UNIVERSITY OF CYPRUS

DEPARTMENT OF CIVIL AND ENVIRONMENTAL ENGINEERING

INVESTIGATING THE SOLAR-DRIVEN ADVANCED CHEMICAL OXIDATION OF OFLOXACIN AND TRIMETHOPRIM IN SEWAGE AND OTHER AQUEOUS MATRICES

DOCTORAL DISSERTATION

IRENE MICHAEL

2012

UNIVERSITY OF CYPRUS

DEPARTMENT OF CIVIL AND ENVIRONMENTAL ENGINEERING

INVESTIGATING THE SOLAR-DRIVEN ADVANCED CHEMICAL OXIDATION OF OFLOXACIN AND TRIMETHOPRIM IN SEWAGE AND OTHER AQUEOUS MATRICES

By

IRENE MICHAEL

Chemical Engineer, National Technical University of Athens, Greece

Submitted to the Department of Civil and Environmental Engineering of the University of Cyprus in partial fulfilment of the requirements for the degree of

DOCTOR OF PHILOSOPHY

Nicosia, May 2012

UNIVERSITY OF CYPRUS

DEPARTMENT OF CIVIL AND ENVIRONMENTAL ENGINEERING

APPROVAL PAGE

DOCTOR OF PHILOSOPHY DISSERTATION

This is to certify that this dissertation prepared

By Irene Michael

Entitled Investigating the solar-driven advanced chemical oxidation of ofloxacin and trimethoprim in sewage and other aqueous matrices

Complies with the University regulations and meets the standards of the University for originality and quality.

This dissertation was successfully presented and defended to the examining committee on Monday 21th of May 2012.

Academic/Research Advisor Despo Fatta Kassinos, *Assistant Professor*

Examination committee Michalis Petrou, *Professor (Chairman of the Committee)*

Panos Papanastasiou, *Professor*

Dionisios Mantzavinos, *Professor*

Ioannis Poulios, *Professor*

Ph.D. examination committee

Academic/Research Advisor

_____

Dr. Despo Fatta-Kassinos
Assistant Professor
Department of Civil
and Environmental Engineering
University of Cyprus

Members of the Committee

_____

Dr. Michalis Petrou
Professor
Department of Civil
and Environmental Engineering
University of Cyprus
(Chairman of the Committee)

_____

Dr. Panos Papanastasiou
Professor
Department of Civil
and Environmental Engineering
University of Cyprus

_____

Dr. Dionisios Mantzavinos
Professor
Department of Environmental
Engineering
Technical University of Crete

_____

Dr. Ioannis Poulios
Professor
Department of Chemistry
Aristotle University of Thessaloniki

Dedicated to my parents

ACKNOWLEDGMENTS

A doctoral thesis requires quite a time of dedication and considerable effort. One can feel lucky, if looking back after such a period can see how many people gave their support to this effort willingly. Therefore I am definitely lucky and I would like to take the opportunity to thank them.

First and foremost, I am deeply grateful to my supervisor, *Assistant Professor Dr. Despo Fatta-Kassinos* for her invaluable help, support and encouraging attitude during the research work. I want to express my gratitude to her for the liberty she gave me to develop my work and pursue my own ideas, for believing in me, for helping me to gain invaluable experiences in research projects, work in other laboratories abroad, to attend international conferences and publish articles in international journals. I appreciate the fact that she provided me time, ideas, and funding to make my Ph.D. experience productive and stimulating. Many thanks Despo for your unconditional and invaluable support and for your continuous heartfelt help and friendship.

Furthermore, I would like to warmly thank the other members of my thesis committee: *Professor Dr. Dionisios Mantzavinos, Professor Dr. Ioannis Poulios, Professor Dr. Panos Papanastasiou* and *Professor Dr. Michalis Petrou* for accepting being examiners of this work.

In addition, I have been very privileged to get to know and collaborate with many other great people. I deeply thank *Dr. Sixto Malato* who helped me during my stay in Plataforma Solar de Almería (PSA) through the interesting scientific discussions, the resolution of many problems during the experimental work and the preparation of scientific papers. A big thanks to all the members and colleague of the PSA group,

especially Ana Zapata, for all their help and support along my stay in Almería. Muchas gracias por toda su ayuda.

I gratefully acknowledge *Professor Dr. Damia Barceló*, *Professor Dr. Mira Petrović* and *Dr. Sandra Pérez* whose experience in analytical chemistry made part of this work possible to be accomplished. A special thanks to *Victoria Osorio* for her valuable help in the transformation products elucidation.

I would like to thank *Dr. Celia Manaia* who offered me the opportunity to work in her laboratory and helped me with the microbiological analysis. I would also like to express my sincere thanks to all the friends that I have made along my stay in Porto; especially *Ana Rita Varela*.

I would like to acknowledge the Waters Corporation (Manchester) and specifically *Simon Cubbon* who made significant contribution to the development of the chromatographic analytical method used in this work. I gratefully acknowledge the funding sources that made my Ph.D. work possible. The experimental work performed in Cyprus has been carried out in the framework of the SolTec project which was co-funded by the Republic of Cyprus and the European Regional Development Fund of the European Union through grant AEIFO/ASTI/0308/01/BIE. Part of the work has been supported by the International Water Research Center "NIREAS" (NEA IPODOMI/STRATH II/0308/09) also co-funded by the Republic of Cyprus and the European Regional Development Fund. Moreover, the experimental work performed in the PSA was funded by the European Commission under SFERA program (Solar Facilities for the European Research Area). The COST (European Cooperation in Science and Technology) awarded a grant through a Short Term Scientific Mission (STSM) within the COST scientific programme on ''Detecting evolutionary hot spots of antibiotic resistances in Europe (DARE)'' for the

training on the method for the determination of antibiotic resistant bacteria in Porto, Portugal.

I want to thank all GAIA members for their contribution and for providing a pleasant and productive working atmosphere. I am particularly thankful to *Dr. Costas Michael* for his encouragement, supervision, invested time and his humour during the difficult times. Sincere thanks to *Dr. Evroula Hapeshi* for her efforts, warm encouragement and friendship throughout these years.

Finally, I would like to thank my parents for their infinite support and love throughout everything. My deepest gratitude to *John Kordatos* for his continued moral support and love.

Irene Michael

University of Cyprus

May, 2012

ABSTRACT

This Ph.D. thesis structure results from different papers published and/or submitted for publication in international journals, during the experimental work carried out at the University of Cyprus (UCY) at the Department of Civil and Environmental Engineering and partly at the Plataforma Solar de Almería (PSA), throughout the period between January 2009 and January 2012.

This work investigated preliminary the application of two solar driven advanced oxidation processes (AOPs) for the degradation of two antibiotic compounds in secondary treated domestic effluents at a bench scale set-up. Ofloxacin (OFX) and trimethoprim (TMP) were chosen as the model contaminants while the two AOPs examined were the homogeneous solar Fenton process ($h\nu/Fe^{2+}/H_2O_2$) and the heterogeneous photocatalysis with titanium dioxide (TiO_2) suspensions. The influence of various operational parameters was evaluated by studying the degradation/removal of the antibiotics in the wastewater solution by UV/Vis spectrophotometry and chromatographic analysis (UPLC-MS/MS) and by monitoring the reduction of dissolved organic carbon (DOC) during the process. A *Daphnia magna* bioassay was also used to evaluate the potential toxicity of the parent compounds and their transformation products generated during the different stages of the oxidation processes. The results indicated that solar Fenton ($[Fe^{2+}]_0$=5 mg L^{-1}; $[H_2O_{2(OFX)}]_0$=2.714 mmol L^{-1}; $[H_2O_{2(TMP)}]_0$=3.062 mmol L^{-1}) has been demonstrated to be more effective than the solar TiO_2 process ($[TiO_2]$=3 g L^{-1}), yielding complete degradation of the examined substrates within 30 min of illumination and DOC reduction of about 41% and 44% at the end of the photocatalytic treatment for OFX and TMP, respectively. The respective values for the TiO_2 process under the optimum

conditions were 60% and 68% degradation of OFX and TMP respectively within 120 min of treatment and 10-13% DOC removal. Kinetic analyses indicated that the homogeneous photodegradation of OFX and TMP can be described by a pseudo-first-order reaction whereas the Langmuir-Hinshelwood (L-H) kinetic expression was used to assess the kinetics of the heterogeneous photocatalytic process. The toxicity of the treated samples was decreased by the end of both processes and the toxicity variations which have been observed illustrated the participation of different oxidation mechanisms during each process.

The solar Fenton process was further investigated in a pilot scale set up. All the experiments were carried out in a two compound parabolic collector (CPC) pilot plants installed at the PSA and at the sewage treatment plant at the UCY for solar photocatalytic applications. The main objectives of the pilot scale study were: (a) the optimization of the solar Fenton process for the determination of the degradation kinetics of the two antibiotics in relatively low concentration level (100 μg L^{-1}); and (b) the structure elucidation of the major oxidation by-products formed during the TMP solar Fenton treatment in four different environmental matrices (demineralized water (DW); simulated natural freshwater (SW); simulated effluent from municipal WWTP (SWW); and real effluent from municipal WWTP (RE)).

DOC removal was lower in the case of SW compared to DW, which can be attributed to the presence of inorganic anions which may act as scavengers of the hydroxyl radicals. On the other hand, the presence of organic carbon and higher salt content in SWW and RE led to lower mineralization per dose of hydrogen peroxide compared to DW and SW. A large number of compounds generated by the photocatalytic transformation of TMP were identified by UPLC-ToF/MS. The degradation pathway

exhibited differences among the four matrices; however hydroxylation, demethylation and cleavage reactions were observed in all matrices.

Solar Fenton process using low iron and hydrogen peroxide doses ($[Fe^{2+}]_0$=5 mg L^{-1}; $[H_2O_2]_0$=75 mg L^{-1}) was proved to be an efficient method for the elimination of these compounds at low concentration level (μg L^{-1}) with relatively high degradation rates. The process was mainly evaluated by a fast and reliable analytical method based on a UPLC-MS/MS technology which was optimized and validated for studying the degradation kinetics of both compounds. Moreover, the solar Fenton application in wastewater treatment at neutral pH had a beneficial impact onto the substrates' degradation due to the formed ferric iron complexes with the dissolved organic matter (DOM). The results demonstrated the capacity of the applied advanced process to reduce the initial toxicity of the non-treated sewage to the examined plant species (*Sorghum saccharatum*, *Lepidium sativum*, *Sinapis alba*) and to the water flea *Daphnia magna*. The phytotoxicity in the treated samples expressed as root or shoot growth inhibition, was higher compared to that observed on the inhibition of seed germination. Enterococci, including those resistant to OFX and TMP, were completely eliminated at the end of the treatment. Solar Fenton was proved to be an efficient and cost effective method considering the requirement for safe wastewater reuse for agriculture irrigation purposes.

ΠΕΡΙΛΗΨΗ

Η δομή της παρούσας διδακτορικής διατριβής είναι αποτέλεσμα διάφορων άρθρων που έχουν δημοσιευτεί και/ή υποβληθεί για δημοσίευση σε διεθνή επιστημονικά περιοδικά, κατά τη διάρκεια των πειραματικών εργασιών που έχουν διεξαχθεί στο Πανεπιστήμιο Κύπρου (ΠΚ) στο Τμήμα Πολιτικών Μηχανικών και Μηχανικών Περιβάλλοντος και μερικώς στην Plataforma Solar de Almería (PSA), καθόλη την περίοδο μεταξύ Ιανουαρίου 2009 και Ιανουαρίου 2012.

Βασικό αντικείμενο της παρούσης έρευνας αποτέλεσε σε αρχικό στάδιο η εφαρμογή δύο προχωρημένων μεθόδων οξείδωσης, αξιοποιώντας ως πηγή φωτός την ηλιακή ακτινοβολία, για την αποικοδόμηση δύο αντιβιοτικών ενώσεων που περιέχονται σε δευτεροβάθμια επεξεργασμένα αστικά λύματα σε εργαστηριακή κλίμακα. Η οφλοξακίνη και η τριμεθοπρίμη επιλέχθησαν ως οι υπό εξέταση ενώσεις ενώ οι δύο προηγμένες τεχνικές οξείδωσης που εξετάσθηκαν ήταν η ομογενής φωτοκατάλυση (φωτο-Φέντον) και η ετερογενής φωτοκατάλυση παρουσία του καταλύτη διοξειδίου του τιτανίου (TiO_2). Η επίδραση διάφορων λειτουργικών παραμέτρων εξετάστηκε μέσω του προσδιορισμού της αποικοδόμησης/απομάκρυνσης των αντιβιοτικών ενώσεων στο απόβλητο με τη χρήση υπεριώδους/ορατής φασματοφωτομετρίας και χρωματογραφικής ανάλυσης (UPLC-MS/MS) και της απομάκρυνσης του διαλυμένου οργανικού άνθρακα (DOC) κατά τη διάρκεια της επεξεργασίας. Επίσης χρησιμοποιήθηκε βιοδοκιμή με τη χρήση των μικροοργανισμών *Daphnia magna*, για τον έλεγχο και την αξιολόγηση της τοξικότητας των εξεταζόμενων ενώσεων και των οξειδωμένων ενδιάμεσων προϊόντων που δημιουργήθηκαν στα διάφορα στάδια των διεργασιών οξείδωσης. Τα αποτελέσματα έδειξαν ότι η διεργασία φωτο-Φέντον ($[Fe^{2+}]_0$=5 mg L^{-1}; $[H_2O_{2(OFX)}]_0$=2.714 mmol L^{-1}; $[H_2O_{2(TMP)}]_0$=3.062 mmol L^{-1})

αποδείχθηκε πιο αποτελεσματική συγκρινόμενη με την ετερογενή ([TiO_2]=3 g L^{-1}), κατά την οποία επιτεύχθηκε πλήρης αποικοδόμηση των εξεταζόμενων ενώσεων σε 30 λεπτά ακτινοβόλησης και απομάκρυνση του διαλυμένου οργανικού άνθρακα περίπου ίση με 41% και 44% στο τέλος της φωτοκαταλυτικής επεξεργασίας για την οφλοξακίνη και τριμεθοπρίμη αντίστοιχα. Οι αντίστοιχες τιμές αποικοδόμησης κατά την ετερογενή φωτοκαταλυτική επεξεργασία στις βέλτιστες συνθήκες ήταν 60% και 68% για την οφλοξακίνη και τριμεθοπρίμη αντίστοιχα στα 120 λεπτά επεξεργασίας και 10-13% απομάκρυνση του διαλυμένου οργανικού άνθρακα. Η μελέτη της κινητικής έδειξε ότι η ομογενής αποικοδόμηση της οφλοξακίνης και της τριμεθοπρίμης μπορεί να περιγραφεί με κινητική ψευδό-πρώτης τάξης ενώ στην περίπτωση της ετερογενούς φωτοκατάλυσης χρησιμοποιήθηκε το κινητικό μοντέλο των Langmuir-Hinshelwood (L-H). Η τοξικότητα των επεξεργασμένων δειγμάτων μειώθηκε στο τέλος των εκάστοτε διεργασιών και οι μεταβολές της τοξικότητας που παρατηρήθηκαν πιθανόν να οφείλονται στη συμμετοχή διαφορετικών μηχανισμών οξείδωσης στην κάθε διεργασία.

Η ομογενής διεργασία φωτο-Φέντον μελετήθηκε περαιτέρω σε πιλοτική κλίμακα. Όλες οι πειραματικές δοκιμές διεξήχθησαν σε δύο παραβολικά πιλοτικά συστήματα τύπου CPC που βρίσκονται εγκατεστημένα στην PSA και στο βιολογικό σταθμό επεξεργασίας του ΠΚ ειδικά σχεδιασμένα για εφαρμογές φωτοκατάλυσης. Οι βασικές συνιστώσες της πιλοτικής έρευνας ήταν: (α) η βελτιστοποίηση της διεργασίας φωτο-Φέντον για τον καθορισμό της κινητικής διάσπασης των αντιβιοτικών σε χαμηλά επίπεδα συγκέντρωσης (100 μg L^{-1}) και (β) η ταυτοποίηση της δομής των βασικών ενδιάμεσων προϊόντων οξείδωσης της τριμεθοπρίμης κατά τη διάρκεια της διεργασίας φωτο-Φέντον σε τέσσερις διαφορετικές περιβαλλοντικές μήτρες (απιονισμένο νερό (DW); προσομοιωμένο φυσικό γλυκό νερό (SW); προσομοιωμένο

απόβλητο από σταθμό επεξεργασίας λυμάτων (SWW) και απόβλητο real από σταθμό επεξεργασίας λυμάτων (RE)).

Η απομάκρυνση του DOC ήταν μικρότερη στο SW σε σχέση με το DW, η οποία μπορεί να αποδοθεί στην παρουσία ανόργανων ιόντων τα οποία μπορούν να δεσμεύσουν τις ρίζες υδροξυλίου. Αφετέρου, η παρουσία του οργανικού φορτίου και του υψηλότερου σε άλατα περιεχόμενου στο SWW και RE οδήγησε σε μικρότερα ποσοστά ανοργανοποίησης ανά δόση υπεροξειδίου του υδρογόνου, σε σύγκριση με το DW και SW. Ένας μεγάλος αριθμός ενώσεων που σχηματίστηκαν κατά την φωτοκαταλυτική οξείδωση της τριμεθοπρίμης ανιχνεύθηκαν με τη χρήση UPLC-ToF/MS. Η πορεία αποικοδόμησης παρουσίασε διαφορές μεταξύ των τεσσάρων μητρών ωστόσο η υδροξυλίωση, η προσθήκη μεθυλομάδων και οι αντιδράσεις διάσπασης του δακτυλίου ήταν εμφανής σε όλες τις μήτρες.

Η διεργασία φωτο-Φέντον με τη χρήση χαμηλών συγκεντρώσεων σιδήρου και υπεροξειδίου του υδρογόνου ($[Fe^{2+}]_0$=5 mg L^{-1}; $[H_2O_2]_0$=75 mg L^{-1}) αποδείχθηκε μια αποδοτική μέθοδος για την απομάκρυνση αυτών των ενώσεων σε χαμηλά επίπεδα συγκέντρωσης (μg L^{-1}) με σχετικά υψηλούς ρυθμούς διάσπασης. Η αξιολόγηση της μεθόδου πραγματοποιήθηκε κυρίως με τη χρήση μιας γρήγορης και αξιόπιστης αναλυτικής μεθόδου βασιζόμενη στην τεχνολογία UPLC-MS/MS η οποία βελτιστοποιήθηκε και επικυρώθηκε για τη μελέτη της κινητικής αποικοδόμησης των δύο ενώσεων. Επιπρόσθετα, η εφαρμογή της διεργασίας φωτο-Φέντον σε ουδέτερο pH στην επεξεργασία αποβλήτων είχε ευεργετική επίδραση στην αποικοδόμηση των υποστρωμάτων λόγω των σχηματιζόμενων συμπλόκων τρισθενούς σιδήρου με τη διαλυμένη οργανικής ύλης (DOM). Τα αποτελέσματα έδειξαν την ικανότητα της προηγμένης διεργασίας να προκαλεί μείωση της τοξικότητας στα υπό εξέταση φυτικά είδη (*Sorghum saccharatum*, *Lepidium*

sativum, *Sinapis alba*) και στον υδρόβιο οργανισμό *Daphnia magna*. Η φυτοτοξικότητα στα επεξεργασμένα δείγματα εκφρασμένη ως αναστολή της ανάπτυξης της ρίζας ή του βλαστού, ήταν υψηλότερη σε σύγκριση με αυτή που παρατηρήθηκε κατά την αναστολή της φύτρωσης των σπερμάτων. Οι εντερόκοκκοι, συμπεριλαμβανομένων των ανθεκτικών στην οφλοξακίνη και στην τριμεθοπρίμη, είχαν εξαλειφθεί εντελώς στο τέλος της επεξεργασίας. Η διεργασία φωτο-Φέντον αποδείχθηκε μια αποτελεσματική και οικονομικά αποδοτική μέθοδος για την ασφαλή επαναχρησιμοποίηση των λυμάτων στη γεωργία για αρδευτικούς σκοπούς.

ABBREVIATIONS

AOPs	*Advanced Oxidation Processes*
APHA	*American Public Health Association*
ATU	*Allylthiourea*
BEH	*Ethylene Bridged Hybrid substrate*
BOD	*Biochemical Oxygen Demand*
CAS	*Conventional Activated Sludge*
CE	*Collision Energy*
CB	*Conduction Band*
CBQF	*Center for Biotechnology and Fine Chemistry*
CFU	*Colony Forming Units*
CIEMAT	*Centro de Investigaciones Energéticas Medioambientales y Tecnológicas*
COD	*Chemical Oxygen Demand*
CPCs	*Compound Parabolic Collectors*
CSIC	*Spanish Council of Scientific Research*
CV	*Cone Voltage*
DAD	*Diode Array Detector*
DBE	*Double Bond Equivalents*
DHFR	*Dihydrofolate Reductase*
DO	*Dissolve Oxygen*
DOC	*Dissolved Organic Carbon*
DOM	*Dissolved Organic Matter*
DW	*Demineralized Water*
EARSS	*European Antimicrobial Resistance Surveillance System*
EDCs	*Endocrine Disrupting Compounds*
EMEA	*European Medicines Agency*
ESI	*Electrospray Ionization*
FA	*Fulvic Acid*
F/M	*Food-microorganism ratio*
FAO	*Food and Agriculture Organization*
GC	*Gas Chromatography*
GI	*Seed Germination Inhibition*
HA	*Humic Acid*
HLB	*Hydrophilic-Lipophilic Balanced polymeric sorbent*

HPLC	*High Performance Liquid Chromatography*
HPLC-DAD	*High Performance Liquid Chromatography with Diode Array Detector*
HRT	*Hydraulic Retention Time*
HSS	*High Strength Silica*
IC	*Ion-exchange Chromatography*
IDÆA	*Institute of Environmental Assessment and Water Research*
LC	*Liquid Chromatography*
LC-MS/MS	*Liquid Chromatography Tandem Mass Spectrometry*
L-H	*Langmuir-Hinshelwood*
LMCT	*Ligand-to-Metal Charge-Transfer*
LOD	*Limit of Detection*
LOQ	*Limit of Quantification*
MF	*Microfiltration*
MIC	*Minimal Inhibitory Concentrations*
MLSS	*Mixed Liquor-Suspended Solids*
MRM	*Multiple Reaction Monitoring*
MS	*Mass Spectrometry*
MS/MS	*Tandem Mass Spectrometry*
MSE	*Mean Square Error*
MWCO	*Molecular Weight Cut-Off*
NDIR	*Non-Dispersive Infrared Detector*
NF	*Nanofiltration*
NHE	*Normal Hydrogen Electrode*
OECD	*Organization for Economic Cooperation and Development*
OFX	*Ofloxacin*
PE	*Population Equivalents*
PMB	*Phosphomolybdenum Blue*
PSA	*Plataforma Solar de Almería*
PTCs	*Parabolic-Trough Concentrators*
QqQ	*Triple Quadrupole*
Q-ToF-MS^2	*Quandrupole-Time of Flight-tandem Mass Spectrometry*
RE	*Real Effluent from municipal WWTP*
RI	*Root growth Inhibition*
RO	*Reverse Osmosis*
RSD	*Relative Standard Deviation*
SBR	*Sequencing Biological Reactor*

SFERA	*Solar Facilities for the European Research Area*
SI	*Shoot growth Inhibition*
SPE	*Solid-Phase Extraction*
SR	*Solar Radiation*
SRT	*Sludge Retention Time*
SS	*Suspended Solids*
SW	*Simulated natural freshwater*
SWW	*Simulated effluent from municipal WWTP*
TIC	*Total Inorganic Carbon*
TIC	*Total Ion Chromatograph*
TKN	*Total Kjeldahl Nitrogen*
TMP	*Trimethoprim*
TOC	*Total Organic Carbon*
ToF	*Time of Flight*
TPs	*Transformation Products*
TQD	*Triple Quadrupole Detector*
TSS	*Total Suspended Solids*
UCY	*University of Cyprus*
UF	*Ultrafiltration*
UPLC	*Ultra Performance Liquid Chromatography*
UPLC	*Ultra Performance Liquid Chromatography*
UPLC-MS/MS	*Ultra Performance Liquid Chromatography tandem Mass Spectroscopy*
UPLC-ToF-MS/MS	*Ultra Performance Liquid Chromatography Time-of-Flight tandem Mass Spectrometry*
UV/Vis	*Ultraviolet/Visible radiation*
VB	*Valence Band*
VSS	*Volatile Suspended Solids*
WAO	*Wet Air Oxidation*
WW	*Wastewater*
WWTP(s)	*Wastewater Treatment Plant(s)*
XIC	*Extracted Ion Chromatograph*

MAIN SYMBOLS

$\hat{y}_i$	*Model predicted values*
$\overline{UV}$	*Average solar ultraviolet radiation*
$\bar{y}$	*Average of the experimental values*
y_i	*Experimental value*
$\bar{\theta}$	*Average temperature*
A	*Acceptor*
A	*Absorbance*
A	*Collector aperture*
A	*Pre-exponentional factor*
Adj-R^2	*Adjusted regression coefficient*
C	*Concentration*
C_0	*Initial concentration*
C_e	*Equilibrium organic substrate concentration*
D	*Donor*
E^0	*Redox potential*
E_a	*Activation energy*
E_{bg}	*Bandgap energy*
e_{CB}^-	*Conduction band electrons*
h_{VB}^+	*Valence hole*
hν	*Photon*
I	*Light intensity*
I_0	*Initial light intensity*
Is	*(%) Respiration inhibition*
k	*Apparent pseudo-first-order rate constant*
k^*	*Kinetic rate constant*
k'	*Retention capacity*
K_d	*Sludge sorption constant*
k_r	*L-H constant*
k_T	*Kinetic rate constant as a function of temperature*
L	*Ligand*
l	*Length*
$logK_{o/w}$	*Octanol/water partition coefficient*
m/z	*Mass-to-charge ratio*

n	*Number of experiments performed*
P	*Micropollutant*
p	*Fit coefficient number*
pK_a	*Ionization constant*
pzc	*Zero point charge*
Q	*Quantification ion*
q	*Confirmation ion*
Q/q	*Intensity ratio of two MS transitions*
R	*Organic substrate*
r	*Degradation rate*
r_0	*Initial rate of degradation*
R^2	*Correlation coefficient*
R_C	*Concentration factor*
R_s	*Respiration rate*
R_{smax}	*Maximum respiration rate*
S_0	*Standard deviation at zero concentration*
T	*Temperature*
$t_{1/2}$	*Half-life time*
$t_{30W,n}$	*Normalized illumination time*
$t_{30WT,n}$	*Normalized illumination time at 25 ^oC*
t_{exp}	*Actual experimental time*
t_R	*Retention time*
V_i	*Irradiated volume of the collector*
V_T	*Total volume of the collector*
ε_λ	*Molar extinction coefficient*
θ_α	*Semi-angle of acceptance*
λ	*Wavelength*
Φ	*Quantum yield*
$\Phi_e{}^n$	*Rate of effective light absorption, n is a power term*

TABLE OF CONTENTS

INDEX OF TABLES

INDEX OF SCHEMATICS

INDEX OF PICTURES

INDEX OF FIGURES

CHAPTER 1: INTRODUCTION AND BACKGROUND OF THE THESIS

1.1 Antibiotics in the aquatic environment

Nowadays, one of the major environmental problems worldwide is the adequate provision of clean water for human consumption. Europe has extensive water resources compared to other regions of the world, and water has long been considered as an inexhaustible public commodity. This position has however been challenged in the last decades by growing water stress, both in terms of water scarcity and water quality deterioration (Hochstrat and Wintgens, 2003). The per capita consumption of water, although different from country to country, tends to increase. Thus in many countries, particularly in those with dry weather conditions such as Cyprus, policies were developed to face the water demand.

In an effort to combat the problem of water stress, a number of governmental authorities have turned their attention to the utilization of treated domestic effluent in order to alleviate water scarcity (Bixio et al., 2006). Treated domestic water recycling for industrial, agricultural, and non-potable municipal uses is an increasingly important component of water resources management practices worldwide. Figure 1.1 (a) ranks European countries according to their water stress index. The water stress index (the ratio of a country's total water withdrawals to its total renewable freshwater resources) serves as a rough indicator of the pressure exerted on water resources. Cyprus is recognised as the first country in European Union facing water stress issues. To this effect, much effort was put by the Cyprus government, during the last fifteen years, to use the treated domestic wastewater for irrigation of agriculture areas and recharging groundwater aquifers (Firure 1.1 (b)). Consequently

huge amounts of fresh water are saved (the water consumption for agricultural irrigation in Cyprus accounts for approximately 70% of the total water consumption).

(a)

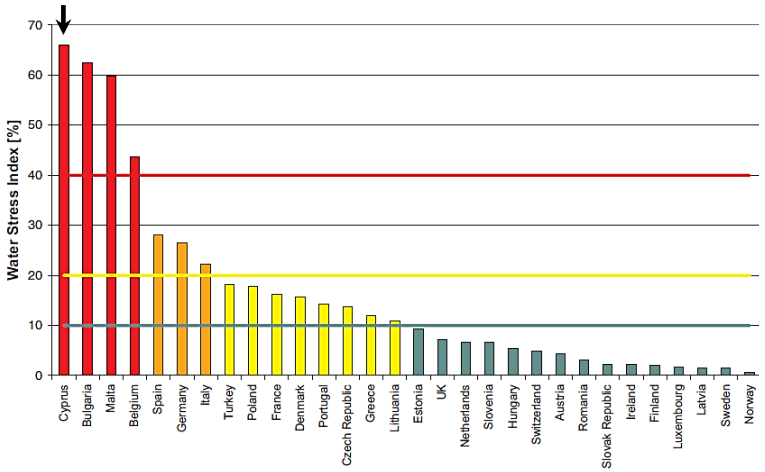

Source: *Hochstrat and Wintgens (2003)*

(b)

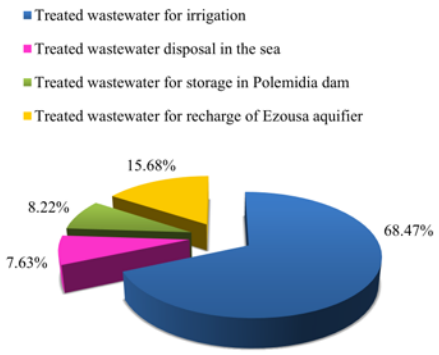

Source: *Water Development Department*

Figure 1.1 (a) Water stress index for the European countries for the year 2000; and (b) Domestic tertiary treated wastewater reuse in 2009 in Cyprus.

Although the treated wastewater reuse practice is accompanied by a number of benefits relating to the enhancement of water balances and soil nutrition by the nutrients existing in the treated effluents (Candela et al., 2007), a number of unanswered questions are still related to this practice. Besides the lack of knowledge in respect to possible elemental interactions that may influence the accumulation of heavy metals and other elements in the soil, during the last several years, the technological progress in respect to innovative analytical methods has enabled the identification and quantitation of a number of organic xenobiotic compounds in treated wastewater (Klamerth et al., 2009; Fatta-Kassinos et al., 2011). Xenobiotic compounds that may be present in treated wastewater effluents include, pesticides, personal care products, endocrine disrupting compounds (EDCs), disinfection by-

products, pharmaceuticals and many other complex compounds (Eriksson et al., 2003; Fatta-Kassinos et al., 2011c).

During the last years, it is recognized that pharmaceuticals constitute a new class of water contaminants of emerging concern with adverse effects on the aquatic life (Watkinson et al., 2009; Fatta-Kassinos et al., 2011). The scientific community, at the beginning, focused on their occurrence and fate in the environment but soon a lot of effort was diverted to the establishment of novel treatment processes particularly for the domestic wastewaters which are recognized as being the main point discharge source of these substances in the environment.

Antibiotics are an important group of pharmaceuticals which were recently classified as a priority risk group (Hernando et al., 2006) due to their high toxicity to microorganisms (algae and bacteria) at low concentrations (Watkinson et al., 2009). Moreover, antibiotics in the aquatic environment have drawn increased attention over the potential relationship between antibiotic resistant infections and humans health (Loftin et al., 2008). Antibiotics can be classified by either their chemical structure or mechanism of action into different sub-groups such as β-lactams, macrolides, sulfonamides, quinolones, tetracyclines and others.

A great number of these compounds, at the ng L^{-1} to the μg L^{-1} level (often referred to as micropollutants), have been detected in various compartments of the aquatic environment worldwide (Fatta-Kassinos et al., 2010; Jeong et al., 2010). This indicates the ineffectiveness of the widespread currently most frequently applied conventional biological treatment processes to remove adequately such compounds from the domestic wastewaters. The reported levels of antibiotic compounds detected in raw sewage appear to differ among countries, possibly reflecting variable prescription practices (Miao et al., 2004) and differences in the per-capita water

consumption leading to various degrees of dilution (Drewes et al., 2007). Seasonal variations in sewage concentrations of antibiotics have also been reported (Le-Minh et al., 2010).

1.1.1 Sources and occurrence of antibiotics in the environment

Antibiotics is a group of chemotherapeutic agents with varying chemical structures, which have the capability to inhibit or abolish the growth of microorganisms (Blom, 2009) and they are mainly used in human medicine for the purpose of preventing or treating microbial infections (Lindberg et al., 2005; Kümmerer, 2009). Besides this fundamental application, antibiotics have also been used for preventing and treating animal's infections as well as for promoting growth in animal farming. Antibiotics have also been used since the 1950s to control certain bacterial diseases of high-value fruit, vegetable and ornamental plants (Martinez, 2009). In addition, some antibiotics have been authorized for use in aquaculture (the farming of aquatic organisms including fish, molluscs, crustaceans and aquatic plants according to Food and Agriculture Organization (FAO)) (Serrano, 2005).

Antibiotics enter the environment though different routes. Many of the antibiotics consumed by humans and animals cannot be completed metabolized in the body therefore a high percentage of antibiotics is excreted unchanged or partially degraded via urine and feces into domestic sewage and discharged further to wastewater treatment plants (WWTPs) (Cha et al., 2006; Li et al., 2009). If they are not eliminated during the conventional wastewater treatment processes, they end up in the environment as a part of the final effluent discharge or as a component of the sludge produced. Residual amounts can also reach surface waters, groundwater or soil. Hospital wastewaters are also considered as the most important source of human

antibiotic compounds, with contributions also from pharmacies, manufacturing industries and from disposal of unused antibiotics into the environment. Discharges from veterinary clinics and runoff from agricultural applications into municipal sewers are also considered as potential sources of veterinary antibiotics in wastewater effluents and the environment.

With conventional treatment processes, most current WWTPs are not capable to remove antibiotics; these compounds have been detected at concentration ranging from ng L^{-1} to μg L^{-1} in the treated effluents taken from various WWTPs in United States (Brown et al., 2006; Karthikeyan and Meyer, 2006; Batt et al., 2007; Massey et al., 2010), Japan (Yasojima et al., 2006; Choi et al., 2007), Spain (Carballa et al., 2004), Sweden (Lindberg et al., 2005; Zorita et al., 2009), China (Xu et al., 2007; Gulkowska et al, 2008), Germany (Joss et al., 2005; Yu et al., 2009), Australia (Choi et al., 2007), Vietnam (Duong et al., 2008), as well as in Taiwan (Lin et al., 2009). Table A1 (Annex) provides an overview of the various studies published in international journals between 2002 and 2011 and it basically gives information about the WWTP and the treatment processes, the effluent quality characteristics, the antibiotic concentrations and some main results based on the antibiotics removal efficiency.

1.1.2 Environmental impact of antibiotics

Once released into the environment, antibiotics are subject to elimination and transformation processes. These processes can be biotic (biodegradation by bacteria and fungi) and non-biotic or abiotic (*e.g.* sorption to soils and sediments, hydrolysis, photolysis, oxidation and reduction) (Knackmuss, 1996; Byrns, 2001; Nikolaou et al., 2007). Elimination means that the antibiotic compound of interest is not detectable

anymore by a specific analytical method in the compartment or phase of sampling. If the compound is converted into CO_2 and inorganic salts (*e.g.* sulphate, phosphate, ammonium and nitrate), it means that complete mineralization took place. If a substance is not completely eliminated, a number of transformation products can reach the environment with the potential of adversely affecting aquatic and terrestrial organisms.

Biotic processes can induce the formation of only a limited degree of transformation because of the high persistence and low biodegradability of many antibiotic compounds (Fatta-Kassinos et al., 2011b). Some antibiotics can biotransformed into innocuous products that may then enter a particular metabolic pathway and be degraded (Byrns, 2001). Abiotic environmental factors (*e.g.* temperature, matrix composition, sunlight, salinity, pH) on the other hand, can make a significant contribution to the transformation of such substances in the environment. Abiotic and biotic processes can also take place during the treatment processes applied at the sewage and drinking water treatment plants.

Routes of transformation of antibiotics into the environment are very important for understanding the fate and behavior of these compounds. It is important to underline however the fact that only little information is currently available with regard to transformation products formed in the environment or WWTPs. The transformation products may preserve the same mode of action of the parent compound (*i.e.* the active moiety remains intact during degradation) or even be more toxic (Boxall et al., 2004; Sirtori et al., 2010). One study dealing with the biological activity of transformation products compared to that of the parent compound was conducted by Kusari et al. (2009) who investigated the degradation of difloxacin and sarafloxacin under natural sunlight conditions. The antibacterial activities of the above antibiotics

and their photoproducts were studied against a group of pathogenic strains. It was found that both compounds revealed potency against both Gram-positive and Gram-negative bacteria while their transformation products also exhibited varying degree of efficacies against the tested bacteria depending on the time duration of the photolysis.

The presence of antibiotics and their transformation products in low concentrations has been associated to chronic toxicity and the prevalence of resistance to antibiotics in bacterial species (Le-Minh et al., 2010). The consequences are particularly worrying in aquatic organisms as they are subjected to multigenerational exposure (Rosal et al., 2010).

1.1.2.1 Ecotoxicity effects

The number of studies focusing on the chronic toxicological assessment of antibiotics in the environment is constantly increasing the aim being to bridge the various knowledge gaps associated with these issues. Toxicity tests with various microorganisms and bacteria indicated that chronic exposure to antibiotics is more critical rather than the acute, due to the fact that the latter approach does not reflect the real environmental conditions, where organisms are continuously exposed to antibiotic residues at sub-therapeutic levels (Lindberg et al., 2007).

Thomulka and McGee (1993) determined the toxicity of a number of antibiotics (*e.g.* novobiocin, tetracycline, chloramphenicol, nalidixic acid, ampicillin, streptomycin) on *Vibrio harveyi* in two bioassay methods. Almost no toxic effects were found after short incubation times when luminescence was used as an endpoint. However, in a long-term assay using reproduction as the endpoint, a toxic effect in environmentally relevant concentrations could be detected for almost all the examined antibiotics.

These results are in accordance with the observations of Froehner et al. (2000). The toxicity of several groups of antibiotics towards *Vibrio fischeri* is also presented in a study of Backhaus and Grimme (1999). The chronic bioluminescence inhibition assay was shown to be sensitive against many of the high volume antibiotics used for veterinary purposes and in aquaculture.

Furthermore, exposure to antibiotics may have adverse reproductive effects in the early life stages of different organisms like the freshwater flea *Daphnia magna* and the crustacean *Artemia salina* (Macrí et al., 1988; Wollenberger et al., 2000). In a study by Kim et al. (2007), sulfonamides (sulfamethoxazole, sulfachloropyridazine, sulfathiazole, sulfamethazine, sulfadimethoxine) and trimethoprim were examined for their acute aquatic toxicity by employing a marine bacterium (*Vibrio fischeri*), a freshwater flea (*Daphnia magna*) and the Japanese medaka fish (*Oryzias latipes*). In this study *Daphnia magna* was in general the most susceptible among the test organisms.

Another issue related with the use of reclaimed wastewater for irrigation is the plant uptake of antibiotics. The fate of antibiotics, including transport and sorption in soil, has been well documented (Kulshrestha et al., 2004; Figueroa and MacKay, 2005; De la Torre et al., 2012) whereas knowledge of their uptake and toxicity to plants is poorly understood (European Medicines Agency-EMEA, 2008). The accumulation may or not affect the growth and development of plants; however, the uptake into plants may represent an important exposure pathway of these compounds to humans and other biota.

Results from a study of Kong et al. (2007) demonstrate that alfalfa (*Medicago sativa L.*) uptake of oxytetracycline (veterinary antibiotic) was pH-dependent. Oxytetracycline inhibited alfalfa shoot and root growth by up to 61% and 85%,

respectively. Migliore et al. (2003) determined the phytotoxicity of enrofloxacin on crop plants *Cucumis sativus*, *Lactuca sativa*, *Phaseolus vulgaris* and *Raphanus sativus* in a laboratory model. Phytotoxicity of enrofloxacin on plants generated both toxic effect and hormesis, related to plant drug uptake.

It is in part not clear if the adverse effects on plants originate from the direct damage of the plant by the antibiotics themselves or if their antimicrobial action on soil microorganisms is responsible for the damage by affecting the plant-microorganism symbiosis (Chander et al., 2005; Fatta-Kassinos et al., 2011c).

1.1.2.2 Antibiotic resistance

The extensive use of antibiotics has contributed to the evolution of antibacterial resistance in human pathogenic microorganisms since a great number of these compounds escape conventional biological treatment and thus enter receiving environmental media either in their parent form or as transformation products (Walter and Vennes 1985; Costanzo et al., 2005). This may pose a serious threat to public health in that more infections may no longer be treatable with known antibiotics (Hirsch et al., 1999). In the event that antibiotic resistance is spread from non-pathogenic to pathogenic bacteria, epidemics may result (Kanay, 1983).

The aquatic and terrestrial ecosystems are the biggest known reservoirs of antibiotic-resistant bacteria (D'Costa et al., 2006; Biyela et al., 2004), and continuous exposure to antimicrobial agents has the potential to enhance both the spread of resistance genes and the selection for resistant bacterial strains in aquatic and soil ecosystems (Kümmerer, 2004). Although antibiotics are found in the environment at sub-inhibitory levels, relatively low concentrations of antimicrobial agents can still

promote bacterial resistance (Castiglioni et al., 2008). Indeed, antibiotic-resistant bacteria have been detected in wastewater effluents (Guardabassi et al, 2002; Akiyama et al, 2010; Novo and Manaia, 2010), surface (Ash et al., 2002) and drinking water (Schwartz et al., 2003).

There are four main genetic reactors in which antibiotic resistance evolves. The primary reactor is constituted by the human and animal microbiota, with more than 500 bacterial species involved, in which therapeutic or preventive antibiotics exert their actions. The secondary reactor involves the hospitals, long-term care facilities, farms, or any other place in which susceptible individuals are crowded and exposed to bacterial exchange. The tertiary reactor corresponds to the wastewater from sewage treatment plants, in which bacterial organisms from many different individuals have the opportunity to mix and genetically react. The fourth reactor is the soil or groundwater environments, where the bacteria originated in the previous reactors mix and counteract with environmental organisms (Baquero et al., 2008; Ding and He, 2010).

The extent to which human activities contribute to the maintenance of environmental reservoirs of antibiotic resistance is poorly understood (Auerbach et al, 2007). Consequently, studies focusing exclusively on wastewater treatment systems regarding removal of antibiotic resistance are limited.

Zhang et al. (2009) recently reported the impact of the wastewater treatment process on the prevalence of antibiotic resistance in *Acinetobacter spp.* in the wastewater and the possible spread of antibiotic resistance to its receiving water bodies. It was found that the prevalence of antibiotic resistance was significantly higher in the downstream samples than in the upstream samples. Specifically, when all samples were considered together, the *Acinetobacter spp.* isolates were most resistant to trimethoprim (97%),

followed by rifampin (74%), chloramphenicol (40%), amoxicillin (20%), sulfisoxazole (8%), ciprofloxacin (6%), and gentamicin (2%). Other studies reported that the prevalence of resistant bacteria in sewage may significantly vary depending on the plant (initial composition of sewage, type of treatment, plant operation, etc.), the target bacterial population and the antimicrobial agent under study, as well as on the methods and the breakpoint values used to determine antimicrobial resistance (Guardabassi et al., 2002).

Luczkiewicz et al. (2010) studied the antimicrobial resistance of *Escherichia coli* and *Enterococci* isolates in municipal wastewater treatment plant based on activated sludge system. Most frequently, among *Escherichia coli* isolates the resistance patterns were found for ampicillin (34%), piperacillin (24.2%) and tetracycline (23.5%). The resistance of *Enterococci* was found to be 2.3-10.7% for ampicillin, 4.2-61.4% for erythromycin, 22.7-38.4% for ciprofloxacin, 11.4-11.6% for levofloxacin, 4.2-9.1% for moxifloxacin, 18.8-75% for tetracycline, 2.7-6.8% for vancomycin and 2.3-2.7% for teicoplanin.

Furthermore, the tetracycline resistance genes in two activated sludge wastewater treatment plants were investigated in comparison with their presence in the nearby receiving lakes by Auerbach et al. (2007). All WWTP samples contained more different types of tet^R genes, compared to the lake water samples. UV disinfection on wastewater effluent did not reduce the number of detectable reduction in the number of detectable tet^R gene types.

Monitoring of the propagation pathways of the antibiotic resistant bacteria in the environmental compartments is required. This is also the objective of the new European Cost Action TD0803 under the title, ‘‘Detecting evolutionary hot spots of antibiotic resistances in Europe’’. Data also collected by the European Antimicrobial

Resistance Surveillance System (EARSS) indicate that antibiotic resistance is an important largely unresolved issue in public health. Antibiotic prescription and/or wastewater treatment must adapt accordingly to face this increasing concern. Moreover, the effect of advanced treatment processes besides conventional treatment on the fate of antibiotic resistant bacteria needs to be explored in the future.

1.2 Wastewater treatment

1.2.1 Conventional wastewater treatment

The conventional wastewater treatment generally consists of a primary, secondary and sometimes a tertiary stage, with different biological and physicochemical processes available for each stage of treatment. Primary treatment is intended to reduce the solid content of the wastewater (oils and fats, grease, sand, grit and settleable solids). This step is performed entirely mechanically by means of filtration and sedimentation and is usually common at all WWTPs. However, the secondary treatment, which typically relies on a biological process to remove organic matter and/or nutrients with aerobic or anaerobic systems, can differ substantially. Several methods are being used in modern WWTPs, but the most common method is conventional activated sludge (CAS). Activated sludge plants use a variety of mechanisms and processes to use dissolved oxygen to promote the growth of a biological floc that substantially remove the organic material. In the final step, tertiary wastewater treatment processes can be applied to remove nitrogen, phosphorus and other pollutants or particles (Batt et al., 2007). In some WWTPs the effluent is also disinfected before it is released into the environment, typically by chlorination or ultraviolet irradiation. A typical flow diagram of a WWTP can be seen in Schematic 1.1.

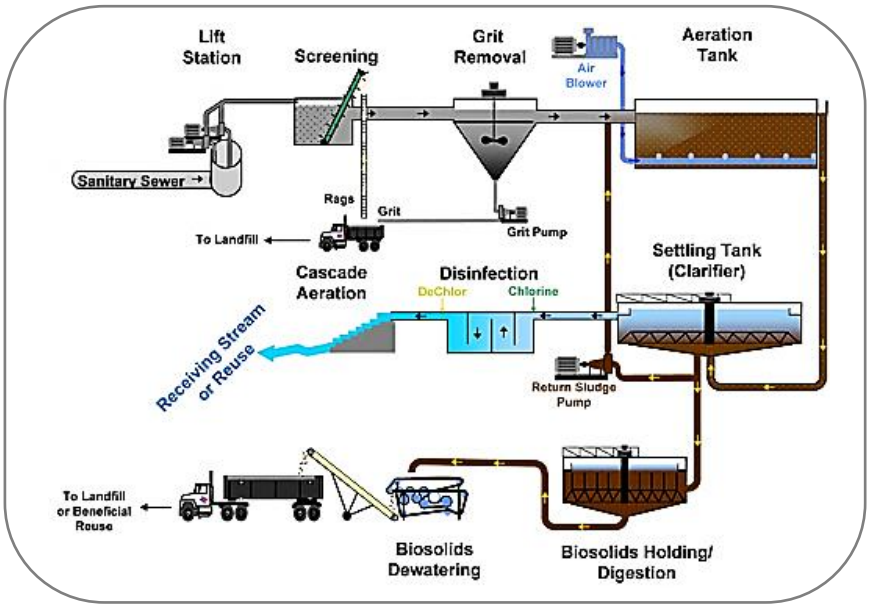

Source: *http://waterschool.brazos.org/category/Wastewater-Treatment.aspx*

Schematic 1.1 Main treatment steps in a WWTP.

1.2.1.1 Removal of antibiotics from wastewater effluents through conventional treatment processes

Previous studies have demonstrated that removal of antibiotic compounds during conventional wastewater treatment processes is highly variable (from nearly complete to very little). Several analytical laboratory studies have been conducted to assess the ability of various conventional wastewater treatment technologies for removing antibiotics from sewage. The performance (expressed as % removal) of some conventional WWTPs for removing antibiotics from wastewater effluents as reported in the literature is summarized in Table A1 (Annex).

The removal efficiency of antibiotic residues during the conventional treatment is affected by their physicochemical properties as well as the operational conditions of the process. These properties will have an influence on whether a compound will

remain in the aqueous phase or interact with solid particles and get adsorbed onto sewage sludge (Drewes, 2007).

The secondary treatment of urban wastewater, which typically relies on a biological process to remove organic matter and/or nutrients with aerobic or anaerobic systems, can differ substantially among various WWTPs. Several methods are being used in modern WWTPs, but the most common method is conventional activated sludge (CAS).

The removal of antibiotics at the different stages of the conventional process mainly depends on their adsorption on the sewage sludge and their degradation or transformation during activated sludge treatment. Hydrophobic antibiotic residues are expected to occur at higher concentrations in primary sludge than hydrophilic ones because they have a greater affinity to solids and hence concentrate in the organic-rich sewage sludge (Le-Minh et al., 2010). Antibiotics can also be removed from aqueous solutions onto solid particulates by ion exchange, complex formation with metal ions and polar hydrophilic interactions (Diaz-Cruz et al., 2003). Antibiotics, adsorbed to flocs, suspended solids and activated sludge, are removed from the aqueous phase by sedimentation and subsequent disposal of excess sludge. The affinity of antibiotics adsorbed to sludge has been represented by sludge sorption constants K_d (L kg^{-1}). The higher K_d values the higher adsorption of the compounds onto sludge. However, antibiotics which are hydrophilic and highly resistant to most conventional biological treatment processes are expected to mainly remain in the aqueous phase of the treated effluent.

The main operational factors that can influence the biological removal of antibiotic residues in activated sludge systems are biochemical oxygen demand (BOD_5),

suspended solids (SS) loading, hydraulic retention time (HRT), sludge retention time (SRT), food-microorganism ratio (F/M), mixed liquor-suspended solids (MLSS), pH and temperature (Drewes, 2007). Frequently, however, these operational details are not provided in the studies available in the literature on the fate and transport of antibiotic residues during wastewater treatment. The SRT is related to the growth rate of microorganisms. High SRTs allow the enrichment of slowly growing bacteria and therefore, provide greater diversity of enzymes, some of which are capable of degrading the antibiotic compounds (Jones et al., 2007). A relationship between SRT/HRT and antibiotic removal has been reported by Le-Minh et al. (2010).

The main groups of antibiotics and their potential removal during conventional wastewater treatment are discussed in the following sections.

1.2.1.1.1 β-Lactams

β-lactams have been reported to be significantly reduced during biological processes with removals higher than 90% (Watkinson et al., 2007; Watkinson et al., 2009). Cha et al. (2006) investigated the fate of four β-lactams (ampicillin, cloxacillin, cephapirin, oxacillin) and the estimated removals were between 17-43%. Ampicillin, which was only detected in Stanley WWTP, was removed by 82% in activated sludge process. A significant removal (96%) of cephalexin from 2000 ng L^{-1} to 78.2 ng L^{-1} has been reported to occur through conventional WWTP processes in Australia (Costanzo et al., 2005). Analysis of amoxicillin conducted by Zuccato et al. (2010) in UWWTPs in Italy and Switzerland showed that is efficiently removed by conventional treatment (removal up to 90%). Similarly, Watkinson et al. (2009) showed that amoxicillin, is quite susceptible to microbial degradation and therefore is not likely to be remained in significant concentration after biological treatment

systems with removal higher than 99%. According to Li et al. (2009) some β-lactams in municipal wastewater samples in Hong Kong were removed by 30.4-100%. β-lactams were also eliminated significantly at both Shatin and Stanley WWTPs as described in the work of Li and Zhang (2011). Cephalexin was removed by 53% in activated sludge treatment at the Shatin WWTP, while it was removed by 91% in activated sludge of Stanley WWTP. Cephalexin was also removed by 36-100% in four Taiwanese WWTPs combining biological treatment and disinfection process (UV or chlorination) (Lin et al., 2009) and by 99.6% in an Australian WWTP using activated sludge process (Watkinson et al., 2009). Those reports are comparable with those in the study of Lin and Zhang (2011) indicating that cephalexin is relatively easy to be eliminated in WWTPs with biological processes whereas cefotaxime, which was only detected in Shatin WWTP was removed by 43% (Li and Zhang, 2011).

1.2.1.1.2 Macrolides

Li and Zhang (2011) reported that roxithromycin was degraded by 46% and 40% in activated sludge processes at the Shatin and Stanley WWTP, respectively. Slightly lower removal (33%) was reported in one German WWTP (Ternes et al., 2007). In the study of Göbel et al. (2007) roxithromycin was removed during primary treatment at two WWTPs in Austria by 3-9% and by 18-38% during secondary treatment. Moreover, roxithromycin removal was higher than 53% in four WWTPs in south China (Xu et al., 2007) whereas a lower removal of about 20% was observed in the study of Joss et al. (2005) in Switzerland.

Erythromycin-H_2O was degraded by 15% and 26% in activated sludge processes at Shatin and Stanley WWTP, respectively (Li and Zhang, 2011). Higher removals were

reported in other studies, that is, 56% in four Taiwanese WWTPs (Lin et al., 2009) and 43.8-100% in a WWTP in the USA (Karthikeyan and Meyer, 2006) by secondary wastewater treatment processes both employing activated sludge. Macrolides may be adsorbed to biomass via cation exchange processes due to the fact that under typical wastewater conditions, many are positively charged through the protonation of the basic dimethylamino group (pK_a > 8.9) and the surface of activated sludge is predominantly negatively charged (Le Minh et al., 2010).

1.2.1.1.3 Sulfonamides

Sulfamethoxazole was reported at concentrations as high as 5450-7910 ng L^{-1} in sewage influent in China with high removal efficiency (Peng et al., 2006). In a Taiwanese WWTP, sulfamethoxazole was detected in influent at concentration range of 500-10000 ng L^{-1} whereas the removal was 65-96% after the applied biological treatment (Yu et al., 2009). Sulfamethoxazole was removed up to 81% (initial concentration 1090 ng L^{-1}) in an American WWTP (Yang et al., 2005), 69-75% (initial concentration in the range 13-155 ng L^{-1}) (Pailler et al., 2009), 68.2-95.7% (initial concentration in the range 146-355 ng L^{-1}) (Li et al., 2009) and 93% (initial concentration in the range 3000 ng L^{-1}) (Watkinson et al., 2009). However, it was only slightly removed (20%) in another WWTP in the USA (Brown et al., 2006) and 24% in a German WWTP (Ternes et al., 2007). Sulfamethoxazole's acetylatedmetabolite, N_4-sulfamethoxazole usually accounts for more than 50% of an administered dose in human excretion and can occur in WWTP influents at concentrations 2.5-3.5 times higher than concentrations of the parent compound (Göbel et al., 2007). Significant removal efficiencies (81-96% and 94% respectively)

of N_4-acetylsulfamethoxazole during secondary treatment were reported by Göbel et al. (2007) and Joss et al. (2005).

Sulfadiazine demonstrated high removals during the activated sludge process of Shatin (100%) and Stanley (87%) WWTPs (Lin and Zhang, 2011). Xu et al. (2007) reported that 50% of sulfadiazine was removed during CAS process which was much lower compared to that observed in the study of Lin and Zhang (2011). The removal of sulfadiazine was 72.8% as reported by Li et al. (2009) and 19% during the primary treatment according to Peng et al. (2006).

Sulfamethazine was removed completely in the activated sludge process in both Shatin and Stanley WWTPs (Lin and Zhang, 2011), WWTP in USA (Karthikeyan and Meyer, 2006) and in WWTP in Korea (Choi et al., 2007). There are very few references available for comparison. Yu et al. (2009) reported a relatively lower removal of 32-85% in a WWTP in Colorado while Yang et al. (2005) reported that the concentration of this drug in the influent was 150 ng L^{-1} and in the effluent was found to be below the limit of detection (30 ng L^{-1}), achieving a removal higher than 80%. Many other sulfonamides were eliminated during conventional processes with removal efficiencies varying from <0 to 100% (Yang et al., 2005; Choi et al., 2007; Göbel et al., 2007; Watkinson et al., 2007; Spongberg et al., 2008; Pailler et al., 2009; Watkinson et al., 2009).

The variation of sulfonamides as that of all pharmaceuticals removal may possibly be explained by the differences in WWTP operating conditions such as SRT, HRT and temperature. Moreover, differences in reported removal efficiencies may, in some cases, be attributed to limitations of employed mass balance techniques. For example, short-term variations of pharmaceutical loads in influent can be significant (Göbel et

al., 2005; Khan and Ongerth, 2005), thus consideration must be taken when comparing influent and effluent concentrations. A further complexity comes from the easily reversible inter-transformation of sulfonamides into their respective metabolites (Göbel et al., 2007), leading to an underestimation of removal efficiencies if these metabolites are not considered.

1.2.1.1.4 Trimethoprim

The presence of trimethoprim can generally be correlated to that of sulfamethoxazole since the two drugs are often administered in combination (Göbel et al., 2005). Trimethoprim was removed by 42% during the activated sludge process at Stanley WWTP, and only by 13% at Shatin WWTP as reported by Lin and Zhang (2011). The removal values of trimethoprim were comparable in American (USA) WWTPs (70%, Brown et al., 2006; 50-100%, Karthikeyan and Meyer, 2006), one German WWTP (69%, Ternes et al., 2007) and one Taiwan WWTP (74%, Yu et al., 2009). Higher removal percentages were obtained in five WWTPs in Australia yielding 94% (Watkinson et al., 2009) and 93.3% (Li et al., 2009). However, the removal of trimethoprim was negligible as reported in the study of Lindberg et al. (2005) and Roberts and Thomas. (2006).

Some studies have indicated that nitrifying microorganisms appear to be capable of degrading trimethoprim. This suggests an important role for aerobic conditions for the biotransformation of trimethoprim (Pérez et al., 2005; Batt et al., 2006).

1.2.1.1.5 Quinolones

Removal efficiencies of quinolones during wastewater treatment in Sweden were reported to be 87% for norfloxacin and ciprofloxacin and 86% for ofloxacin

(Lindberg et al., 2005). A later study reported the removal of ciprofloxacin (90%), ofloxacin (56%), and norfloxacin (70%) during activated sludge treatment followed by chemical coagulation/flocculation (Zorita et al., 2009). A study by Golet et al. (2003) revealed that a conventional wastewater treatment process resulted in the removal of 88-92% of fluoronoquinolones from the aqueous phase, due to the sorption on sewage sludge. High removals of ofloxacin were achieved in WWTPs in Cyprus (>83%) (Fatta et al., 2010) and in Australia (100%) (Watkinson et al., 2009).

1.2.1.1.6 Tetracyclines

Tetracycline is one of the most frequently detected antibiotics in wastewater (Watkinson et al., 2007). According to the study of Yang et al. (2005) tetracycline was removed by 85% in a WWTP in Colorado. Tetracycline was eliminated by 24% and 36% in activated sludge processes of Shatin and Stanley WWTPs, respectively (Lin and Zhang, 2011). Higher removals were reported in two USA WWTPs (67.9-100%) (Karthikeyan and Meyer, 2006) and four Taiwanese WWTPs (66-90%) (Lin et al., 2009). The removals of chlortetracycline were 85% and 82% during the activated sludge processes at Shatin and Stanley WWTP, respectively (Lin and Zhang, 2011). Furthermore, chlorotetracycline and doxycycline have been reported after secondary treatment and chlorination with removal efficiencies of 78% and 67%, respectively (Yang et al., 2005). Choi et al. (2007) reported high removal values for minocycline and democlocycline (92 and 89%, respectively).

The pH and temperature have been reported to have an important effect on hydrolysis rates of tetracyclines and therefore it is possible that this mechanism may further contribute to the degradation of these chemicals in wastewater (Le Minh et al., 2010).

1.2.1.1.7 Others

Several studies reported the occurrence of lincosamides antibiotics such as lincomycin and clindomycin in wastewater influents and effluents with maximum removal efficiencies of 67% (Zuccato et al., 2010). A study by Watkinson et al. (2009) showed that removals of polyether ionophores (monensin and salinomycin) in wastewater were up to 95%. Limited information on the behaviour of polyether ionophores through WWTP processes is available, due to the less likely occurrence of these antibiotics in urban wastewater except where there is runoff from agricultural lands into sewers. Glycopeptides such as vancomycin was analysed by Lin and Zhang (2011) and the removal after the activated sludge process was found to be as high as 52%.

In summary, the removal efficiency of antibiotics during conventional wastewater treatment processes can be strongly variable, and in most cases incomplete. The concentrations of the antibiotics in WWTP influents and effluents vary significantly, depending on their physicochemical properties as well as the operational conditions of the biological processes employed.

1.2.2 Advanced treatment processes

Conventional wastewater treatment processes appear to be highly variable in their ability to remove most antibiotics, with performance apparently dependent upon specific operational conditions (McArdell et al., 2003; Miao et al., 2004). Accordingly, advanced treatment processes may be necessary to provide further reduction of these compounds, in order to minimise environmental and human exposure. Advanced treatment includes processes like membrane filtration, activated carbon adsorption treatment and chemical or biological oxidation processes.

Membrane filtration is pressure- or vacuum-driven separation process in which particulate matter is rejected by an engineered barrier, primarily through a size-exclusion mechanism. These processes include common membrane classifications such as microfiltration (MF, pore size range: 0.1-0.2 μm), ultrafiltration (UF, pore size range: 0.01-0.05 μm), nanofiltration (NF, pore size range: 0.001 μm) and reverse osmosis (RO, pore size range < 0.001 μm). The main rejection mechanisms are size exclusion, electrostatic interactions (attractive or repulsive) and hydrophobic interaction (diffusion and partitioning) between compounds and the membrane (Le Minh et al., 2011). These mechanisms are mostly dependent on the physicochemical properties of the compound (molecular weight cutoff (MWCO), pK_a, hydrophobicity/hydrophilicity), the solution (pH, ionic strength) and the membrane characteristics (material, surface morphology, pore size). Membrane bioreactor (MBR) process which combines membrane filtration technology with biological treatment, received considerable attention the last decades for wastewater treatment and water reuse applications.

Adsorptive treatment with activated carbon can be used for removing many hydrophobic pharmaceuticals from water (Le Minh et al., 2010). The removal

effectiveness of the activated carbon adsorptive treatment system depends mainly on the properties of the adsorbent (*e.g.* specific surface area, porosity, surface polarity and physical shape of the material) and the characteristics of the compound (*e.g.* shape, size, charge and hydrophobicity). Moreover, the sorption efficiencies of many contaminants to activated carbon may be significantly altered by the initial concentrations of the target compounds, the pH, the temperature and the presence of other species in the solution (Aksu and Tunc, 2005).

Advances in chemical water and wastewater treatment have led to a range of processes termed advanced oxidation processes (AOPs) to be developed. These processes have shown great potential in the treatment of micropollutants, either in high or in low concentrations and have found applications in the wastewater treatment field (Legrini et al., 1993; Klavarioti et al., 2009). AOPs have been studied over the past 30 years and the scientific literature surrounding their development and application is extensive.

These processes involve the use and generation of powerful transitory species, principally the hydroxyl radical ($HO^{\bullet}$) (Goslich et al., 1997; Andreozzi et al., 1999). Second to fluorine (E^0 = 3.03 V) the hydroxyl radical is the strongest known oxidant with a potential of 2.80 V. The relative strength of various oxidizing species compared to the hydroxyl radical is shown in Table 1.1. Hydroxyl radicals are powerful oxidizing agents that oxidize a broad range of organic pollutants quickly, yielding CO_2 and inorganic ions (Litter, 2005). Rate constants (k_{HO}, $r=k_{HO}\,[HO^{\bullet}]\,C$) for most reactions involving hydroxyl radicals in aqueous solution are usually on the order of 10^6-10^9 M^{-1} s^{-1} (Andreozzi et al., 1999). This property is of great importance especially in wastewater treatment because they attack non-selectively the oxidisable part of organic molecules.

Table 1.1 Redox potential of common oxidizing species.

Species	E^0 **(V, 25 ºC)***
Fluorine	3.03
Hydroxyl radical	**2.80**
Atomic oxygen	2.42
Ozone	2.07
Hydrogen peroxide	1.78
Perhydroxyl radical	1.70
Permanganate	1.68
Chlorine dioxide	1.57
Hypochlorous acid	1.49
Chlorine	1.36

(*) Redox potential referred to normal hydrogen electrode (NHE).

The versatility of the AOPs is enhanced by the fact there are different ways of producing hydroxyl radicals, facilitating compliance with the specific treatment requirements. Table 1.2 lists those AOPs that have been developed so far and whilst the list is not comprehensive it does highlight the range and variety of the main processes developed which have applications in water and wastewater treatment. The most common AOPs that have been used and evaluated (mainly at a bench scale but many of the processes are being developed at a pilot scale) are: photolysis under ultraviolet (UV) irradiation; combinations of hydrogen peroxide (H_2O_2), ozone (O_3) and UV irradiation; homogeneous photocatalysis with Fenton reagent and heterogeneous photocatalysis with semiconductor materials (*e.g.* TiO_2).

Table 1.2 AOPs used for water and wastewater treatment (*italicized* processes are covered in the following sections).

AOP	Key reactions	Fundamentals
UV	$R\text{-}R + h\nu \rightarrow R\text{-}R^* \rightarrow 2R^\bullet$ $R\text{-}R^* + O_2 \rightarrow R\text{-}R^{\bullet+} + O_2^{\bullet-}$ $^3DOM^* + {}^3O_2 \rightarrow DOM + {}^1O_2$	▪ Direct irradiation leads to the promotion of a molecule from the fundamental state to an excited singlet state. The formed radicals initiate chain reactions; for example the carbon-centered radicals ($R^\bullet$) react with dissolved oxygen leading to peroxyl ($RO_2^\bullet$) and oxy ($RO^\bullet$) radicals. ▪ Photolysis (indirect or sensitised) may be favoured in the presence of naturally occurring substances in the system (*e.g.* DOM) which can act as photosensitizers which generate strong reactive agents *e.g.* singlet oxygen ($^1O_2$), hydroxyl radicals ($HO^\bullet$). ▪ Disadvantages: UV irradiation with lamps is expensive.
UV/H_2O_2	$H_2O_2 + h\nu \rightarrow HO^\bullet + HO^\bullet$ $HO^\bullet + H_2O_2 \rightarrow HO_2^\bullet + H_2O$ $HO_2^\bullet + H_2O_2 \rightarrow HO^\bullet + H_2O + O_2$	▪ Hydroxyl radicals are formed through the photolytic cleavage of H_2O_2. ▪ High concentration of H_2O_2 scavenges the radicals, making the process less effective. ▪ Disadvantages: low radical formation through low molar extinction coefficient of H_2O_2 (18.7 mol cm^{-1} at 254 nm).
O_3	$O_3 + R \rightarrow R_{ox}$ $2O_3 + 2H_2O \rightarrow 2HO^\bullet + O_2 + 2HO_2^\bullet$	▪ In the absence of light, ozone can react directly with an organic substrate (R), through a slow and selective reaction, or through a fast and non-selective radical reaction that produces hydroxyl radicals. ▪ Disadvantages: low solubility of O_3 in water, O_3 is selective, formation of by-products (bromates), elevated costs.
H_2O_2/O_3	$O_3 + H_2O_2 \rightarrow HO^\bullet + O_2 + 2HO_2^\bullet$	▪ H_2O_2 initiates O_3 decomposition by electron transfer ▪ Disadvantages: additional cost of H_2O_2
UV/O_3	$O_3 + h\nu + H_2O \rightarrow H_2O_2 + O_2$ $O_3 + h\nu \rightarrow O_2 + O(^1D)$ $O(^1D) + H_2O \rightarrow 2\,HO^\bullet$	▪ The generated hydrogen peroxide is photolyzed (see UV/H_2O_2 process), generating hydroxyl radicals, and also reacts with the excess of ozone. ▪ If $\lambda < 300$ nm, photolysis of O_3 takes place, generating additional hydroxyl radicals and other oxidants, with a subsequent increase in the efficiency. ▪ Disadvantages: high operating costs
UV/H_2O_2/O_3	$O_3 + H_2O_2 + h\nu \rightarrow O_2 + HO^\bullet + HO_2^\bullet$	▪ The addition of light to the H_2O_2/O_3 process produces a net increase in the efficiency through the additional generation of hydroxyl radicals. ▪ Disadvantages: elevated costs
UV/TiO_2	$TiO_2 + h\nu \rightarrow TiO_2\,(e_{CB}^- + h_{VB}^+)$ $HO^- + h_{VB}^+ \rightarrow HO^\bullet$ $O_2 + e_{CB}^- \rightarrow O_2^{\bullet-}$	▪ When a particle of semiconductor excited by light of energy higher than that of the band gap, electron-hole pairs are formed. ▪ The valence holes (h_{VB}^+) are strong oxidants and are able to oxidize various contaminants, as well as water, resulting in the formation of hydroxyl radicals while the conduction band electrons (e_{CB}^-) are good reductants reducing the dissolved

		oxygen to $O_2^{\bullet-}$. ▪ Disadvantages: low quantum yield, catalyst removal and regeneration.
Fenton	$Fe^{2+} + H_2O_2 \rightarrow Fe^{3+} + HO^- + HO^{\bullet}$	▪ The Fenton process (or dark Fenton) involves the use of H_2O_2 and a catalyst, usually iron (in the form of ferrous or ferric ions) in acidic medium. ▪ Fe^{2+} oxidation leads to the formation of hydroxyl radicals. ▪ Disadvantages: low pH (2.8-3.0) and requirement for iron removal.
Photo-Fenton	$Fe^{2+} + H_2O_2 \rightarrow Fe^{3+} + HO^- + HO^{\bullet}$ $Fe^{3+} + H_2O \rightarrow Fe^{2+} + H^+ + HO^{\bullet}$	▪ The photo-Fenton process involves irradiation with sunlight or from an artificial light source. In the presence of light the process can be made more efficient, by photoreducing the Fe^{3+} to Fe^{2+}, and the generation of additional hydroxyl radicals. ▪ Disadvantages: low pH (2.8-3.0) and requirement for iron removal.
Electro-Fenton	$Fe^{3+} + e^- \rightarrow Fe^{2+}$ $O_2 + 2H^+ + 2e^- \rightarrow H_2O_2$	▪ There are two main types of Fenton process involving the use of electrochemically produced reagents. ▪ In cathodic process the iron is added as a Fe^{2+} (or Fe^{3+}) salt. The source of H_2O_2 may be either via direct H_2O_2 addition or it may be produced by reduction of oxygen at the cathode. ▪ In anodic Fenton process the source of the iron is a sacrificial iron anode. ▪ Disadvantages: elevated costs, requirement for high iron concentration (g L^{-1}).
Sonolysis	$H_2O \rightarrow H^{\bullet} + HO^{\bullet}$	▪ The sonochemical degradation in aqueous phase involves several reaction pathways and zones such as pyrolysis inside the bubble and/or at the bubble-liquid interface and hydroxyl radical-mediated reactions at the bubble-liquid interface and/or in the liquid bulk. ▪ Pyrolytic reactions inside or near the bubble as well as solution radical chemistry are the two major pathways of sonochemical degradation. ▪ Disadvantages: high operational cost
Wet air oxidation (WAO)	*Substrate* + $O_2 \rightarrow$ *Degradation products*	▪ WAO is defined as the oxidation of substances in an aqueous solution by means of oxygen or air at elevated temperatures and pressures (T=100-372 ^oC; P=20-200 bar). ▪ Disadvantages: high operational cost
References: Herrmann et al., 1993; Legrini et al., 1993; Goslich et al., 1997; Arslan and Balcioglu, 1999; Huston and Pignatello, 1999; Mantzavinos et al., 1999; Andreozzi et al., 2003; Balcioglu and Otker, 2003; Sakthivel et al., 2003; Parsons, 2004; Litter, 2005; Bautitz and Nogueira, 2007; Esplugas et al., 2007; Klavarioti et al., 2009; Malato et al., 2009; Naddeo et al., 2009; Ikehata et al., 2010; Le-Minh et al., 2010.		

A detailed description of the aforementioned AOPs is beyond the scope of this study. The research of the work focus lies on the two AOPs which can be conducted under solar irradiation, which are the homogeneous photocatalysis with Fenton reagent and the heterogeneous photocatalysis with TiO_2. Their process fundamentals and mechanisms are described thoroughly in the next sections.

1.2.2.1 Homogeneous photocatalysis with Fenton reagent

Fenton reagent was discovered about a century ago, but its application as an oxidizing process for destroying toxic organic compounds was not applied until the late 1960s (Neyens and Baeyens, 2003). The Fenton reagent refers to a mixture of hydrogen peroxide and ferrous (or ferric) salts, which is an effective oxidant of a large variety of organic substrates (Goldstein et al., 1993).

Fenton's reagent oxidation is a homogeneous oxidation process and is considered to be a metal-catalyzed oxidation reaction, in which iron acts as the catalyst (Tekin et al., 2006; Saritha et al., 2007). The chain reactions that take place in the process produce a range of free radicals, including the highly reactive and non-selective hydroxyl radicals, which are capable to react with a wide range of organic compounds in water matrices and cause their chemical decomposition (Lucas and Peres, 2006).

The renewed interest of researchers for this classic, old reactive system, discovered by Fenton (Fenton, 1894), is today underlined by a significant number of investigations devoted to its application in water and wastewater treatment (Andreozzi et al., 1999). In the recent years, the Fenton process has been extensively used with success for the oxidation of many classes of organic compounds (pesticides (Lin et al., 2004; Lapertot et al., 2006); chlorophenols (Liang et al., 2007; Kuo and Wu, 2010); phenols (Kavitha and Palanivelu, 2004; Zazo et al., 2009); dye pollutants (Garcia-Montano et

al., 2006; Nunez et al., 2007), pharmaceuticals (Mendez-Arriaga et al., 2010; Perez-Estrada et al., 2005), etc.) due to its high efficiency to generate hydroxyl radicals during decomposition of H_2O_2 by Fe^{2+} in acidic medium (Muruganandham and Swaminathan, 2004).

This reagent is an attractive oxidative system for the wastewater treatment due to the fact that iron is abundant (and may be naturally occurring in the system being treated) and is a non-toxic element (Andreozzi et al., 1999). Moreover, hydrogen peroxide is easy to transport and handle, as well as being environmentally safe (Parsons, 2004). The Fenton reaction offers the possibility to be driven under solar irradiation (photo-Fenton) and therefore becoming a cost-effective process (Pérez et al., 2002; Garcia-Montano et al., 2006). Moreover, the depth of light penetration is high and the contact between the pollutant and the oxidizing agent is close, since the process is homogenous (Evgenidou et al., 2007). The design of reactors for the technological application of Fenton process is rather simple (Litter, 2005). Fenton's oxidation can also be an effective pretreatment step by transforming organic constituents to by-products that are more readily biodegradable and reducing the overall toxicity to microorganisms in the downstream biological treatment processes (Miller et al., 1996).

The main disadvantages of the process are the low pH values (2.8-3.0) which are required, since iron precipitates at higher pH and the final separation of soluble iron species from the treated water in order to recover the metal and comply with the regulatory limits for aqueous effluent discharge (Melero et al., 2007; Santos et al., 2007).

The use of Fenton reaction for the degradation of organic contaminants has received extensive attention but the mechanisms and the key intermediates in the Fenton chemistry are still under intense and controversial discussion.

1.2.2.1.1 Chemical fundamentals

The most abundant iron species in an aqueous solution are ferrous (Fe^{2+}) and ferric iron (Fe^{3+}). Fe^{2+} and Fe^{3+} may exist in the form of a range of hydrolysis species or other inorganic complexes depending on the pH, the concentration of iron and the concentration of inorganic ligands (Malato et al., 2009). In the absence of other complexing substances, iron is complexed by water and hydroxyl ligands. In this case, the number of the hydroxyl ligands depends strongly on the pH of the solution, which influences directly the acid/base equilibrium of the aquo complex. Ferric iron is the more critical iron species in the Fenton process, because its hydroxides precipitate at lower pH than those of ferrous iron. It is crucial to understand the hydrolytic speciation of Fe^{3+} species in order to accurately interpret their absorption spectra and photochemical behavior.

The pH-dependent hydrolytic speciation of Fe^{3+} can be represented by the following iron aquo complexes (eqs. (1.1)-(1.4)) (Faust et al., 1990; Buda et al., 2001). Figure 1.2 illustrates the equilibrium concentrations of the ferric iron complexes in aqueous solution at different pH and at constant ferric iron concentration (20 mg L^{-1}).

$$[Fe(H_2O)_6]^{3+} \leftrightarrow [Fe(H_2O)_5(OH)]^{2+} + H^+ \quad (1.1)$$

$$[Fe(H_2O)_5(OH)]^{2+} \leftrightarrow [Fe(H_2O)_4(OH)_2]^{+} + H^+ \quad (1.2)$$

$$[Fe(H_2O)_4(OH)_2]^{3+} \leftrightarrow [Fe(H_2O)_3(OH)_3] + H^+ \quad (1.3)$$

$$2Fe_{aq}^{3+} \leftrightarrow [Fe_2(OH)_2]^{4+} + 2H^+ \quad (1.4)$$

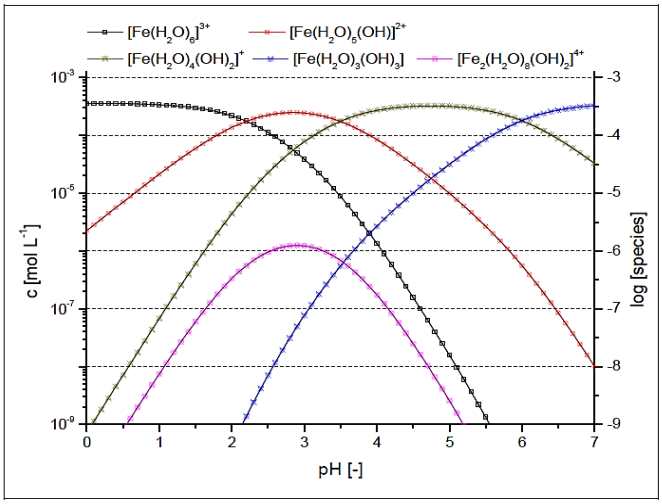

Source: *Malato et al. (2009)*

Figure 1.2 Ferric (Fe^{3+}) iron species present in aqueous solution at different pH at a concentration of 20 mg L^{-1}, calculated with equilibrium constants provided by (Flynn, 1984) at T=20 ^{o}C.

As shown in Figure 1.2, $[Fe(H_2O)_5(OH)]^{2+}$ (data in red color) is the dominant monomeric Fe^{3+}-hydroxy complex species between pH 2.5 and 3.0. At pH < 2.0 the ferric ions form $[Fe(H_2O)_6]^{3+}$ which at higher pH this complex undergoes hydrolysis and subsequent precipitation. The precipitation process starts at pH=2.5-3.5 with the formation of dimers and oligomeres, which gradually polymerise further and lose water until forming finally insoluble iron hydroxides.

1.2.2.1.2 Fenton reactions and mechanisms

Two reaction pathways for the Fenton system have been proposed; a radical pathway, which considers a hydroxyl radical ($HO^{\bullet}$) production and a non-radical pathway considering ferryl ion (Fe^{4+}) production.

In 1894, Henry Fenton discovered that in the presence of low concentrations of ferrous salts and hydrogen peroxide, tartaric acid was oxidized to dihydroxy maleic acid (Fenton, 1894). Later, he has shown that some other hydroxy acids were also oxidized in the presence of this reagent (Fenton, 1899). Two years after Fenton's death the hydroxyl radical mechanism was mentioned for the first time in 1931 by Haber and Willstätter in a paper on radical chain mechanisms (Haber and Willstätter, 1931). They suggested that the hydroxyl radicals could be produced by one-electron reduction of H_2O_2 to $HO_2^{\bullet}$ (today known as a very slow reaction in the absence of catalytic redox cycling metals) and that the hydroxyl radicals could abstract hydrogen from a carbon-hydrogen bond and initiate radical chain reactions.

Haber and Weiss (1934) proposed that during the decomposition of hydrogen peroxide, catalyzed by iron salts, hydroxyl radical is formed as an active intermediate via the oxidation of ferrous ion by hydrogen peroxide. Fenton reaction (eqn. (1.5)) was first reported by Haber and Weiss (1934) (although Fenton never wrote it) and involves the reaction between the dissolved ferrous iron and hydrogen peroxide in acidic aqueous solution which leads to the oxidation of Fe^{2+} to Fe^{3+} and the subsequent formation of hydroxyl radicals ($HO^{\bullet}$). This reaction is spontaneous and can occur in the absence of light (Parsons, 2004).

$$Fe^{2+} + H_2O_2 \rightarrow Fe^{3+} + HO^- + HO^{\bullet} \qquad (1.5)$$

The formation of hydroxyl radical was confirmed by Baxendale et al. (1946), showing that the Fenton reagent initiates and catalyzes the polymerization of olefins via the addition of hydroxyl radicals to the double bond. The fact that in many systems this reagent was an efficient hydroxylating agent supported the formation of hydroxyl radicals as reactive intermediates (Merz et al., 1947). The original mechanism of Haber and Weiss has been subsequently modified by Barb et al. (1951) and Walling

(1975). The Fenton reaction initiates the chain reaction (eqn. (1.5)) which is then followed by chain reactions (eqs. (1.6) and (1.7)) while the chain termination is caused by the reaction in eqn. (1.8) (Neyens and Baeyens, 2003).

$$HO^{\bullet} + H_2O_2 \rightarrow H_2O + O_2^{\bullet-} + H^+ \quad (1.6)$$

$$O_2^{\bullet-} + H^+ + H_2O_2 \rightarrow O_2 + HO^{\bullet} + H_2O \quad (1.7)$$

$$Fe^{2+} + HO^{\bullet} + H^+ \rightarrow Fe^{3+} + H_2O \quad (1.8)$$

Moreover, the formed ferric ions may catalyse hydrogen peroxide, which is decomposed into water and oxygen (eqs. (1.9)-(1.14)). The reactions of hydrogen peroxide with ferric ions are referred to as Fenton-like reactions.

$$Fe^{3+} + H_2O_2 \rightarrow Fe\text{-}OOH^{2+} + H^+ \quad (1.9)$$

$$Fe\text{-}OOH^{2+} \rightarrow HO_2^{\bullet} + Fe^{2+} \quad (1.10)$$

$$HO_2^{\bullet} + Fe^{2+} \rightarrow HO_2^- + Fe^{3+} \quad (1.11)$$

$$HO_2^{\bullet} + Fe^{3+} \rightarrow O_2 + Fe^{2+} + H^+ \quad (1.12)$$

$$Fe\text{-}OOH^{2+} \rightarrow HO_2^{\bullet} + Fe^{2+} \quad (1.13)$$

$$HO^{\bullet} + H_2O_2 \rightarrow HO_2^{\bullet} + H_2O \quad (1.14)$$

Some studies suggested that the classical Fenton reaction occurs using Fe^{2+} as an electron donor to H_2O_2. Such would be an outer sphere electron transfer reaction with no direct bonding interactions between the electron donor and the acceptor, (Mechanism I, Schematic 1.2). However, the outer sphere mechanism is thermodynamically unfavorable and unlikely to occur (Parsons, 2004).

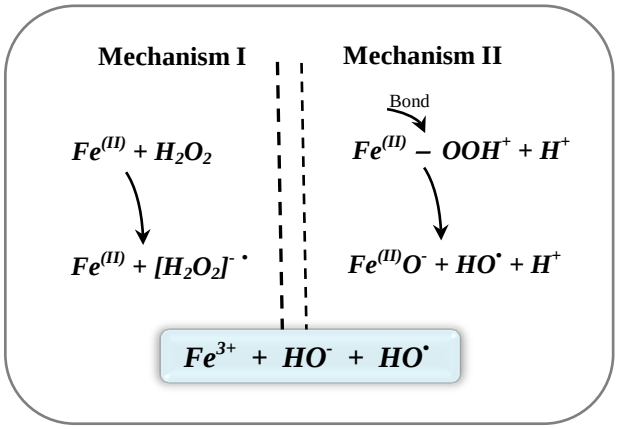

Schematic 1.2 Basic reactions and intermediates involved in the classic Fenton process (Fentona et al., 2009).

On the other hand, recent studies have shown and favored the inner sphere electron transfer mechanisms, which involve direct bonding between the iron and the hydrogen peroxide. This interaction can produce an iron-peroxo complex, $Fe–OOH^+$ which may react further to generate hydroxyl radicals (one-electron oxidant) (Mechanism II, Schematic 1.2) (Fentona et al., 2009).

There have also been suggestions that a ferrous peroxide complex ($[Fe^{2+}. H_2O_2]$) may be involved in the oxidation reaction of Fe^{2+} and H_2O_2 with a subsequent formation of a highly reactive iron-oxo complex such as the ferryl ion (Fe^{4+}) species, FeO^{2+} (Bray and Gorin, 1932, Kremer et al., 1999). Bray and Gorin (1932) were the first to propose ferryl ion as the active intermediate in the Fenton chemistry according to the eqs. (1.15) and (1.16).

$$Fe^{2+} + H_2O_2 \rightarrow FeO^{2+} + H_2O \quad (1.15)$$

$$FeO^{2+} + H_2O_2 \rightarrow Fe^{2+} + H_2O + O_2 \quad (1.16)$$

Schematic 1.3 demonstrates the Fenton mechanism proposed by Kremer (1999). This mechanism involves the formation of $[FeOFe]^{5+}$ species and the FeO^{2+} is considered to be the active oxidizing species rather than the hydroxyl radical. The FeO^{2+} species can react either with Fe^{2+} ions to produce Fe^{3+} (k_5) or with H_2O_2 to produce O_2 (k_4). FeO^{2+} can further react with Fe^{3+} and form a binuclear species $[FeOFe]^{5+}$ (k_6). This species can react with H_2O_2 to produce O_2 (k_8) or to decompose back to FeO^{2+} and Fe^{3+} (k_7).

Kremer (1999) concluded that it is difficult to accept the existence of the radical mechanism because this mechanism either in the formulation of Haber and Weiss or in that of Barb et al. (1951), recognizes only Fe^{2+} and Fe^{3+} as the forms of iron in the system.

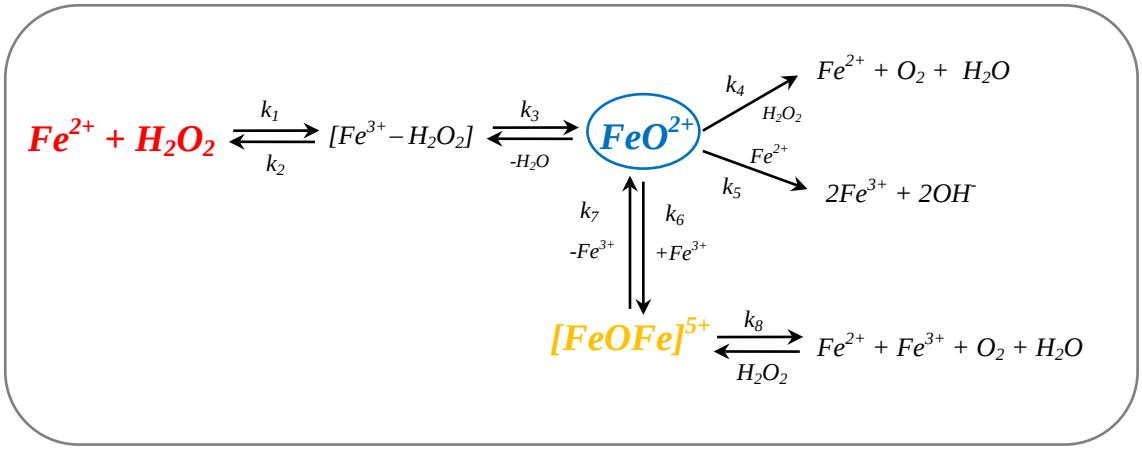

Schematic 1.3 Mechanism of Fenton reaction (Kremer, 1999).

The mechanisms of Fenton reactions are still poorly understood and there is much disagreement in the literature on the exact intermediates they form including whether or not the hydroxyl radical itself forms (Dunford, 2002).The discussion about the mechanism of Fenton reaction is still on-going and the occurrence of ferryl iron (Fe^{4+}) has been proposed by several authors (Buda et al., 2001; Ensing et al., 2002).

The set of the main consecutive reactions in the Fe^{2+}/H_2O_2 system (Table 1.3) that is regarded as generally accepted has been proposed by many research groups, one example being Sychev and Isak (1995). The table includes only reactions taking place between the species in eqn. (1.5) and excludes other species that may be present in the solution.

Table 1.3 Rate constants for the elementary reactions of ferrous iron (Fe^{2+}), ferric iron (Fe^{3+}) and hydrogen peroxide (H_2O_2) in the absence of other interfering ions and organic substances (Sychev and Isak, 1995).

Reaction	**Rate constants (*k*)***
$Fe^{2+} + H_2O_2 \rightarrow Fe^{3+} + HO^- + HO^\bullet$	53-76
$Fe^{2+} + HO^\bullet \rightarrow Fe^{3+} + HO^-$	$2.6\text{-}5.1\ 10^8$
$Fe^{2+} + HO_2^\bullet \rightarrow Fe^{3+} + HO_2^-$	$0.72\text{-}1.5\ 10^6$
$Fe^{3+} + H_2O_2 \rightarrow Fe^{2+} + H^+ + HO_2^\bullet$	$1\text{-}2\ 10^{-2}$
$Fe^{3+} + HO_2^\bullet \rightarrow Fe^{2+} + O_2 + H^+$	$0.33\text{-}2.1\ 10^6$
$Fe^{3+} + O_2^{\bullet-} \rightarrow Fe^{2+} + O_2$	$0.05\text{-}1.9\ 10^9$
$H_2O_2 + HO^\bullet \rightarrow H_2O + HO_2^\bullet$	$1.7\text{-}4.5\ 10^7$

* The rate constants are expressed in L mol^{-1} s^{-1} (M^{-1} s^{-1}).

It should be mentioned that since the reduction of ferric iron is generally much slower than the oxidation of ferrous iron, iron exists mainly in the ferric (Fe^{3+}) form (Pignatello, 1992; Neyens and Baeyens, 2003). The regeneration of ferrous iron from ferric iron is the rate limiting step in the catalytic iron cycle during the Fenton process.

In the presence of organic substrates (such as in the case of wastewater matrices where various organic pollutants exist), the reaction pathways are more complicated as the organic substrates (*R*) react with various ways with the generated hydroxyl radicals yielding organic radicals ($R^{\bullet}$) (Malato et al., 2009). Some reactions (*e.g.* hydrogen abstraction, electrophilic addition to organic π-systems) of the Fenton reagent with organic substrates have been proposed by Legrini et al. (1993).

Several reactions can take place with the generated organic radicals (eqs. (1.17)-(1.23)). The reaction of organic radicals with dissolved oxygen (eqs. (1.22)-(1.23)), known as Dorfman-mechanism, is of special interest because the formed peroxyl radical ($RO_2^{\bullet}$) can regenerate hydrogen peroxide (by reaction in eqn. (1.11) and (1.18)) and thereby contribute to reduce the consumption of oxidant in wastewater treatment by Fenton process.

$$R^{\bullet} + Fe^{3+} \rightarrow R^{+} + Fe^{2+} \quad (1.17)$$

$$R^{\bullet} + Fe^{2+} \rightarrow R^{-} + Fe^{3+} \quad (1.18)$$

$$R^{\bullet} + R^{\bullet} \rightarrow R\text{-}R \quad (1.19)$$

$$R^{\bullet} + HO_2^{\bullet} \rightarrow RO_2H \quad (1.20)$$

$$Fe^{2+} + RO_2H \rightarrow Fe^{3+} + OH^{-} + OR^{\bullet} \quad (1.21)$$

$$R^{\bullet} + O_2 \rightarrow RO_2^{\bullet} \quad (1.22)$$

$$RO_2^{\bullet} + H_2O \rightarrow ROH + HO_2^{\bullet} \quad (1.23)$$

The Fenton process can be made more efficient in the presence of light, by photoreducing the ferric iron to ferrous iron, and the generation of additional hydroxyl radicals (eqn. (1.24)). The combined process is known as the photo-Fenton (or photo-assisted) reaction (Huston and Pignatello, 1999). Schematic representation of the

photo-Fenton process, where it is evidence that the light increases the catalytic iron cycle and the formation of hydroxyl radicals, is illustrated in Schematic 1.4.

$$Fe^{3+} + H_2O + h\nu \rightarrow Fe^{2+} + H^+ + HO^{\bullet} \quad (1.24)$$

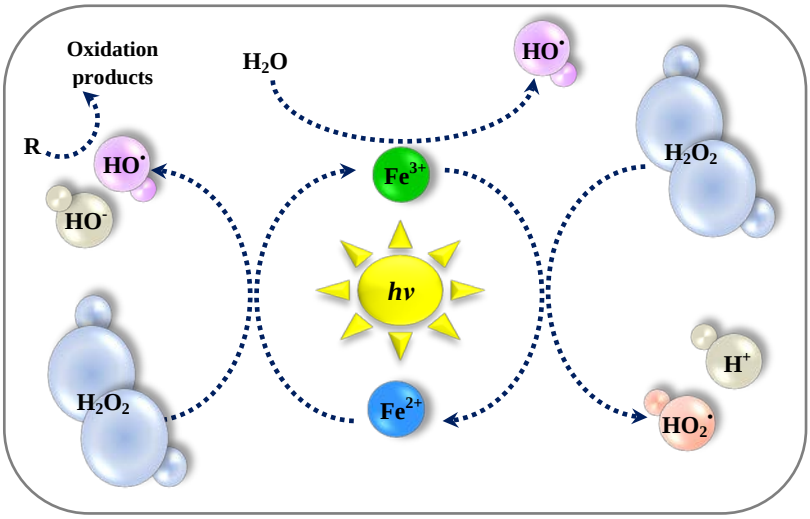

Schematic 1.4 Representation of the main photo-Fenton reactions.

The quantum yield of ferrous iron production in eqn. (1.24) is relatively low and has been estimated by Faust and Hoigne (1990) to be $\Phi_{Fe(II)}$=0.14 at 313 nm. Dissolved ferric iron undergoes ligand-to-metal charge-transfer (LMCT) reactions in the excited state. As a consequence iron complexes are formed with the ligand (*L*) being any Lewis base able to form a complex with ferric iron (*e.g.* OH^-, H_2O, HO_2^-, Cl^-, etc.). The product may be a hydroxyl radical such as in eqs. (1.26) and (1.27) or another radical derivated from the ligand.

$$[Fe^{3+}L] + h\nu \rightarrow [Fe^{3+}L]^{\bullet} \rightarrow Fe^{2+} + L^{\bullet} \quad (1.25)$$

$$[Fe(H_2O)]^{3+} + h\nu \rightarrow Fe^{2+} + HO^{\bullet} + H^+ \quad (1.26)$$

$$[Fe(OH)]^{2+} + h\nu \rightarrow Fe^{2+} + HO^{\bullet} \quad (1.27)$$

The quantum yield of the ferric reduction reaction can increase when ferrous iron is complexed with organic ligands such as carboxylic acid anion (*e.g.* oxalate).

A pH range of 2.8-3.0 is frequently postulated as the optimum operating condition for the Fenton process, to avoid the formation and subsequent precipitation of iron hydroxides. Additionally, at this pH range the predominant species is the $[Fe(H_2O)_5(OH)]^{2+}$ which is able to undergo excitation yielding hydroxyl radicals (Larson et al., 1991; Ciesla et al., 2004):

$$[Fe(H_2O)_5(OH)]^{2+} + H_2O + h\nu \rightarrow [Fe(H_2O)_6]^{2+} + HO^{\bullet} \qquad (1.28)$$

The capacity of the Fenton and photo-Fenton systems to degrade a great variety of toxic and non-biodegradable organic pollutants in various water matrices is affected by several operating parameters, such as hydrogen peroxide and iron concentrations, solar irradiation, pH, initial concentration of the substrate, temperature and solution salinity. The effect of these parameters is discussed in the next chapters.

1.2.2.2 Heterogeneous photocatalysis with TiO_2 suspensions

1.2.2.2.1 Chemical fundamentals

In a heterogeneous photocatalytic system, photo-induced molecular transformations or reactions take place at the surface of a catalyst, normally a wide-band semiconductor (Linsebigler et al., 1995). Photocatalytic reactions on semiconductor powders have attracted much attention because of their applicability to the treatment of a variety of pollutants and utilization of solar energy (Hoffmann et al., 1995).

The electronic structure of a semiconductor material comprises a highest occupied band full of electrons called the valence band (VB) and a lowest unoccupied band

called the conduction band (CB). These bands are separated by a region that is largely devoid of energy levels and the difference in energy between the two bands is called the bandgap energy, E_{bg} (Parsons, 2004). The ability of a semiconductor to undergo photo-induced electron transfer to adsorbed species on its surface is governed by the band energy positions of the semiconductor and the redox potentials of the adsorbed substrate.

Ultra-bandgap illumination of the semiconductor leads to the formation of electron-hole pairs ($e_{CB}^{-} - h_{VB}^{+}$) which can migrate on the surface of the catalyst and participate in redox reactions with the compounds that are adsorbed on the catalyst's surface (Herrmann et al., 1993; Schiavello et al., 1993; Robertson et al., 1996). In competition with charge transfer to adsorbed species is the electron and hole recombination. Recombination of the separated electron and hole can occur in the volume of the semiconductor particle or on the surface with the release of thermal energy.

The valence holes are strong oxidants (E^0=1.0-3.5 V) and can migrate to the catalyst's surface where an electron from a donor (*D*) can combine with the surface hole oxidizing the donor species and subsequent resulting in the formation of hydroxyl radicals. Similarly, the conduction band electrons are good reductants (E^0=-1.5-0.5 V) and can react with electron acceptors (*A*) adsorbed on the surface (Munter et al., 2001). The probability and rate of the charge transfer processes for electrons and holes depends upon the respective positions of the band edges for the conduction and valence bands and the redox potential levels of the adsorbed species. The overall reactions can be summarized as follows while a schematic representation of the mechanisms associated with the process are illustrated in Schematic 1.5.

$$TiO_2 + h\nu \rightarrow e_{CB}^- + h_{VB}^+ \quad (1.29)$$

$$A + h_{VB}^+ \rightarrow A^{\bullet -} \quad (1.30)$$

$$D + e_{CB}^- \rightarrow D^{\bullet +} \quad (1.31)$$

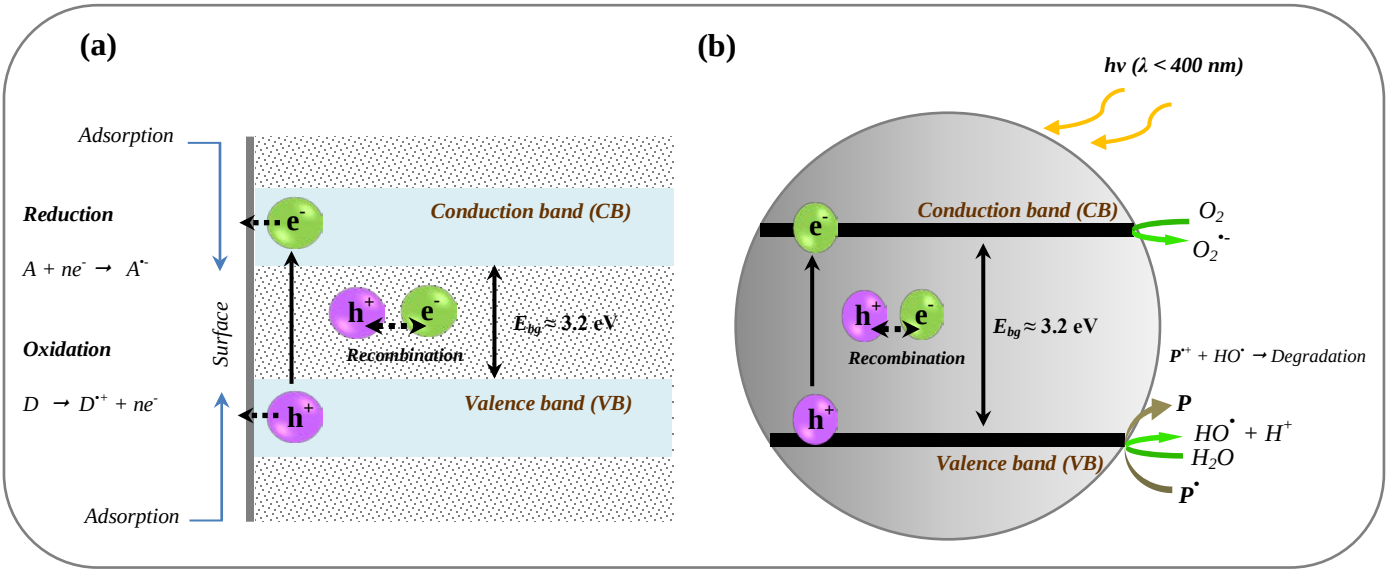

Schematic 1.5 (a) Energy band diagram and fate of electrons and holes in a semiconductor particle (Herrmann et al., 2010); and (b) Commonly adopted but misleading energy band diagram.

Normally, in environmental applications, the photocatalytic process takes place in aerobic environments; therefore the electron acceptor (A) is the dissolved oxygen yielding the superoxide radical anion ($O_2^{\bullet -}$) and the electron donor (D) is particular the water or hydroxyl anions (HO^-) generating hydroxyl radicals and/or other radicals. It appears from the literature that the rate-determining step in the overall photocatalytic process is the reduction of dissolved oxygen by the photogenerated electrons (eqn. (1.34)).

$$HO^- + h_{VB}^+ \rightarrow HO^\bullet \quad (1.32)$$

$$H_2O + h_{VB}^+ \rightarrow HO^\bullet + H^+ \quad (1.33)$$

$$O_2 + e_{CB}^- \rightarrow O_2^{\bullet-} \quad (1.34)$$

$$O_2^{\bullet-} + H^+ \rightarrow HO_2^\bullet \quad (1.35)$$

$$2HO_2^\bullet \rightarrow H_2O_2 + O_2 \quad (1.36)$$

It is worthwhile to point out, however, that the until recently widely-used schematic associated with the semiconductor photocatalysis can be considered a bit misleading since it indicates that the photo-excited species formed at the surface escape from this surface to react in the ambient liquid phase. A revised schematic representation was recently proposed, and critically discussed and explained thoroughly by Hermann et al. (2010).

Among the various semiconductors which have been so far tested, titanium dioxide (TiO_2) has generally been demonstrated to be the most active. It seems to possess the most interesting features, such as high chemical stability in a wide pH range, strong resistance to chemical breakdown and photocorrosion, commercial availability and good performance. The catalyst is also cheap, innocuous and can be reused (Andreozzi et al., 1999; Malato et al., 2009).

Two different crystal structures of TiO_2, rutile and anatase, are commonly used in photocatalysis, with anatase showing a higher photocatalytic activity (Abellan et al., 2009). The structure of rutile and anatase can be described in terms of chains of TiO_6 octahedra. The two crystal structures differ by the distortion of each octahedron and by the assembly pattern of the octahedra chains (Linsebigler et al., 1995). The structures differences cause different mass densities and electronic band structures between the two forms of TiO_2 (Ohno et al., 2001).

Although there are many different sources of TiO_2, Aeroxide® TiO_2 P25 has effectively become a standard catalyst in the field of photocatalytic reactions because it has (i) a reasonably well defined nature (70:30 anatase:rutile mixture, non-porous, BET surface area 55±15 m^2 g^{-1}, average particle size 30 nm) and (ii) a substantially higher photocatalytic activity than most other commercial available TiO_2 products (Serpone et al., 1996; Malato et al., 2009). TiO_2 has a large bandgab energy ($E_{bg} \approx$ 3.0-3.2 eV) and is only able however to absorb ultraviolet irradiation (typically $\lambda <$ 380 nm).

1.2.2.3 Removal of antibiotics from wastewater effluents through other advanced treatment processes

1.2.2.3.1 Membrane filtration and membrane bioreactor treatment

From the results presented in Table A2 (Annex), membrane filtration treatment appears to be a process that is more effective than CAS process in removing most antibiotics from wastewaters. Various studies showed up to 90% removal of several antibiotics including quinolones, sulfonamides, tetracyclines and trimethoprim (Kimura et al., 2004; Morse and Jackson, 2004; Sahar et al., 2010). A study undertaken by Kosutic et al. (2007) on the treatment of model wastewater of a manufacturing plant producing pharmaceuticals for veterinary use showed that sulfonamides were effectively removed by NF and RO. Zhang et al. (2006) reported a high removal (98.5-99.7%) of amoxicillin from wastewater which contains high level of TOC using RO. In a study of Li et al. (2004) oxytetracycline at very high concentration (1000 mg L^{-1}) in wastewater from pharmaceutical manufacturing was reduced to 80 mg L^{-1} (< 92% removal). Clara et al. (2005) also reported removals

between 50-60% of roxithromycin during ultrafiltration treatment combined with membrane bioreactor (MBR).

Some investigations reveal that the fouling of membranes can also lead to improved rejection of many solutes (Schafer et al., 1994; Drewes et al., 2006; Xu et al., 2006). This interesting observation is believed to be due to increased negative surface charge leading to increased electrostatic rejection of ionic species; along with simultaneously increased adsorptive capacity for non-ionic solutes (Xu et al., 2006).

1.2.2.3.2 Activated carbon adsorption treatment

In wastewater treatment, some studies on the removal of antibiotics by activated carbon have been reported (Adams et al., 2002; Westerhoff et al., 2005; Putra et al., 2009; Rivera-Utrilla et al., 2009). With dosages between 10 mg L^{-1} and 20 mg L^{-1} of powdered activated carbon, the concentrations of several antibiotics in wastewater have been reduced by 49-99% after 4 h contact time (Adams et al., 2002; Westerhoff et al., 2005). Putra et al. (2009) compared the adsorption capacity of activated carbon and bentonite, using amoxicillin and reported that 94.67% of amoxicillin was removed from wastewater using activated carbon at a dose as high as 1.5 g $(50\ mL)^{-1}$.

1.2.2.3.3 Direct photolysis

Direct photolytic process, especially under ultraviolet irradiation (UV), has been widely used for the treatment of waters and wastewaters worldwide. Several studies have reported the effective treatment of UV irradiation for removal of antibiotics in wastewater effluents (Adams et al., 2002; Ryan et al., 2011; Yuan et al., 2011). It has been recently reported that at high UV doses of nearly 11000-30000 mJ cm^2, an almost complete removal of tetracyclines and ciprofloxacin was achieved (Yuan et al.,

2011). Kim et al. (2009) reported that sulfonamides (sulfamethoxazole and sulfadimethoxine) and quinolones (norfloxacin and nalidixic acid) showed a quite high removal efficiency in the range of 86-100% during the UV process. In contrast to this, macrolides (clarithromycin, erythromycin and azithromycin) were removed by 24-34%. Among tetracyclines, chlorotetracycline concentration decreased to lower levels than the limit of detection during the UV process while only 15% removal efficiency was achieved for tetracycline. This can be explained by the low molar extinction coefficient of tetracycline (ε_λ=4108 M^{-1} cm^{-1}) comparing to that of chlorotetracycline (ε_λ=18868 M^{-1} cm^{-1}). Generally, the degradation of a compound by UV irradiation is affected by the UV energy absorption and the quantum yield of the compound. UV energy absorption is expressed as molar extinction coefficient, which is a measure of how strongly a chemical species absorbs light at a given wavelength that can be used for its degradation (Kim et al., 2009). Another study of photolysis was conducted by Arslan-Alaton and Dogruel (2004) in which penicillin in the form of formulation effluent with total COD=1555 mg L^{-1} was treated under UV irradiation or UV combined with H_2O_2. In this study the removal efficiency was very low compared to the others described above (COD removal max=22% and TOC removal max=10% with 30 and 40 mM of peroxide respectively) and this may be attributed to the complexity of the formulation effluent (high COD and TOC values). Zuccato et al. (2010) also reported the complete elimination of amoxicillin in a WWTP in Varese, Italy with UV-light treatment.

The organic matter (DOC, COD), UV dose and contact time are important factors governing the removal efficiency of antibiotics during direct photolysis whereas it seems that this process is extremely dependent on the chemical structure of the compound. This technology is only applicable to wastewater containing photo-

sensitive compounds and waters with low COD concentrations (*e.g.* river, drinking waters) (Homem and Santos, 2011). Furthermore, wastewater effluents have different organic compounds that may either inhibit or enhance the process by scavenging or generating oxidant species (humic and inorganic substances like dissolved metals) (Jiao et al., 2008). Generally, photolysis has been proved to be less effective in degrading antibiotics in wastewater effluents than the other AOPs described herein.

1.2.2.3.4 Ozonation

Huber et al. (2005) observed that using ozonation at ozone doses > 2 mg L^{-1}, up to 90% of sulfonamides and macrolides were removed in secondary wastewater effluents. The study by Adams et al. (2002) showed that ozonation removed more than 95% of several sulfonamides and trimethoprim from river water within 1.3 min contact time at ozone dose of 7.1 mg L^{-1}. Balcioglu and Otker (2003) also found that up to 80% of β-lactams removal from wastewater was achieved during ozonation treatment after 60 min and ozone dose 2.96 g L^{-1} h^{-1}. In a study of Arslan-Alaton et al. (2004) the COD of an antibiotic formulation effluent containing penicillin (COD=830 mg L^{-1}) was removed by 10-56% during the ozonation process while the addition of small amounts of hydrogen peroxide increased the removal efficiency (83%). In another study of Arslan-Alaton and Dogruel (2004), the COD and TOC of the formulation effluent containing penicillin was removed by 49% and 52% respectively under alkaline conditions (pH=11), whereas the removal efficiency was much lower under acidic conditions (pH=3) (COD removal max=15%; TOC removal max=2%). Many authors (Balcioglu and Ötker, 2003; Arslan-Alaton et al., 2004; Andreozzi et al., 2005) suggested that pH is a critical parameter in the ozonation process and a decrease of pH usually affects the reaction rate and also the absorption rates of ozone.

During wastewater ozonation, many antibiotics, including β-lactams, sulfonamides, macrolides, quinolones, trimethoprim and tetracyclines, have been shown to be transformed predominantly via direct oxidation by O_3 during wastewater ozonation whereas penicillin G, cephalexin and N_4-sulfamethoxazole were transformed to a large extent by hydroxyl radicals (Dodd et al., 2006). Ozone treatment performance is enhanced if ozone is combined with UV irradiation, hydrogen peroxide or catalysts (usually iron or copper complexes) (Klavarioti et al., 2009).

1.2.2.3.5 Fenton oxidation

Wastewater contained amoxicillin with high TOC (TOC=18925 mg L^{-1}) and low biodegradability was treated using a combined process of extraction, Fenton oxidation and a two-stage reverse osmosis (RO) (Zhang et al., 2006). TOC and COD were reduced by 88.4% and 89.6%, respectively. Trovo et al. (2008) observed that amoxicillin degradation was not influenced by the source of the irradiation during the photo-Fenton process and the removals of the antibiotic obtained were 89 and 85% under black light and solar irradiation, respectively. A similar study by Bautitz and Nogueira (2007) showed that tetracycline was removed by 80% during the photo-Fenton treatment using two types of iron and irradiation. Moreover, in a study by Arslan-Alaton and Dogruel (2004) good removals of the COD (>55%) and TOC (>50%) were achieved during the photo-Fenton and photo-Fenton-like treatment of the formulation effluent containing penicillin.

1.2.2.3.6 Heterogeneous photocatalysis with TiO_2

The study of Elmolla and Chaudhuri (2011) examined the feasibility of using combined TiO_2 photocatalysis ($UV/TiO_2/H_2O_2$) and a sequencing batch biological

reactor (SBR) process for the treatment of an antibiotic wastewater containing amoxicillin and cloxacillin. The complete removal of these compounds was observed at TiO_2 and H_2O_2 doses of 1000 and 250 mg L^{-1}, respectively. Amoxicillin was also completely removed from urban wastewater treatment plant effluent using [TiO_2]=0.8 g L^{-1} after 120 min of treatment as reported by Rizzo et al. (2009). Ofloxacin in wastewater samples was removed by 60% using [TiO_2]=3 g L^{-1} (Michael et al., 2010) while Hapeshi et al. (2010) reported that the DOC of a solution contained ofloxacin at 10 mg L^{-1} was reduced by 79% after 120 min of photocatalytic treatment using [TiO_2]=250 mg L^{-1} and [H_2O_2]=0.07 mmol L^{-1}.

1.2.2.3.7 Sonolysis

Ultrasound irradiation or sonolysis is a relatively new process in water and wastewater treatment and therefore, has unsurprisingly received less attention than other AOPs. This is also reflected by the small number of publications concerning the treatment of pharmaceutical compounds. Naddeo et al. (2009) evaluated the ultrasonic process on the degradation of amoxicillin spiked in urban wastewater effluent. It was found that the amoxicillin conversion was enhanced at increased applied power densities, acidic conditions and in the presence of dissolved air and the maximum removal observed was 40%.

1.2.3 Solar reactors for the photocatalytic wastewater treatment

There is much literature on the design and layout of different kinds of solar reactors for photocatalytic applications; however, this section provides only a brief overview on the topic.

1.2.3.1 Concentrating or Parabolic-trough concentrators (PTCs)

The first solar photoreactor designs for photochemical applications were based on line-focus parabolic-trough concentrators (PTCs) (Goswami, 1997). The parabolic-trough collector consists of a structure that supports a reflective concentrating parabolic surface; an absorber tube (reactor) is placed in the focus of this parabolic reflector (Schematic 1.6 (a)). With regard to the reflecting/concentrating materials, aluminium is the best option due to its low cost and high reflectivity in the solar UV spectrum on earth surface. All the solar radiation available on the aperture plane is reflected and concentrated on the absorber tube that is located at the geometric focal line of the parabolic trough. The reflector redirects radiation parallel to the axis of the parable towards the absorber tube in the focus. Consequently, this type of concentrator has to track the sun and can use only parallel direct radiation. One-axis and two-axis tracking systems can be used for this purpose (Malato et al., 2007).

A disadvantage of PTCs is that due to their geometry they can use only direct radiation, which makes them practically useless, when the sky is clouded. They are also rather expensive systems due to the necessary sun tracking system. This applies to the investment as well as to the maintenance costs, because moving parts are prone to require enhanced maintenance effort. Another aspect that has to be taken into account is the possibility of overheating water in large-scale installations with residence times in the concentrating collectors in the range of several minutes.

1.2.3.2 Non-concentrating collectors

The non-concentrating (or one-sun) collectors (Schematic 1.6 (b)) are, in principle, cheaper than PTCs as they have no moving parts or solar-tracking devices (Goswami,

1997). They do not concentrate radiation so that efficiency is not reduced by factors associated with concentration and solar tracking. Consequently, they can as well be operated under cloudy sky conditions, although of course with reduced efficiency compared to sunny conditions. However, these systems require resistant and chemically inert ultraviolet-transmitting materials. Additionally, non-concentrating systems require significantly more photoreactor area than concentrating collectors (Malato et al., 2007; Malato et al., 2009).

1.2.3.3 Compound parabolic collectors (CPCs)

CPCs are an interesting combination between PTCs and non-concentrating collectors without their respective disadvantages. CPCs are static collectors with a reflective surface formed by two connected parabolic mirrors with an absorber tube in the focus and have been found to provide the most efficient light-harvesting optics for low concentrating systems (Schematic 1.6 (c)). They have no tracking system and the design permits the solar rays to be reflected onto the absorber tube attaining a low concentration factor (R_C). The concentration factor is defined as the ratio of the collector aperture (A) to the absorber tube perimeter and is usually between 1 and 1.5 depending on the type of application (eqn. (1.37)).

$$R_C = \frac{1}{\sin \theta_\alpha} = \frac{A}{2\pi r} \tag{1.37}$$

The normal values for the semi-angle of acceptance (θ_α), for photocatalytic applications, are between 60 and 90^o. This wide angle of acceptance allows the receiver to collect both direct and a large part of the diffuse light (1/ R_C of it), with the additional advantage of decreasing errors of both the reflective surface and receiver tube alignment, which become important for achieving a low cost photoreactor. A

special case is the one in which θ_α = 90^o, whereby R_C = 1 (non-concentrating solar system) (Malato et al., 2009).

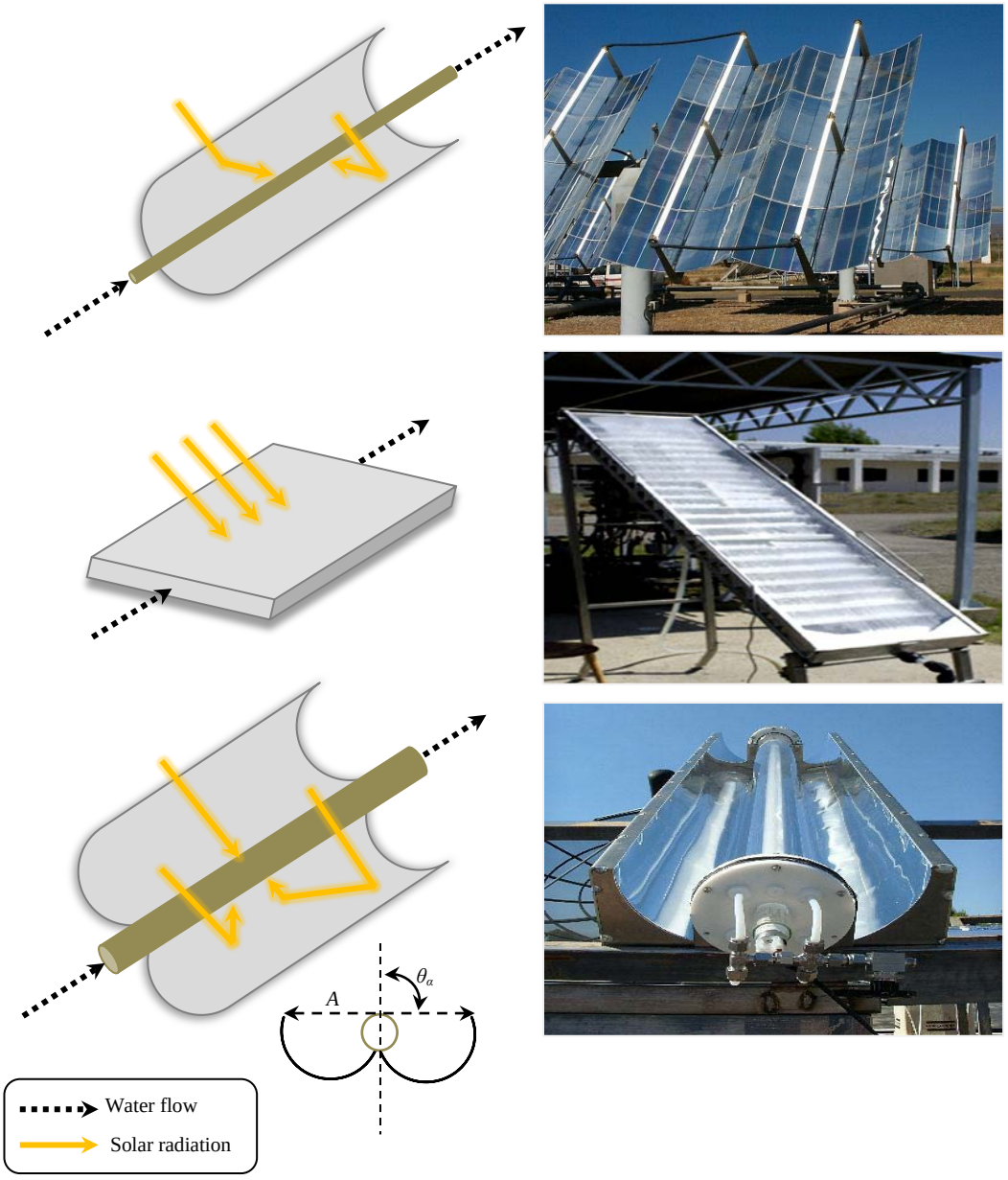

Schematic 1.6 Schematic drawings and photographs (taken from Plataforma Solar de Almería) of the solar reactors: (a) Concentrating or parabolic-trough concentrator (PTC); (b) Non-concentrating collector; and (c) Compound parabolic collector (CPC).

1.3 Ofloxacin and trimethoprim: The target contaminants

Ofloxacin (OFX) and trimethoprim (TMP) are synthetic antibiotics frequently used in human and veterinary medicine for the prevention and treatment of various infections. Investigations for the occurrence of ofloxacin and trimethoprim in wastewater effluents and natural waters have been conducted in several European countries (Miao et al., 2004; Batt et al, 2007; Gulkowska et al., 2008) (Table 1.4). Significant concentrations ($\mu g\ L^{-1}$) of these antibiotics were also detected in secondary and tertiary treated effluents taken from WWTPs in Cyprus (Fatta-Kassinos et al., 2010) (see Table 1.4).

OFX is a fluoroquinolone widely used as a broad-spectrum antibiotic and has established efficacy in the treatment of urinary tract infections (Okeri and Arhewoh, 2008; Ghosh et al., 2010). Its pharmacological activity is associated with inhibition of the bacterial topoisomerase (Lhiaubet-Vallet et al., 2009). It is active against most Gram-negative bacteria, many Gram-positive bacteria and some anaerobes while it also demonstrates favorable pharmacokinetic properties (Monk and Campoli-Richards, 1987; Himmelfarb et al., 1993; Nau et al., 1994). It is widely prescribed for the treatment of infectious diseases on account of its safety, good tolerance and broad antibacterial spectrum with less resistance (Park et al., 2006; Koo et al., 2008).

TMP is used clinically either alone or in combination with sulfonamides (*e.g.* sulfamethoxazole, sulfadiazine, sulfamoxole) for the treatment of specific bacterial infections (Mengelers et al., 1989; Ni et al., 2006). It is a broad-spectrum antimicrobial agent which acts as an inhibitor of bacterial dihydrofolate reductase (Fresta et al., 1996; Barbarin et al, 2002; Li et al., 2005). TMP is mainly used in the prophylaxis and treatment of urinary tract infections, as well as for prevention and

treatment of respiratory or gastro-intestinal tract infections (Abellan et al., 2009). Indeed, the combination of sulfonamides with trimethoprim is widely used in veterinary medicines.

Table 1.4 Occurrence of OFX and TMP in urban wastewater effluents.

Antibiotic	Concentration (ng L^{-1})	Reference
OFX	503	*Xiao et al., 2008*
	53-991	*Lin et al., 2009*
	2.1-556	*Li et al., 2009*
	183	*Castiglioni et al., 2008*
	96-7870	*Zuccato et al., 2005*
	4.9-77	*Zuccato et al., 2010*
	50-210	*Miao et al., 2004*
	110	*Brown et al., 2006*
	7-52	*Lindberg et al., 2005*
	740-5700	*Peng et al., 2006*
	1290-4820	*Fatta-Kassinos et al., 2010*
TMP	250	*Watkinson et al., 2009*
	70-480	*Watkinson et al., 2007*
	340	*Ternes et al., 2007*
	203-415	*Lin et al., 2009*
	11-66	*Li et al., 2009*
	290	*Gros et al., 2006*
	550	*Karthikeyan and Meyer,2006*
	210-2400	*Batt et al., 2007*
	120-230	*Gulkowska et al., 2008*
	180	*Brown et al., 2006*
	1070	*Renew and Huang, 2004*
	60-90	*Fatta-Kassinos et al., 2010*

Schematic 1.7 shows the chemical structure of the two compounds with their most important physicochemical properties summarized in Table 1.5.

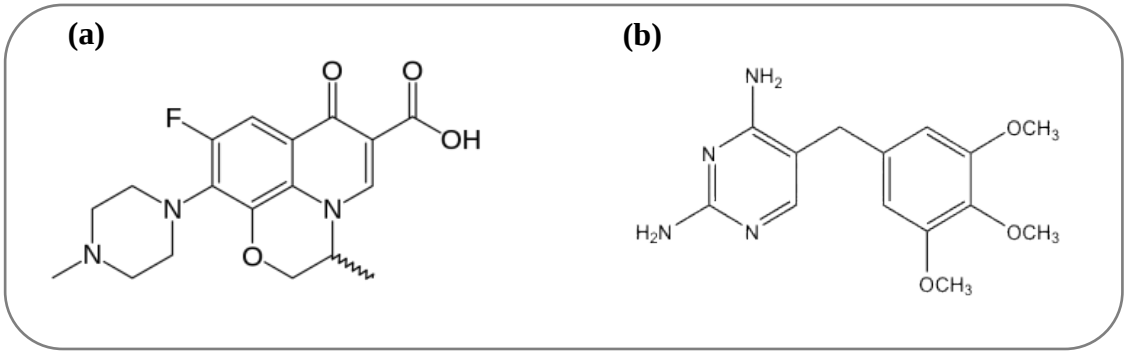

Schematic 1.7 Chemical structure of: (a) OFX and (b) TMP.

Table 1.5 Main physicochemical properties of OFX and TMP.

Property	OFX	TMP
Therapeutic group	Fluoroquinolone	Trimethoxybenzylpyrimidine
IUPAC name	[(±)-9-Fluoro-2,3-dihydro-3-methyl-10-(4-methylpiperazin-1-yl) 7oxo7Hpyrido [1,2,3 benzoxazine-6-carboxylic acid]	[2,4-diamino-5-(3,4,5-trimethoxybenzyl) pyrimidine]
Chemical formula	$C_{18}H_{20}FN_3O_4$	$C_{14}H_{18}N_4O_3$
Molecular weight (g mol^{-1})	361.4	290.3
Melting point (^oC) [1], [5]	270-273	199-203
Solubility in H_2O (mg mL^{-1}) [2], [5]	60 (pH=2-5), 4 (pH=7), 303 (pH=9.8)	0.4
Octanol/water partition coefficient ($logK_{o/w}$) [3], [6]	0.41 (pH 7), 0.33 (pH 7.2), 0.28 (pH 7.3)	0.91 (pH=2-4)
Ionization constants (pK_a) [1], [7]	pK_{a1}=6.05, pK_{a2}=8.25	pK_{a1}=3.2, pK_{a2}=7.1
Pharmacokinetic parameters [4]	Bioavailability (%)=70-90 Time of half life (h)=5.0-7.4 Excretion in urine (%)=80	Bioavailability (%)=90-100 Time of half life (h)=8-10 Excretion in urine (%)= 50-60

[1] Okeri and Arhewoh, 2008; [2] Hapeshi et al., 2010; [3] Nau et al., 1994; [4] National prescriptions National Organization for Medicines, Athens, Greece, 2000; [5] PhysProp Database Demo, Syracuse Research corporation, 2007 (http://www.syrres.com/esc/physdemo.htm); [6] Gros et al., 2006; [7] Dodd et al., 2006.

1.4 Objectives of the study

The aim of this thesis was to study the solar-driven advanced chemical oxidation of two selected antibiotics-OFX and TMP-in secondary domestic treated effluents at a pilot scale. Therefore, preliminary experiments were performed to optimize two advanced oxidation systems for the degradation of OFX and TMP in secondary effluents at a bench scale under simulated solar irradiation. The two AOPs examined were the homogeneous solar Fenton process ($h\nu/Fe^{2+}/H_2O_2$) and the heterogeneous photocatalysis with titanium dioxide (TiO_2) suspensions. Subsequently the most efficient method was chosen for implementing a pilot scale study for determining the degradation kinetics, the main transformation products, toxicity, etc.

1.4.1 Bench scale experiments

The first part of the experimental work was dedicated to the degradation study of the examined antibiotics during the two advanced treatment processes. At the beginning, bench scale experiments with a solar simulator in combination with a photochemical batch reactor were carried out to evaluate the efficiency of each one of the two processes and the influence of various operational parameters on the degradation of the two antibiotics. The bench scale experiments were performed at substrates concentration level of 10 mg L^{-1}. The evaluation of the processes was performed by studying the degradation/removal of individual antibiotics in solution by chromatographic analysis and/or by UV/Vis spectrophotometry of the parent compounds and by monitoring the observed reduction of dissolved organic carbon (DOC) during the process. In more detail the following have been studied:

Homogeneous photocatalysis ($hv/Fe^{2+}/H_2O_2$)

- The effect of ferrous (Fe^{2+}) and hydrogen peroxide (H_2O_2) concentration
- The effect of pH
- The effect of the solar irradiation
- The effect of the temperature
- The effect of the initial substrate concentration
- The degradation kinetics
- Mineralization (DOC removal)

Heterogeneous photocatalysis (hv/TiO_2)

- The effect of the catalyst (TiO_2) concentration
- The effect of pH
- The effect of oxidants
- The effect of initial substrate concentration
- The degradation kinetics
- Mineralization (DOC removal)

Furthermore, a *Daphnia magna* bioassay was used to evaluate the potential toxicity of the parent compounds and their photo-oxidation by-products in different stages of treatment.

The examined substrates concentration level (10 mg L^{-1}), although considerably greater than the concentration range typically found in wastewaters, was chosen so as to allow the sufficient UV-light absorption of ofloxacin and the accurate determination of residual concentrations with the UV/Vis spectrophotometric system. At this point it is worth noting that in the case of OFX substrate, the concentration was evaluated using the UV/Vis spectrophotometric system for

two reasons: (1) a characteristic evolution of the UV/Vis absorbance (λ_{max}=288 nm) along the degradation process can be distinguished even when using wastewater; and (2) the UV/Vis system was the only available and appropriate technique for these measurements during the experimental period (2009). On the other hand, TMP substrate concentration was determined using an ultra-performance liquid chromatography tandem mass spectrometry (UPLC-MS/MS) system which was made available in the laboratory in October 2010.

1.4.2 Pilot scale experiments

From the bench scale experiments it has been demonstrated that the homogeneous photocatalysis (solar Fenton) was more effective than the heterogeneous process (solar TiO_2). Therefore the solar Fenton was further investigated in a pilot scale set up.

The main objectives of the pilot scale study were:

(a) the optimization of the solar Fenton process for the determination of the degradation kinetics of the two compounds in relative low concentration level (100 $\mu g\ L^{-1}$). This concentration, although far from the real concentrations in effluents, was considered to be low enough to simulate the environmental concentrations quite accurately and it is at the same time high enough to be detected in the UPLC-MS/MS system.

(b) the structure elucidation of the major oxidation by-products formed during the photocatalytic treatment of TMP in four environmental matrices (demineralized water (DW); simulated natural freshwater (SW); simulated effluent from municipal WWTP (SWW); and real effluent from municipal WWTP (RE)). As domestic wastewater

treatment plant effluents are a complex mixture, a step by step approach from demineralized water to real effluent from municipal wastewater treatment plant was applied to clarify the possible negative effects of the water matrix on the degradation behavior of the selected compounds. The formation of these by-products allows the degradation process to be better understood and evaluated. Moreover, the identification of those by-products is the key to maximizing the overall process efficiency. On the other hand, some of the degradation by-products obtained may be more toxic and persistent than the parent compounds. This is one of the most fascinating parts of this work and unique characteristics of the overall oxidation process. For these experiments a concentration of 10 mg L^{-1} was applied in order to credibly elucidate the oxidation by-products.

The aforementioned experimental procedures (a, b) were carried out in two compound parabolic collector (CPC) solar pilot plants: (i) at the sewage treatment plant at the University of Cyprus (UCY); and (ii) at the Plataforma Solar de Almería (PSA) in Tabernas (Almeria, Spain), respectively.

Additionally, various toxicity assays (*i.e. Daphnia magna*, *Vibrio fischeri*, phytotoxicity test) were performed to evaluate the potential toxicity of the parent compounds and their transformation products during the various stages of the oxidation process. Considering the fact that the treated effluent samples are intended for irrigation purposes, the toxicity measurements were considered as an indispensable task.

An important issue that concerns the presence of antibiotic residues in the effluents after wastewater treatment is the evolution of antibacterial resistance in human pathogenic microorganisms. Therefore, the efficiency of solar Fenton on pilot scale in removing antibiotic resistance bacteria was assessed. The training on the method for

the determination of antibiotic resistant bacteria was carried out at the laboratory of ''Center for Biotechnology and Fine Chemistry-CBQF'' at the Escola Superior de Biotecnologia, Universidade Católica Portuguesa in Porto, Portugal. This training was funded by the COST (European Cooperation in Science and Technology) through the Short Term Scientific Mission (STSM) within the COST scientific programme on ''Detecting evolutionary hot spots of antibiotic resistances in Europe (DARE)''.

A UPLC-MS/MS method has been also developed and validated for studying the degradation kinetics during the solar Fenton process of ofloxacin and trimethoprim in secondary treated wastewater at low concentration levels. The development of the analytical method was achieved in collaboration with Waters Corporation (Waters MS Technology Centre, Manchester) which specializes in the manufacture, operation and development of innovative analytical instruments.

The experimental work performed in Cyprus has been carried out in the framework of the **SolTec** project (Project title: Development of a solar technology for the removal of effluent organic matter from urban wastewaters). This project was co-funded by the Republic of Cyprus and the European Regional Development Fund of the European Union through grant AEIFO/ASTI/0308/01/BIE. Part of the work has been supported by the International Water Research Center "NIREAS" (NEA IPODOMI/STRATH II/0308/09) also co-funded by the Republic of Cyprus and the European regional development fund.

Moreover, part of the experimental work was funded by the European Commission under SFERA program (Solar Facilities for the European Research Area) ('G.Agreement no: 228296 FP7-INRASTRUCTURES-2008-1'). The experiments were carried out at the Plataforma solar detoxification laboratory in PSA from 31 May 2010 to 28 June 2010. The PSA, which belongs to the Centro de Investigaciones

Energéticas Medioambientales y Tecnológicas (CIEMAT), is the largest European center for research, development and testing of concentrating solar technologies. It is located in the Tabernas Desert, 35 km from the city of Almeria in Spain (Picture 1.1). PSA deals with various activities that configure the environmental applications of solar energy which encompass the following lines of research: (i) solar water detoxification and disinfection; (ii) solar air detoxification and disinfection; (iii) solar seawater and saltwater desalination; and (iv) characterization and measurement of solar radiation.

Picture 1.1 Aerial view of the Plataforma Solar de Almería.

Moreover, the elucidation of the oxidation intermediates generated during the solar Fenton process performed at the PSA pilot plant, was conducted at the Institute of Environmental Assessment and Water Research (IDÆA) of the Spanish Council of Scientific Research (CSIC) in Barcelona (31 June-20 July).

The main tasks of this research are summarized and shown in Schematic 1.8.

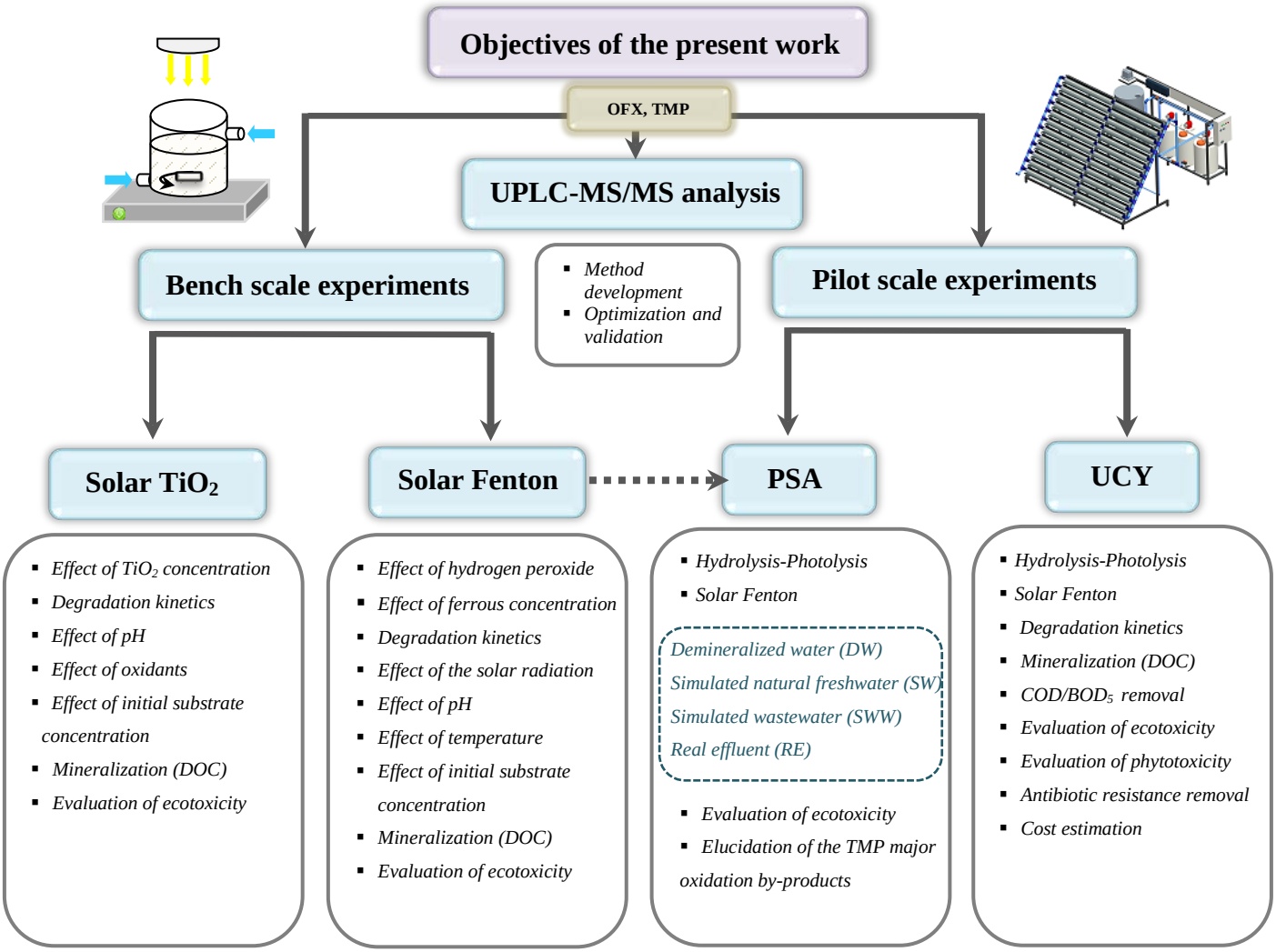

Schematic 1.8 The main tasks included in this work.

CHAPTER 2: EXPERIMENTAL

2.1 Materials and methods

2.1.1 Chemicals

2.1.1.1 Antibiotics

The antibiotic standards (OFX, Sigma Aldrich; TMP, Fluka) used were of high purity grade (≥ 98.5%) and were not subjected to any further purification. Two concentration levels of antibiotics were examined: (i) 10 mg L^{-1} for the bench scale experiments; and (ii) 100 μg L^{-1} for the pilot scale experiments.

Solutions containing each compound separately at initial concentration of 10 mg L^{-1} were prepared by dissolving a quantity of the powdered standard in the appropriate volume of secondary treated effluent samples taken from a municipal wastewater treatment plant (WWTP) in Cyprus. The solution was stirred for several hours in the dark to ensure complete dissolution of the compound. Solutions at 100 μg L^{-1} were prepared by dissolving a specified mass of each compound in deionized water (milli-Q) water and then spiking the appropriate volume into the secondary effluent contained in the storage tank of the pilot plant.

It should be noted that the range of concentration of OFX and TMP in the original secondary wastewater taken form the WWTP in Limassol, was in the ng L^{-1} range ($[OFX]_{average}$=1150 ng L^{-1}; $[TMP]_{average}$=30 ng L^{-1}); thus it was not taken into account. Moreover, these antibiotics were not detected in the wastewater effluent taken form the WWTP at UCY campus.

2.1.1.2 Reagents used in experiments and chromatographic analysis

The reagents used in the solar Fenton experiments were iron sulfate heptahydrate ($FeSO_4 \cdot 7H_2O$, Sigma Aldrich) and hydrogen peroxide (H_2O_2 30% w/w, Merck). The pH of the wastewater was adjusted by 2N H_2SO_4 (Merck). The Fenton reaction was terminated at specific time intervals by adding: (i) methanol (Fluka) for the chromatographic analysis; (ii) anhydrous sodium sulfite (Na_2SO_3, Sigma Aldrich) for the DOC measurements; and (iii) manganese dioxide (MnO_2, particle size 10 μm, reagent grade ≥ 90%) (Sigma Aldrich) for the COD determination. Titanium dioxide (TiO_2) was Aeroxide® TiO_2 P25, supplied by Aeroxide® (anatase:rutile 75:25, particle size 21 nm and 50 $m^2\ g^{-1}$ BET area). Sodium persulfate ($Na_2S_2O_8$) was purchased by Riedel-de Haen.

Calcium sulfate dehydrate ($CaSO_4.2H_2O$, Panreac), magnesium sulfate ($MgSO_4$, Sigma Aldrich) and potassium chloride (KCl, J.T. Baker) were used for the simulated natural freshwater (SW) preparation. Peptone (Biolife), meat extract (Biolife), urea (Fluka), magnesium sulfate heptahydrate ($MgSO_4.7H_2O$, Fluka), dipotassium phosphate (K_2HPO_4, Riedel-de Haën), calcium chloride dehydrate ($CaCl_2.2H_2O$, Riedel-de Haën) and sodium chloride (NaCl, Merck) were used for the simulated wastewater (SWW) preparation. SW and SWW were prepared according to APHA Standards Methods (Standard Methods for the Examination of Water and Wastewater, 20th ed, 1998).

For toxicity and microbiological analyses the treated solutions were neutralized by 2N NaOH (Merck). In the case of the solar Fenton process, the residual hydrogen peroxide was removed from the treated samples with catalase (*Micrococcus lysodeikticus* 170000 U mL^{-1}, Fluka). *Enterococcus* medium agar (Enterococcus Selective Agar) was supplied by Fluka.

For the chromatographic analysis, stock solutions of each analyte (1 mg mL^{-1}) were prepared by dissolving the appropriate amount of standard in MeOH (Fluka) and stored in the dark at 4 ^{o}C. Working standard solutions were prepared daily by diluting the appropriate volume of stock solution with 10:90 v/v MeOH:H_2O to yield concentrations in the range of 0.01-0.1 μg L^{-1} and 0.1-100 μg L^{-1}. Ofloxacin-d_3 (10 mg, powder) and trimethoprim-d_3 (100 ng μL^{-1} in acetonitrile) obtained from Dr. Ehrenstorfer (Augsburg, Germany) were used as surrogate standards. LC/MS-grade methanol (Fisher Scientific; Fluka) and acetonitrile (Fisher Scientific; Sigma Aldrich) were used as the main solvents. Formic acid (98%) was purchased by Fluka. Ammonium acetate (> 98%) was supplied by Sigma Aldrich.

Other reagents used for the analytical measurements are: Potassium hydrogen phthalate (KHP, Sigma Aldrich), acetic acid ($C_2H_4O_2$, Sigma Aldrich), ascorbic acid (Sigma Aldrich), ammonium metavanadate (NH_4VO_3, Fluka), 1,10-phenantholine (Sigma Aldrich), Cd granules (Fluka), copper sulfate ($CuSO_4$, Sigma Aldrich), ammonium chloride (NH_4Cl, Riedel-de Haën), EDTA (Sigma Aldrich), ammonium persulfate ($(NH_4)_2S_2O_8$, Sigma Aldrich), ammonium molybdate ($(NH_4)_2MoO_4$, Sigma Aldrich), potassium antimonyl tartrate ($C_8H_4K_2O_{12}Sb_2.3H_2O$, Fluka), sodium acetate ($C_2H_3O_2Na$, Fluka) and allylthiourea (Sigma Aldrich).

Ultrapure water (milli-Q PURELAB Ultra ELGA Water Dispenser; Millipore) was used throughout the experimental procedure and chromatographic analyses.

2.1.2 Water matrices used for the experiments performed at the University of Cyprus

2.1.2.1 Secondary treated wastewater for the bench scale experiments

The secondary treated wastewater samples used as the matrix for the bench experiments were collected from a municipal WWTP in Cyprus. The specific WWTP situated in Limassol (Moni) serves a population of about 272 000 equivalents (PE) and receives both industrial and domestic discharges. Water treatment includes primary, secondary and tertiary treatment while chlorination is used as disinfection method. The WWTP facility (Schematic 2.1) includes screening, grid/grease chamber, skimmer tanks and large solids removal via fine screens (3 mm) in its primary processes. A primary sedimentation tank follows and then conventional secondary activated sludge treatment is applied. The secondary treatment process consists of two interconnected aeration tanks where nitrogen is removed biologically in two processes - nitrification and denitrification. Nitrification and denitrification are achieved by operating the aeration tanks under alternating conditions. From the aeration tanks the water is led to four final settlement tanks where the water is separated from the biological sludge. The sampling points from which the secondary wastewater effluent was collected are depicted in Schematic 2.1 (red dashed lines). In the tertiary treatment, the biologically treated water that overflows from the secondary tanks passes through sand filters for removing small particles before the water is disinfected by chlorination. The treated water is mainly reused for irrigation purposes. The WWTP is operating with an average daily flow of 15 000 m^3 day^{-1} with an average influent BOD_5 of about 121 mg L^{-1}.

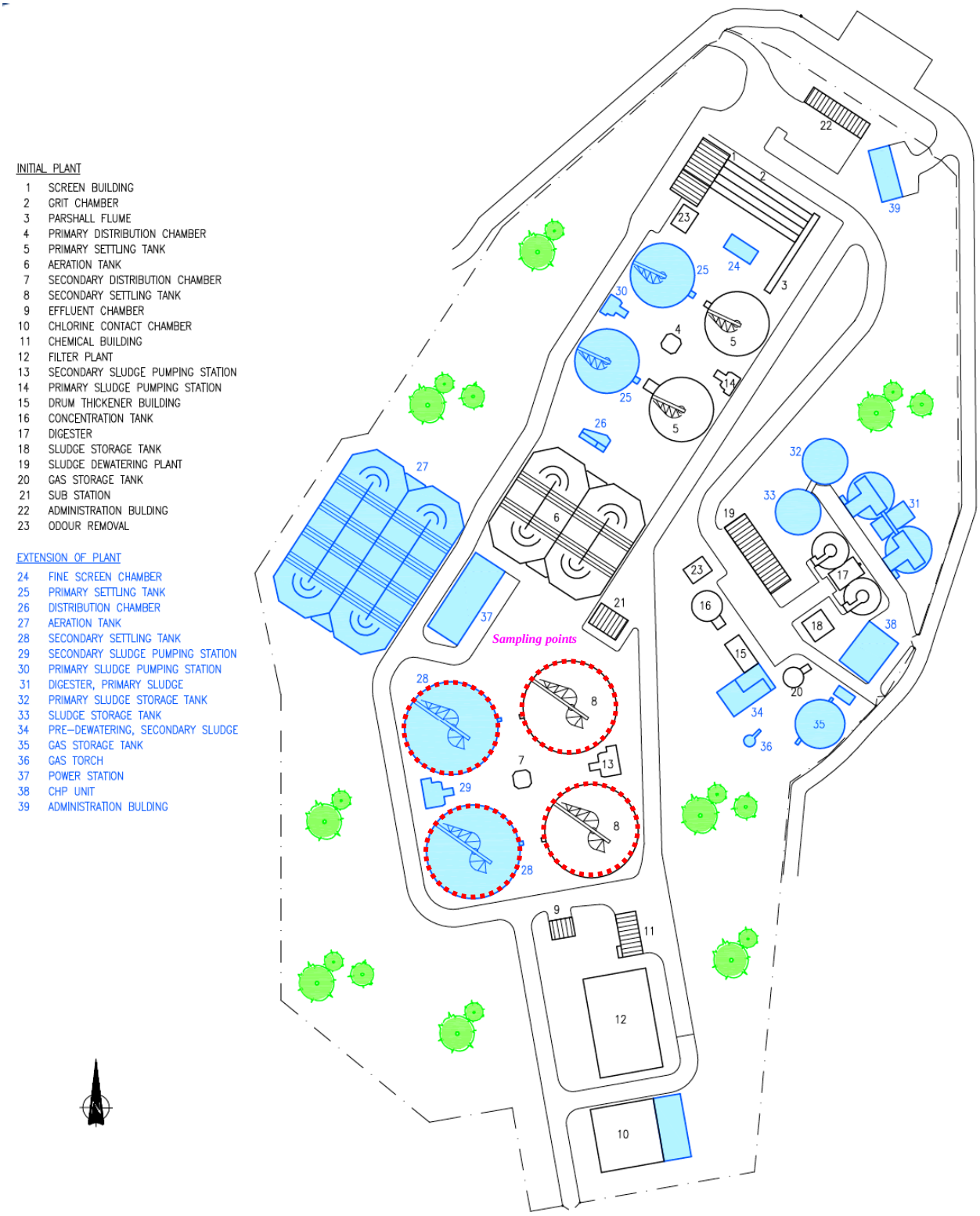

Source: *Kruger-Cybarco Consortium*

Schematic 2.1 WWTP (Moni, Limassol) facility.

The secondary treated wastewater samples were analyzed before use for a number of qualitative characteristics which were provided by the plant operators (Table 2.1). All wastewater samples analyzed in this work were grab samples collected in amber glass bottles (1 L each), placed in a cool box and vacuum filtered through 0.45 μm glass fibre filters (GF/D, Whatman, USA) immediately after being brought to the laboratory. Samples were stored in the dark at 4 ^{o}C and used within one week.

Table 2.1 Main qualitative parameters of the secondary effluent samples taken from the WWTP (Moni, Limassol).

Parameter	**Value***
pH (20 ^{o}C)	8.04
Conductivity (μS cm^{-1}) (20 ^{o}C)	1477
TSS (mg L^{-1})	27.2
Total N (mg L^{-1})	11.5
NO_3^- (mg L^{-1})	5.90
NH_4^+ (mg L^{-1})	1.38
Total P (mg L^{-1})	1.90
COD (mg L^{-1})	28.0
DOC (mg L^{-1})	8.53

* Mean value of three measurements

2.1.2.2 Secondary treated wastewater for the pilot scale experiments

The UCY WWTP is operating with an average daily flow of 400 m^3 day^{-1} and it serves the student houses and offices at the UCY campus. The treatment plant consists of three basic areas: (i) the pumping station; (2) the main building which is constructed over the irrigation tanks and houses a blower room and odour control

filter, a generator room, a chemical room and a tertiary filter; and (iii) the main control panel room. The other section of the plant is an over ground construction of tanks which basically consists of: one splitter box, two selectors, two grease traps, two aeration tanks, two settlement tanks, one common sludge holding tank and one common backwash tank. The electrical installation consists of three panels: the main control panel, the tertiary filter control panel and the irrigation control panel.

At the inlet to the treatment plant the wastewater passes through mechanical screens and then is pumped to the splitter box where flow is equally split to the two grease traps and after to the two aeration tanks. After the activated sludge treatment, the treated wastewater is displaced to the settlement tank where the effluent is separated from the biological mass and pumped through the tertiary filter. After the tertiary filter stage the flow is passed through the chlorine contact tank, where removal of pathogens takes place and from there it is diverted to the irrigation tank compartments. The treated effluent is used for irrigation purposes.

The main qualitative characteristics of the secondary treated wastewater are illustrated in Table 2.2.

Table 2.2 Main qualitative characteristics of the secondary treated effluent taken from the WWTP at UCY campus.

Parameter	Value *
pH (20 ^{o}C)	7.05
Conductivity (μS cm^{-1}) (20 ^{o}C)	1677
TSS (mg L^{-1})	48.33
NO_3^- (mg L^{-1})	36.07
Total N (mg L^{-1})	38.00
PO_4^{3-} (mg L^{-1})	2.65
Total P (mg L^{-1})	3.53
COD (mg L^{-1})	27.00
DOC (mg L^{-1})	8.60
BOD_5 (mg L^{-1})	12.00
Fe (mg L^{-1})	0.302
Cu (mg L^{-1})	0.195
Cd (mg L^{-1})	0.11
Na (mg L^{-1})	13.24
K (mg L^{-1})	26.84

* Mean value of three measurements

2.1.3 Water matrices used for the experiments performed at Plataforma Solar de Almería (PSA)

The experiments at PSA were performed in four different matrices; demineralized water (DW), simulated natural freshwater (SW), simulated effluent from municipal WWTP (SWW) and real effluent from municipal WWTP (RE).

2.1.3.1 Demineralized water

DW used in the pilot plant was supplied by the PSA distillation plant (conductivity < 10 μS cm^{-1}, Cl^- = 0.2-0.3 mg L^{-1}, SO_4^{2-} = 0.2-0.3 mg L^{-1}, NO_3^- < 0.5 mg L^{-1}, organic carbon < 0.5 mg L^{-1}).

2.1.3.2 Simulated natural freshwater

SW was prepared by mixing 60 mg L^{-1} of $CaSO_4.2H_2O$, 60 mg L^{-1} of $MgSO_4$ and 4 mg L^{-1} of KCl (Standard Methods for the Examination of Water and Wastewater of 1998, 20th edition). Although SW recipe includes bicarbonates (96 mg L^{-1} $NaHCO_3$), it was decided to avoid this addition because previous experiments have confirmed that the presence of carbonate species (CO_3^{2-}, HCO_3^-) compete with organic contaminants for hydroxyl radicals leading to extremely slow degradation kinetics (Klamerth et al., 2009).

2.1.3.3 Simulated wastewater

In the literature, there is not any recipe that describes the preparation of wastewater effluent. So the recipe for standard municipal wastewater (Standard Methods for the Examination of Water and Wastewater of 1998, 20th edition) was taken and the organic content was reduced to 20% (an assumed 80% organic removal which is a common efficiency in WWTPs). The SWW was prepared by mixing SW and various compounds such as: 32 mg L^{-1} peptone, 22 mg L^{-1} meat extract, 6 mg L^{-1} urea, 2 mg L^{-1} $MgSO_4.7H_2O$, 28 mg L^{-1} K_2HPO_4, 4 mg L^{-1} $CaCl_2.2H_2O$ and 7 mg L^{-1} NaCl which derived to an initial dissolved organic carbon (DOC) of 25 mg L^{-1} (OECD, 1999).

2.1.3.4 Real effluent

The RE was a secondary treated effluent sample taken from the municipal WWTP of El Ejido (40 km east of Almería). The WWTP treats water of a medium sized community (6800 inhabitants). It consists of primary clarification process (sand, grit and grease removal) and a biological treatment based on the activated sludge process followed by a nitrification-denitrification step and a subsequent anaerobic sludge digestion. The WWTP is designed to treat up to 12 500 m^3 day^{-1} with a maximum flow of 1765 m^3 h^{-1}, BOD_5 of 350 mg L^{-1}, TSS of 375 mg L^{-1} and total Kjeldahl nitrogen (TKN) of 60 mg L^{-1}.

The composition of the water matrices used is illustrated in Table 2.3.

Table 2.3 Main qualitative characteristics of the water matrices used for the experiments at PSA.

Matrix	Parameter	Value *
DW	pH (20 °C)	6.1
	Conductivity (μS cm^{-1}) (20 °C)	< 10
	Cl^- (mg L^{-1})	0.2-0.3
	SO_4^{2-} (mg L^{-1})	0.2-0.3
	NO_3^- (mg L^{-1})	< 0.5
	DOC (mg L^{-1})	< 0.5
SW	$CaSO_4.2H_2O$ (mg L^{-1})	60
	$MgSO_4$ (mg L^{-1})	60
	KCl (mg L^{-1}	4
SWW	$CaSO_4.2H_2O$ (mg L^{-1})	60
	$MgSO_4$ (mg L^{-1})	60
	KCl (mg L^{-1})	4
	Peptone (mg L^{-1})	32
	Meat extract (mg L^{-1})	22
	Urea (mg L^{-1})	6
	$MgSO_4.7H_2O$ (mg L^{-1})	2
	K_2HPO_4 (mg L^{-1})	28
	$CaCl_2.2H_2O$ (mg L^{-1})	4
	NaCl (mg L^{-1})	7
	DOC (mg L^{-1})	~25
RE	pH (20 °C)	7.8
	Conductivity (μS cm^{-1}) (20 °C)	3.05
	Cl^- (g L^{-1})	0.54
	SO_4^{2-} (g L^{-1})	1.05
	NO_3^- (g L^{-1})	0.02
	NH_4^+ (g L^{-1})	0.11
	Na^+ (g L^{-1})	0.37
	K^+ (g L^{-1})	0.045
	Mg^{2+} (g L^{-1})	0.064
	Ca^{2+} (g L^{-1})	0.12
	COD (mg L^{-1})	63.7
	DOC (mg L^{-1})	10.72

* Mean value of three measurements

2.2 Experimental procedure

2.2.1 Experimental set up in bench scale

Solar Fenton and TiO_2 suspension experiments were performed in a continuously magnetically stirred (500 rpm) photochemical batch reactor (inner diameter 8 cm; height 9.5 cm) with a maximum capacity of 300 mL. The reactor, constructed with double wall Pyrex glass was connected to a thermostatic bath for maintaining the temperature at the selected value of 25±0.1 ^{o}C. A laboratory-scale solar simulator (Newport 91193) equipped with 1 KW Xenon lamp was used. The irradiation intensity of the simulator was determined using a radiometer (Newport 70260) and it was found 272.3 W m^{-2}. The xenon lamp used spectrum differs from the solar spectrum because of the intense line output in the 800-1100 nm region while the rest of its spectrum simulates very well the natural sunlight one. At specific time intervals, samples were withdrawn from the reactor and were analyzed with UV/Vis spectrophotometer (Jasco V-530), UPLC-MS/MS (ACQUITY TQD) and TOC analyzer (Shimadzu TOC-$V_{CPH/CPN}$). Schematic 2.2 shows the basic experimental features and the picture of the photochemical reactor and the simulator.

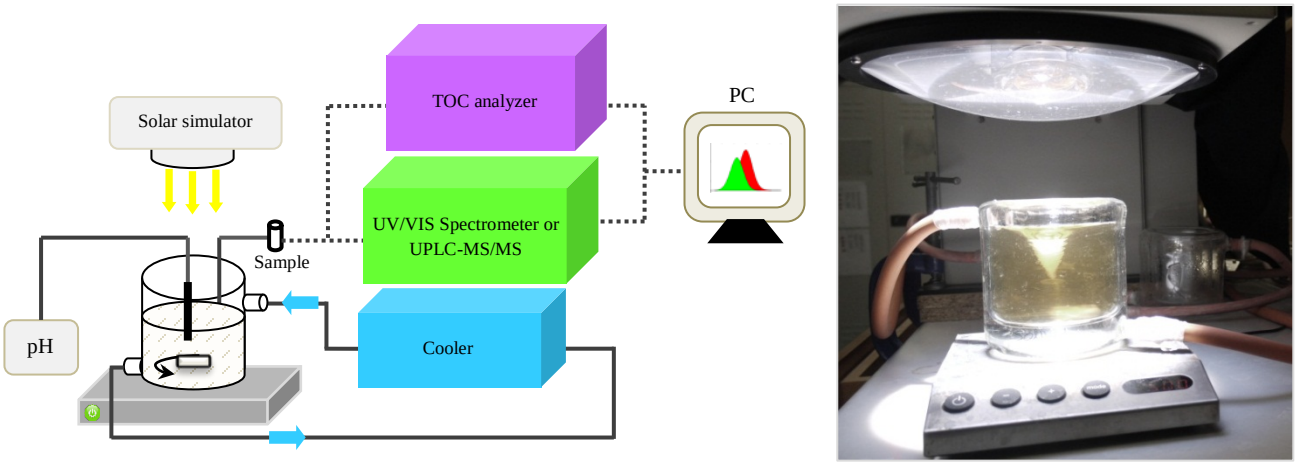

Schematic 2.2 Bench scale experimental set-up.

2.2.1.1 Solar Fenton

The antibiotic solution (10 mg L^{-1}) was fed into the reactor and the pH was adjusted to 2.9-3.0 by adding the required amount of 2N H_2SO_4 aqueous solution. No further adjustment of the pH was performed during the experiments. Then, the appropriate amount of Fe^{2+} was added (aqueous solution of $FeSO_4 \cdot 7H_2O$) and the mixture was mixed well. The reaction was initiated by adding the appropriate volume of H_2O_2 (30% w/w) ensuring vigorous mixing until the end of the experiment. Irradiation started just after the addition of the H_2O_2 and the time at which the system started to be irradiated was considered time zero. Samples were withdrawn at specific time intervals from the reactor and were transferred in vials containing 1 mL of 0.2 M Na_2SO_3 solution in order to stop the reactions. In the case that samples were intended to be analyzed with UPLC-MS/MS the reactions were terminated with MeOH. For the COD determinations, samples were transferred in vials containing a small quantity (one spatula tip) of MnO_2 powder. Samples were further analyzed after been filtered through a 0.22 μm syringe-driven filter (Millipore).

2.2.1.2 Solar TiO_2

The reactor was charged with the antibiotic solution and the catalyst loading ([TiO_2]=0.25-4.0 g L^{-1}) and the resulting suspension was continuously stirred. The pH of the solution was kept at the inherent pH value (pH=7-8) of the wastewater. At the beginning, the suspension was stirred for 30 minutes in the dark to ensure complete equilibration of the adsorbed substrate and the other organic compounds contained in the wastewater sample on the catalyst surface. This test was also performed overnight with no further increase in the adsorption. Samples were periodically withdrawn from

the reactor and were further analyzed after filtration through a 0.22 μm filter (Millipore).

2.2.2 Experimental set up in pilot scale

The experiments were carried out in two compound parabolic collector (CPC) pilot plants installed: (i) at the Plataforma Solar de Almería (PSA, pilot plant A) in Tabernas (Almería, Spain); and (ii) at the sewage treatment plant at the University of Cyprus (UCY, pilot plant B), for solar photocatalytic degradation applications (Picture 2.1 (a) and (b), respectively).

(a)

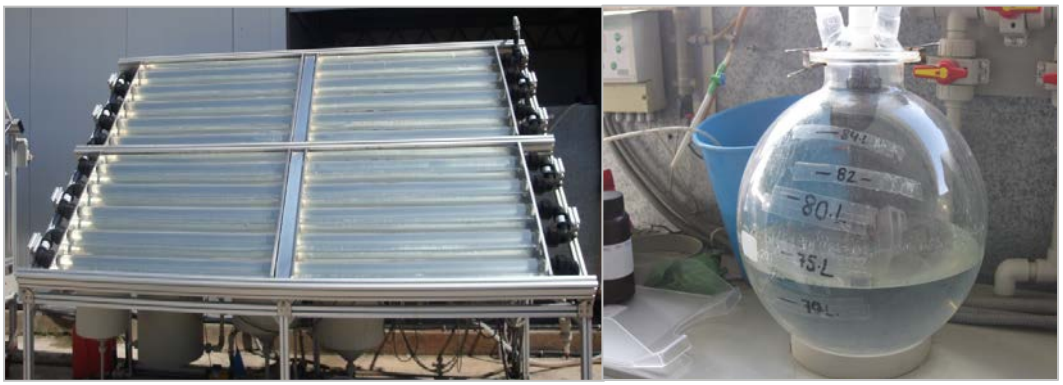

(b)

Picture 2.1 Solar pilot plant at: (a) PSA and (B) UCY.

Both pilot plants comprised of glass tubes mounted on a fixed platform tilted at the local latitude (37^o at PSA; 35^o at UCY) and they were operated in batch mode. The reflecting surface is constructed of resistant and highly reflecting polished aluminium. The contaminated water flows directly from one tube to the other tank (meander flow) and finally to a reservoir. A centrifugal pump returns the water to the collectors in a closed circuit. The overall capacity of the reactor V_T consists of the total irradiated volume V_i (tubes volume) and the dead reactor volume (tank, piping and valves). Storage tank, flow meters, sensors (pH, DO and *T*), air blower, UV radiometer, control panel, pipes, and fittings complete the installations' configuration. The control panel is directly connected to a PC for the on-line data acquisition. Furthermore, three reagent tanks along with their dosing pumps are installed at both plants, which can automatically dose reagents (H_2SO_4, H_2O_2, $FeSO_4.7H_2O$) directly to the storage tank. The automated dosing system was not used for the experiments because both pilot plants were operated in batch mode. The temperature and pH in the reactor as well as the UV solar radiation was continuously recorded. The UV radiometer (Kipp & Zonen) at PSA; UV_air_ABC at UCY) is mounted on the platform of the CPCs. The flow diagram for each plant is illustrated in Schematic 2.3 (a, b) whereas the specific characteristics of each plant are presented in Table 2.4.

(a)

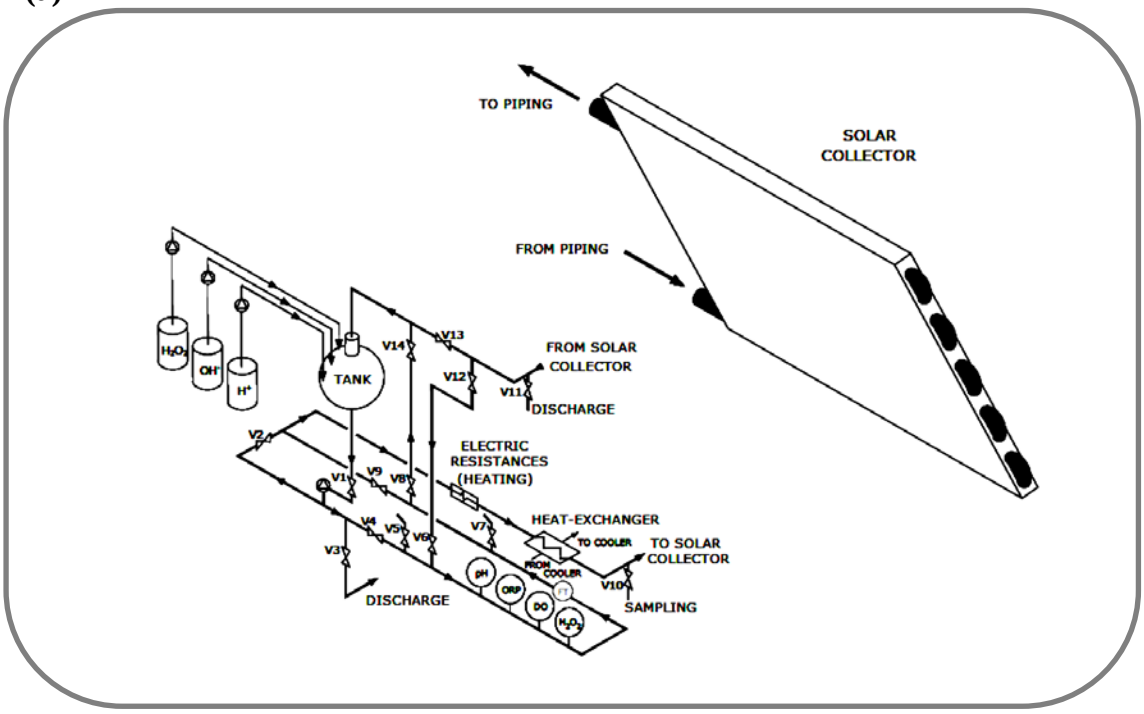

(b)

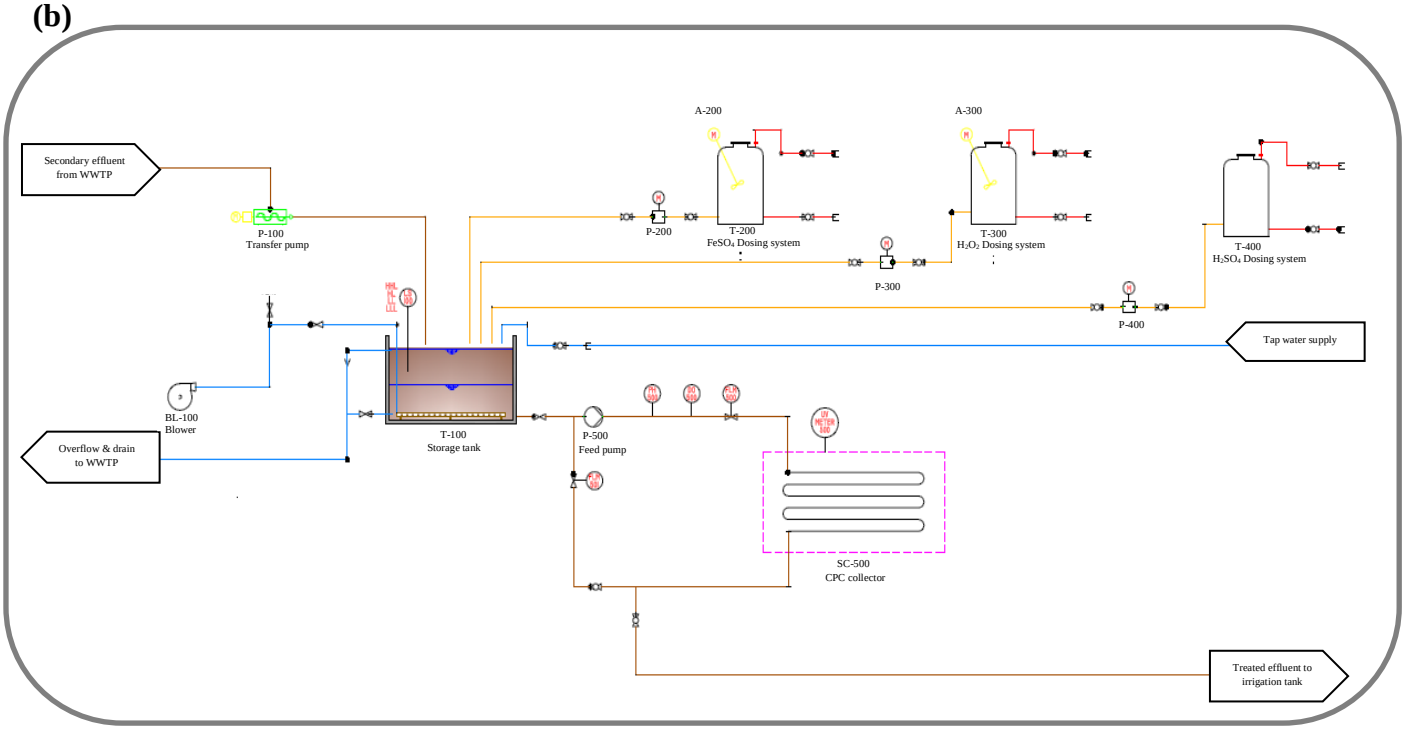

Schematic 2.3 Flow diagrams for the pilot plants used in this study:

(a) PSA; and (b) UCY.

During the loading of the reactor with the chemicals, the collectors were covered to avoid any photoreaction. At the beginning, the reactor was filled with the water matrix. It should be noted that, the storage tank of the pilot unit at the UCY is directly connected to the main secondary tank of the sewage treatment plant at the UCY campus. The secondary effluent before entering the tank passes through a cylindrical filter (pore size 200 μm) installed at the entrance of the storage tank. This was deemed necessary for avoiding fouling problems in the mechanical parts of the pilot plant.

Then, a predetermined volume of standard solution of OFX or TMP was added and after homogenization by stirring (15 min) a sample was taken representing the initial drug concentration. The pH was then adjusted with 2N H_2SO_4 and the appropriate volume of ferrous solution was added. Then the solution was stirred for 15 min. The hydrogen peroxide was then added. A sample was taken after some minutes of dark Fenton oxidation (zero-illumination time) and the collectors were uncovered. This was the time when photo-Fenton process began.

Pilot plant A was used for experiments where the initial concentration of the selected compounds was 10 mg L^{-1} and samples were withdrawn during the process when the hydrogen peroxide was completely consumed and another dose was added. The experiments normally lasted 4-5 hours and in the case of experiments which lasted longer than that, the plant was covered at the end of the day and the next day after recirculation for 15 min, a sample was taken, peroxide was added and the covers were removed again. Pilot plant B was used for experiments where the initial concentration of the examined compounds was 100 μg L^{-1} with an excess of hydrogen peroxide. The decision to examine the concentration levels 10 mg L^{-1} and 100 μg L^{-1} was based on the reasons stated in the previous chapter in section 1.4

Table 2.4 Main characteristics of the pilot plants used in this work.

Pilot plant	**A**	**B**
Platform slope (^{o})	37	35
Coordinates	Latitude: 37° N Longitude: 2.27° W	Latitude: 35° N Longitude: 33.25 E
Modules	4	2
Total volume V_T (L)	85.4	250
Irradiated volume V_i (L)	44.6*	85.4
Number of tubes	20	24
Tube material	Borosilicate	Borosilicate
Tube length (mm)	1320	1500
Diameter (mm)	50	50
Storage tank material	Borosilicate	Stainless Steel
Flow (L h^{-1})	1500	600
UV meter	Kipp & Zonen	UV_air_ABC
T sensor	PT-100	PT-100
Cover material	Tailor-made aluminium sheets	Thick grey plastic sheet

* The irradiated volume in the solar collector can vary between 8.9 L and 44.6 L, corresponding to uncovering 20% and 100% of the collector surface, respectively. This can be done by covering the corresponding part of the collector with tailor-made aluminium sheets.

All runs in bench and pilot scale experiments were performed in triplicate and mean values are quoted as results. The uncertainty in this assay, quoted as the relative standard deviation (RSD) of three separate measurements, was never higher than 20%.

2.3 Analytical methods

2.3.1 UV/Vis Spectrophotometer

Absorbance spectroscopy involves comparing the light transmitted through a blank to the light transmitted through an absorbing species solution. If the incident light (at a specific wavelength, λ) has intensity I_0, and it passes through a sample that absorbs at the wavelength λ, the light intensity, I, leaving the sample is attenuated. These two quantities are related by the molar extinction coefficient at the wavelength of interest, ε_λ (L mol^{-1} cm^{-1}), the concentration of the absorbing species, C (mol L^{-1}), and the length of the path that the light traverses through the sample, l (cm) according to Lambert-Beer's law (Ochsenkuehn-Petropoulou, 2006).

$$I = I_0 e^{-\varepsilon_\lambda C l} \tag{2.1}$$

The eqn. (2.1) can be transformed to eqn. (2.2).

$$-log\left(\frac{I}{I_0}\right) = \varepsilon_\lambda C l = A \tag{2.2}$$

The quantity that is measured in absorption spectroscopy is the logarithmic term, which is commonly called absorbance, A.

The photometric measurements and recording of UV spectra were performed using a UV-Vis Jasco V-530 spectrophotometer at UCY and a Unicam-2 spectrophotometer at PSA.

UV/Vis spectrophotometry, during the experiments performed at UCY, was also used to evaluate the conversion of the OFX substrate in the photo-treated samples (in bench scale experiments). The conversion of OFX was carried out by measuring the absorbance of the treated solution at 288 nm. This wavelength corresponds to the absorption of the aromatic ring of the OFX molecule. Figure 2.1 illustrates the

absorption spectra of wastewater with and without OFX (WW+OFX, WW) at pH=8.0.

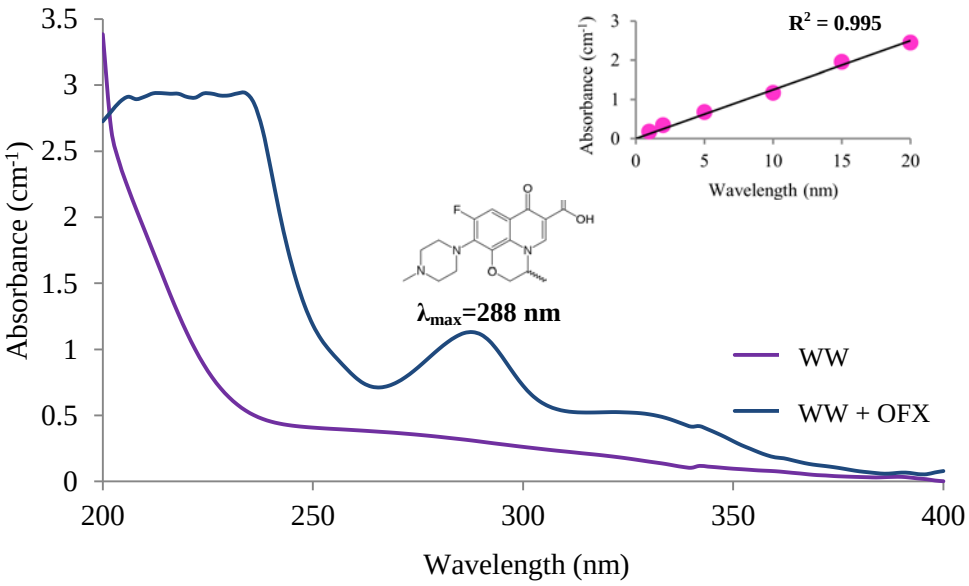

Figure 2.1 UV absorbance spectrum of wastewater (WW) and wastewater spiked with 10 mg L^{-1} OFX (WW+OFX). Inset graph: Calibration curve for OFX spiked wastewater solutions demonstrating linearity in the range of 0-20 mg L^{-1}.

A calibration curve was established using spiked wastewater samples with various concentrations of OFX. Linear correlation was observed up to 20 mg L^{-1} of OFX (Inset graph of Figure 2.1). It is important to mention that the UV absorbance measurements at 288 nm of the treated solutions represent both the concentration of the non-oxidized parent compound and the potentially produced oxidation by-products that may also absorb at the same region. The term 'substrate conversion' is used to express the conversion of both the parent compound and the oxidation by-products resulted by the photocatalytic process (Hapeshi et al., 2010).

2.3.2 High performance liquid chromatography with diode array detector (HPLC-DAD)

High performance liquid chromatography (HPLC) is a dynamic physicochemical method of separation in which the components to be separated are distributed between two phases, one of which is stationary (stationary phase) while the other (mobile phase) moves relatively to the stationary phase (McDonald, 2009 Waters Corporation). The stationary phase may be a solid or a liquid that is immobilized or adsorbed on solid particles. The mobile phase can be run as a single or mixed solvent at a constant composition (isocratic elution) or two (or more) separate mobile phases can be pumped simultaneously at varying concentrations (gradient elution).

The sample solution is injected into the mobile phase through the injector port. As the sample solution flows with the mobile phase through the stationary phase, the components of that solution will migrate according to the non-covalent interactions of the compounds with the two phases. These interactions determine the degree of migration and separation of the components contained in the sample. For example, solutes which have stronger interactions with the mobile phase than with the stationary phase will elute from the column faster and thus have a shorter retention time (t_R). The composition of the mobile phase can be modified in order to manipulate the interactions of the sample and the stationary phase. Additionally, in order to improve the separation and peak resolution, the pH of the mobile phase can be adjusted accordingly.

The type of liquid chromatography (LC) used for the analytical determinations in this thesis was a reversed phase LC. The separation mechanism in reversed phase LC depends on the hydrophobic binding interaction between the solute molecule in the mobile phase and the hydrophobic stationary phase. Reverse phase operates by using

a stationary phase that consists of silica-based packings with n-alkyl chains (e.g. C_8, C_{18}) covalently bound to them. C_8 signifies an octyl chain and C_{18} an octadecyl ligand in the silica medium. The distribution of the solute between the two phases depends on the binding properties of the medium, the hydrophobicity of the solute and the composition of the mobile phase. The more hydrophobic the medium on each ligand, the greater is the tendency of the column to retain hydrophobic compounds.

A UV-diode array (UV-DAD) was used as detector in the HPCL system of this study. A diode array consists of a number of photosensitive diodes placed side by side and insulated from one another in the form of a multi-layer sandwich. The light source is usually polychromatic (*e.g.* light from a deuterium lamp) and after passing through the cell, the light is dispersed by a quartz prism or a diffraction grating onto the surface of the diode array. Many organic compounds have characteristic spectra in the UV which can be used to help identify the substance passing though the sensor cell. The analytes eluted through the sensor cell and all the outputs from the array can be processed by a computer device. The result is used to construct absorption spectra that can be compared with standard spectra for identification purposes.

An HPLC-UV-DAD system at PSA (Agilent Technologies, series 1100) was used to monitor the concentration of the parent compounds during photodegradation. Chromatographic separation was achieved on a C_{18} column (LUNA®, 5 μm, 3×150 mm from Phenomenex). The elution was isocratic (0.5 mL min^{-1}) and the mobile phase consisted of a mixture of 10% methanol HPLC grade and 90% ultrapure water (Millipore) with 0.25 mM formic acid for TMP and a mixture of 10% acetonitrile HPLC grade and 90% ultrapure water (Millipore) with 25 mM formic acid for OFX. Samples were filtered through a 0.22 μm filter (Millipore) and transferred into HPLC vials. The detection of TMP and OFX was done at 254 nm (t_R=6.4 min) and 290 nm

(t_R=12 min), respectively. The system control and the data evaluation were conducted via a PC interface with Agilent ChemStation® software. Schematic 2.4 depicts the HPLC instrument used for the analytical determinations along with the schematic representation of the chromatographic process.

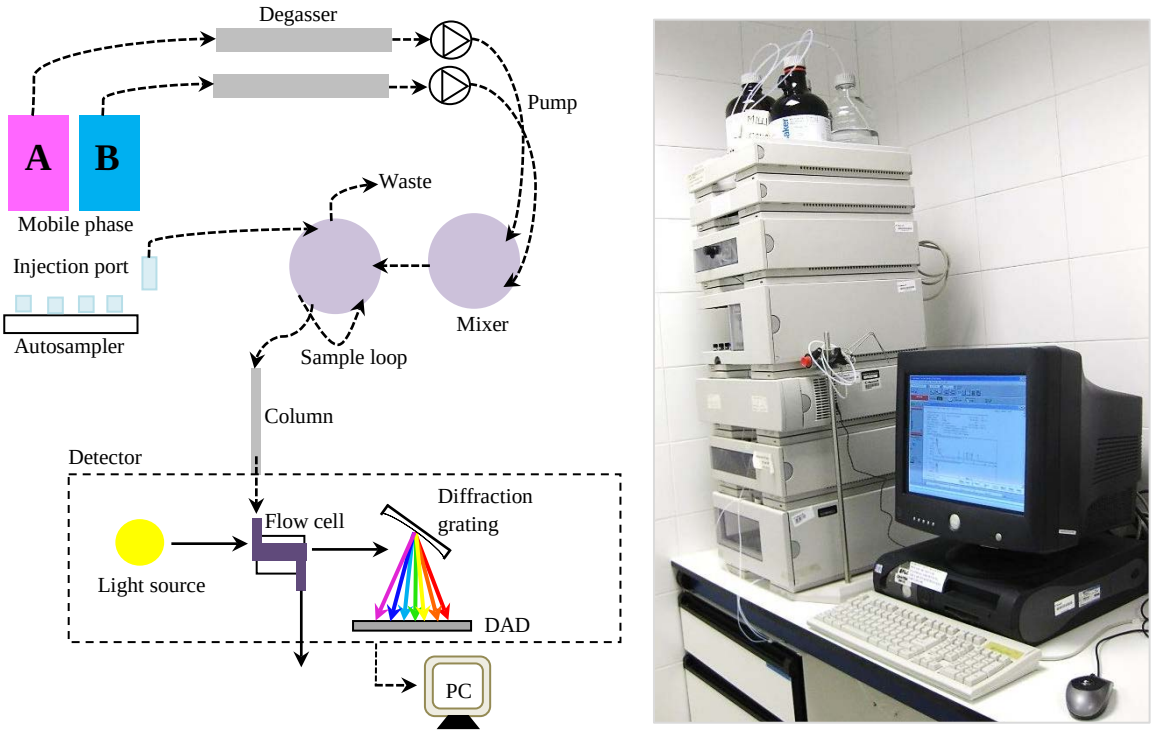

Schematic 2.4 Description and picture of the HPLC (Agilent 1100) used for the analytical determinations at PSA.

2.3.3 Ultra performance liquid chromatography tandem mass spectrometer (UPLC-MS/MS)

The recently introduced improvements of LC, like the use of ultra-performance liquid chromatography (UPLC), has made this technology more attractive and powerful when combined with tandem mass spectrometry (MS/MS) (Petrović et al., 2007). An ultra-high pressure system operates using small particle-packed columns with small diameter (< 2 μm), which allows for operation at high pressures (> 15000

psi), providing an increased chromatographic resolution compared to HPLC (Jin et al., 2010). The high speed of analysis and low mobile phase flow rates enabling direct introduction of analytes into the ion source from LC without splitting are some of the main advantages of the UPLC-MS/MS method when compared to other multi-residue methods using HPLC for analytes separation (Cahill et al., 2004; Gros et al., 2006). Furthermore, improved tandem quadrupole (QqQ) mass analyzers have become the favoured analytical tool for the analysis of pharmaceuticals in environmental samples because their application has allowed the simultaneous determination of a great number of compounds, especially polar compounds that previously were difficult or even impossible to analyze (Batt et al., 2008; Chang et al., 2008; Li et al., 2009).

Mass spectrometry (MS) is based on the production of gas-phase ions of a compound. Each product ion derived from the molecular ion can undergo fragmentation. These ions are separated according to their mass-to-charge ratio (*m/z*) and detected in proportion to their abundance. A mass spectrometer contains the following elements: a sample inlet to introduce the compound that is analyzed (LC outlet); an ionization source to produce ions from the sample; one or several mass analyzers to separate the ions; a detector to measure the abundance of the produced ions and produce electrical signals; and finally a data processing system that produces the mass spectrum in a suitable form (Hoffmann and Stroobant, 2007).

A variety of ionization techniques are used for MS. Electrospray ionization (ESI) is one of the most common ionization techniques that is widely used for MS applications. ESI is produced by applying a strong electric field, under atmospheric pressure, to a liquid passing through a capillary tube with a weak flow (1-10 μl min^{-1}). The electric field is obtained by applying a potential difference of 3-6 kV between this

capillary and the counter-electrode, separated by 0.3-2 cm, producing electric fields of the order of 10^6 V m^{-1}. This field induces a charge accumulation at the liquid surface located at the end of the capillary (the shape of the droplet appears as Taylor cone), which will break to form highly charged droplets. A gas injected coaxially at a low flow rate allows the dispersion of the spray to be limited in space. These droplets then pass either through a curtain of heated inert gas (nitrogen) or through a heated capillary to remove the last solvent molecules. The solvent contained in the droplets evaporates, which causes them to shrink and their charge per unit volume to increase. Under the influence of the strong electric field, deformation of the droplets occurs and finally smaller droplets are released (Hoffmann and Stroobant, 2007). These small droplets will continue to lose solvent and when the electric field on their surface becomes high enough, desorption of analyte ions from the surface occurs (Schematic 2.5).

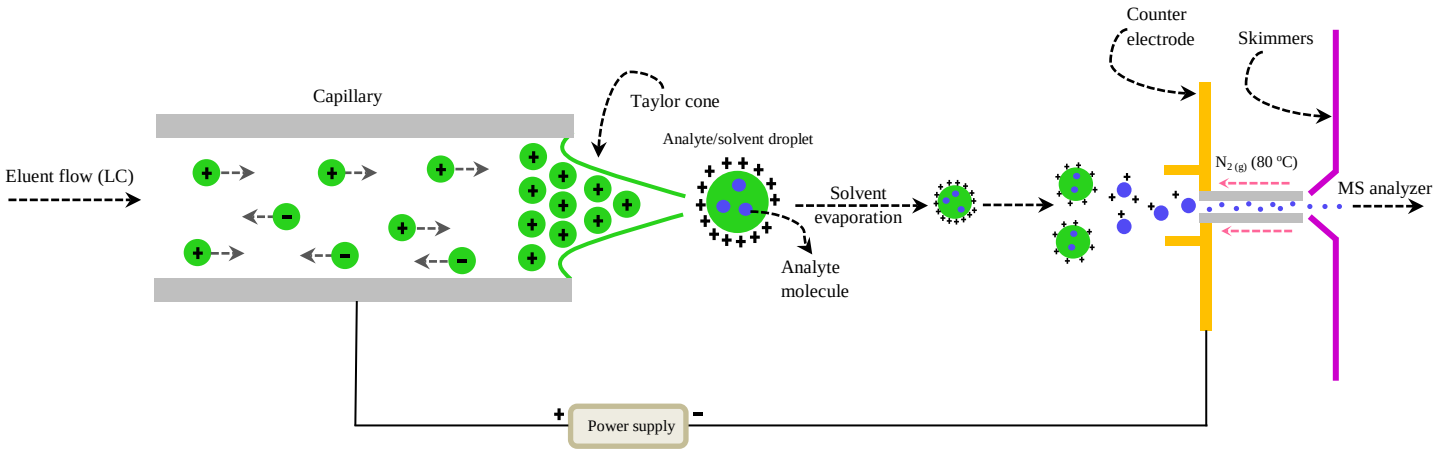

Schematic 2.5 Diagram of ESI.

The quadrupole analyzer (Schematic 2.6) is a device which uses the stability of the trajectories in oscillating electric fields to separate ions to their *m/z* ratios. Quadrupole

analyzers consist of four parallel rods of circular section. The analyzer used in this work consists of three single quadrupole mass analyzers (Triple quadrupole). The first and the latter quadrupole are symbolized by upper case Q whereas the centre quadrupole, which is a quadrupole using radio frequencies only, with a lower case q. The first quadrupole Q_1 acts like a mass filter where ions with specific *m/z* value can pass; in the second quadrupole q_2 a collision gas (argon) is introduced at a pressure such that an ion entering q_2 undergoes one or several collisions which generate small ion fragments; and in quadrupole Q_3 the ion fragments are analyzed.

.

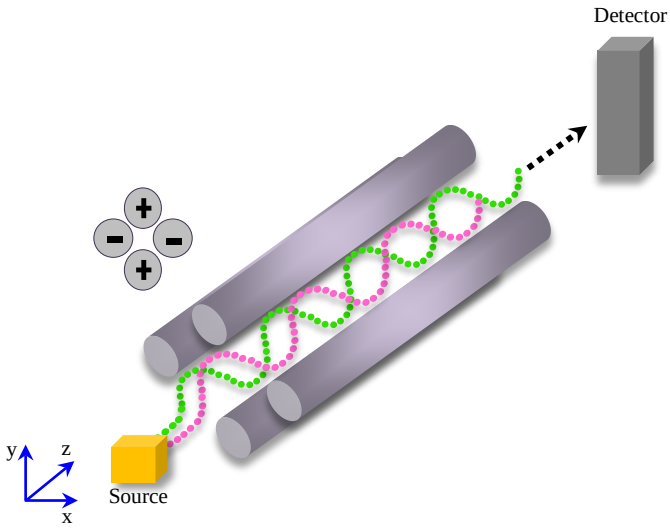

Schematic 2.6 Quadrupole mass analyzer.

All analyses at UCY were performed on an ACQUITY TQD UPLC-MS/MS system (Waters Corporation) using a method specifically developed for this application (Picture 2.2). Data acquisition was performed with positive electrospray in multiple reaction monitoring mode (MRM), recording the transitions between the precursor ion and the most abundant fragment ions. The most abundant transition product ion was typically used for quantification of the target compound while the second

transition product together with the ratio of the intensities of the two transitions, were used for confirmation purposes.

Column BEH Shield RP18 (1.7 μm; 2.1×50 mm; Waters) was used for the chromatographic analysis with mobile phase consisting of 0.1 mM ammonium acetate in water + 0.01% formic acid (eluent A) and 0.1 mM ammonium acetate in methanol + 0.01% formic acid (eluent B). Oasis HLB cartridges (200 mg, Waters) were used for the sample preconcentration.

Picture 2.2 ACQUITY TQD UPLC-MS/MS system (Waters) used for the analytical determinations at UCY.

The development of the chromatographic method and its optimization was part of the present thesis; therefore a detailed analysis on the chromatographic method applied is described thoroughly in CHAPTER 3.

2.3.4 Quadrupole-Time of Flight-tandem mass spectrometer (Q-ToF-MS^2)

The Time of Flight (ToF) analyzer separates ions after their initial acceleration by an electric field, according to their velocities when they pass in a free-field region that is called flight tube. Ions are produced from a source (*e.g.* ESI, laser) and then these ions are accelerated towards the flight tube by a difference of potential applied between an electrode and an extraction grid. As all the ions acquire the same kinetic energy, ions characterized by a distribution of their masses and their velocities. When leaving the acceleration region, they enter into a field-free (E=0) region where they are separated according to their velocities, before reaching the detector positioned at the end of the flight tube. The principle of operation of ToF instrument is illustrated in Schematic 2.7.

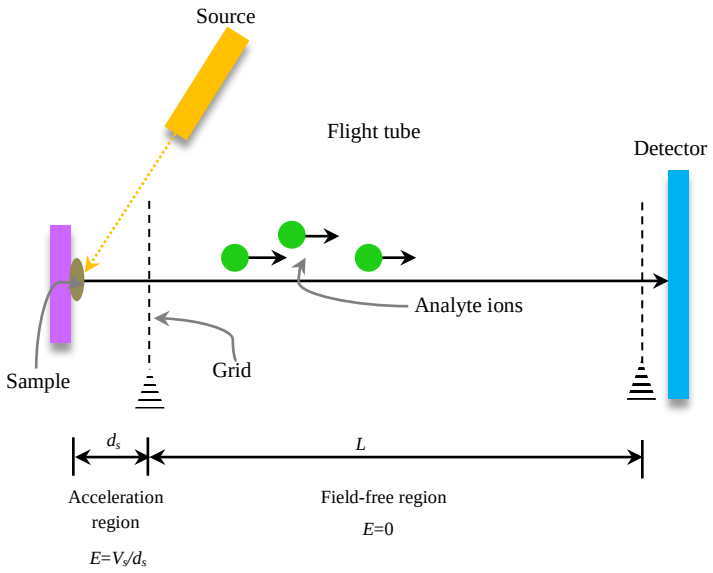

Schematic 2.7 Principle of operation of a ToF instrument. After their formation, the ions are subject to the applied electric field. Ions are continuously accelerated and drift in a free-field region. They travel through this region with a velocity that depends on their *m/z* ratios.

Mass-to-charge ratios are determined by measuring the time (known as time of flight) that ions take to move through the field-free region between the source and the detector (Cotter, 1992).

$$t^2 = \frac{m}{z}\left(\frac{L^2}{2eV_s}\right) \quad (2.3)$$

This equation shows that *m/z* can be calculated from a measurement of t^2, the terms in parenthesis being constant. Moreover, this equation shows that, all other factors being equal, the lower the mass of an ion, the faster it will reach the detector.

The intermediates generated during the pilot-scale solar Fenton treatment of TMP were monitored on Q-ToF-MS (Waters) connected to an UPLC ACQUITY system (Waters) equipped with a reverse phase C_{18} analytical column (1.7 μm; 2.1×50 mm) (Picture 2.3). The injection volume was 10 μL. Column temperature was maintained at 40 ^{o}C. Mobile phases A and B were acetonitrile and water with 0.01% formic acid, respectively at a flow rate of 0.4 mL min^{-1}. The chromatographic method held the initial mobile phase composition (5% A) constant for 0.5 min, followed by a linear gradient to 95% A in 8.5 min and then maintained at 5% for 2 min. The analysis lasted 11 min. The Q-ToF-MS system was equipped with an electrospray interface operating in positive mode. The accurate mass and composition for the precursor and the fragment ions were calculated using software MassLynx^{TM} incorporated in the instrument. The above analysis took place at CSIC. Detailed information is discussed further in CHAPTER 6.

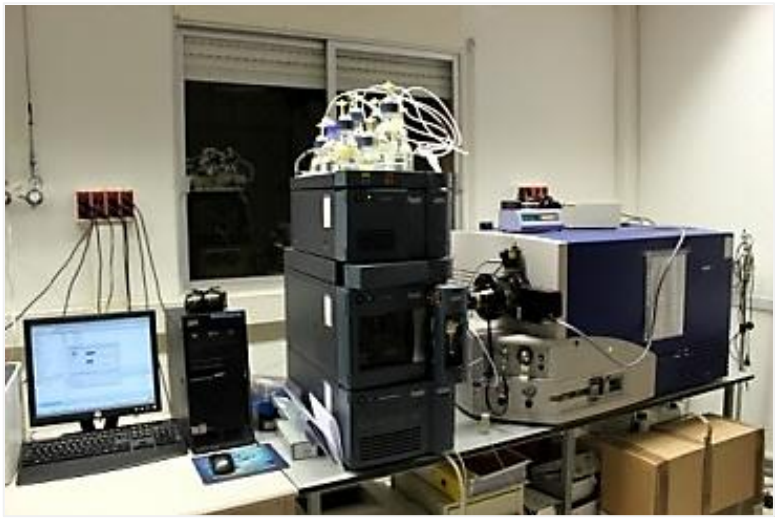

Picture 2.3 Q-ToF-MS system used for the analytical determinations at CSIC.

2.3.5 Ion-exchange chromatography (IC)

Separation in ion-exchange chromatography is based mainly on differences in the ion-exchange affinities of the sample components. Separation is obtained since different substances have different degrees of interaction with the ion exchanger due to differences in their charges, charge densities and distribution of charge on their surfaces. These interactions can be controlled by varying conditions such as ionic strength and pH.

An ion exchanger consists of an insoluble matrix to which charged groups have been covalently bound. The most common ion exchangers are synthetic resins. There are two types of resins depending on the nature of the ion to be retained. These are the anion exchangers (resin with positive functional groups) or cation exchangers (resin with negative functional groups) (Schematic 2.8).

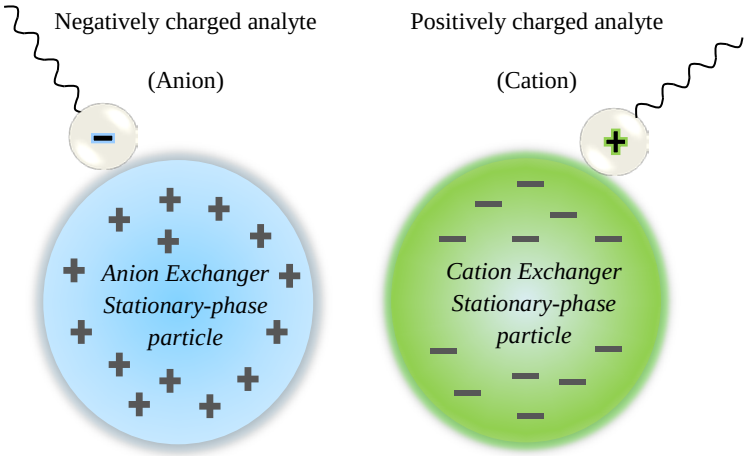

Schematic 2.8 Ion-exchange chromatography principle.

The mobile phase usually consists of an aqueous solution containing ions that compete with the analytes for the active sites on the stationary phase. In the case of anion IC the most common mobile phases contain hydrogen carbonate/carbonate, hydroxide or boric acid/tetraborate. Cation IC mobile phase usually contains sulphuric acid, methanesulphonic acid or hydrochloric acid.

The detector is a membrane suppression electric conductivity detector which neutralises the eluent by supplying hydronium or hydroxyl ions generated by electrolysis via ion exchange membranes. The response of the electric conductivity detector does not have a linear response over a wide dynamic range; therefore the calibration applied in this work consisted of three partial linear calibration curves (0.1-1, 1-10 and 10-50 mg L^{-1}). Operation and data analysis were done by a PC interface with Chromeleon® software from Dionex.

The organic acids generated during the photo-Fenton process were separated on a Dionex DX-600 Ion Chromatograph in anion mode, equipped with an auto sampler (Dionex AS40), a quaternary gradient pump (Dionex GP50), a thermostatic column

oven (Dionex LC30) and a conductivity detector (Dionex ED50). The mobile phase passes through an anion trap column (Dionex Ionpac ATC-3) before the injection valve to guarantee the purity of the mobile phase. Then the eluent passes through a precolumn (Dionex Ionpac AS11-HC 4×50 mm), the chromatographic column (Dionex Ionpac AS11-HC 4×250 mm), the suppressor (Dionex ASRS-Ultra II 4 mm) and finally the electric conductivity detector. Samples were filtered using 0.22 μm syringe driven filters (Millipore) into the sample vials provided for the Dionex Autosampler. Standard solutions were injected with every run to ensure the correct operation of the system.The gradient elution was performed using NaOH (1-60 mM) solution at 1.5 mL min^{-1}. The eluent program is shown in Table 2.5.

Table 2.5 Gradient program and operating conditions for the ion-exchange system in anion mode.

Acids	**Flow/Mobile phase**	**Gradient**
Acetic	1.5 mL min^{-1}	80/20: 0-18 min
Oxalic	H_2O / 5 mM NaOH	85/15: 18-28 min
Propionic	H_2O / 100 mM NaOH	70/30: 28-38 min
Formic		

2.3.6 Total organic carbon (TOC) analyzer

In order to evaluate the extent of mineralization, dissolved organic carbon (DOC) was monitored by direct injection of the filtered samples into a Shimadzu TOC analyzer. The basic principle for the quantitation of TOC relies on the oxidation of organic

matter present in water sample to CO_2 by dry combustion. The final determination of CO_2 is carried out by infrared spectrometry (ISO 8245:2000).

Prior to the determination of TOC, a filtered and acidified water sample is sparged with oxygen to remove total inorganic carbon (TIC). The acidification is usually performed using HCl solution. The water is then injected onto a combustion column packed with platinum-coated alumina beads held at 680 °C. Non-purgeable organic carbon compounds are combusted and converted to CO_2 and then a CO_2 free carrier gas delivers the sample combustion products to the cell of a non-dispersive infrared detector (NDIR) gas analyser, where CO_2 is detected. The absorbance of CO_2 generates a signal which is evaluated by the equipment's software and which is proportional to the quantity of carbon in the sample.

The TOC analysers used in this study were provided by Shimadzu (Shimadzu TOC-$V_{CPH/CPN}$; Shimadzu-5050A) both equipped with an auto sampler. Due to the narrow capillary tubes in both analyzers, any suspended solids in the sample have to be removed prior the injection in the system. Therefore, the analyzers can only be used to measure dissolve organic carbon (DOC). Samples (~20 mL) were filtered through 0.22 μm pore size syringe driven filters (Millipore) prior to direct injection into the TOC system. Each measurement was based on two injections with a maximum variance coefficient of less than 2% (otherwise automatic sample re-injection takes place). The calibration curve was made from a standard aqueous solution of potassium hydrogen phthalate (KHP) over the range 0-20 mg L^{-1}. Calibration and quality maintenance were performed regularly to ensure the correct operation of the equipment.

2.3.7 Other analytical measurements

2.3.7.1 Biological oxygen demand (BOD)

The BOD test measures the molecular oxygen utilized during a specified incubation period for the biochemical degradation (in presence of microorganisms) of organic material (carbonaceous demand) and the oxygen used to oxidize inorganic material such as sulfides and ferrous iron.

The method consists of filling with sample, to overflowing, an airtight bottle of the specified size and incubating it at the specified temperature (20 ^{o}C) for 5 days. Dissolved oxygen (DO) is measured initially and after incubation, and the BOD is computed from the difference between initial and final DO. Because the initial DO is determined shortly after the dilution is made, all oxygen uptake occurring after this measurement is included in the BOD measurement. BOD measurements in a 5-day test period are known as BOD_5 (APHA 5210B). BOD was determined using the 444406 OxiDirect meter.

2.3.7.2 Chemical oxygen demand (COD)

Chemical oxygen demand (COD) is defined as the quantity of oxygen which is required to oxidize the organic matter present in a sample under controlled conditions (temperature, time, oxidizing agent).

The organic matter in a sample is oxidized in an acidic solution of potassium dichromate ($K_2Cr_2O_7$) in presence of silver sulfate (Ag_2SO_4) which acts as a catalyst. Under these conditions and when the sample is digested, dichromate ion ($Cr_2O_7^{2-}$) is reduced to the chromic ion (Cr^{3+}). The produced Cr^{3+} ions, which generate a green color, are measured photometrically (APHA 5220D).

Merck®Spectroquant kits were used for the COD determination. The measurement range for the samples analysed was between 10 and 150 mg_{O2} L^{-1}. 3 mL of a sample, which was filtered with 0.22 μm filters (Millipore), was mixed with the reaction solution in the test tube and heated for two hours at 148 ^{o}C in a thermo block. After cooling down to room temperature the test tube was introduced into the photometer (Photolab S6) and measured at 445 nm. The calibration was made from a standard aqueous solution of potassium hydrogen phthalate (KHP) over the range 10-150 mg L^{-1}.

2.3.7.3 Hydrogen peroxide concentration

The residual peroxide concentration during photo-Fenton process is a very important parameter to evaluate. When H_2O_2 is completely consumed, which can happen in a very short time depending on the organic matter concentration, the degradation reaction practically stops making new additions of the oxidant necessary.

Hydrogen peroxide consumption during the solar Fenton process was determined by a fast, simple spectrophotometric method using ammonium metavanadate in acidic medium, based on the red-orange color of peroxovanadium cation (VO_2^{3+}) formed during the reaction of H_2O_2 with metavanadate, at λ_{max}=450 nm (Nogueira et al., 2005). The presence of H_2O_2 in the treated samples was also monitored using Merckoquent® test sticks.

The procedure for measuring H_2O_2 is as follows: 4 mL of sample was mixed with 4 mL of ammonium metavanadate solution and 2 mL of deionized water. The reaction generates a red-orange color which does not change within 2 hours. The absorbance of the samples was measured at 450 nm using a spectrophotometer and the H_2O_2 concentration was obtained by a calibration curve.

2.3.7.4 Metals

Metals present in the wastewater samples were determined by atomic absorption spectrometry. In flame atomic absorption spectrometry, a sample is aspirated into a flame and atomized. A light beam is directed through the flame, into a monochromator, and onto a detector that measures the amount of light absorbed by the atomized element in the flame. Because each metal has its own characteristic absorption wavelength, a source lamp composed of that element is used. The amount of energy at the characteristic wavelength absorbed in the flame is proportional to the concentration of the element in sample. Stock standard solutions can be obtained from several commercial sources. A standard curve is obtained by plotting the absorbance of standards against the concentration. The sample concentration is computed directly from the standard curve (APHA 3111C).

2.3.7.5 Nitrates (NO_3^-)

Nitrates (NO_3^-) are reduced to nitrites (NO_2^-) when passed through a copperized cadmium reduction column. This method uses commercially available Cd granules treated with copper sulfate ($CuSO_4$) and packed in a glass column. The column is activated by passing through it, 100 mL of a solution (10 mL min^{-1}) composed of 25% standard solution of nitrates (NO_3^-) and 75% NH_4Cl-EDTA solution. The NO_2^- produced is determined by diazotizing with sulphanilamide and coupling with N-(1-naphthyl)-ethylenediamine dihydrochloride (colour reagent) to form a highly coloured azo dye that is measured photometrically (λ=543 nm). Concentration of NO_3^- in sample is determined by comparison of absorbance signal with calibration results obtained from standards of varying concentrations (APHA 4500E).

2.3.7.6 Orthophosphates (PO_4^{3-})

Ammonium molybdate and potassium antimonyl tartrate react in acidic medium with orthophosphate ions to form a heteropoly acid-phosphomolybdic acid. Ascorbic acid reduces this acid to phosphomolybdenum blue (PMB) that is determined photometrically. A standard curve is obtained by plotting absorbance of standards against phosphate concentration. The sample PO_4^{3-} concentration is calculated directly from the standard curve (APHA 4500-PE).

2.3.7.7 pH and conductivity

Laboratory pH measurements were carried out using a PL-600 lab pH meter (EZDO pH/mV/Temp meter) equipped with a standard glass electrode. A calibration of the pH-meter was performed using two standard buffer solutions at pH 4.00 and pH 7.00 (obtained from Panreac).

In the pilot plant A (PSA), the pH was measured with a WTW® Sensolyt SEA electrode inserted in a WTW Sensolyt® 700IQ sensor having integrated internal temperature compensation. The WTW sensor was connected to the WTW IQ sensornet® controller for signal processing and re-transmission. In the pilot plant B (UCY) pH measurements were performed with a Dulcometer® pH-meter provided by Prominent (Germany). The pH-meter system includes a pH controller, a pH sensor and a pH probe. A portable pH-meter (Gondo EZDO) was also used. Conductivity measurements were carried using an inoLab Multi Level 3 WTW meter.

2.3.7.8 Total iron concentration

Total iron concentration was monitored by colorimetric determination with 1,10-phenanthroline, according to ISO 6332:1996, using a spectrophotometer. Dissolved iron forms a stable red-orange colored complex with 1,10-phenanthroline, which is strongly absorbed at 510 nm. A series of iron standards is measured at this wavelength and a calibration plot of absorbance vs. concentration is prepared. The absorbance of the unknown sample is measured and the calibration curve is used to calculate the concentration of iron in the sample.

4 mL of sample was mixed with 1 mL of 1,10-phenanthroline (0.1% w/v in deionised water), 1 mL of acetate buffer solution (250 g L^{-1} ammonium acetate and 700 mL acetic acid in deionised water), and a spatula tip of ascorbic acid. After some minutes of reaction the absorbance was measured at 510 nm in a spectrophotometer against a blank (1,10-phenantroline was replaced with the same volume of distilled water). The ascorbic acid reduces any Fe^{3+} to Fe^{2+}, and degrades H_2O_2, so that the iron was measured is the total iron present in the sample.

2.3.7.9 Total nitrogen

Total nitrogen can be determined through oxidative digestion of all nitrogenous compounds to nitrate according to the persulfate method. Alkaline oxidation at 100 ^{o}C to 110 ^{o}C converts organic and inorganic nitrogen to nitrate. Total nitrogen is determined by analyzing the nitrate in the digestate. A standard curve is prepared by plotting the absorbance of the standard nitrate solutions carried through the digestion procedure against their concentrations. The total N of the sample is computed by the standard curve (APHA 4500-NC).

The total N values obtained from the method described above were confirmed using another method (Koroleff's method). For this method, Merck®Spectroquant kits were used. Organic and inorganic nitrogen compounds are transformed into nitrate (NO_3^-) according to Koroleff's method by treatment with an oxidizing agent in a thermoreactor. In a solution acidified with sulfuric and phosphoric acid, the nitrates react with 2,6-dimethylphenol to form 4-nitro-2,6-dimethylphenol that is determined photometrically.

2.3.7.10 Total phosphorus

Total phosphorus is measured by the persulfate digestion procedure. The sample is digested with a sulfuric acid solution containing ammonium persulfate. Ammonium molybdate and potassium antimonyl tartrate react in acidic medium with orthophosphate ions to form a phosphomolybdic acid. Ascorbic acid reduces this acid to phosphomolybdenum blue (PMB) that is determined photometrically. A standard curve is prepared by plotting the absorbance of the standard P solutions carried through the digestion procedure against their concentrations. The total P of the sample is computed by the standard curve (APHA 4500-PB).

2.3.7.11 Total suspended solids (TSS)

Total suspended solids (TSS) refer to matter suspended in water or wastewater. A well-mixed sample is filtered through a weighed standard glass-fiber filter (Sartorius Stedim Biotech) and the residue retained on the filter is dried to a constant weight at 103 ^oC to 105 ^oC. The increase in weight of the filter represents the TSS (APHA 2540 D).

$$mg_{TSS}/L = \frac{(A-B)\times 100}{sample\ volume,mL} \quad (2.4)$$

where *A* is the weight of filter with the dried residue (mg) and *B* is the weight of filter (mg).

2.4 Toxicity assays

Toxicity bioassays are applied worldwide as tools for wastewater quality control. These tests have the ability to distinguish different degrees of toxicity and toxic specificity of the compounds on target organisms (Hernando et al., 2005). Therefore, the use of single organisms to evaluate wastewater toxicity cannot provide a real assessment of the risk. An appropriate way to assess the risk of wastewater is the use of variety of toxicity tests with representative organisms of different biological organization (Hernado et al., 2005).

Toxicity assays rely on measuring the response of test organisms exposed to contaminants compared to their response exposed to a control. The test organisms incorporated in these bioassays can be grouped in: microorganisms, plants and algae, invertebrates and fishes (Rizzo, 2011).

Toxicity measurements were carried out in samples at various times of the photocatalytic treatment using various types of toxicity assays. The toxicity assays used in the present study are: (i) Daphtoxkit F^{TM} toxicity test; (ii) Microtox$^{®}$ toxicity test; (iii) Respirometric test; and (iv) Phytotestkit microbiotest toxicity test.

It is important to mention that the H_2O_2 present in the solar Fenton treated samples could affect the toxicity measurements and therefore it had to be eliminated. The residual H_2O_2 was removed from the treated samples with catalase solution. Catalase is an enzyme which catalyzes the decomposition of H_2O_2 to water and molecular

oxygen. One unit of catalase corresponds to the amount of enzyme which decomposes 1 μmol H_2O_2 per minute at pH 7 and 25 °C.

2.4.1 Daphtoxkit F^{TM} toxicity test

This test, which is currently used in many laboratories worldwide for toxicity monitoring purposes, is based on the observation of the freshwater species *Daphnia magna* (Picture 2.4) immobilization after 24 and 48 hours of exposure in the samples. *Daphnia magna* is a component of freshwater zooplankton and it refers to group Arthropoda (phylum), Branchiopoda (class), and Daphniidae (family) (ISO 6341:1996).

The experimental procedure for conducting this assay was based on the ISO 6341 standard protocol. The water used to activate and hatch the organisms (72-90 h) was synthetic freshwater containing $NaHCO_3$, $CaCl_2$, $MgSO_4$ and KCl (dilution solution). Sufficient amount of dissolved oxygen (~5 mg L^{-1}) was achieved by aeration. The dilution water was prepared a day prior to its use, in order to provide oxygen saturation and ensure complete salts dissolution and homogenization. Cultures were grown under continuous illumination of 6000 lux at a constant temperature of 20-22 ºC. Appropriate adjustment of the pH value of the samples in the range of 7±0.5 was carried out with 1M solution of NaOH or HCl. Two hours before testing, the neonates were fed using a dilution of *Spirulina* microalgae in order to preclude mortality by starvation, thus avoiding biased test results. Analysis was carried out on specific test plates which were filled with the examined samples. For statistically acceptable evaluation of the effects, each test sample as well as the control, was tested in quadruplicate. After the transfer of five *Daphnia* neonates into the cells, the test plates were covered and incubated at 20 ºC in the dark. Observations of test populations

were made at 24 and 48 hours of exposure and any dead or immobilized neonates were recorded. The neonates were considered immobile, if after 24 or 48 h of incubation with the toxicant they remained settled at the bottom or did not resume swimming within the observation period. It should be noted that tests in which the control survival was less than 90% were invalid and were repeated.

Source: *http://en.wikipedia.org/wiki/File:Daphnia_pulex.png*

Picture 2.4 *Daphnia magna* species.

2.4.2 Microtox® toxicity test

The procedure employs the bioluminescent marine gram negative bacterium *Vibrio fischeri* (earlier referred as *Photobacterium phosphoreum*) as the test organism (Picture 2.5). Light production is directly proportional to the metabolic activity of the bacterial population and any inhibition of enzymatic activity causes a corresponding decrease in bioluminescence (Parvez et al., 2006). In this test, toxicity is assessed by measuring the extent to which light production by the bacteria is inhibited after they have been exposed to a sample (Jennings et al., 2001). A difference in light output (between the sample and the control) is attributed to the effect of the sample on the

bacteria. The main advantages of this toxicity assay include short time of analysis, simplicity of operation and cost effectiveness.

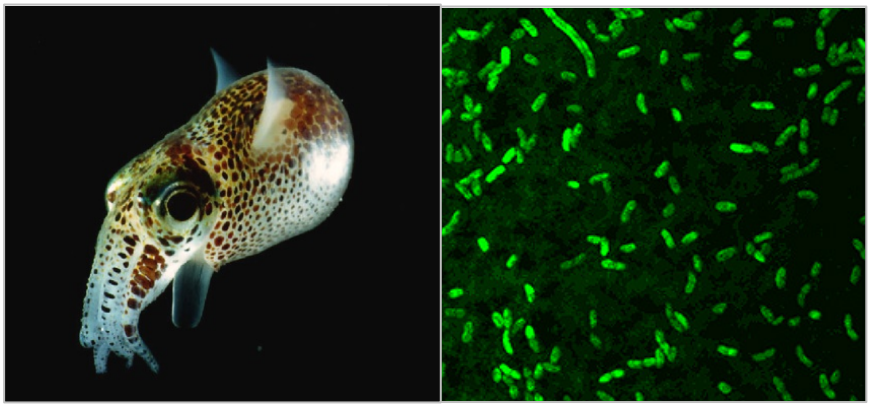

Source: *http://dels-old.nas.edu/oceans.html; http://www.flickr.com/photos/pabloo/page4/*

Picture 2.5 *Vibrio fischeri* species.

The experimental procedure for conducting the bacterial bioluminescence assay was based on the ISO 11348-3:2007 standard protocol and was carried out with a commercially available kit (Biofix®Lumi-10). The freeze-dried *Vibrio fischeri* (NRRL-B 11177) was reconstituted with 11 ml of 2% NaCl and incubating at 4 ^{o}C for 30 min and at 15 ^{o}C for 15 min before use. Samples were filtered through a 0.22 μm filter (Millipore) to remove suspended solids and hydrogen peroxide was removed with catalase. Adjustment of the samples pH to 7±0.5 was carried out prior to analysis while the osmotic pressure of the samples in order to obtain salinity 2% was adjusted with NaCl. 500 μL of bacterial suspension was transferred into a test vial (cuvette), which contained 5 mL of sample and 500 μL of saline solution (2% w/v NaCl solution). Temperature was kept at 15 ^{o}C. The (%) inhibition of chemiluminescence of bacteria was measured at 5, 15 and 30 min of time exposure and was compared

with a non-toxic control solution (2% NaCl solution). The measurements of light were made using a luminometer (spectra range: 380-630 nm).

2.4.3 Respirometric test

The activated sludge respiration inhibition test has been established as an effective method for evaluating the toxicity of chemicals to activated sludge bacteria. Respiration inhibition test evaluates the effect of a compound on microorganisms from activated sludge by measuring their respiration rate (uptake oxygen rate) in the presence of different concentrations of the test compound.

The principle of this test is based on the consumption of oxygen by the microorganisms present in the activated sludge. Its operation is based on a batch closed circuit in which the dissolved oxygen contained in the sludge is measured in a continuous mode. This dissolved oxygen is the result of the respiration of the activated sludge microorganisms in the process of the metabolism of the organic matter and its own consumption. The oxygen demand obtained by respirometry test has become an excellent control parameter, since it represents a direct measurement of the viability and proper activity of the microorganisms present in the activated sludge.

Activated sludge from the municipal WWTP of Almería was mixed with the samples in a respirometer BM-T (Surcis SA) equipped with a biological reactor of 1 L capacity, a temperature control system (to maintain the temperature by external circuit of 20 ^{o}C) and an oxygen meter (Stratos 2402 Oxy). The respirometric test instrumentation is shown in Picture 2.6.

Picture 2.6 Respirometric test instrumentation.

At first, activated sludge was collected from the municipal WWTP of Almería and maintained in aeration without the addition of organic source for a day in order to remove any traces of organic substrate and to obtain the sludge in endogenous respiration phase. The supply of oxygen was continuously maintained to keep the saturation in the water.

In addition, the amount of volatile suspended solids (g_{VSS} L^{-1}) present in the sludge was determined. In order to remove ammonia and therefore eliminate any possibility of nitrification, allylthiourea (ATU) was added to the sludge in the proportion of ATU 3 mg $(g_{VSS})^{-1}$ and left airing 30 minutes before starting the test. The analysis was performed comparing the bacterial activity developed in two essays: (i) the reference which consisted of 900 mL of sludge and 100 mL of distilled water with added substrate and; (ii) the mix which consisted of 900 mL of sludge and 100 mL of sample with added substrate.

The substrate was 0.5 g sodium acetate $(g_{VSS})^{-1}$ dissolved in 100 mL of distilled water. The test of the reference was extended until it reached the maximum respiration rate (R_{smax}). After obtaining the R_{smax} of the reference, the analysis was performed for each sample (Mix). This test was maintained during the same or longer time than the one needed for the reference to achieve R_{smax}.

If there is no toxicity, the respiration rate of the examined sample should be equal or higher than in the reference test. When $R_s << R_{smax}$ toxicity is expressed quantitatively through the inhibition percentage (I_s, %), determined as follows:

$$I_s(\%) = 100 \times \left(1 - \frac{R_S}{R_{smax}}\right) \quad (2.5)$$

2.4.4 Phytotestkit microbiotest toxicity test

The Phytotestkit microbiotest is measuring the decrease (or the absence) of germination and early growth of plants which are exposed directly to the samples spiked onto a thick filter paper. A control test was performed using tap water. The plants used for the Phytotestkit microbiotest were: the monocotyl Sorgho (*Sorghum saccharatum*), the dicotyl garden cress (*Lepidium sativum*) and the dicotyl mustard (*Sinapis alba*) (Picture 2.7). These species are frequently used in phytotoxicity analyses due to their rapid germination and growth of roots and shoots and their sensitivity to low concentrations of phytotoxic substances.

Seeds of the selected test plant(s) are positioned at equal distance near the middle ridge of the test plate, on a black filter paper placed on top of the spiked filter paper (20 mL sample). After closing the test plates with their transparent cover, the test plates are placed vertically in a holder and incubated at 25 ^{o}C and for 3 days. At the end of the incubation period a digital picture was taken of the test plates which the

germinated plants can clearly be seen underneath the transparent cover. The pictures were stored in a computer file and the length measurements of the roots and the shoots were performed using the Image Tool 3.0 for Windows. Measurements of roots and shoots length were also performed manually using a ruler. The bioassays were carried out in three replicates for each sample and for each type of plant.

Picture 2.7 Phytotest kit plant types: (i) *Sorghum saccharatum*; (ii) *Lepidium sativum*; and (iii) *Sinapis alba*. The above photos were taken after the exposure of these plants to the solar Fenton treated samples for 3 days.

2.5 Membrane filtration system for the enumeration of total cultivable and antibiotic resistant bacteria

In order to assess the removal of antibiotic resistant bacteria of enteric origin, commonly found in wastewaters and used as microbiological indicators of water quality, total and antibiotic resistant enterococci were monitored. Enterococci enumeration was based on the membrane filtration method (Picture 2.8).

Picture 2.8 Membrane filtration system (Microfil®, Millipore) used in this study. (Membranes: Mixed cellulose ester; Funnels: Polypropylene; Filtration supports and manifolds: Stainless steel).

In the membrane filtration method, a measured volume of the sample or diluted sample is filtered through a membrane filter, typically composed of cellulose-based fibres. The membrane filters have grid-marks which facilitate counting of colonies. The pore size of the membrane filter is such that the target organisms to be enumerated are retained on or near the surface of the membrane filter, which is then placed (face upward) on a differential medium, selective for the target organisms. Colonies of the target organisms (of characteristic morphology and colour) are enumerated after 48

hours and the bacterial load in the original sample is calculated based on that number (Ferreira da Silva et al., 2006; Novo and Manaia, 2010).

Enterococci bacteria are enumerated on m-Enterococcus agar or on this medium supplemented with 1 mg L^{-1} of TMP or OFX. The culture medium is prepared by dissolving 42 g of m-Ent powder in 1L of distilled water with stirring and heating to aid dissolution. When the medium cools down to less than 45 ^{o}C it is then dispensed (7 mL) into petri dishes (50 mm). Antibiotic stock solutions (0.5 g L^{-1}) were prepared by dissolving a specified mass of each compound in deionized water and sterilized by filtration. These were then spiked in the appropriate volume, into the medium solution. The final antibiotic concentrations in the culture medium were determined according to the minimal inhibitory concentrations (MIC) as reported by Andrews (2009).

Samples from the solar Fenton experiments were mixed with catalase solution to remove the residual hydrogen peroxide and were neutralized with 2N NaOH. Serial dilutions were prepared in saline solution (NaCl 0.85%) and filtered through filtering membranes (mixed cellulose ester, 0.45 mm pore size, 47 mm diameter, Millipore). The membranes were placed onto the culture media and incubated for 48 h at 37 °C. After the incubation period, the number of colony forming units (CFU) was registered on the basis of filtering membranes containing between 10 and 100 colonies (Picture 2.9).

The preparation of the agar media as well as the filtration procedure were performed in microbiological safety cabinets.

The prevalence of antibiotic resistant enterococci was calculated as the ratio between the CFU ml^{-1} observed on antibiotic supplemented culture medium and the CFU ml^{-1}

observed on the same medium without antibiotic (Novo and Manaia, 2010). All analyses were made in triplicate for each sample.

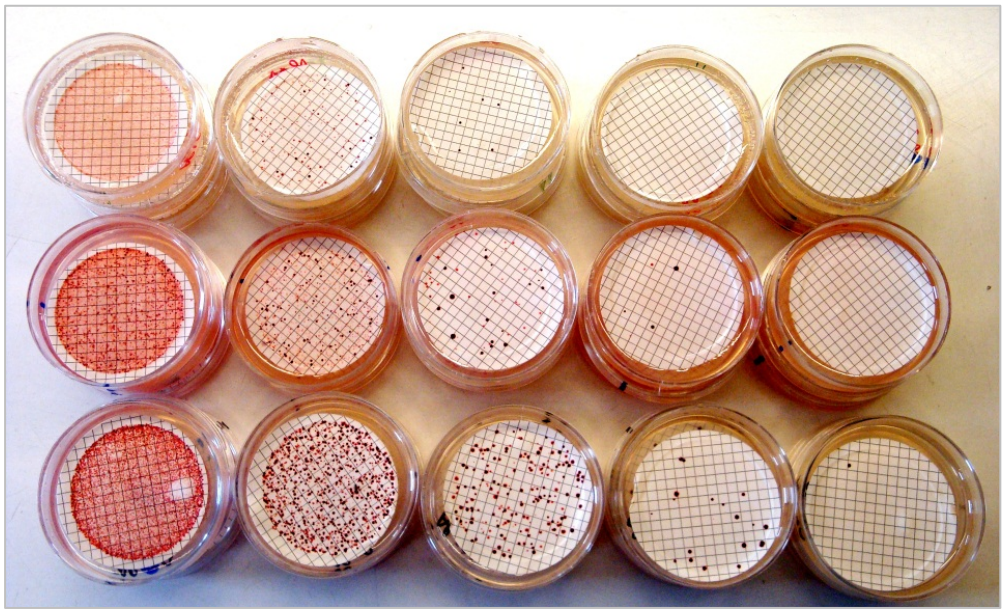

Picture 2.9 Enterococci colonies on the membranes after an incubation period of 48 h.

CHAPTER 3: DEVELOPMENT AND VALIDATION OF A UPLC-MS/MS METHOD FOR STUDYING THE DEGRADATION OF THE TARGET CONTAMINANTS DURING THE PHOTOCATALYTIC TREATMENT

A growing number of analytical methods for the determination of pharmaceuticals in the aquatic environment can be found in the literature (Petrović et al., 2006; Kasprzyk-Hordern et al., 2007; Ibanez et al., 2009). Depending on the concentration level and the polarity of the compounds to be determined these methods include gas and liquid chromatographic methods (GC, LC) in combination with mass spectrometry (MS) and, although with less sensitivity, capillary electrophoresis (Petrović et al., 2005; Himmelsbach et al., 2006). Liquid chromatography in combination with tandem mass spectrometry (LC-MS/MS) has been widely used during the last few years to analyze antibiotics and other pharmaceuticals at trace concentration levels in complex environmental and wastewater samples (Li et al., 2009; Fatta et al., 2007).

Recent developments in LC include the application of ultra-performance liquid chromatography (UPLC) for analysis of environmental contaminants (Hernando et al., 2007; Li et al., 2009; Sui et al., 2010). An ultra-high pressure system operates using sub-2 μm particle-packed columns, which offers significant benefits over today's HPLC systems equipped with standard 5 μm particle-packed columns (Jin et al., 2010). The use of smaller particles provides enhanced chromatographic speed, resolution and sensitivity (Dongre et al., 2008). A combined UPLC tandem MS technique mainly using triple quadrupole analyzer (QqQ) has made impressive progress within the environmental field (Kasprzyk-Hordern et al., 2008; Baker and Kasprzyk-Hordern, 2011).

This chapter describes the development and validation of a fast and reliable UPLC-MS/MS method for the detection and quantification of OFX and TMP in secondary treated wastewaters at the ng L^{-1} levels. Three different chromatographic columns were tested on a UPLC-MS/MS instrument working in the electrospray ionization (ESI) mode with twelve combinations of eluting solvents. Samples were enriched prior to the analysis by solid phase extraction using the hydrophilic-lipophilic balanced (HLB) reversed phase polymeric sorbent. This method was specifically designed to study the degradation kinetics for both antibiotics during the photocatalytic processes applied in this thesis which is more sensitive and reliable than the HPLC method regularly used to study the degradation kinetics of pharmaceuticals at these concentration trace levels in wastewaters.

3.1 Preparation of standard solutions

Stock standard solutions were prepared as described in Chapter 2 (section 2.1.1).

3.2 Solid-phase extraction (SPE)

Sample preparation is a key component of every analytical method. The importance of sample preparation, particularly solid phase extraction (SPE), stems from four major concerns: (i) eliminating matrix interferences (including ion suppression); (ii) lowering method variability; (iii) concentrating analyte(s) of interest; and (iv) improving analytical system performance (Hennion, 1999; Poole et al., 2000; Petrović et al., 2005; Kasprzyk-Hordern et al., 2008).

SPE has proven to be an effective tool for removing matrix interferences enabling sensitive, selective and robust LC-MS/MS analysis. In addition, SPE materials successfully remove phospholipids and lysophospholipids, which are considered as key contributors to ion suppression. Moreover, removal of these interferences, results in lowering the method variability, increasing the MS signal response and extending analytical column lifetime (reducing system maintenance). SPE enables also the enrichment of selected analytes without concentrating the matrix interferences (Waters Corporation).

Oasis HLB cartridges (200 mg, Waters Corporation) were used for all SPE steps. Oasis HLB is a Hydrophilic-Lipophilic-Balanced, water-wettable, reversed phase polymeric sorbent, which provides excellent pH stability across the entire pH range (0 to 14). This broader pH range allows the flexibility of SPE methods development. It is made from a specific ratio of two monomers, hydrophilic N-vinylpyrrolidone and lipophilic divinylbenzene (Petrović et al., 2005). It provides excellent retention

capacity (*k'*) for a wide range of analytes. This sorbent also exhibits three to five times higher retentivity/capacity than traditional silica-based sorbents like C_{18} (Liu et al., 2008; Waters Corporation). The advantage of having higher retention capacity is that more analytes are retained improving the recovery and overall reproducibility of the applied SPE method.

SPE method development requires the knowledge of the nature of the sample matrix and the analytes of interest. pK_a values of analytes is an important criterion for SPE because the pH of sample significantly influences the chemical form of analytes, their stability and the interaction between the analyte and SPE cartridge packing material (Babić et al., 2006; Seifrtova et al., 2009). OFX has two ionizable functional groups, a carboxylic group and an amino group in the heterocyclic ring (namely piperazinyl). The first ionization constant (pK_{a1}) corresponds to the dissociation of a proton from the carboxyl moiety while pK_{a2} corresponds to the dissociation of proton from the N_4 in the piperazinyl group (Table 1.5, CHAPTER 1). OFX is primarily cationic below pK_{a1}, anionic above pK_{a2}, and zwitterionic *i.e.*, net neutral between pK_{a1} and pK_{a2}. The piperazinyl quinolones present in cationic form at acidic conditions, are retained well on the polymeric Oasis HBL column (Senta et al., 2008; Seifrtova et al., 2009). TMP has positive charge at pH below its pK_a because of the protonation of the two heterocyclic nitrogen atoms that it contains; therefore it is retained well on HLB cartridges (Renew et al., 2004). It is important to mention that the wastewater samples spiked with the above antibiotics were acidified (pH=2.8-3.0) for the solar Fenton experiments; therefore acidification yielded both compounds in their cationic form.

Sample processing in SPE consists of four basic steps. Initially, the sorbent is conditioned with solvent to improve the reproducibility of analyte retention and to reduce the carry-through of sorbent impurities at the elution stage. Then the aqueous

sample is passed through the conditioned cartridge at a controlled flow rate. After the sample is processed, the sorbent is rinsed with a weak solvent to displace undesired matrix components from the sorbent without displacing the analytes. A drying step between processing the aqueous sample and eluting the retained analyte follows for reducing the volume of water retained by the eluting solvent. Finally, the analytes of interest are eluted from the sorbent in a small volume of solvent for subsequent determination (Poole et al., 2000; Feng et al., 2009).

The SPE cartridges were conditioned with 4 mL MeOH followed by 4 mL of deionized water (pH ≈ 3) at a flow rate of 1 mL min^{-1}. After the conditioning step, 10 mL of sample were percolated through the cartridges at a flow rate of 1 mL min^{-1} followed by 3 mL of deionized water. The cartridges were then dried under vacuum for 15-20 minutes. The final elution was performed with 2×2 mL of MeOH at 1 mL min^{-1}. The SPE procedure is presented in Schematic 3.1.

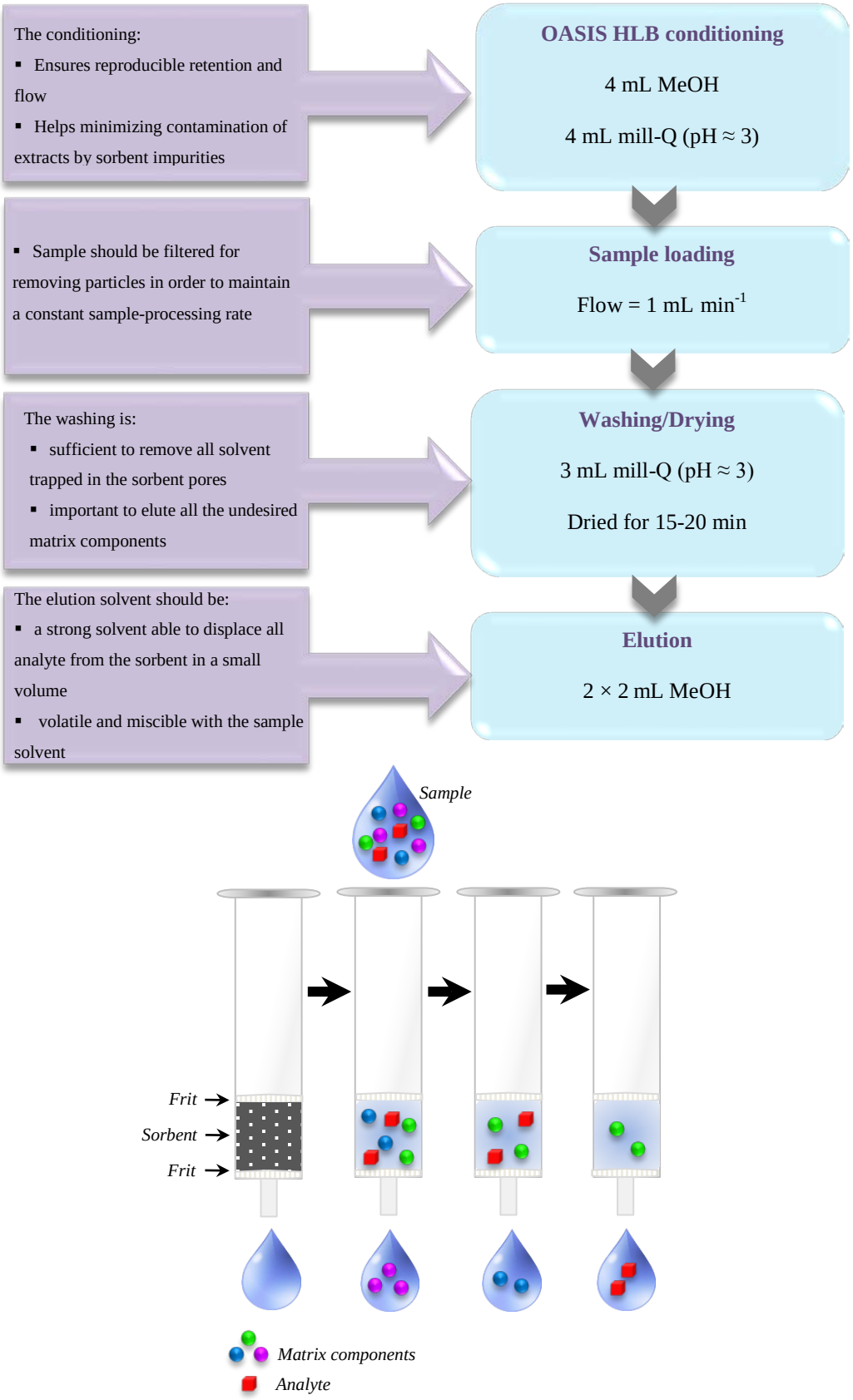

Schematic 3.1 Solid phase extraction protocol applied.

3.3 Chromatographic instrumentation

All analyses were performed on an ACQUITY TQD UPLC-MS/MS system (Waters Corporation) equipped with auto sampler, binary solvent manager, and column manager. Electrospray ionization (ESI) in positive mode was used for all the experiments. Data acquisition was performed with MassLynx^{TM}.

Three different LC columns were tested for the analysis: (i) HSS C_{18} SB (1.8 μm; 2.1×50 mm); (ii) BEH Shield RP18 (1.7 μm; 2.1×50 mm); and (iii) BEH Phenyl (1.7 μm; 2.1×50 mm) (all provided by Waters). Columns characteristics are illustrated in Table 3.1.

Four solvents were used for the binary elution: (i) A_1: 0.1 mM ammonium acetate in water + 0.01% formic acid; (ii) B_1: Methanol; (iii) A_2: 0.1 mM ammonium acetate in methanol + 0.01% formic acid; and (iv) B_2: Acetonitrile. Twelve combinations between columns and solvents were examined in order to optimize chromatographic separation (reduction of peak tailing and better resolution) and the ESI ionization. The column temperature was maintained at 60 ^{o}C, the solvent flow was 0.3 mL min^{-1} and the sample injection volume 10 μL.

Table 3.1 Main technical characteristics of the columns used for LC analysis.

Name	Dimensions (mm)	Particle size (µm)	pH Range (*)	Temperature Limits (°C)	Surface Area ($m^2 g^{-1}$)	Carbon Load (%)
HSS C_{18} SB (1) *(High Strength Silica)*	2.1×50	1.8	2-8	Low pH: 45 High pH: 45	230	8
BEH Shield RP18 (2) *(Bridged Hybrid Substrate)*	2.1×50	1.7	2-11	Low pH: 50 High pH: 45	185	17
BEH Phenyl (3) *(Bridged Hybrid Substrate)*	2.1×50	1.7	1-12	Low pH: 80 High pH: 60	185	15

(1) Intermediate coverage tri-functionally bonded C_{18}, no endcapping, bonded to High Strength Silica (HSS) UPLC particles

(2) Monofunctional embedded polar C_{18}, fully endcapped, bonded to Ethylene Bridged Hybrid (BEH) substrate

(3) Trifunctional C_6 Phenyl, fully endcapped, bonded to Ethylene Bridged Hybrid (BEH) substrate

(*) Room Temperature

A tandem quadrupole mass spectrometer ACQUITY TQD (Waters Corporation) was used for the detection of target analytes. In order to achieve sensitive target quantitative analysis, data acquisition was performed with electrospray ionization in multiple reaction monitoring mode (MRM), recording the transitions between the precursor ion and the most abundant fragment ions.

MRM consists of selecting a specific fragmentation reaction. The ions selected by the first quadrupole (Q_1) are only detected if they produce a given fragment, by a selected reaction. The MS analysis is focussed only on analytes of specific masses, while all others are excluded. The absence of scanning allows one to focus on the precursor and fragment ions over long times, enhancing the sensitivity of the method.

The target parent ion is selected in the first quadrupole (Q_1) and enters the second quadrupole (Q_2) where it undergoes collision-induced dissociation. One or more

fragment ions are then selected according to the predefined transitions and the signal produced provides the counts for quantification. Where more than one transition is selected for a given precursor ion, the accumulative counts are used for quantification (Hoffmann and Stroobant, 2007; Kitteringhama et al., 2009).

The ESI was operated in positive mode and the protonated molecular ion $[M+H]^+$ was selected as precursor ion for both analytes. The analyses were performed with capillary voltage of 2 kV, source temperature at 150 ^oC and desolvation gas (N_2) temperature at 500 ^oC. A cone gas flow of 10 L h^{-1} and desolvation gas flow of 1000 L h^{-1} were used whereas the collision gas (Ar) flow was 0.15 mL min^{-1}. Manual optimization of compound-dependent MS parameters (collision energy (CE), capillary voltage, cone voltage (CV)) was performed individually for each compound in a continuous-flow mode through a direct infusion of standard solutions into the stream of the mobile phase (10% MeOH-90% H_2O with 0.1% formic acid) using the on-board fluidics system; IntelliStart was used to generate/confirm the MRM transitions (automated MRM development software). The MS tune was performed by using the stock solutions at 1 mg mL^{-1}.

Precursor and product ions with associated collision energies and retention times are summarized in Table 3.2, together with the operating MS/MS parameters. The choice of the two most abundant fragmentation products for each compound was done according to the intensity and the signal to noise ratio. The most abundant transition product ion was typically used for quantification of the target compound, while the second transition product, together with the ratio of the intensities of the two transitions, were used for confirmation purposes.

Table 3.2 Retention times and MS/MS parameters for the target analytes.

Analyte	Retention time (min)	Precursor ion (*m/z*)	Cone Voltage (V)	Capillary Voltage (kV)	Product ions (*) (*m/z*)	CE (eV)
OFX	2.59	362.1	28	3	**261.2**	27
					58.1	35
TMP	2.67	291.1	38	2	261.1	24
					230.2	23
					123.1	24
					110.1	32
					81.1	46

* The most intensive fragment ion (**in green bold**) from each precursor ion was selected for quantification. A less sensitive secondary transition (**in bold**) was used as the second criterion for confirmation purposes.

MRM chromatograms of the standard solutions (10 μg L^{-1}) of the investigated analytes are shown in Figure 3.1.

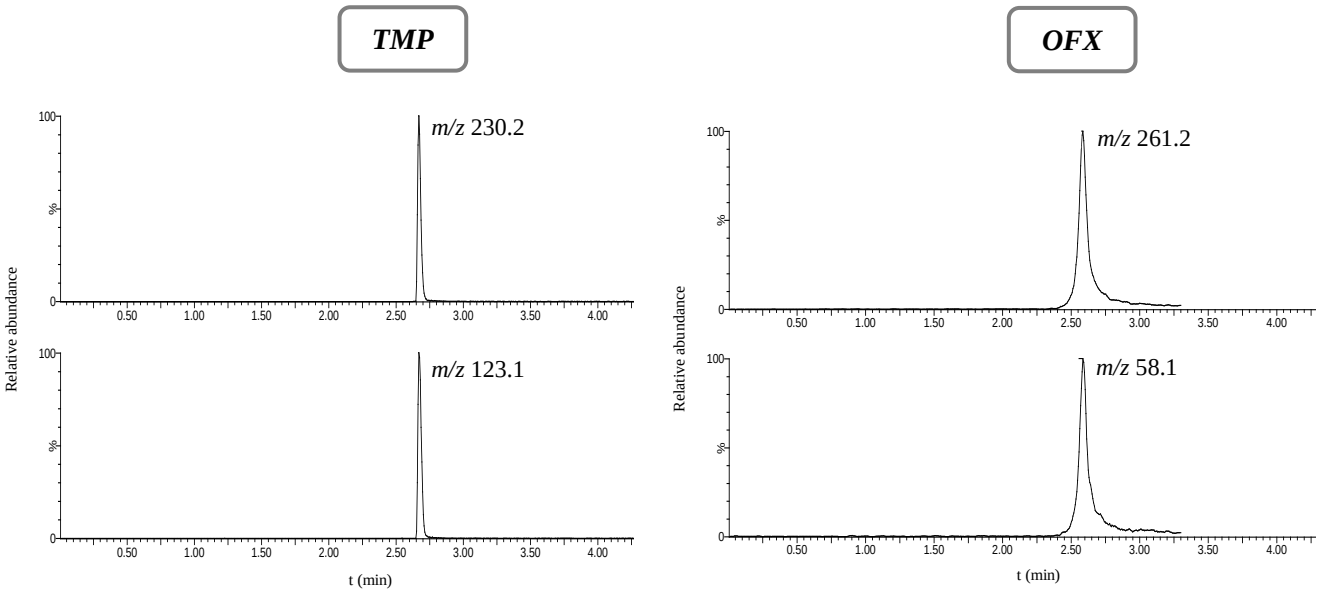

Figure 3.1 MRM chromatograms of the target analytes in a standard solution of 10 μg L^{-1} (for the applied MRM transitions see Table 3.2).

3.4 Method optimization

To optimize the chromatographic separation different mobile phases containing acidic additives were investigated (see section 3.3). Retention time, peak shape and resolution were the main criteria for the method optimization.

Column BEH Shield RP18 was found to be the most efficient for separation and determination of OFX and TMP using 0.1 mM ammonium acetate in water + 0.01% formic acid (A_1) and 0.1 mM ammonium acetate in methanol + 0.01% formic acid (A_2) as mobile phase. The gradient elution program is illustrated in Table 3.3. Chromatographic analysis lasted 9 min. The weak wash was H_2O + 0.1% formic acid, whereas the strong wash was the eluent A_2. The gradient elution described in Table 3.3 was runned before sample analysis in order to equilibrate the column. The other combinations caused broad peak shapes (higher retention times) and poor sensitivity for both compounds.

Table 3.3 LC gradient elution program.

Time (min)	A_1 (%)	A_2 (%)
0.0	95	5
1.5	95	5
2.0	70	30
3.0	50	50
5.0	30	70
6.0	10	90
7.0	10	90
7.1	95	5
9.0	95	5

The formic acid applied into the mobile phase at concentration 0.01% was found to provide both good sensitivity and better peak shapes. Formic acid which is one of the most common acids used for chromatographic analysis has the ability to effectively mitigate the effect of residual silanols on the stationary phase and possibly even salvage residual metals (Zhu et al., 2001; Lykkeberg et al., 2004). Additionally, formic acid is known to promote positive ionization of acidic molecules and as a result an increase of the signal in the ESI source operating in positive mode takes place (Kasprzyk-Hordern et al., 2007).

Formic acid at concentration level of 0.005-0.5% was chosen as the optimum mobile phase additive in pharmaceuticals analysis by other research groups (Lee et al., 2007; Pailler et al., 2009; Gracia-Lor et al., 2010). Many researchers also reported that formic acid dissociation affects the ionization efficiency thus providing good chromatographic separation (Becker et al., 2004; Cai et al., 2008; Li et al., 2009).

3.5 Validation study

The method was validated in terms of linearity, limit of detection (LOD) and limit of quantification (LOQ), recovery, accuracy, precision (or reproducibility) and identification.

3.5.1 Linearity

Linearity was examined from five point calibration curves using a set of working standard solutions (in triplicate) at concentration levels in the range 0.01-0.1 μg L^{-1} and 0.1-100 μg L^{-1} typically measured in wastewater effluents. Calibration curves were generated using the QuanLynx^{TM} application manager from MassLynx^{TM} software by plotting the peak area versus the measured standard concentrations.

Correlation coefficients (R^2) were greater than 0.98 for both analytes over the examined concentrations range demonstrating an excellent linearity. The representative standard curves for each compound are shown in Figure 3.2.

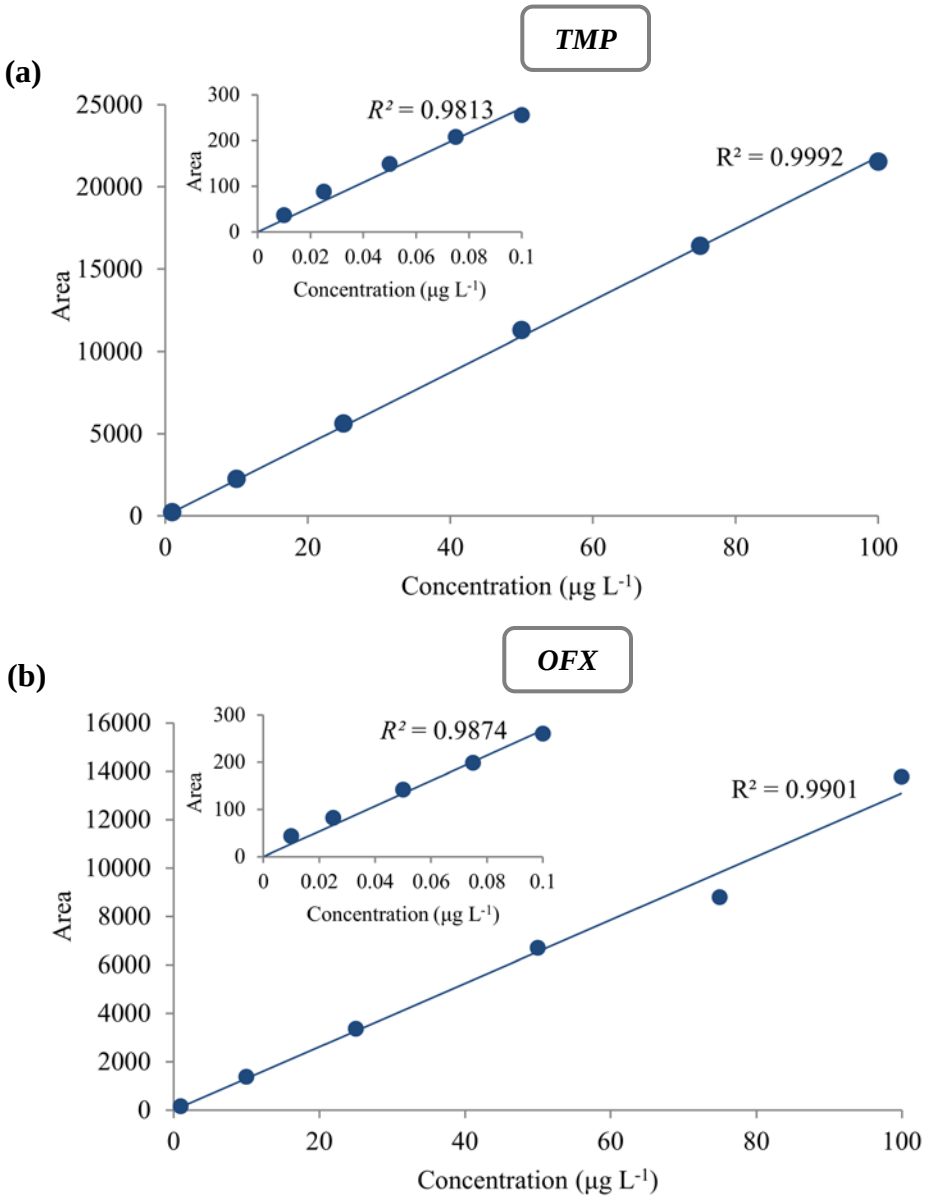

Figure 3.2 Representative standard curves demonstrating the method linearity in the range of 0.1-100 µg L^{-1} and 0.01-0.1 µg L^{-1} (inset graphs): (a) TMP; (b) OFX.

3.5.2 Limit of detection (LOD) and Limit of quantification (LOQ)

The LOD of the method was calculated according to ISO 11843-2 (Ternes et al., 2001), with a confidence interval of 99% using the standard deviation of a linear regression curve for a concentration range from 0.01 to 100 μg L^{-1}. LOD is defined as $3S_0$, where S_0 is the value of the standard deviation at zero concentration of the analyte. The value of S_0 can be obtained by extrapolation from a plot of standard deviation (y axis) versus concentration (x axis). LOQ is calculated by multiplying S_0 by 10.

Stock solutions of TMP and OFX were diluted serially to low, mid and high concentrations and used to determine the LOD and the LOQ. LOD of the target analytes was found to be 4.6 ng L^{-1} for OFX and 5.5 ng L^{-1} for TMP, whereas the LOQ was 8.8 ng L^{-1} and 9.5 ng L^{-1} for OFX and TMP, respectively. This makes the method useful for the determination of very low concentration levels of these antibiotics in many environmental matrices.

3.5.3 Accuracy/Recovery

Recovery experiments were performed to examine the possible effect of the environmental matrix. Recovery was assessed by extracting spiked wastewater samples with deuterated internal standards (OFX-d_3; TMP-d_3) at concentration levels of 0.01, 0.1, 50 and 100 μg L^{-1} for each individual compound. The samples in triplicate were eluted through separate cartridges. As shown in Table 3.4, recoveries were at all ranges of concentrations examined, higher than 90%. Some recovery data for OFX and TMP reported by other research groups are depicted in Table 3.4 for comparison purposes.

Table 3.4 SPE recovery for OFX and TMP at various concentrations.

Analyte	Concentration (μg L^{-1})	Recovery (%)±RSD (%) (*n=3*)	Recovery (%) *(reported in the literature)*
TMP	0.01	91.87±2.66	85±6 [1]; 109±56 *sec* [4]; 98±39 *ef* [4]; 88±7 *ef* [5]; 111±1 *in* [5]; 83±15 *ef* [6]; 106±2 *in* [6]; 100±8 *ef* [7]; 100±4 *in* [7]; 106±8.4 *ef* [8]; 138±19 *in* [8]; 102±7 *ef* [9]; 74±16 *in* [9]; 109.7±2.9 *in* [10]; 82.7±9.0 [11]; 92±6 [12]
	0.1	92.48±4.14	
	50	91.25±1.79	
	100	96.47±1.78	
OFX	0.01	91.70±5.14	90±2 [1]; 81±13 *ef* [2]; 89.8±4.0 *in* [2]; 115±13 *ef* [3]; 132±25 *in* [3]; 129±25 *sec* [4]; 114±24 *ef* [4]; 106±2 *ef*; 95±4 *in* [5]; 89.8±4.2 *in* [10]
	0.1	93.52±14.32	
	50	91.38±1.74	
	100	98.59±3.05	

Notes: *in* → influent; *sec* → secondary effluent; *ef* → final effluent

[1] Lindberg et al., 2005; [2] Xiao et al., 2008 (1 μg L^{-1}); [3] Peng et al., 2006 (2-5 μg L^{-1}); [4] Renew et al., 2004 (1 μg L^{-1}); [5] Gros et al., 2006 (1 and 10 μg L^{-1}); [6] Fatta-Kassinos et al., 2010 (10 ng μL^{-1}); [7] Gulkowska et al., 2008; [8] Karthikeyan and Meyer, 2006 (0.5 μg L^{-1}); [9] Sui et al., 2010; [10] Li et al., 2009 (1 μg L^{-1}); [11] Yu et al., 2009; [12] Watkinson et al., 2009.

3.5.4 Precision

Method precision data was obtained by measuring multiple samples at each concentration (0.01-100 μg L^{-1}) for each analyte. The precision (or reproducibility), expressed as the relative standard deviation (RSD) of independent multiple analyses (n=3) was typically found in the range of 0.98% to 1.54% for OFX and 0.85% to 5.54 % for TMP in the range of 0.01-1.0 μg L^{-1}. For the higher concentration level of 10-100 μg L^{-1}, RSD was 2.36-14.65% and 2.59-5.54% for OFX and TMP, respectively.

3.5.5 Identification

Positive confirmation of the analytes was made using the intensity ratio (*Q/q*) of the two MS transitions in the samples (Hernandez et al., 2005; Senta et al., 2008). The *Q*/*q* ratio is defined as the ratio between the intensity of the quantification ion (*Q*) and the confirmation

ion (*q*) (Cervera et al., 2010). The experimental average *Q*/*q* value for each compound was calculated as the mean value obtained from standard solutions at different concentration levels in the range of 0.01-0.1 μg L^{-1} and 1-100 μg L^{-1} injected in triplicate (see Table 3.5). The average *Q/q* ratios were less than 1.88 for TMP and less than 4.70 for OFX.

A ratio tolerance of ±20% (*Q/q* ratio lower than 2) and ±25% (*Q/q* ratio between 2 and 5) was accepted for TMP and OFX respectively to confirm a finding as positive according to the European Commission Decision (2002/657/EC). Despite the fact that this Decision was originally defined for the determination of organic contaminants in food samples, it is being increasingly used for the confirmation of positive findings in other matrices such as environmental and biological samples. The *Q/q* ratio for each analyte in each treated sample was calculated and it was found to be within the above tolerance levels. Furthermore, an agreement in the retention time between the reference standard and the sample was also required to characterize a detection as positive.

Table 3.5 Average *Q*/*q* value for each compound, calculated at various concentrations. The RSD percentage of the calculations (*n=3*) is given in parenthesis.

Analyte	Concentration (µg L^{-1})	*Q/q* (RSD (%)) (*n=3*)
TMP	0.01	1.02 (1.49)
	0.025	1.07 (6.17)
	0.05	1.88 (9.88)
	0.075	1.25 (3.88)
	0.1	1.18 (4.34)
	1	1.21 (4.17)
	10	1.31 (7.76)
	25	1.45 (7.66)
	50	1.37 (5.68)
	75	1.26 (6.24)
	100	1.34 (2.00)
OFX	0.01	2.40 (5.28)
	0.025	3.47 (9.44)
	0.05	3.25 (3.79)
	0.075	3.09 (7.17)
	0.1	3.47 (3.84)
	1	2.99 (7.63)
	10	3.78 (9.88)
	25	4.70 (9.47)
	50	4.50 (4.88)
	75	4.30 (8.86)
	100	3.58 (2.57)

The chromatographic method developed is quick and reliable, suitable for the identification and quantification of OFX and TMP in secondary treated municipal effluents down to low μg L^{-1} levels. The method was optimized and showed very good performance characteristics and was successfully applied to study the degradation kinetics of the selected antibiotics during the two AOPs applied in further experiments.

CHAPTER 4: BENCH SCALE STUDY OF SOLAR FENTON AND SOLAR TiO_2

4.1 Solar Fenton oxidation process

4.1.1 Effect of ferrous salt (Fe^{2+}) and hydrogen peroxide (H_2O_2) concentration

Preliminary experiments were carried out to determine the suitable ferrous salt (Fe^{2+}) and hydrogen peroxide (H_2O_2) doses needed to degrade the target compounds. To obtain the optimal initial Fe^{2+} and H_2O_2 concentrations, experiments were conducted with several combinations of catalyst and oxidant. The efficiency of the H_2O_2 use with respect to the theoretically needed stoichiometric amount of the oxidant highly depends on the substrate and its concentration (Oller et al., 2006). The stoichiometric ratio of H_2O_2 required for total mineralization of OFX and TMP, according to the following equations (eqs. (4.1) and (4.2)), is 1:49 and 2:89 (1:44.5), respectively.

OFX: $C_{18}H_{20}FN_3O_4 + 49H_2O_2 \rightarrow 18CO_2 + 57H_2O + 3HNO_3 + HF$ (4.1)

TMP: $2C_{14}H_{19}N_4O_3 + 89H_2O_2 \rightarrow 28CO_2 + 104H_2O + 8HNO_3$ (4.2)

Therefore, the minimum concentration of H_2O_2 required to achieve total mineralization of the solution of 10 mg L^{-1} OFX (0.0277 mmol L^{-1}) is 1.357 mmol L^{-1} (0.0277×49). In the case of TMP, the minimum concentration of H_2O_2 required for total mineralization of the solution of 10 mg L^{-1} TMP (0.0344 mmol L^{-1}) is 1.531 mmol L^{-1} (0.0344×44.5).

The examined concentrations of H_2O_2 for the solar Fenton experiments were multiples of the peroxide stoichiometric concentration for each compound. It is important to point out that to render the solar Fenton system effective, it is essential that its application represents a low cost operation, which basically implies a better

control of H_2O_2 dosage. Moreover, considering that the regulations in Cyprus (Cyprus Law: 106(I)/2002) set the value of 5 mg L^{-1} as the maximum iron concentration in treated effluents that can be discharged in water dams and other water bodies, the influence of Fe^{2+} was examined in the range of 1-5 mg L^{-1}.

Figure 4.1 (a, b) depicts the effect of ferrous initial concentration on the conversion of OFX and the degradation of TMP at pH=2.9-3.0. The original concentration of Fe^{2+} was altered from 1 to 5 mg L^{-1}, while the initial concentration of H_2O_2 was kept constant ($[H_2O_2]_0$=2.714 mmol L^{-1} for OFX; $[H_2O_2]_0$=3.062 mmol L^{-1} for TMP).

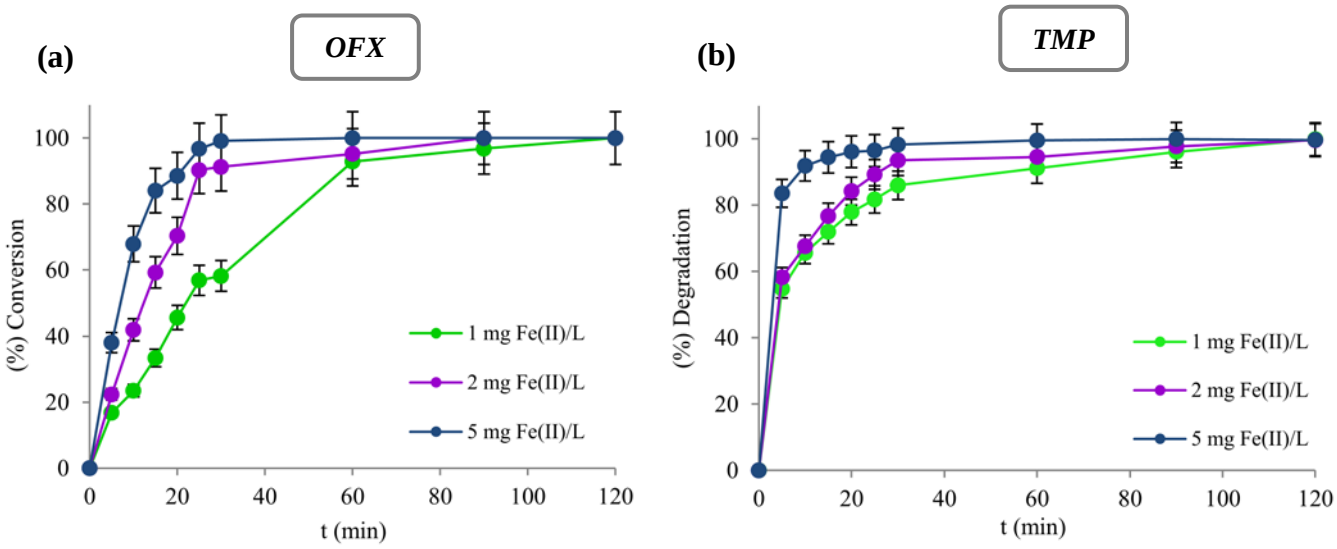

Figure 4.1 Effect of initial ferrous concentration on the photooxidation of: (a) OFX and (b) TMP spiked wastewater solutions. Experimental conditions: $[Fe^{2+}]_0$=1-5 mg L^{-1}; $[H_2O_{2(OFX)}]_0$=2.714 mmol L^{-1}; $[H_2O_{2(TMP)}]_0$=3.062 mmol L^{-1}; $[OFX]_0$=0.0277 mmol L^{-1}; $[TMP]_0$=0.0344 mmol L^{-1}; pH=2.9-3.0 and T=25±0.1 ^oC.

The complete conversion of OFX substrate was achieved within 30 min of illumination at $[Fe^{2+}]$=5 mg L^{-1}, while at $[Fe^{2+}]$=2 mg L^{-1} and $[Fe^{2+}]$=1 mg L^{-1} within 90 and 120 min, respectively. TMP was degraded completely within 30 min of

photocatalysis at $[Fe^{2+}]$=5 mg L^{-1} but more time was needed for the complete TMP degradation at lower ferrous concentrations.

As already mentioned, Fe^{2+} is the main species that can catalyze H_2O_2 to produce $HO^{\bullet}$. The chain reactions that take place in the process produce additional $HO^{\bullet}$, which are capable to react with a wide range of organic compounds in water matrices and cause their chemical decomposition. In the presence of higher iron concentrations, the process is accelerated mainly by two mechanisms. First, the photocatalytic regeneration of Fe^{2+} from ferric (Fe^{3+}) iron results to the rapid generation of additional $HO^{\bullet}$. H_2O_2 is also more efficient, as it is mainly consumed in ‘‘useful’’ reactions yielding substrates degradation. When iron concentration is low, part of the H_2O_2 is decomposed into molecular oxygen and water but does not participate in the oxidation of the polluting molecules (Zapata et al., 2009).

The ferrous concentration is considered to be a crucial parameter for large-scale wastewater treatment plants since it can influence not only the application costs as it determines the size of the photoreactor but also the operating costs as shorter reaction times are required (Malato et al., 2009). However, if iron concentration is very high, the problem of the resulting iron-separation step arises at the end of the photocatalytic process. Consequently, it is preferable to select a system with small concentration of iron by which it would be possible to achieve relatively high degradation rates and to avoid the requirement of iron removal, according to the existing regulations.

Furthermore, the inner filter effects present in the treated solution are considered as an important issue regarding the effect of iron concentration on the degradation rate during the solar Fenton process. Inner filter effects are the competitive absorption of photons by other light absorbing species, usually the various organic contaminants present in the wastewater matrix (Malato et al., 2009). The photons absorbed by the

contaminants instead of the catalyst (especially at low concentrations of iron) may be considered lost in terms of efficient photon use. The competitive light absorbance may lead also to some direct photolysis reactions; however photolysis reactions usually have a low efficiency in the degradation (See section 4.1.3).

The effect of H_2O_2 initial concentration on OFX and TMP substrate oxidation was studied in the range of 1.357-8.142 mmol L^{-1} and 1.531-9.186 mmol L^{-1} respectively, at pH=2.9-3.0 and at constant ferrous concentration of 5 mg L^{-1} (Figure 4.2 (a, b)).

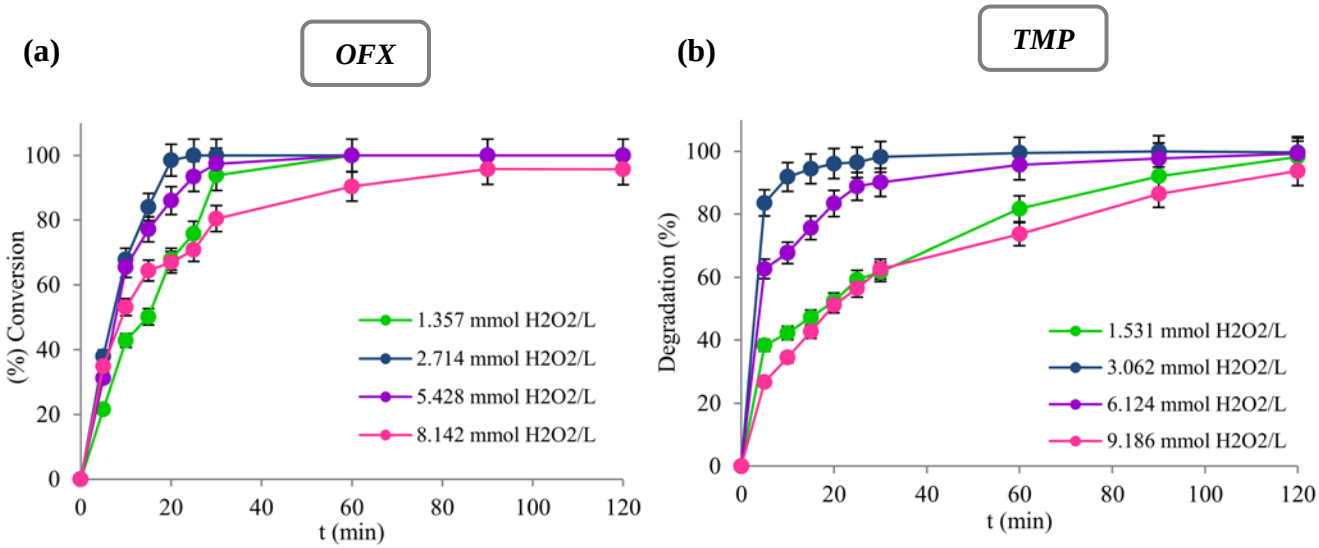

Figure 4.2 Effect of initial hydrogen peroxide concentration on the photooxidation of (a) OFX and (b) TMP spiked wastewater solutions. Experimental conditions: $[Fe^{2+}]_0$=5 mg L^{-1}; $[OFX]_0$=0.0277 mmol L^{-1}; $[TMP]_0$=0.0344 mmol L^{-1}; pH=2.9-3.0 and T=25±0.1 ^oC.

The results indicate that the degradation of both compounds is increased when increasing the concentration of peroxide. With increasing H_2O_2 concentration from 1.357 to 2.714 mmol L^{-1}, the conversion of OFX increases due to the additionally produced $HO^{\bullet}$. The same behavior was observed in the case of TMP with increasing

H_2O_2 concentration from 1.531 to 3.062 mmol L^{-1}. However, at higher H_2O_2 concentrations (5.428-8.142 mmol L^{-1} for OFX; 6.124-9.186 mmol L^{-1} for TMP) an adverse effect on the substrates degradation was observed. This may be attributed to the recombination of the $HO^{\bullet}$ produced as well as the reaction of $HO^{\bullet}$ with H_2O_2, contributing to the $HO^{\bullet}$ scavenging capacity (eqs. (4.3)-(4.5)) (El-Morsi et al., 2002; Tamimi et al., 2008).

$$HO^{\bullet} + HO^{\bullet} \rightarrow H_2O_2 \quad (4.3)$$

$$HO^{\bullet} + H_2O_2 \rightarrow HO_2^{\bullet} + H_2O \quad (4.4)$$

$$HO_2^{\bullet} + HO^{\bullet} \rightarrow H_2O + O_2 \quad (4.5)$$

The above reactions reduce the overall solar Fenton effectiveness, as H_2O_2 consumption and $HO^{\bullet}$ generation are unrelated to the substrate degradation. In addition, saturation of active iron ion sites resulting from the excess dosage of H_2O_2 could be another explanation as reported by Chen et al. (2010).

Under the conditions of these experiments, it appears that 2.714 mmol L^{-1} and 3.062 mmol L^{-1} of H_2O_2 was the optimal dosage for OFX and TMP degradation respectively during the solar Fenton process.

It is worth noting that the different degradation behavior of the substrates (especially in the early stages) as shown in Figure 4.1 (a, b) and Figure 4.2 (a, b), indicates the different breakdown of the substrates molecules and subsequently the formation of various by-products which influence the overall decomposition pathway of the compounds.

4.1.2 Degradation kinetics

Generally, the reaction rate (*r*) can be expressed using the following equation (Abellan et al., 2009):

$$r = \frac{dC}{dt} = k\, f(C) \tag{4.6}$$

where *k* is the kinetic constant and *f(C)* is a function of the target compound concentration.

Assuming that among the reactions taking place during the solar Fenton process, the reaction between HO• and the substrate (OFX or TMP) is the rate-determining step, the rate equation can be given by eqn. (4.7) (Huston and Pignatello, 1999).

$$r = \frac{dC}{dt} = k^{*}[HO\cdot]C \tag{4.7}$$

where *C* is the concentration of the substrate, $[HO\cdot]$ is the concentration of the hydroxyl radicals and k^{*} is the reaction rate constant.

The hypothesis that was further taken into account for the system employed in the present work is that HO• rapidly achieve a constant steady-state concentration in the solution (Evgenidou et al., 2007); therefore eqn. (4.7) can be written as a pseudo-first-order reaction rate:

$$r = \frac{dC}{dt} = k^{*}\,[HO\cdot]\,C = kC \tag{4.8}$$

where *k* is the apparent pseudo-first-order constant.

Therefore the concentration of the substrate can be given by the kinetic expression (eqn. (4.9)):

$$C = C_0 e^{-kt} \tag{4.9}$$

Accordingly, in order to evaluate the kinetics of OFX and TMP degradation the logarithm graph $-ln(C/C_0)=f(t)$, where C_0 and C are the concentrations of the substrate at times 0 and t (min) respectively, was plotted. The apparent rate constant, k (min^{-1}), was determined from the slope of the $-ln(C/C_0)=f(t)$ plot and has been chosen as the basic kinetic parameter to compare the different systems, since it is independent of the concentration and therefore, enables to determine the catalytic activity. Also, to have a better knowledge of the degradation process the time necessary to reduce the initial concentration of each substrate to 50%, the half-life time ($t_{1/2}$) and the initial rate of degradation (r_0) were calculated and presented in Table 4.1.

The half-life time ($t_{1/2}$) is determined by eqn. (4.10):

$$t_{1/2} = \frac{ln2}{k} \tag{4.10}$$

The calculation of the initial rate of the reaction is based on the mathematical definition of derivative. The derivative of a continuous function $C=f(t)$ is defined as follows:

$$\frac{dC}{dt} = lim_{\Delta t \to 0} \frac{\Delta C}{\Delta t} \tag{4.11}$$

The above function can be developed in Maclaurins' formula as follows:

$$\frac{\Delta C}{\Delta t} = f(0) + \frac{\Delta t}{1!} f'(0) + \frac{(\Delta t)^2}{2!} f"(0) + \cdots + \frac{(\Delta t)^n}{n!} f^{(n)}(0) \tag{4.12}$$

For very small values of Δt, eqn. (4.12) can be approximated by keeping only the first two terms.

$$\frac{\Delta C}{\Delta t} = f(\Delta t) = f(0) + \Delta t\, f'(0) \tag{4.13}$$

The point of intersection of the above function with the axis of the $\frac{\Delta C}{\Delta t}$ *(f(0))* is the initial rate of the reaction.

The degradation kinetic parameters described above were estimated under different conditions of ferrous and oxidant concentration. Each degradation experiment described in section 4.1.1 was used to calculate the rate constant by the linear fit, using only the experimental data from the first 20 minutes of reaction in order to avoid variations as a result of competitive effects of intermediates, pH changes, wastewater matrix, etc. The experimental data fit well the linear kinetic equation as depicted in Figure 4.3 (a, b) and consequently OFX and TMP oxidation was found to follow the pseudo-first-order kinetic law.

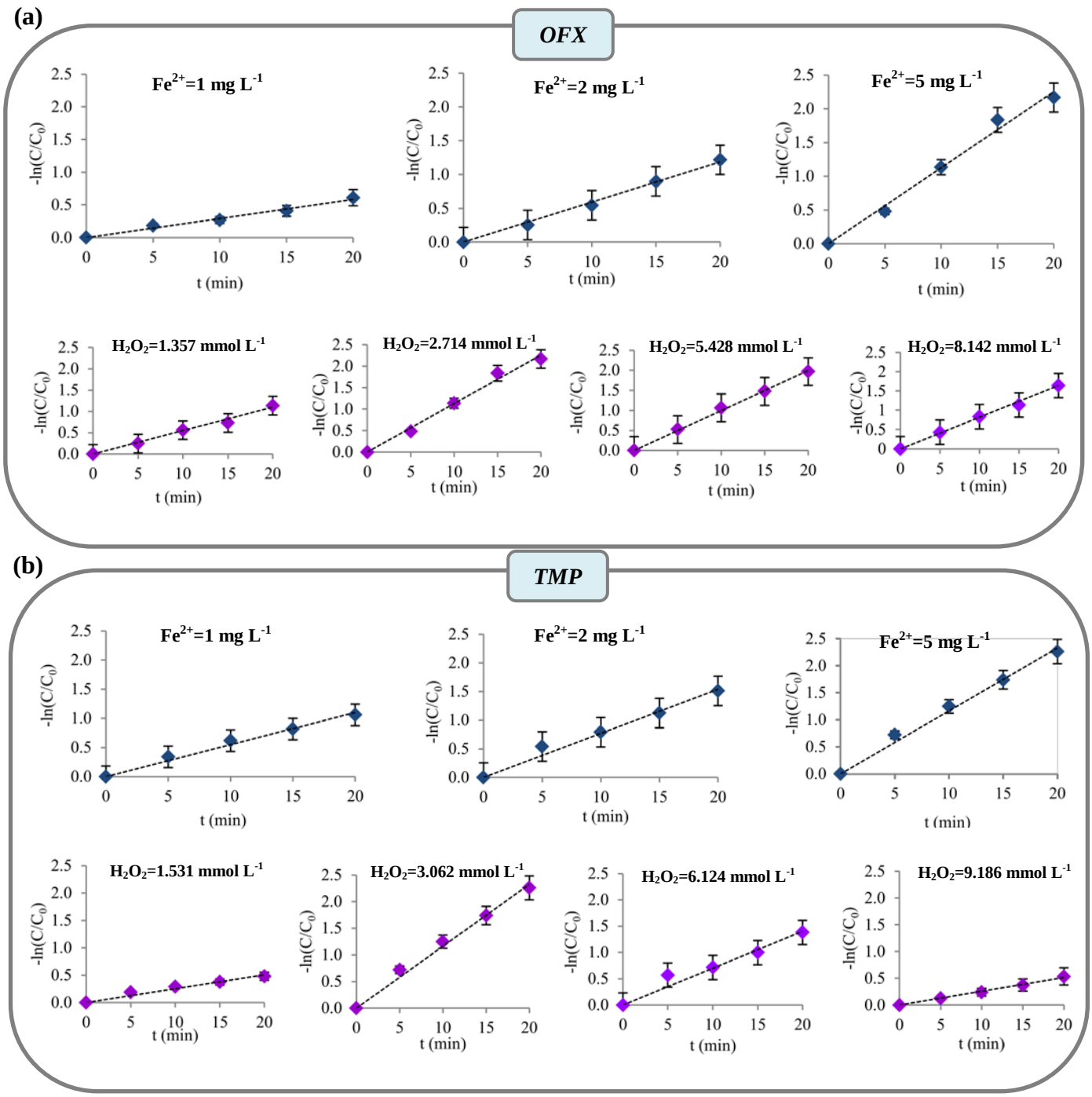

Figure 4.3 Fitting of the experimental data to the linear kinetic model for solar Fenton process: (a) OFX and (b) TMP. Experimental conditions: $[Fe]^{2+}$=1-5 mg L^{-1}; $[H_2O_2]_{OFX}$=1.357-8.142 mmol L^{-1}; $[H_2O_2]_{TMP}$=1.531-9.186 mmol L^{-1}; pH=2.9-3.0 and T=25±0.1 ^{o}C.

It is obvious from Figure 4.4 (a, b) that the increase of Fe^{2+} concentration (from 1 mg L^{-1} to 5 mg L^{-1}) causes an increase of the rate constant. In many photo-Fenton applications, an increase of iron concentration always leads to an increased degradation rate (Lin et al., 2004; Zapata et al., 2009; Mendez-Arriaga et al., 2010). When the iron concentration is very low, the catalyst concentration is the photo-Fenton limiter, and H_2O_2 is consumed by less desirable reactions (Zapata et al., 2009).

Moreover, the fate of Fe^{2+} in the photo-Fenton system has important consequences on the degradation kinetics. As reported by Larson et al. (1991) dissolved oxygen may react with Fe^{2+} to produce superoxide ($O_2^{\bullet-}$), which is susceptible to disproportionation to H_2O_2 and oxygen. Ultimately, additional $HO^{\bullet}$ could be produced by the Fenton reaction of H_2O_2 with Fe^{2+}. The overall process is summarized by the following equations.

$$Fe^{2+} + O_2 \rightarrow Fe^{3+} + O_2^{\bullet-} \quad (4.14)$$

$$2O_2^{\bullet-} + 2H^+ \rightarrow H_2O_2 + O_2 \quad (4.15)$$

$$Fe^{2+} + H_2O_2 \rightarrow HO^{\bullet} + HO^- + Fe^{3+} \quad (4.16)$$

In addition, an increase of peroxide concentration causes an increase of the rate constant (inset diagrams), since more $HO^{\bullet}$ are produced; however, this increase of the reaction rate constant continues up to a level which corresponds to the optimum peroxide concentration (Muruganandham and Swaminathan, 2004). The influence of oxidant concentration on the kinetics during photo-Fenton process was investigated by several studies (Lucas et al., 2006; Santos et al., 2007; Poulopoulos et al., 2008; Tamimi et al., 2008) and the main findings can be reduced to the fact that neither too

low H_2O_2 concentration (leading to a rate reduction of the Fenton reaction) nor a too high concentration may be applied (H_2O_2 competes successfully for $HO^{\bullet}$).

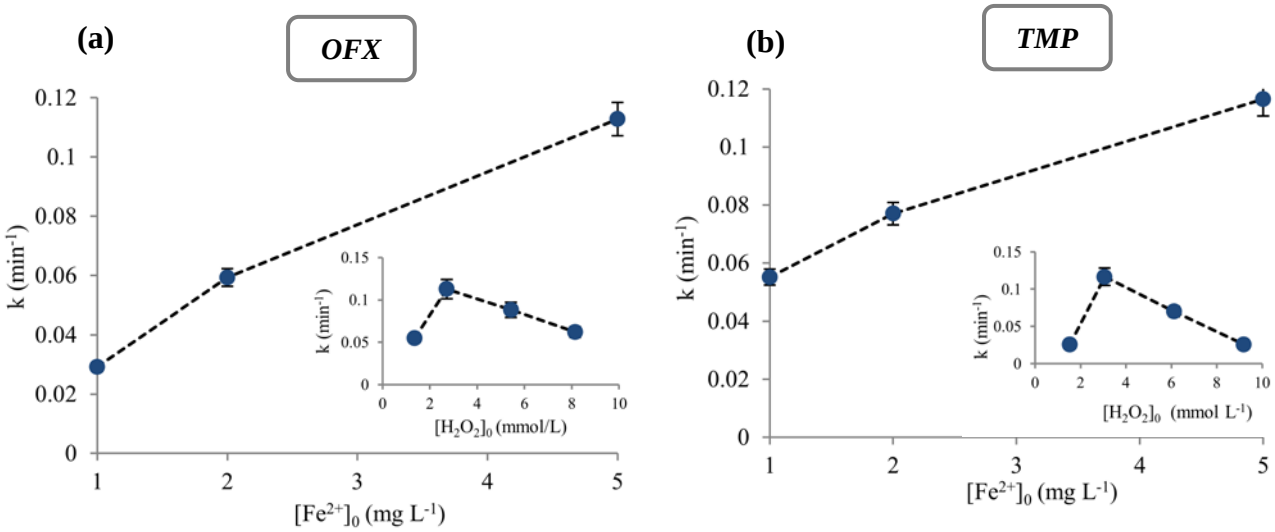

Figure 4.4 Effect of initial ferrous and hydrogen peroxide concentration (inset graph) on the rate constant, *k*: (a) OFX and (b) TMP.

Table 4.1 Kinetic parameters for the solar Fenton system at constant hydrogen peroxide concentration ($[H_2O_{2(OFX)}]_0$=2.714 mmol L^{-1}; $[H_2O_{2(TMP)}]_0$=3.062 mmol L^{-1}).

$[Fe^{2+}]_0$ (mg L^{-1})	k (min^{-1})	$t_{1/2}$ (min)	r_0 (mg L^{-1} min^{-1})
	OFX		
1	0.0292 (R^2=0.982)	23.7	0.310 (R^2=0.992)
2	0.0593 (R^2=0.994)	11.7	0.358 (R^2=0.998)
5	0.1128 (R^2=0.989)	6.14	0.538 (R^2=0.989)
	TMP		

1	0.0551 (R^2=0.984)	12.6	0.432 (R^2=0.992)
2	0.0770 (R^2=0.992)	9.00	0.713 (R^2=0.985)
5	0.1165 (R^2=0.990)	5.95	0.830 (R^2=0.968)

4.1.3 Effect of the solar irradiation

To evaluate the efficiency of the Fenton reagent and the benefit of solar irradiation (SR) on the photocatalytic process, experiments were carried out with the following combinations: (1) Substrate + SR (photolysis); (2) Substrate + Fe^{2+} + SR; (3) Substrate + H_2O_2 + SR (photo-bleaching); (4) Substrate + Fe^{2+} + H_2O_2 (dark Fenton) and; (5) Substrate + Fe^{2+} + H_2O_2 + SR (solar Fenton).

The photolysis (solar radiation alone) of substrate solution (10 mg L^{-1}) showed no significant degradation of the investigated compounds since less than 6% degradation was observed for both compounds after 120 min of solar illumination.

Photolytic degradation can be either direct or indirect. In direct photolysis, the target contaminant (in this case the antibiotic compound) absorbs a solar photon which leads to a break-up of the molecule. In an indirect photolysis mechanism, naturally occurring molecules in the system such as dissolved organic matter (DOM) act as sensitizing species which generates strong reactive agents *e.g.* singlet oxygen ($^1O_2$), hydroxyl radicals ($HO^{\bullet}$) or alkyl peroxyl radicals ($^{\bullet}OOR$) and hydrate electrons under solar radiation (Arnold and McNeill, 2007; Fatta-Kassinos et al., 2011b).

For the determination of the rates of direct photolysis, the two fundamental parameters necessary are the molar absorptivity of the compound as a function of wavelength (ε_λ, which is easily measured with a UV/Vis spectrophotometer) and the quantum yield, Φ. The quantum yield (Φ) determines the efficiency of direct photolysis and is defined as the moles of a compound that are transformed per mole of

photons that were absorbed by the compound (Baeza and Knappe, 2011). Andreozzi et al. (2003) reported the quantum yield value for OFX (Φ = 7.79 $\times 10^{-9}$ mol einstein^{-1} at pH 5.5) obtained from solar irradiation and lamp-light irradiation experiments. TMP was found to exhibit higher quantum yield value compared to OFX (Φ = 1.18 $\times 10^{-3}$ mol einstein^{-1} at pH 7.85, Baeza and Knappe, 2011; Φ = 1.2 $\times 10^{-3}$ at pH 8, Ryan et al., 2011).

Some studies indicate the indirect photolysis of OFX and TMP from the singlet oxygen. Hapeshi et al. (2010) showed that when aqueous OFX solutions were irradiated with UVA under N_2 sparging (anoxic conditions) only 5% conversion was observed. The negligible degradation attained by the photolytic reactions can only be attributed to photo-oxidation of substrate from the singlet oxygen, generated photochemically from the oxygen dissolved in the reaction mixture. Additionally, a major role for singlet oxygen in the photolysis of TMP was reported by Ryan et al. (2011) and Luo et al. (2012). Moreover, Dedola et al. (1999) reported the slow degradation of TMP during photolysis due to the presence of aromatic amines in its structure which are characterized by a little photochemical reactivity. Other authors studied the photolytic degradation of TMP achieving very low removals or very long reaction times to obtain a high degradation (Adams et al., 2002; Sirtori et al., 2010). As reviewed by Boreen et al. (2003), many investigations have focused on the photostability of pharmaceutical compounds. In some cases, these studies have used conditions relevant to environmental conditions (*e.g.* an aqueous solution of the compound irradiated with wavelengths of light > 300 nm). Generally photolysis is relatively ineffective in treating wastewater matrices contaminated with antibiotics. This technology is only applicable to wastewater containing photo-sensitive compounds and waters with low COD concentrations (*e.g.* river, drinking waters).

The combined action of solar radiation and Fe^{2+} at acidic conditions (pH = 2.9-3.0) alone was not able to oxidize the compounds completely, leading to a very small degradation of only 5% and 9% for OFX and TMP respectively within 120 min of the photocatalytic treatment. It must be noted that even in the absence of the oxidant, photodegradation still occurs due to charge transfer photolysis of Fe^{3+}. At pH≈3.0 the predominant species is the $[FeOH(H_2O)_5]^{2+}$ complex which is able to undergo excitation. This excitation is followed by electron transfer producing Fe^{2+} aqua complex and $HO^{\bullet}$ (Larson et al., 1991; Ciesla et al., 2004). However, the degradation in the presence of iron alone is relatively slow.

Additional experiments were also performed to assess the contribution of photo-bleaching in the presence of 2.714 and 3.062 mmol L^{-1} H_2O_2 which are the optimum H_2O_2 concentrations for OFX and TMP, respectively (as determined in section 4.1.1). The results showed that 30% of OFX and 35% of TMP was degraded within 120 min. This degradation can be attributed to the photochemical cleavage of H_2O_2 to yield $HO^{\bullet}$ by solar light absorption (Tuhkanen, 2004). Moreover, the degradation profile of the compounds indicates that the SR/H_2O_2 process enhanced the degradation of TMP substrate more than OFX degradation. An important remark is the fact that under these experimental conditions, DOC did not decrease. Thus, the composition of the remained organic solution after 120 min of the SR/H_2O_2 process could be addressed to the by-products formed during OFX and TMP oxidation.

Dark Fenton experiments were conducted to assess the oxidation power of the Fenton reagent in the absence of solar light. In the dark Fenton, OFX conversion was completed at 90 min whereas TMP was degraded completely within 120 min. However, the substrates' oxidation was strongly accelerated by solar irradiation (solar Fenton) and was completed at 30 min for both compounds. The acceleration observed

in the solar Fenton is due to the formation of additional $HO^{\bullet}$ and to the recycling of ferrous catalyst by photoreduction of Fe^{3+} to Fe^{2+} (Huston and Pignatello, 1999; Kavitha and Palanivelu, 2004). In addition, DOC removal was enhanced under the irradiated conditions in the solar Fenton system. The maximum DOC removal for both substrates solutions was around 35% and 40% during the dark Fenton and solar Fenton process, respectively.

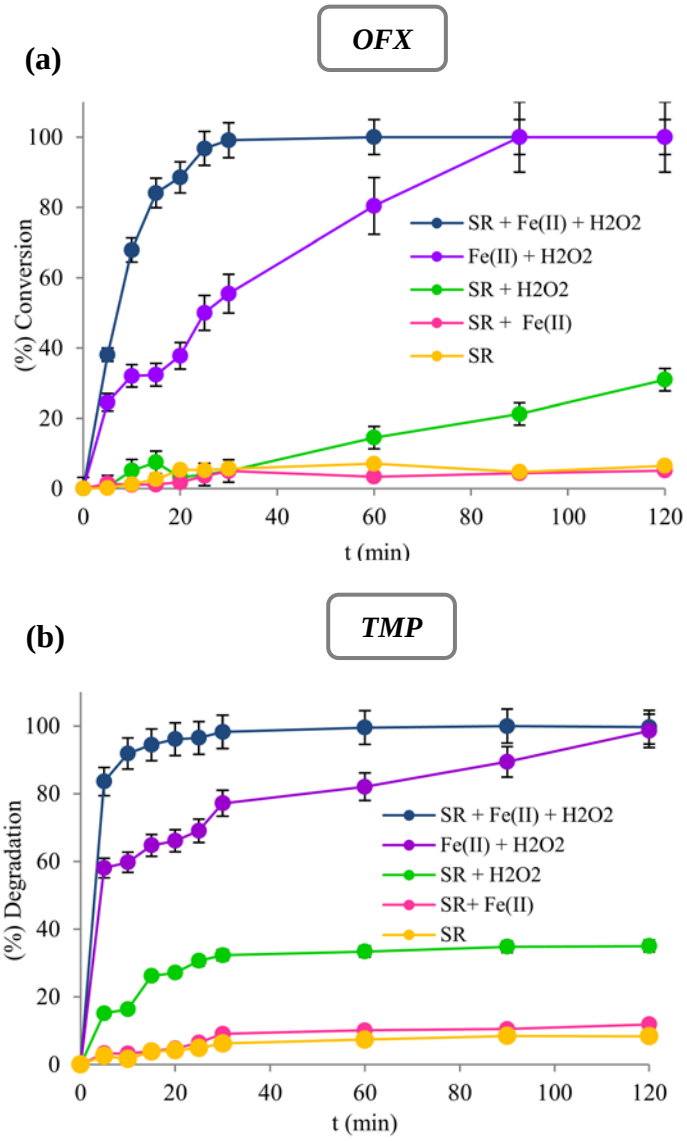

Figure 4.5 Degradation of (a) OFX and (b) TMP spiked wastewater solutions under different conditions. Initial experimental conditions: $[Fe^{2+}]_0$=5 mg L^{-1}; $[H_2O_{2(OFX)}]_0$=2.714 mmol L^{-1}; $[H_2O_{2(TMP)}]_0$=3.062 mmol L^{-1}; $[OFX]_0$=0.0277 mmol L^{-1}; $[TMP]_0$=0.0344 mmol L^{-1}; pH=2.9-3.0 and T=25±0.1 ^oC.

Hence, the relative efficiencies of the above processes can be given in the following order: Substrate + Fe^{2+} + H_2O_2 + SR: solar Fenton > Substrate + Fe^{2+} + H_2O_2: dark Fenton > Substrate + H_2O_2 + SR (photo-bleaching) > Substrate + Fe^{2+} + SR ≈ Substrate + SR (photolysis). The corresponding results are presented in Figure 4.5 (a, b).

4.1.4 Effect of pH

The pH plays a crucial role in the efficiency of the solar Fenton process since it significantly affects the formation of the oxidizing agents ($HO^{\bullet}$) and the concentration of the dissolved ferrous complexes (Tamimi et al., 2008; Malato et al., 2009). Experiments were carried out at pH levels in the range 2.0-4.5 by adding the appropriate amount of 1M H_2SO_4 solution. Figure 4.6 (a_1, a_2, b_1, b_2) shows the influence of pH on the photocatalytic oxidation and on the degradation rate constant of OFX and TMP.

At pH 2.0 the OFX conversion was approximately 75% in 120 min but by increasing the pH to 3.0, complete conversion was observed in 30 min and the highest rate constant was achieved. TMP degradation was 61% at pH 2.0 whereas TMP was degraded completely at pH 3.0 (30 min). For pH values below 3.0, the reaction of H_2O_2 with Fe^{2+} is seriously affected, causing a reduction in $HO^{\bullet}$ production. The low degradation at pH 2.0 is also due to the $HO^{\bullet}$ scavenging by the H^+ ions (eqn. (4.17)) as this was suggested by Lucas and Peres (2006) and Tamini et al. (2008).

$$HO^{\bullet} + H^{+} + e^{-} \rightarrow H_2O \quad (4.17)$$

Another reason for the inefficient degradation at pH < 3.0 may be attributed to the reaction of H_2O_2 with H^+ ions to form stable oxonium ion $[H_3O_2]^+$. An oxonium ion makes peroxide electrophilic to enhance its stability and substantially reduces the reactivity with Fe^{2+} (Abo-Farha, 2010). Moreover, at low pH the reaction is slowed down due to the formation of complex species $[Fe(H_2O)_6]^{3+}$, which reacts more slowly with peroxide and therefore, produce less $HO^{\bullet}$ (Xu et al., 2009). Furthermore, at pH < 3.0, the reaction system is autocatalytic, because Fe^{3+} decomposes H_2O_2 in O_2 and H_2O through a chain mechanism (eqs. (4.18)-(4.22)) (Litter, 2005).

$$Fe^{3+} + H_2O_2 \rightarrow Fe\text{-}OOH^{2+} + H^{+} \quad (4.18)$$

$$Fe\text{-}OOH^{2+} \rightarrow HO_2^{\bullet} + Fe^{2+} \quad (4.19)$$

$$HO_2^{\bullet} + Fe^{2+} \rightarrow Fe^{3+} + HO_2^{-} \quad (4.20)$$

$$HO_2^{\bullet} + Fe^{3+} \rightarrow Fe^{2+} + O_2 + H^{+} \quad (4.21)$$

$$HO^{\bullet} + H_2O_2 \rightarrow HO_2^{\bullet} + H_2O \quad (4.22)$$

On the other hand, at pH 4.5 the conversion was further reduced to 46% for OFX and 57% for TMP in 120 min, due to iron precipitation as hydroxide and the resulted reduction of the transmission of the radiation (Faust et al., 1990). The oxidation potential of $HO^{\bullet}$ also decreases, by increasing the pH (Lucas and Peres, 2006; Babuponnusami and Muthukumar, 2011).

A pH range of 2.8-3.0 is frequently postulated as the optimum operating condition for the photo-Fenton process (Pignatello et al., 1992; Safarzadeh-Amiri et al., 1996), to avoid the formation and subsequent precipitation of iron hydroxides (Klavarioti et al., 2009). Additionally, at pH 2.8-3.0 the predominant species is the $[FeOH(H_2O)_5]^{2+}$

complex which is able to undergo excitation. The excitation is followed by electron transfer producing Fe^{2+} aqua complex and $HO^{\bullet}$ radicals (Larson et al., 1991; Ciesla et al., 2004):

$$[FeOH(H_2O)_5]^{2+} + H_2O + h\nu \rightarrow [Fe(H_2O)_6]^{2+} + HO^{\bullet} \quad (4.23)$$

At this pH range the dominant ferric species in the solution are $[Fe(OH)]^{2+}$ (eqn. (4.24)); the most photoactive ferric iron-water complex (Malato et al., 2009).

$$[Fe(OH)]^{2+} + h\nu \rightarrow Fe^{2+} + HO^{\bullet} \quad (4.24)$$

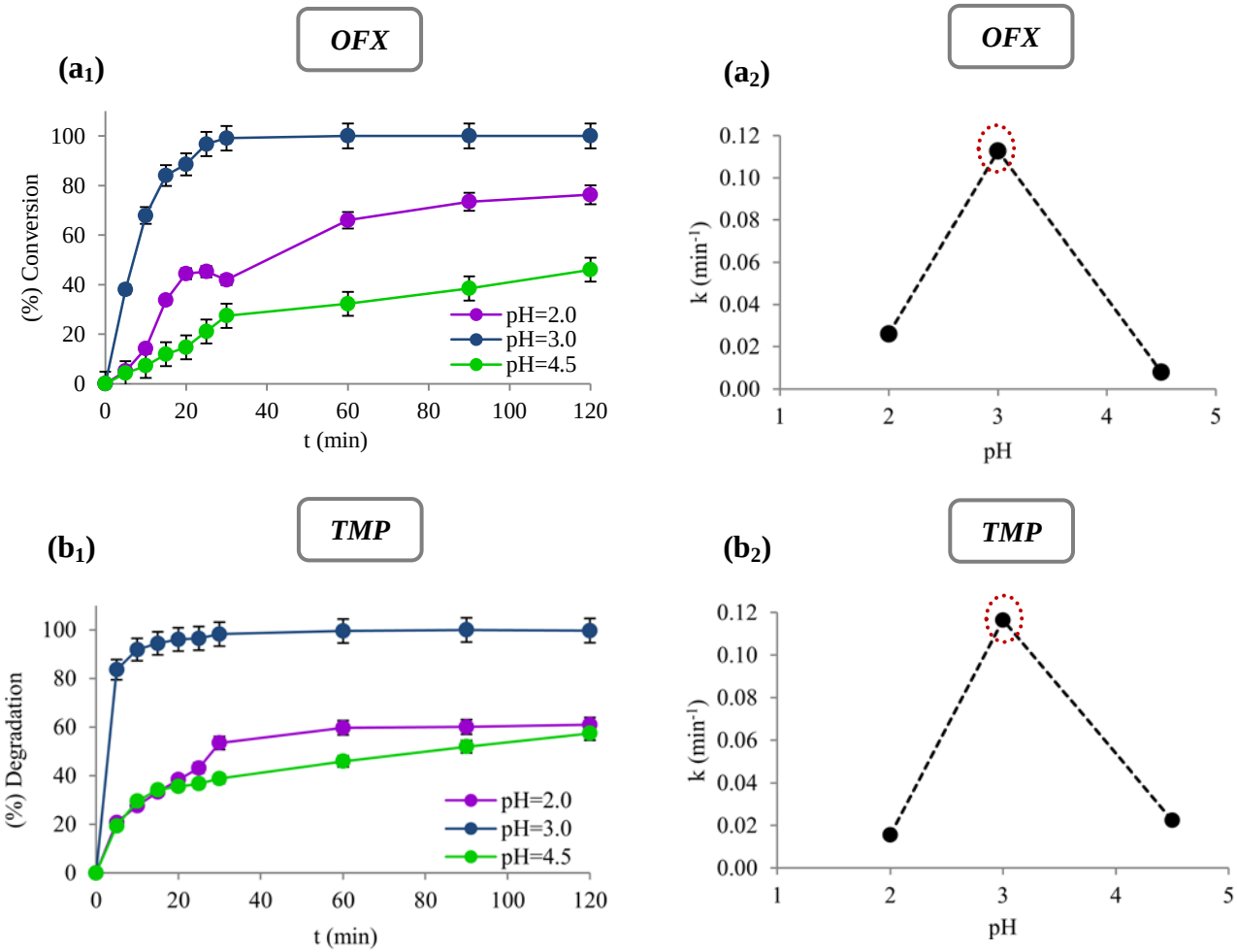

Figure 4.6 Effect of initial solution pH on photooxidation and on the degradation rate constant, *k* of: (a) OFX (a_1, a_2) and (b) TMP (b_1, b_2) spiked wastewater solutions. Experimental conditions: $[Fe^{2+}]_0$=5 mg L^{-1}; $[H_2O_{2(OFX)}]_0$=2.714 mmol L^{-1}; $[H_2O_{2(TMP)}]_0$=3.062 mmol L^{-1}; $[OFX]_0$=0.0277 mmol L^{-1}; $[TMP]_0$=0.0344 mmol L^{-1} and T=25±0.1 ^oC.

The need for acidification in the Fenton process is often outlined as one of its major drawbacks. Not only does this mean additional cost through the consumption of reagents for acidification but also an increase of the salinity of the treated solution. In order to avoid the need for acidification of the wastewater and to maintain iron stably dissolved, some researchers are performing the photo-Fenton reaction in the presence of iron complexing agents (Sun and Pignatello, 1992). The addition of oxalic acid or the direct addition of ferric oxalate as iron source which are photoactive in the UV/Vis region, have been proposed by Nogueira et al. (2005).

A new approach aimed at performing photo-Fenton treatment at neutral pH has been proposed by Moncayo-Lasso et al. (2008), Klamerth et al. (2010) and De la Cruz et al. (2012). The efficiency of the modified photo-Fenton system is based on the reaction of dissolved organic matter (DOM) present in wastewaters with Fe^{2+} leading to the formation of soluble iron-complexes. However, contaminants degradation and mineralization tend to be slower at neutral pH than at pH 3.0. The efficiency of the solar Fenton process at neutral pH was examined in detail in a pilot scale set-up and it is discussed further in CHAPTER 5.

4.1.5 Effect of temperature

The temperature significantly increases the activity of the photo-Fenton system and has a beneficial effect on the reaction kinetics (Gob et al., 2001; Torrades et al., 2003; Gernjak et al., 2006). The photooxidation of OFX and TMP was investigated with reaction temperatures ranging from 15 to 45 ^{o}C. Temperatures over 45 ^{o}C were not examined, as solar photocatalytic plants cannot be operated at higher temperatures in real-life applications which was the objective of the present study. Figure 4.7 (a, b) shows the degradation process and the rate constant (inset graphs) for OFX and TMP at each temperature level studied.

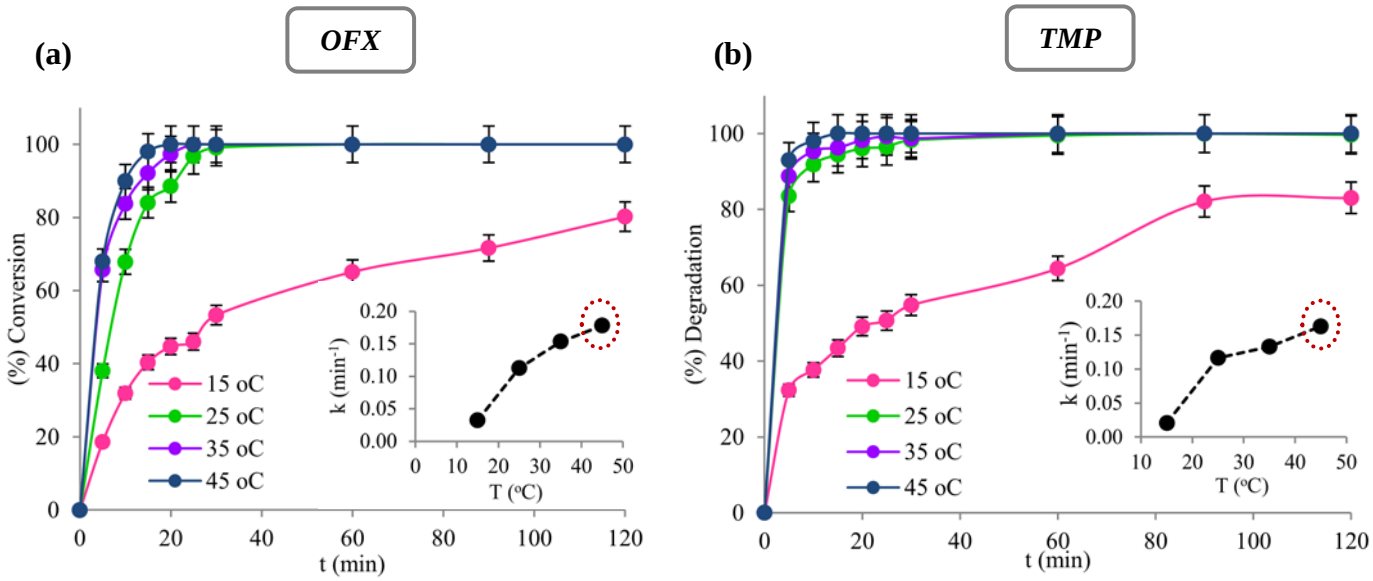

Figure 4.7 Effect of temperature on photooxidation of (a) OFX and (b) TMP spiked wastewater solutions. Inset graph shows the effect of temperature on the rate constant, *k*. Experimental conditions: $[Fe^{2+}]_0$=5 mg L^{-1}; $[H_2O_{2(OFX)}]_0$=2.714 mmol L^{-1}; $[H_2O_{2(TMP)}]_0$=3.062 mmol L^{-1}; $[OFX]_0$=0.0277 mmol L^{-1}; $[TMP]_0$=0.0344 mmol L^{-1} and pH=2.9-3.0.

As expected, the highest treatment efficiency (*i.e.* faster substrate degradation, shorter illumination time required for complete removal and less hydrogen peroxide

consumption) was obtained at 45 ^{o}C. This could be explained by a faster rate of ferrous regeneration from ferric ion, which is even faster as the temperature increases. This enhancement can be also attributed to the increase of the $Fe(OH)^{2+}$ concentration and to the temperature dependence of the quantum yield of the photochemical reduction of Fe^{3+} (Lee and Yoon, 2004). Furthermore, higher temperatures in the solar-Fenton process lead to a faster thermal decomposition of the H_2O_2, increasing the available $HO^{\bullet}$ (Santos et al., 2007). It is remarkable that the existence of $HO^{\bullet}$ scavengers, contained in wastewater samples, can also influence the temperature dependence of the $HO^{\bullet}$ concentration in the $h\nu/Fe^{3+}/H_2O_2$ system (Malato et al., 2009). Moreover, it must be noted that temperatures higher than 50 ^{o}C are known to enhance the iron precipitation during the photo-Fenton process (Krysóvá et al., 2003; Zapata et al., 2009b).

The dependence of the rate constant on the temperature is described by the Arrhenius-type equation (eqn. (4.25)):

$$k_T = A\, exp\left(-\frac{E_a}{RT}\right) \tag{4.25}$$

where E_a is the activation energy of the reaction, A is a pre-exponentional factor, R is the Universal gas constant and T is the temperature (in Kelvins). It should be noted that the activation energy (E_a) of the reaction represents the temperature dependence, and a higher value of E_a indicates a higher temperature dependence of the reaction (Lee and Yoon, 2004).

Arrhenius equation can be linearized as follows:

$$lnk = lnA - \frac{E_a}{RT} \tag{4.26}$$

The rate constant (*k*) vs *1/T* was found to be linear, obeying Arrhenius equation (E_{aOFX} = 58.0 kJ mol^{-1}; E_{aTMP} = 68.9 kJ mol^{-1}) indicating the dependence of OFX and TMP degradation on *T* (Figure 4.8). Arrhenius temperature dependence for some antibiotics (*e.g.* trimethoprim, lyncomycin and ciprofloxacin) was observed also in a recent study by Hu et al. (2010) with activation energies ranging from 49 to 68 kJ mol^{-1}.

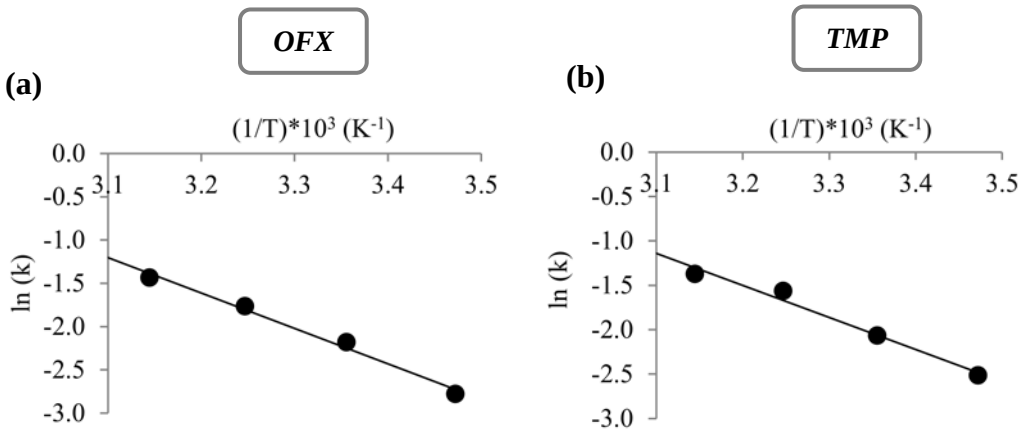

Figure 4.8 Logarithm of kinetic constant (ln(*k*)) plotted against inverse temperature (1/T): (a) OFX and (b) TMP spiked wastewater solutions.

4.1.6 Effect of initial substrate concentration

The influence of the initial substrate concentration on the photocatalytic degradation of OFX and TMP was investigated at different levels of concentrations (2-10 mg L^{-1}; 100 μg L^{-1}) and the results are depicted in Figure 4.9 (a, b).

OFX substrate was degraded completely at 2 mg L^{-1} (25 min), 5 mg L^{-1} (25 min) and 10 mg L^{-1} (30 min) while TMP degradation was 100% at 2 mg L^{-1} (20 min), 5 mg L^{-1} (30 min) and 10 mg L^{-1} (30 min). At higher concentration of 20 mg L^{-1} the substrates degradation was decreased to 85% and 91% for OFX and TMP within 120 min, respectively.

Additionally, it was observed that the degradation rate constant decreased with increasing the initial concentration of the substrate from 2 to 20 mg L^{-1} (inset graphs). Many studies (Lucas and Peres, 2006; Malato et al., 2009; Tamimi et al., 2008) reported that degradation of substrate in distilled water at levels of mg L^{-1} during photo-Fenton process increases with decreasing the initial substrate concentration. The presumed reason is that higher substrate concentrations need a longer treatment time under identical process conditions (Malato et al., 2009).

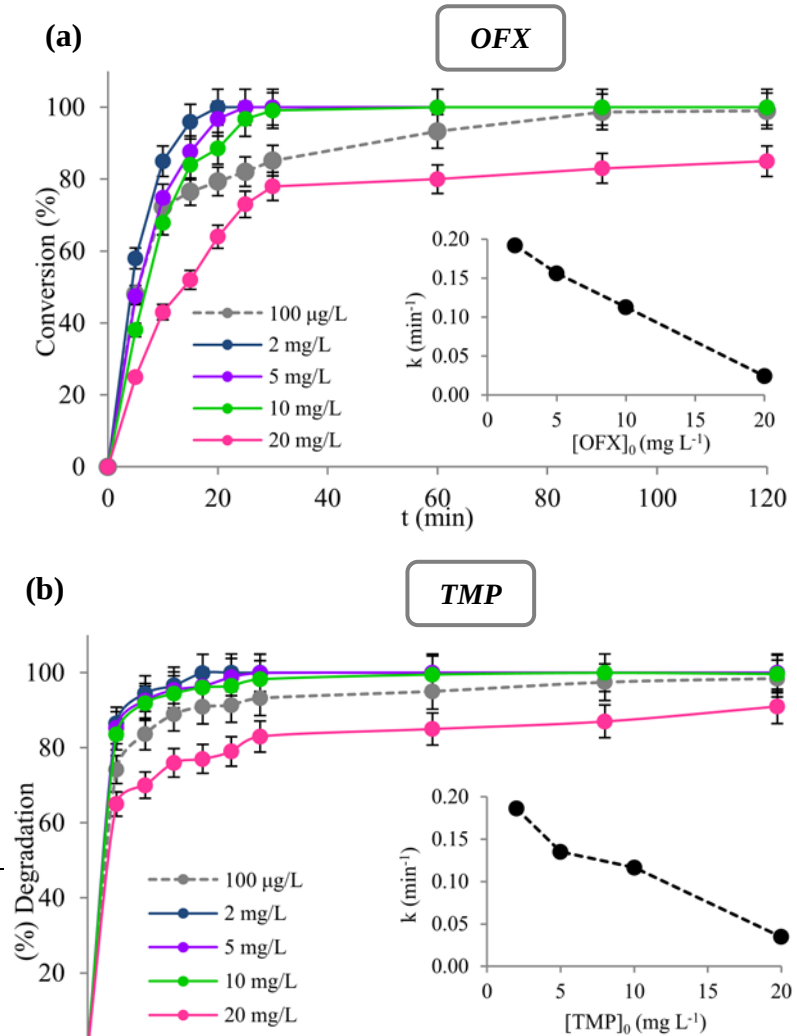

Figure 4.9 Effect of initial substrate concentration on photooxidation of (a) OFX and (b) TMP spiked wastewater solutions. Inset graph shows the effect of initial substrate concentration on the rate constant, *k*. Experimental conditions: $[Fe^{2+}]_0$=5 mg L^{-1}; $[H_2O_{2(OFX)}]_0$=2.714 mmol L^{-1}; $[H_2O_{2(TMP)}]_0$=3.062 mmol L^{-1}; $[OFX]_0$=0.0277 mmol L^{-1}; $[TMP]_0$=0.0344 mmol L^{-1}; pH=2.9-3 and T=25±0.1 ^oC.

In further experiments the degradation of OFX and TMP solution at lower level concentration (100 μg L^{-1}) was examined considering that the typical environmental concentrations of antibiotics in the effluents are in the ng-μg L^{-1} range. As can be seen from Figure 4.9 (a, b), OFX and TMP degradation proceeded more slowly at 100 μg L^{-1} compared to that at mg L^{-1} level (except 20 mg L^{-1}). Although in the previous experiments the degradation increased with decreasing the initial concentration it seems that when substrate concentration is in the μg L^{-1} level the degradation is slower. The complete degradation of the compounds was achieved within 120 min of solar illumination while the respective degradation constant values were lower than those observed at mg L^{-1} level (except 20 mg L^{-1}) (k = 0.0345 min^{-1} for OFX; k = 0.0768 min^{-1} for TMP). The possible explanation for these results is that at very low substrate concentration, the generated $HO^{\bullet}$ cannot easily attack the substrate molecules contained in a complex wastewater matrix and thereby lowering the degradation rates.

4.2 Solar TiO_2 oxidation process

4.2.1 Effect of catalyst concentration

Preliminary dark adsorption experiments were conducted to assess the extent of OFX and TMP adsorption onto TiO_2 particles at catalyst loadings ranging from 0.25 to 4.0 g L^{-1}. Experiments were performed with substrate solution of 10 mg L^{-1} in the dark under continuous stirring for 24 h. It was observed that equilibrium was reached within 30 min with less than 8% of OFX and TMP adsorbed on the catalyst's surface.

Further experiments were conducted in the presence of solar irradiation and catalyst loading varying from 0.25-4.0 g L^{-1}. The results are presented in Figure 4.10 (a, b). The results demonstrate that the degradation of the antibiotics and the initial degradation rate (r_0) increased by increasing the catalyst amount up to a level after which a sharp drop of the r_0 (inset graphs) was observed.

From Figure 4.10 (a, b) it is apparent that the optimum concentration of TiO_2, under the experimental conditions, was 3 g L^{-1} for both compounds yielding 60% and 68%

degradation of OFX and TMP, respectively. Moreover, as shown in Figure 4.10 (a, b), the degradation profile of the substrates was different indicating the different degradation pathway of the two substrates.

The total active surface area increases by increasing catalyst dosage up to a level which corresponds to the optimum of light absorption (Daneshvar et al., 2004). Above the optimum amount of TiO_2 the increased turbidity of the solution reduced the light transmission through the solution. Below this level, it is assumed that the catalyst surface and the absorption of light are the limiting factors for the process (Evgenidou et al., 2005). Furthermore, at high concentrations of the catalyst, agglomeration (particle-particle interactions) can also take place resulting to the loss of surface area available for light absorption (Sakthivel et al., 2003).

(a)

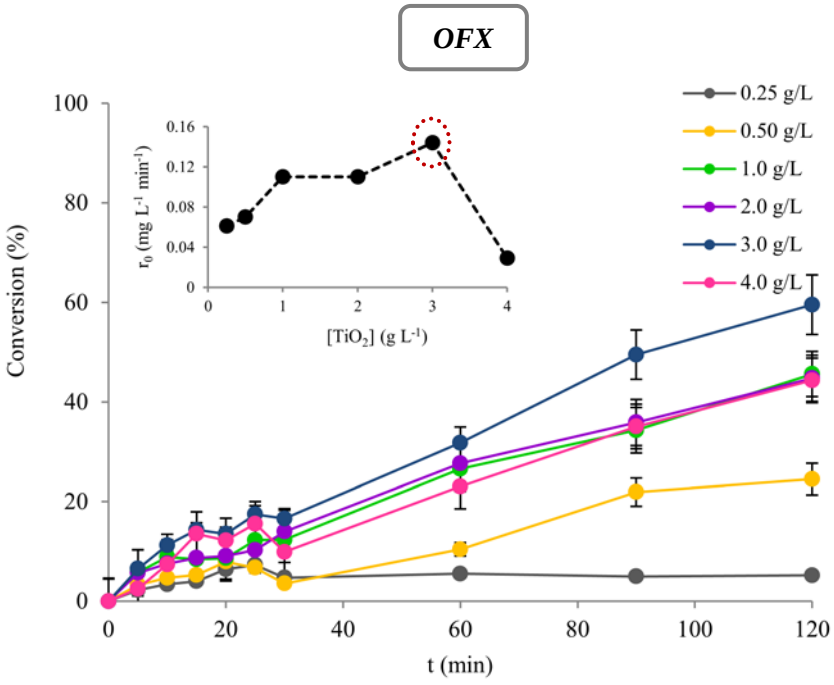

(b)

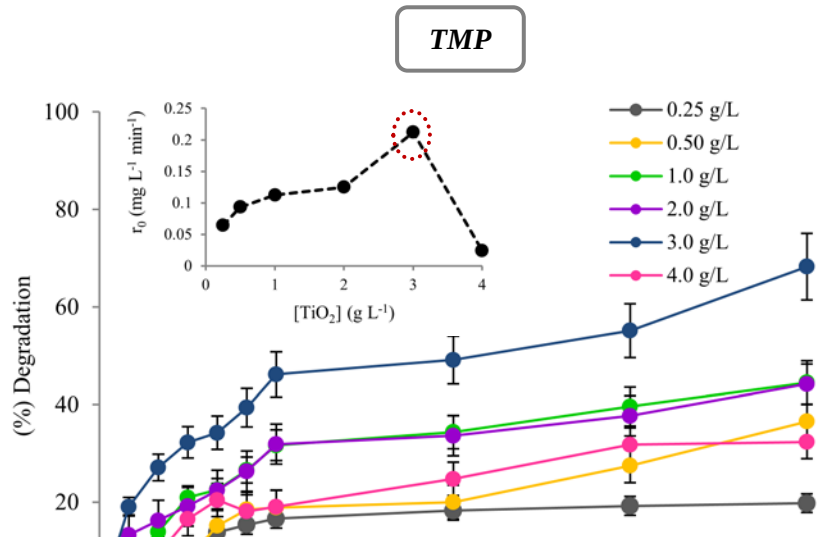

Figure 4.10 Effect of catalyst loading on photooxidation of: (a) OFX and (b) TMP spiked wastewater solutions. Inset graph shows the effect of TiO_2 concentration on the initial rate, r_0. Experimental conditions: $[OFX]_0$=0.0277 mmol L^{-1}; $[TMP]_0$=0.0344 mmol L^{-1}; pH=7.0 and T=25±0.1 ^oC.

4.2.2 Effect of pH

In the heterogeneous photocatalytic process, the adsorption of the investigated substrate on the catalyst surface and the degradation rate is strongly dependent on the pH of the solution. The initial pH of the 10 mg L^{-1} OFX or TMP solution was approximately 7.0 and was adjusted to alkaline or acidic range by adding the appropriate amount of NaOH or HCl solutions. The degradation and rate constant of the substrates oxidation at various pH values (pH 2.0, 7.0 and 10.0) are given in Figure 4.11 (a, b) and Figure 4.12 (a, b), respectively.

The experimental results showed that, the degradation of both compounds and the rate constant is higher in acidic conditions compared to alkaline conditions. The higher degradation of the substrates was observed at pH 2.0; 91.6% for OFX and 68.3% for TMP within 120 min of heterogeneous photocatalytic treatment. The effect of the pH on degradation is a complex issue since it concerns: (i) the charge of TiO_2 surface with respect to its point of zero charge (*pzc*); (ii) the ionization state of the substrate and its degradation by-products formed during the process (Hapeshi et al., 2010); (iii) the equilibrium of water dissociation which affects the generation of $HO^{\bullet}$

(Xekoukoulotakis et al., 2010); and (iv) the oxidative power of the photogenerated holes, radicals or other reactive species in the reaction mixture (Konstantinou and Albanis, 2004).

The point of zero charge (*pzc*) of the TiO_2 (Aeroxide® P25) is at pH 6.8. Thus, the TiO_2 surface is positively charged in acidic media (pH < 6.8), whereas it is negatively charged under alkaline conditions (pH > 6.8) (Poulios et al., 1998).

$$TiOH + H^+ \rightarrow TiOH_2^+ \quad (4.27)$$

$$TiOH + OH^- \rightarrow TiO^- + H_2O \quad (4.28)$$

The equilibrium constants of these reactions are $pK_{TiOH_2^+}$=2.4 and pK_{TiOH}=8.0 (Kormann et al., 1991).

OFX has two ionizable functional groups, the carboxylic group (–COOH) and the N of the piperazinyl substituent (Okeri and Arhewoh, 2008). According to Schematic 4.1, OFX is primarily cationic below pK_{a1}, anionic above pK_{a2}, and zwitterionic *i.e.*, net neutral between pK_{a1} and pK_{a2}.

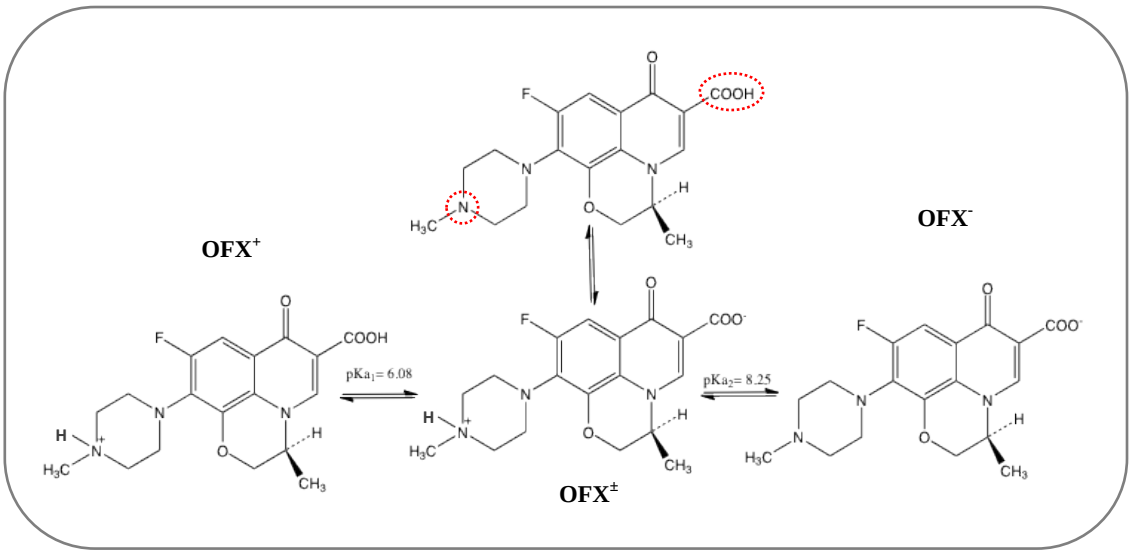

Schematic 4.1 Ionisation of OFX: OFX^+ = cationic ofloxacin; $OFX^{\pm}$ = zwitterionic ofloxacin; and OFX^- = anionic ofloxacin.

TMP contains two reactive sites: an activated aromatic ring (1,2,3-trimethoxybenzene) and a secondary amine-moiety (2,4-diaminopyrimidine). The reaction of the amine-moiety depends on the solution pH, while the reaction of the aromatic ring does not. Consequently, the reaction of TMP depends on the pK_a of the amines and the pH of the solution. In the case of a basic drug as TMP, when the pH is below the pK_a values, the drug has positive charge because of the protonation of the aniline moieties that it contains (Dodd et al., 2007) (Schematic 4.2).

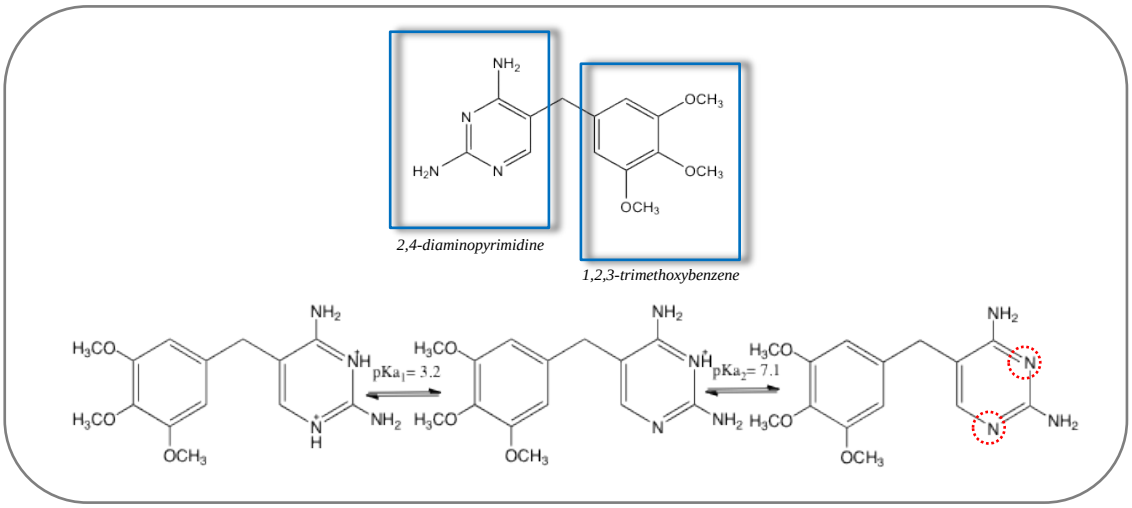

Schematic 4.2 Ionisation of TMP molecule.

When pH was increased from 7.0 (inherent pH) to 10.0, the adsorption of OFX and TMP (see inset figures) increased from 7.5% to 15.4% and from 9.5% to 13.3%, respectively. The adsorption increased noticeably to 29.5% and 26.8% in acidic conditions (pH 2.0) for OFX and TMP, respectively. Under these conditions catalyst surface gradually becomes positively and negatively charged at acidic and alkaline conditions, respectively. Logically this should have led to an electrostatic repulsion

between the substrates and the catalyst. It should be noted that at pH 7.0, a pH value in the close vicinity of TMP pK_a value, the adsorption of the compound is very low because TMP molecules and the catalyst particles are completely neutral.

Concerning the above, the effect of the pH of the solution on the photocatalytic degradation of OFX and TMP cannot be explained in terms of the ionization state of the catalyst and the substrate alone, since both have either negative or positive charges at alkaline or acidic conditions, respectively; *i.e.* neither environment should particularly favour substrate adsorption onto the catalyst surface (Hapeshi et al., 2010). Therefore, the behaviour shown in Figure 4.11 (a, b) may be due to the relative contribution of various non-determined herein complex reactions.

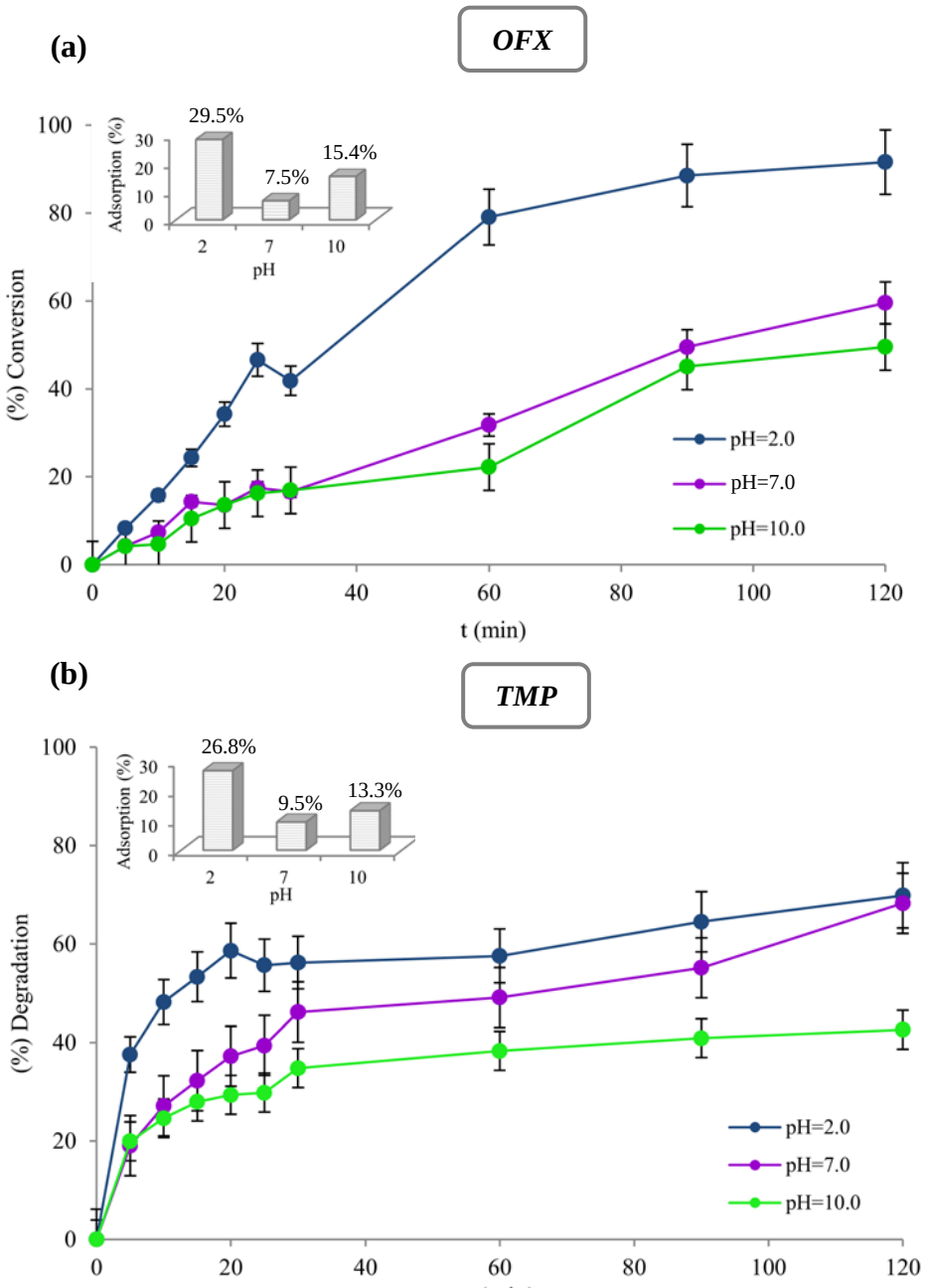

Figure 4.11 Effect of initial solution pH on adsorption and degradation of: (a) OFX and (b) TMP spiked wastewater solutions. Experimental conditions: $[TiO_2]$=3 g L^{-1}; $[OFX]_0$=0.0277 mmol L^{-1}; $[TMP]_0$=0.0344 mmol L^{-1} and T=25±0.1 ^oC.

At low pH values, positive holes are the major oxidation species, while at neutral or high pH, $HO^{\bullet}$ are considered the major species (Konstantinou and Albanis, 2004); it seems that at pH 2.0 OFX and TMP degradation is driven primarily by valence band holes rather than radicals. On the other hand, at high pH values the $HO^{\bullet}$ are rapidly scavenged and they do not have the opportunity to react with organic compounds (Davis and Huang, 1989).

The degradation rate of some antibiotic compounds increases with decreasing pH as reported elsewhere and cannot be explained in terms of the ionization states of the TiO_2 and the investigated substrates (Giraldo et al., 2010; Xekoukoulotakis et al., 2010; Xekoukoulotakis et al., 2011).

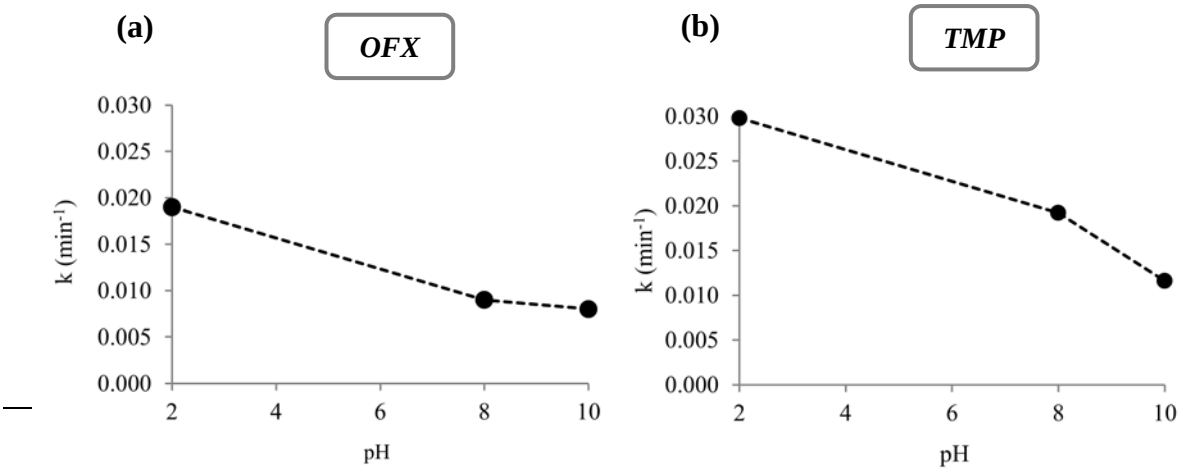

Figure 4.12 Effect of initial solution pH on the degradation rate constant, *k*: (a) OFX and (b) TMP spiked wastewater solutions. Experimental conditions: $[TiO_2]$=3 g L^{-1}; $[OFX]_0$=0.0277 mmol L^{-1}; $[TMP]_0$=0.0344 mmol L^{-1} and T=25±0.1 ^oC.

4.2.3 Effect of oxidants

One practical problem in using TiO_2 as photocatalyst is the electron-hole ($e_{CB}^- - h_{VB}^+$) recombination which in the absence of proper electron acceptors, is extremely efficient and thus represents a major energy-wasting step, limiting the achievement of a high quantum yield. The use of inorganic powerful oxidizing species such as hydrogen peroxide (H_2O_2) and peroxodisulphate ($S_2O_8^{2-}$) has been demonstrated to enhance the photodegradation rate of a variety of organic compounds using TiO_2 (Malato et al., 2000; Hapeshi et al., 2010). In further experiments, the addition of the aforementioned oxidizing species to TiO_2 suspensions was investigated by employing different concentrations of the oxidant and results are shown in Figure 4.13 (a, b).

The above oxidants are considered to have two functions in the process of photocatalytic degradation. They accept a photo-generated electron from the conduction band and thus promote the charge separation (inhibiting $e_{CB}^- - h_{VB}^+$ recombination on the semiconductor surface) and the production of $HO^{\bullet}$ (eqn. (4.29))

and $SO_4^{\bullet-}$ (eqn. (4.31)) radicals. They also form $HO^{\bullet}$ radicals according to eqn. (4.30) and eqn. (4.32) (Malato et al., 2009).

$$H_2O_2 + e_{CB}^- \rightarrow HO^{\bullet} + HO^- \quad (4.29)$$

$$H_2O_2 + O_2^{\bullet-} \rightarrow HO^{\bullet} + HO^- + O_2 \quad (4.30)$$

$$S_2O_8^{2-} + e_{CB}^- \rightarrow SO_4^{2-} + SO_4^{\bullet-} \quad (4.31)$$

$$SO_4^{\bullet-} + H_2O \rightarrow SO_4^{2-} + HO^{\bullet} + H^+ \quad (4.32)$$

$$H_2O_2 + 2h_{VB}^+ \rightarrow O_2 + 2H^+ \quad (4.33)$$

Generally, it was found that an increase of the oxidant concentration causes an increase of the reaction rate constant, especially in the presence of $S_2O_8^{2-}$. This is valid up to an upper concentration after which a reduction of the rate constant was observed.

The optimum $S_2O_8^{2-}$ concentration, under the studied experimental conditions, was approximately 5 and 6 mmol L^{-1} for OFX and TMP, respectively; above these values a decrease to the reaction rate was observed. The superior behavior of the photocatalytic degradation when using $S_2O_8^{2-}$ is not only due to the prevention of the recombination of the $e_{CB}^- - h_{VB}^+$ pair but also due to the photolytic activity of the oxidant (ability to absorb light and act as sensitizer through the production of sulfate radicals which are very strong oxidizing agents; E^0 = 2.6 V)) (Evgenidou et al., 2007b, 2007c).

On the other hand, the optimum H_2O_2 concentration was 5.5 mmoL L^{-1} for OFX and 3 mmol L^{-1} for TMP while at higher oxidant concentration an inhibition on the rate constant was observed for both compounds. H_2O_2 at high concentration can become a

scavenger of valence band holes and $HO^{\bullet}$ (Kritikos et al., 2007) thus reducing the degradation of the substrates (eqs. (4.34)-(4.35)).

$$H_2O_2 + 2h_{VB}^{+} \rightarrow O_2 + 2H^{+} \quad (4.34)$$

$$H_2O_2 + HO^{\bullet} \rightarrow H_2O + {}^{\bullet}OH_2 \quad (4.35)$$

Another adverse effect of H_2O_2 addition at high concentration is that the peroxide reacts with TiO_2 and forms peroxo compounds, which are detrimental to the photocatalytic efficiency (Poulios et al., 2000). This explains the need for an optimal concentration of H_2O_2 for maximum effect (Poulios et al., 1998).

Moreover, comparing the two substrates degradation, the addition of $S_2O_8^{2-}$ was obviously more effective on OFX substrate decomposition comparing that observed with the peroxide addition; on the other hand, this tendency was not observed for TMP.

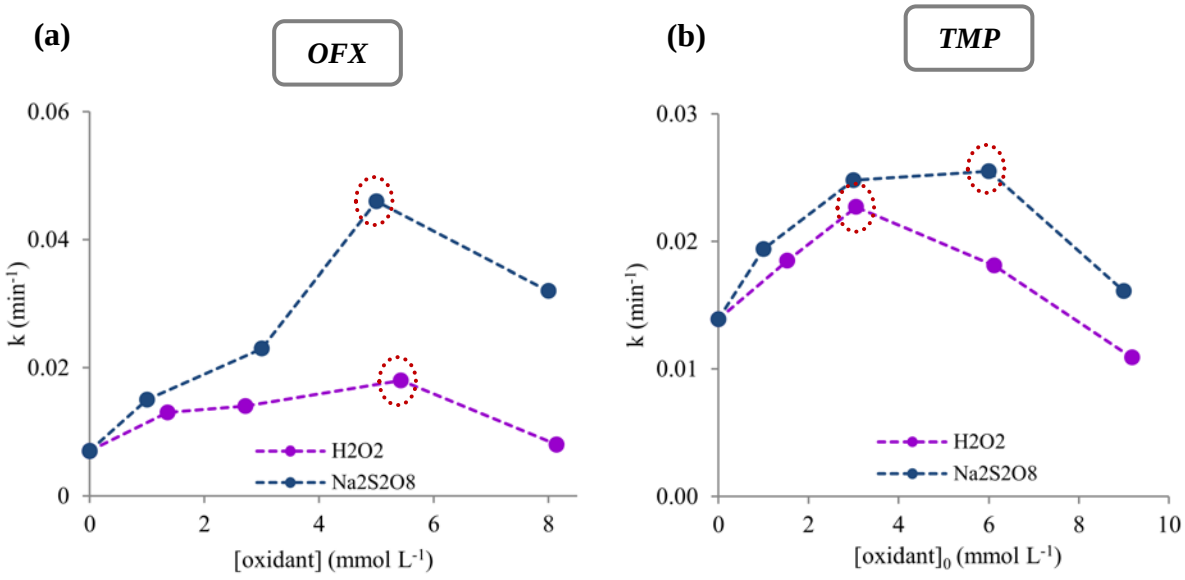

Figure 4.13 Effect of H_2O_2 and $S_2O_8^{2-}$ concentration on the rate constant, *k*: (a) OFX and (b) TMP spiked wastewater solutions. Experimental conditions: $[TiO_2]_0$=3 g L^{-1}; $[TMP]_0$=0.0344 mmol L^{-1}; pH=7.0 and T=25±0.1 ^{o}C.

4.2.4 Effect of initial substrate concentration

The influence of the initial concentration of the substrate on the heterogeneous photocatalytic degradation rate of most of the organic compounds is described by a pseudo-first kinetics order, which is rationalized in terms of the Langmuir-Hinselwood (L-H) model (eqn. (4.35)), modified to accommodate reactions occurring at a solid-liquid interface (Poulios et al., 1998; Bouzaida et al., 2004; Kumar, 2008).

$$r = -\frac{dC}{dt} = \frac{k_r KC}{1+KC} \tag{4.35}$$

where r is the rate of disappearance of the organic substrate and C is its concentration. K represents the equilibrium constant for the adsorption of the organic substrate onto TiO_2 surface, and k_r is a constant which provides the limiting rate of reaction at maximum coverage for the experimental conditions. It was found that k_r is proportional to Φ_e^n, where Φ_e is the rate of effective (able to form $e_{CB}^- - h_{VB}^+$) light absorption and n is a power term ($n \leq 1$), at high or low intensities, respectively (Malato et al., 2009).

The term r in eqn. (4.35) is represented in terms of initial reaction rate (r_0), as a function of the C_e, where C_e is the equilibrium organic substrate concentration in solution after the completion of dark experiments.

$$r_0 = \frac{k_r KC_e}{1+KC_e} \tag{4.36}$$

The parameters k_r and K can be predicted by linearizing the eqn. (4.36) as follows:

$$\frac{1}{r_0} = \frac{1}{k_r} + \frac{1}{k_r KC_e} \tag{4.37}$$

A series of experiments at different initial substrate concentrations (2-20 mg L^{-1}) was performed to demonstrate whether the experimental results could fit the L-H

linearization. The r_0 values were independently obtained from the degradation curves, by the linear fit using only the experimental data obtained during the first 15 min of illumination. The effect of the initial substrate concentration on the degradation of the substrates is shown in Figure 4.14 (a, b) whereas the inset figures illustrates that the degradation follows the L-H kinetic model (regression coefficient (R^2) of the linear fitting is 0.994 and 0.996 for OFX and TMP, respectively). The linear transformation of this expression yields: $k_{r(OFX)}$ = 0.27 mg (L min)$^{-1}$; $k_{r(TMP)}$ = 0.43 mg (L min)$^{-1}$; K_{OFX} = 0.16 L mg^{-1} and K_{TMP} = 0.11 L mg^{-1}.

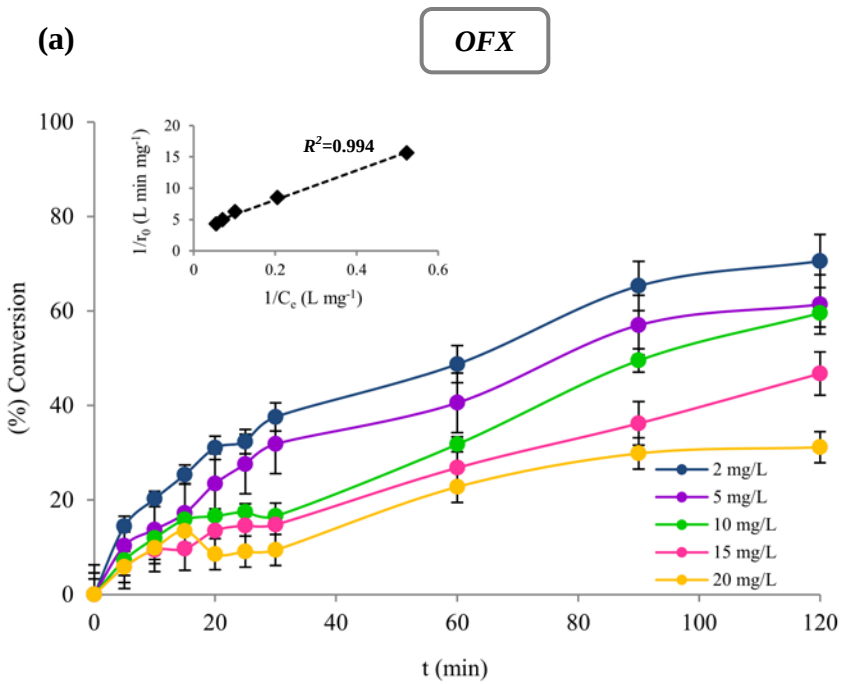

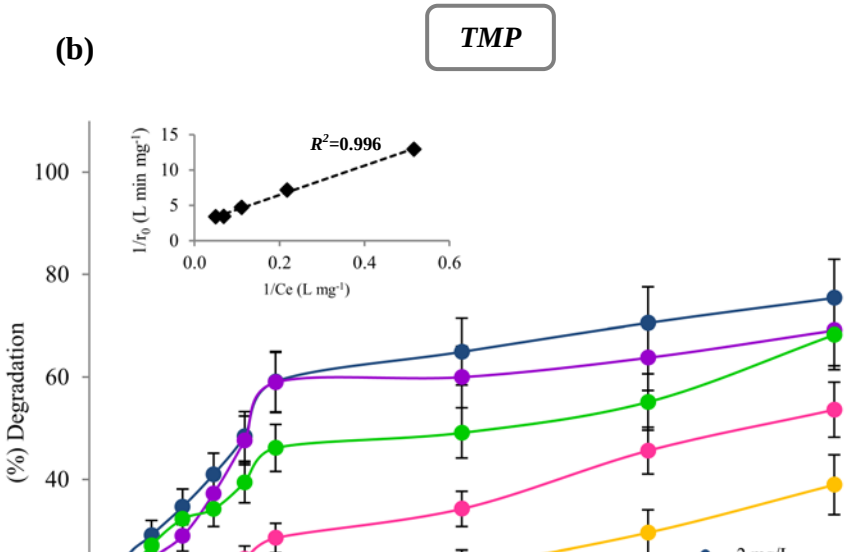

Figure 4.14 Kinetic study of OFX and TMP heterogeneous photodegradation. Experimental conditions: $[TiO_2]_0$=3 g L^{-1}; $[OFX]_0$=0.0277 mmol L^{-1}; $[TMP]_0$=0.0344 mmol L^{-1}; pH=7.0 and T=25±0.1 ^oC.

4.3 Mineralization

In order to assess the degree of mineralization reached in the treated wastewater samples during the two AOPs applied, the removal of TOC was measured. In the present work, TOC measurements represent the DOC because the samples were filtered before use. In the various operating conditions studied, mineralization was found to be relatively low compared to the degradation of the substrates, which means that the organic load remained, can be attributed to the presence of the oxidation by-products. The great difference between degradation and mineralization efficiencies also implies that the by-products of substrates oxidation are stable under the present experimental conditions.

It should be mentioned that the secondary wastewater contains (a) an extra DOC of about 8.5 mg L^{-1} (this accounts for about 60% of the organic carbon content of the 10 mg L^{-1} OFX or TMP solution) and (b) a considerable concentration of carbonates and chlorides that could act as radical scavengers. It should be emphasized that DOC of the wastewater matrix is attributed to the dissolved organic matter (DOM). Substrates

photodegradation and mineralization is influenced by DOM (mainly humic and fulvic compounds) that interacts readily with $HO^{\bullet}$ (Dong et al., 2010; Navarro et al., 2011; Li et al., 2012). As a result, DOM can be expected to be the primary reaction substrate in all practically relevant conditions of AOP treatment. Still, most of the experiments reported in prior literature were carried out using pharmaceutical compounds dissolved in deionized water, with only a few studies reporting the degradation of pharmaceuticals in real wastewater (Klamerth et al., 2010, Klamerth et al., 2011).

DOC concentrations in the solar Fenton treated wastewater samples were measured at varying Fe^{2+} concentrations at a constant H_2O_2 concentration for each compound ($[H_2O_{2(OFX)}]_0$=2.714 mmol L^{-1}; $[H_2O_{2(TMP)}]_0$=3.065 mmol L^{-1}). Similar experiments were also performed for solar Fenton treatment at a constant Fe^{2+} concentration (5 mg L^{-1}) and varying H_2O_2 concentrations.

DOC removal profiles as a function of the treatment time and the catalyst concentration ($[Fe^{2+}]$) are shown in Figure 4.15 (a, b). The consumed peroxide for the solar Fenton process vs time (at the optimum concentrations: $[Fe^{2+}]_0$=5 mg L^{-1}, $[H_2O_{2(OFX)}]_0$=2.714 mmol L^{-1}; $[H_2O_{2(TMP)}]_0$=3.065 mmol L^{-1}) is presented in the inset of Figure 4.15 (a, b). In the case of OFX solution, the highest DOC removal achieved was approximately 41% (~2.6 mmol L^{-1} of H_2O_2 consumed) after 120 min of treatment. Similar DOC removal behavior was observed for TMP. DOC removal was approximately 44% within 120 min (~1.55 mmol L^{-1} of H_2O_2 consumed) of solar Fenton treatment. Furthermore, the results showed that an increase in DOC removal occurred by increasing $[Fe^{2+}]$ from 1 to 5 mg L^{-1} due to the catalytic decomposition effect on H_2O_2 induced by the initial Fe^{2+}.

In experiments with varying H_2O_2 doses, the DOC removal increased gradually by increasing the oxidant concentration due to the formation of additional $HO^{\bullet}$. However,

as clearly seen in Figure 4.16 (a, b), the use of excessive concentrations of peroxide may have an adverse effect on the mineralization for both substrates. Thus, although OFX mineralization is enhanced in the presence of 1.531-5.428 mmol L^{-1} H_2O_2, higher peroxide concentrations (*i.e.* 8.142 mmol L^{-1}) yield reduced DOC removal. Similarly to the observations concerning the mineralization of OFX solution, the DOC removal in the TMP samples increases with increasing H_2O_2 concentration from 1.531 to 6.124 mmol L^{-1} but above this range no improvement was observed.

The DOC removal during the heterogeneous photocatalysis was determined at varying TiO_2 concentrations and treatment times (Figure 4.17 (a, b)). The results indicate that DOC removal increases with increasing catalyst loading due to an increased number of catalyst active sites that are available for photocatalytic reactions. However, at higher TiO_2 concentration (4 g L^{-1}) a screening effect of excess particles occurs, thus reducing the DOC removal. The maximum DOC removal was achieved within 120 min of treatment at TiO_2=3 g L^{-1} yielding 10% and 13% for OFX and TMP, respectively. It should be noted that solar Fenton ([Fe^{2+}]=5 mg L^{-1}) was proved to be more effective than the TiO_2 process (3 g L^{-1}) for removing DOC.

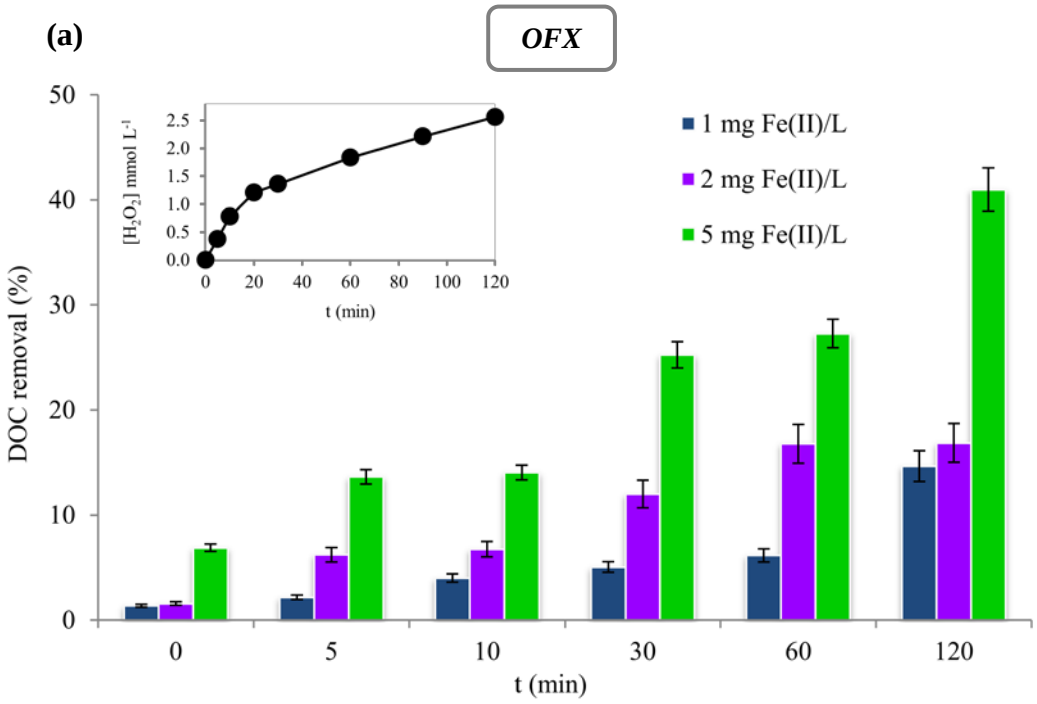
(a)
OFX
DOC removal (%)
t (min)
1 mg Fe(II)/L
2 mg Fe(II)/L
5 mg Fe(II)/L
[H2O2] mmol L-1
t (min)

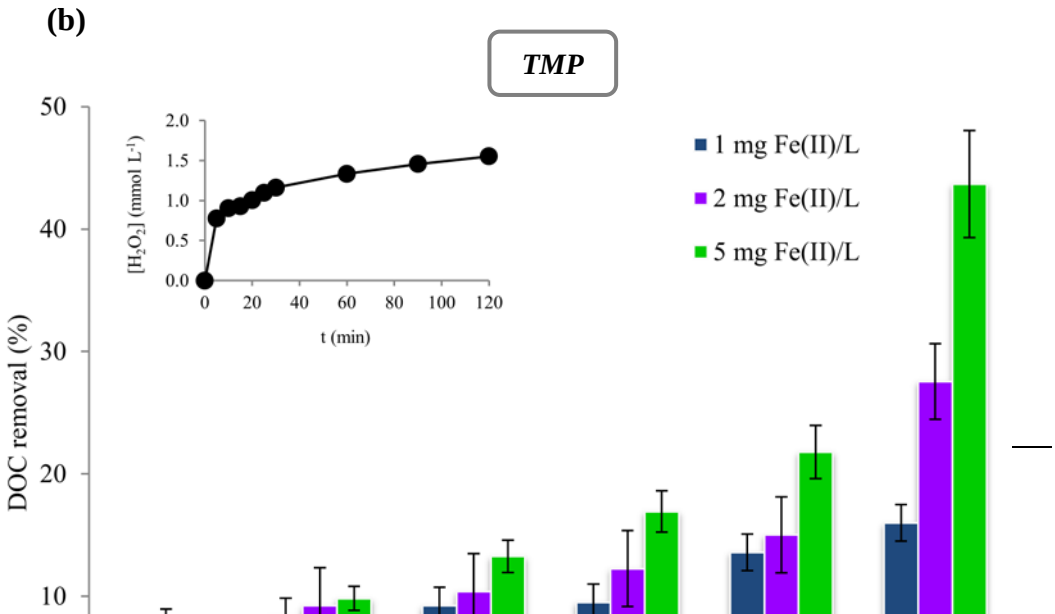
(b)
TMP
DOC removal (%)
t (min)
1 mg Fe(II)/L
2 mg Fe(II)/L
5 mg Fe(II)/L
[H2O2] (mmol L-1)
t (min)

Figure 4.15 Effect of $[Fe^{2+}]$ on the mineralization of: (a) OFX (0.0277 mmol L^{-1}) and (b) TMP (0.0344 mmol L^{-1}) spiked wastewater solutions. The inset graph shows the consumed peroxide with the time at the optimum experimental conditions ($[Fe^{2+}]_0$=5 mg L^{-1}; $[H_2O_{2(OFX)}]_0$=2.714 mmol L^{-1}; $[H_2O_{2(TMP)}]_0$=3.062 mmol L^{-1}).

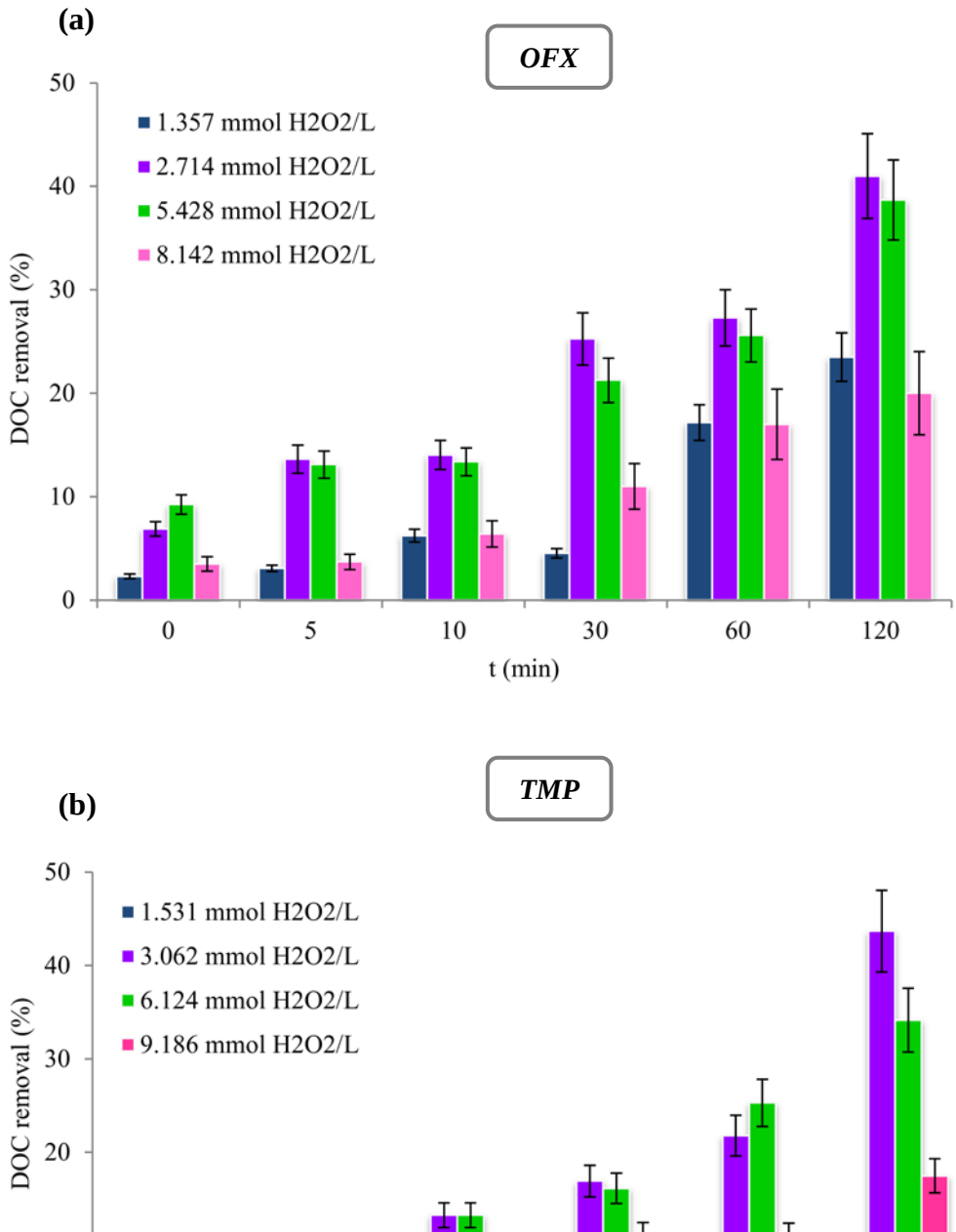

Figure 4.16 Effect of initial H_2O_2 concentration on the DOC removal: (a) OFX and (b) TMP spiked wastewater solutions. Experimental conditions: $[Fe^{2+}]_0$=5 mg L^{-1}; $[OFX]_0$=0.0277 mmol L^{-1}; $[TMP]_0$=0.0344 mmol L^{-1}; pH=2.9-3.0 and T=25±0.1 ^oC.

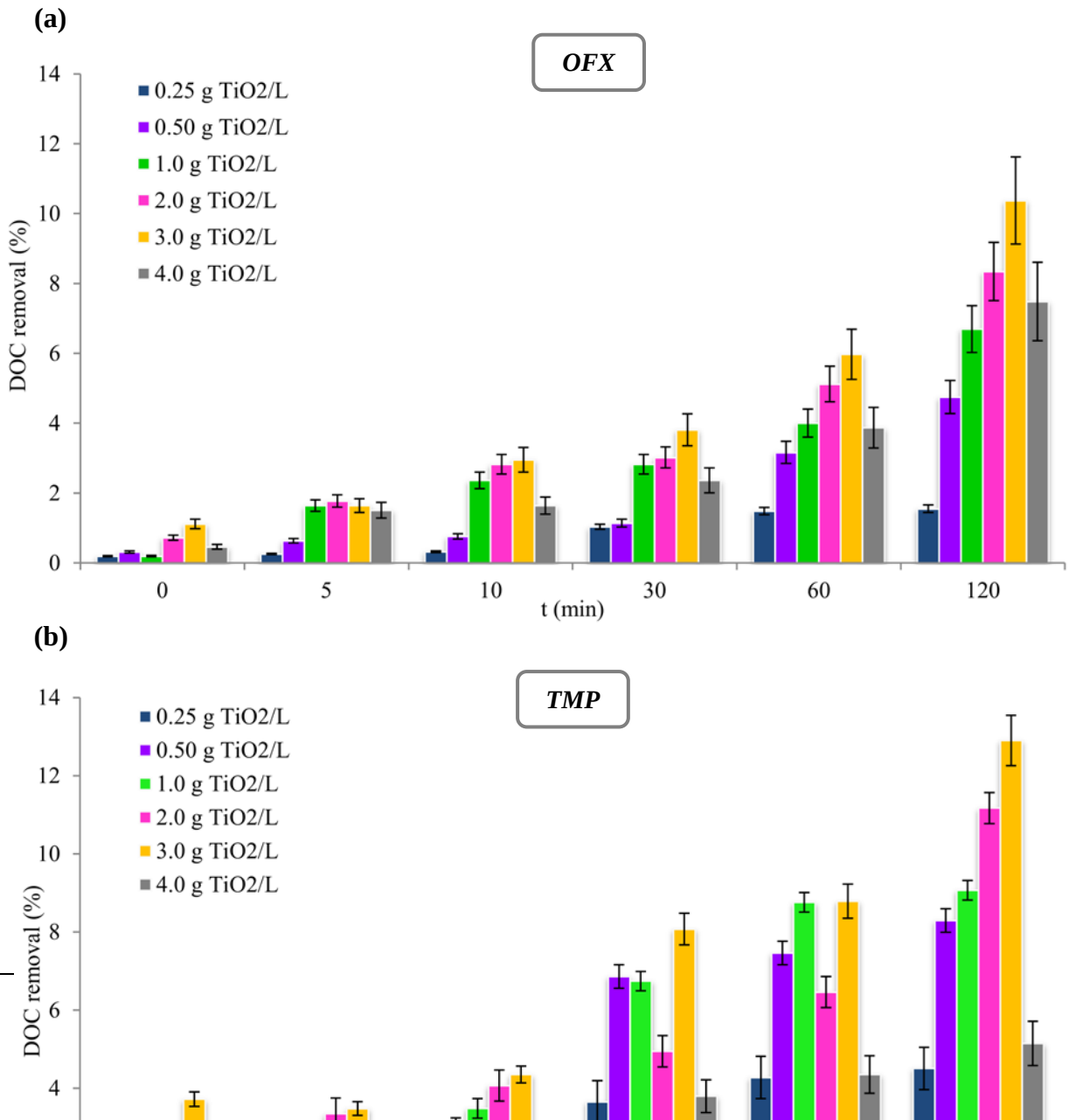

Figure 4.17 Effect of [TiO_2] on the mineralization of: (a) OFX and (b) TMP spiked wastewater solutions. Experimental conditions: $[OFX]_0$=0.0277 mmol L^{-1}; $[TMP]_0$=0.0344 mmol L^{-1}; pH=7.0 and T=25±0.1 ^oC.

Additional experiments examined the effect of solar Fenton and solar TiO_2 process (at the optimum experimental conditions) in DOC removal of the wastewater matrix in the absence of the antibiotic compounds. As can be seen from Figure 4.18, the DOC removal was much higher in the homogeneous photocatalytic treatment compared to the heterogeneous process.

During the initial phase, a negligible DOC removal was observed in solar Fenton experiments. However, in the second phase, DOC removal increased from 17% (30 min) to 33% (120 min) indicating the degradation of some organics contained in the wastewater matrix and thus the formation of oxidation by-products. In the case of TiO_2 process, DOC removal was carried out with slower rates and in lower percentages. Little additional DOC removal took place when the treatment time increased from 30 to 120 min (5.6% to 8.4%).

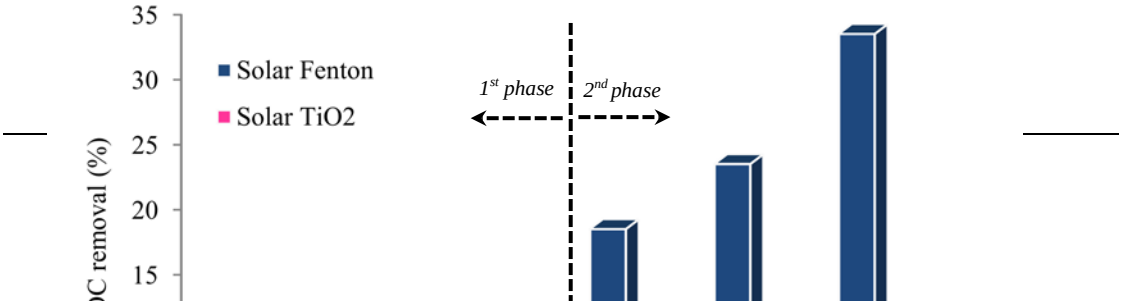

Figure 4.18 Effect of solar Fenton and solar TiO_2 on the mineralization of the secondary wastewater (without spiking OFX or TMP) at the optimum experimental conditions ($[Fe^{2+}]$= 5 mg L^{-1}; $[TiO_2]$=3 g L^{-1}).

4.4 Evaluation of toxicity

Considering the fact that complete mineralization was not achieved, it was decided to investigate the possible toxicity of the oxidation products formed during the degradation of OFX and TMP. This would enable establishing a more complete evaluation of the efficiency and environmental safety of the technologies applied. The aim of this assay was to evaluate the toxicity reduction or increase following the two processes at their optimum conditions. Toxicity measurements were carried out in samples at various times of the photocatalytic treatment using the Daphtoxkit F^{TM} magna toxicity test. The examined samples were not subjected to further dilutions.

At first, a set of control toxicity tests was performed by exposing *D. magna* to the secondary treated wastewater samples. The control tests (without OFX or TMP spiking) showed no toxicity to *D. magna* after 24 and 48 h of exposure.

The untreated solution of OFX (wastewater spiked with 10 mg L^{-1} OFX) was found to be non-toxic to *D. magna* (0% immobilization after 24 and 48 h of exposure). In

Figure 4.19 (a), the variation of toxicity during the photocatalytic treatment of OFX is presented.

A slight toxicity to *D. magna* for 24 h was observed for the solar Fenton treated samples at 0, 15 and 30 min whose immobilization was 20±0.5, 30±0.58 and 10±0.58%, respectively. Finally, after 60 and 120 min of treatment no immobilization was observed after 24 h of exposure. As clearly seen, OFX decomposes rapidly to oxidation by-products, whose 24 h-toxicity is low throughout the experiment. The samples taken at 0 and 15 min of photocatalysis showed 20±0.5 and 40±0.86 % of immobilization to *D. magna* after 48 h of exposure, respectively. However, the toxicity of the treated effluents at 30 and 60 min of the photocatalytic treatment was dramatically increased up to 90% after 48 h of exposure. The increase is attributed to the organic intermediates formed by the oxidation of the parent compound, causing toxicity effects on daphnids at longer time of exposure. Finally, after 120 min of irradiation a decrease on immobilization was observed (50%) after 48 h of exposure.

On the other hand, OFX treated effluents with heterogeneous photocatalysis were relatively non-toxic to daphnids (the highest immobilization was 25% at 48 h of exposure). However, the heterogeneous photocatalytic treatment did not completely reduce the toxicity under the investigated conditions (maximum catalyst loading 3 g L^{-1} TiO_2).

The toxicity of the samples collected from different stages of the treatment of TMP solution during both photocatalytic processes was monitored and the results are illustrated in Figure 4.19 (b). The standard solution of TMP (wastewater spiked with 10 mg L^{-1} TMP) was found to be very toxic to *D. magna* yielding 93% and 100% immobilization after 24 and 48 h of exposure, respectively. In a further study, the solution was subjected to photocatalytic treatment at 5 mg L^{-1} Fe^{2+} and 3.062 mmol L^{-}

[1] H_2O_2 (solar homogeneous treatment) and at 3 g L^{-1} TiO_2 (solar heterogeneous treatment) and then evaluated for its toxicity. A high toxicity to *D. magna* for 24 h was observed for the solar Fenton treated samples at 0, 15 and 30 min whose immobilization was 86.7, 80.0 and 66.7%, respectively (RSD was not higher than 5%). Finally, after 60 and 120 min of treatment, lower immobilization was observed after 24 h of exposure (40.0% and 26.7%, respectively). This behaviour can be attributed to the oxidation by-products formed which may have lower toxicity than the parent compound. Similar behaviour was observed during TiO_2 photocatalysis, although in this case higher values of toxicity were recorded during the last stages of the process (30, 60 and 120 min), due to the potentially slower decomposition of the toxic by-products. However, as clearly seen from the Figure 4.19 (b) the immobilization of daphnids after 24 h of exposure decreases throughout the treatment with both processes.

The immobilization of daphnids increased after 48 h of exposure as shown in Figure 4.19 (b). This increase is attributed to the organic intermediates formed by the oxidation of the parent compound, indicating the toxicity effects on daphnids at longer time of exposure. Finally, after 120 min of irradiation a decrease on immobilization was observed after 48 h of exposure; 33 and 47% immobilization for solar Fenton and solar TiO_2, respectively.

As an overall observation of all the results presented here, which indicate different toxicity profiles for the treated effluents by solar Fenton and TiO_2 method, it can be emphasized that the oxidation mechanisms of each process and the pathways of transformation that the by-products follow, seem to play a significant role in the toxicity changes during the photocatalytic treatment during the experimental conditions applied in this study.

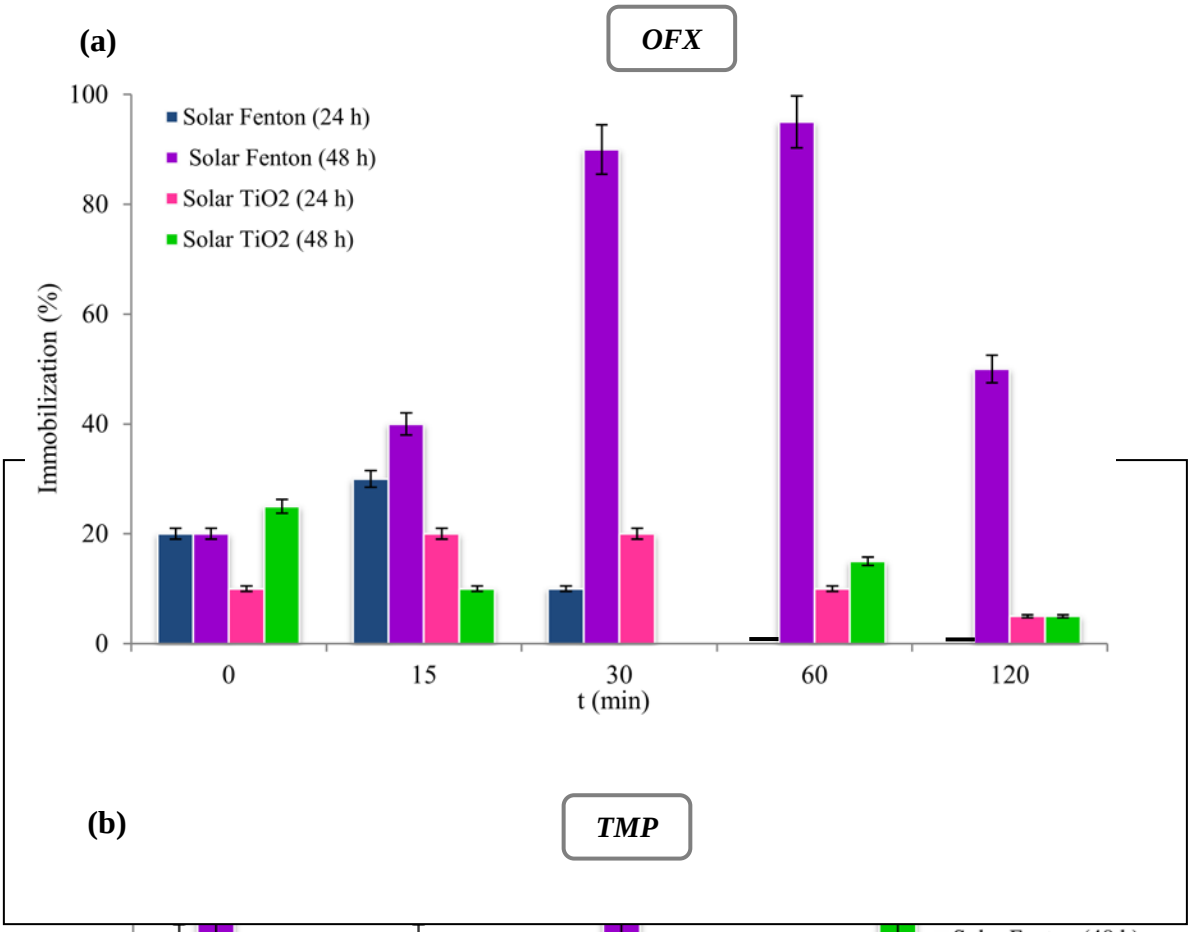
(a)
OFX
Solar Fenton (24 h)
Solar Fenton (48 h)
Solar TiO2 (24 h)
Solar TiO2 (48 h)
Immobilization (%)
100
80
60
40
20
0
0
15
30
60
120
t (min)

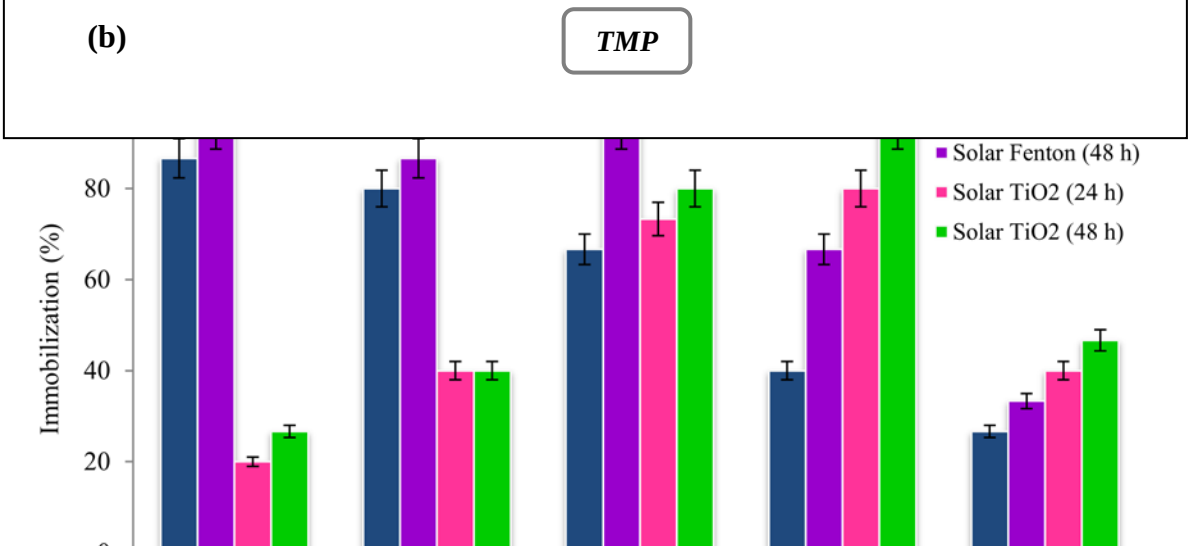
(b)
TMP
Solar Fenton (48 h)
Solar TiO2 (24 h)
Solar TiO2 (48 h)
Immobilization (%)
80
60
40
20

Figure 4.18 Evolution of toxicity to *D. magna* during the photocatalytic degradation of: (a) OFX and (b) TMP spiked wastewater solutions. Experimental conditions: Solar Fenton: $[Fe^{2+}]_0$=5 mg L^{-1}; $[H_2O_{2(OFX)}]_0$=2.714 mmol L^{-1}; $[H_2O_{2(TMP)}]_0$=3.062 mmol L^{-1}; pH=2.9-3.0 and T=25±0.1 ^oC; TiO_2 suspensions: $[TiO_2]_0$=3 g L^{-1}; pH=7.0 and T=25±0.1 ^oC.

Solar Fenton was proved to be more efficient for the degradation of the examined antibiotics than TiO_2 photocatalysis. OFX and TMP substrates at concentration of 10 mg L^{-1} can be successfully removed by solar Fenton at low iron and low initial hydrogen peroxide concentrations within 30 min of treatment. However, the maximum degradation of OFX and TMP substrates with the heterogeneous photocatalysis at the optimum conditions was 60% and 68% for OFX and TMP, respectively. The substrates degradation follows during the solar Fenton first-order kinetic law in the first 20 min while the Langmuir-Hinshelwood kinetic model was used to determine the degradation kinetics during the heterogeneous photocatalysis. The kinetic parameters were found to be influenced by the operating conditions employed such as the concentration of iron salt and hydrogen peroxide, the pH of solution, the solar irradiation, the temperature and the initial concentration of the substrate in the case of the solar Fenton process. The substrates degradation by the TiO_2 process depends on the concentration of catalyst, initial substrate concentration, solution pH and the addition of an oxidant. The mineralization was lower compared to the substrates degradation indicating the formation of stable oxidation by-products during the application of both processes. Toxicity variations were observed which can be attributed to the potentially different oxidation by-products produced during the AOPs applied.

CHAPTER 5: PILOT SCALE STUDY OF SOLAR FENTON

5.1 Pilot scale experiments at Plataforma Solar de Almería (PSA)

The main objective of the pilot scale study at PSA was the structure elucidation of the major transformation products formed during the TMP solar Fenton process in four different environmental matrices; thus, a concentration of 10 mg L^{-1} was applied in order to convincingly elucidate the oxidation by-products

5.1.1 Hydrolysis and photolysis experiments

Preliminary hydrolysis and photolysis experiments were carried out in order to determine the contribution of these effects in the overall photocatalytic process. Hydrolysis and photolysis experiments were performed with 10 mg L^{-1} concentration of each compound in demineralized water (DW) at pH 6.5 and 6.8 for OFX and TMP, respectively. Hydrolysis experiments were performed using amber glass bottles (1 L), which were kept in the dark at room temperature during the tests. Photolysis was performed in Pyrex beakers (1 L) having high UV transmissivity (UV transmissivity > 80% between 320 and 400 nm, around 40% at 300 nm, 15 cm internal diameter). Beakers were exposed to direct sunlight and were continuously stirred during the photolysis tests. The temperature, which was monitored during the photolysis experiments, varied between 25-37 ^{o}C. The hydrolysis experiments lasted 15 days (360 hours) and the photolysis 500 min (> 8 h).

Figure 5.1 (a, b) illustrates the concentration profile of OFX and TMP substrate during the hydrolysis and photolysis experiments. The direct photolysis (solar radiation alone) showed that 20% of TMP was removed after 500 min of solar

illumination. The long irradiation time required for this low degradation demonstrated that TMP is highly stable to photolysis (Sirtori et al., 2010). OFX was more photosensitive since 72% of the initial concentration was removed after 500 min of exposure; however this degradation was achieved in much longer time than the one used during the photocatalytic tests. On the other hand, no mineralization was observed at the end of the photolysis indicating the formation of intermediates, which are resistant to photodegradation ($[DOC]_0 \approx 6$ mg L^{-1}).

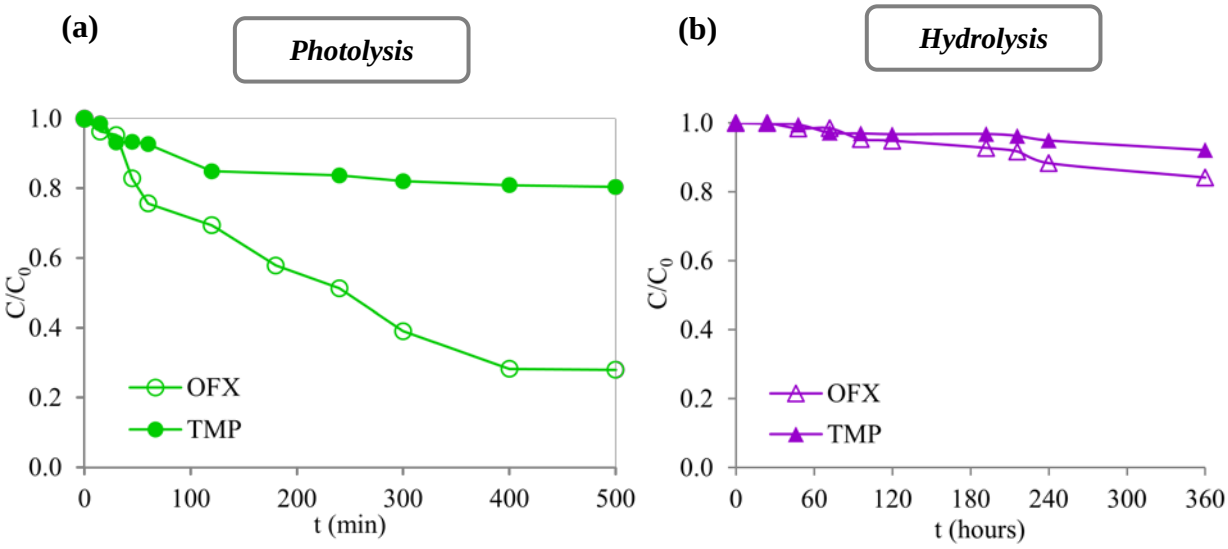

Figure 5.1 OFX and TMP degradation during photolysis and hydrolysis experiments.

The hydrolysis experiments showed no significant degradation of the investigated compounds. The concentration of the substrates was almost constant after 360 h. Hydrolysis of OFX or TMP was not expected because these compounds do not possess structural features that can be readily hydrolyzed at the temperatures relevant to environmental conditions.

5.1.2 Solar Fenton experiments

The experimental protocol to estimate the matrix effect on the solar Fenton efficiency was first designed with relatively non-complex water matrices (demineralized water (DW) and simulated natural freshwater (SW)), and then with matrices of increased complexity by studying simulated effluent from municipal wastewater treatment plant (SWW) and finally real effluent from municipal wastewater treatment plant (RE).

Solar Fenton degradation of OFX and TMP was evaluated using ferrous iron (Fe^{2+}) at 2 mg L^{-1} and hydrogen peroxide in doses of 2.5 mg L^{-1}. When the initial hydrogen peroxide dose was consumed the reagent was replaced.

Figure 5.2 (a-d) shows the mineralization and the corresponding hydrogen peroxide requirements during the oxidation of the substrates in the various water matrices. As can be seen, the extent of mineralization decreases in the order DW > SW > SWW > RE. Table 5.1 illustrates the DOC removal achieved at the end of the treatment in each water matrix.

No significant differences in the DOC reduction were observed between DW and SW and the DOC curves showed approximately the same tendency. It should be noted that the DOC removal needed a little bit more of hydrogen peroxide in the case of SW compared to DW, which can be attributed to the presence of various anions (*e.g.* Cl^-, SO_4^{2-}) which may act as scavengers of the hydroxyl radicals and other reactive moieties. The occurrence of these inorganic anions in the SW influences the mineralization rate; however the solar Fenton efficiency is still sufficient even if salt concentrations are high (Bacardit et al., 2007).

Table 5.1 DOC removal at the end of solar Fenton process ($[H_2O_2]_{consumption}$=12 mg L^{-1}) in each water matrix.

Substrate / **Water matrix**	**OFX**	**TMP**
	DOC removal (%)	DOC removal (%)
DW	78.1	77.6
SW	58.1	61.4
SWW	40.5	37.3
RE	35.8	34.4

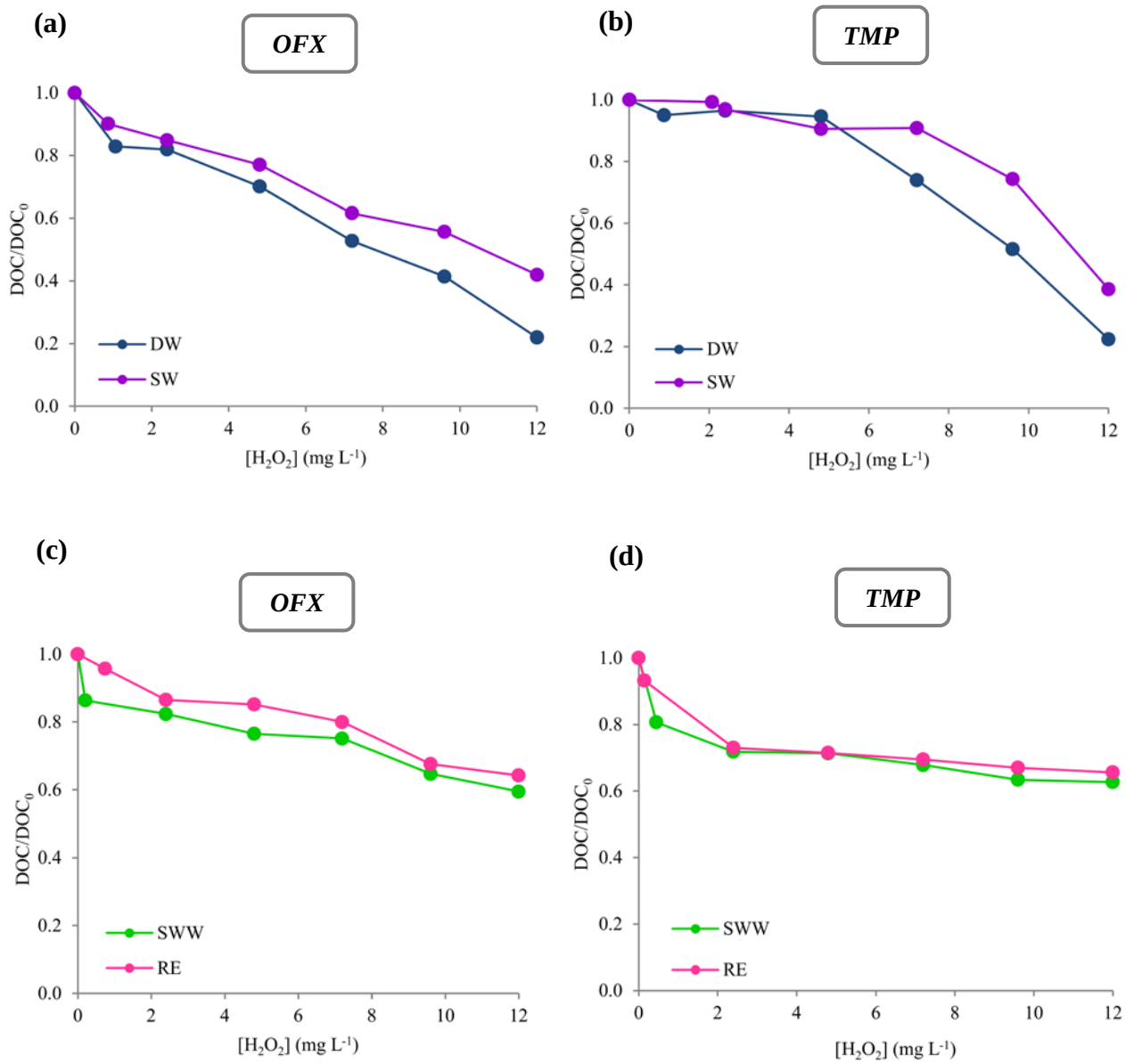

Figure 5.2 OFX and TMP mineralization during solar Fenton experiments in each type of water matrix: (a) OFX: DW-SW; (b) TMP: DW-SW; (c) OFX: SWW-RE; and (d) TMP: SWW-RE. Experimental conditions: $[Substrate]_0$=10 mg L^{-1}; $[Fe^{2+}]_0$=2 mg L^{-1}; $[H_2O_2]_0$=2.5 mg L^{-1}; pH_0=2.8-2.9.

The possible implications of these anions are: (i) complexation reactions with Fe^{2+} or Fe^{3+} which can affect the distribution and the reactivity of the iron species as a result of the generation of iron-chloride (or -sulfate) complexes (this slows down the reduction of Fe^{3+} to Fe^{2+} which is necessary for the continuity of the solar Fenton mechanism); (ii) scavenging of the hydroxyl radicals and formation of less reactive inorganic radicals ($Cl^{\bullet-}$, $Cl_2^{\bullet-}$ and $SO_4^{\bullet-}$); and (iii) oxidation reactions involving these inorganic radicals (De Laat et al., 2004).

De Laat et al. (2004) presented a rather comprehensive review of the additional reactions in the Fenton system in the presence of significant amounts of chlorides and sulfates. Table 5.2 reports some representative reactions.

Table 5.2 Main reactions in the presence of chlorides and sulfates for the photo-Fenton system (De Laat et al., 2004).

Chloride	**Sulfate**
$Cl^- + HO^\bullet \rightarrow [ClOH]^{\bullet-}$	$SO_4^{2-} + H^+ \leftrightarrow HSO_4^-$
$[ClOH]^{\bullet-} + H^+ \rightarrow [HClOH]^\bullet$	$HSO_4^- + HO^\bullet \rightarrow H_2O + SO_4^{\bullet-}$
$[HClOH]^\bullet + Cl^- \rightarrow Cl_2^{\bullet-} + H_2O$	$SO_4^{\bullet-} + H_2O \rightarrow H^+ + SO_4^{2-} + HO^\bullet$
$Cl_2^{\bullet-} + H_2O_2 \rightarrow HO_2^\bullet + 2Cl^- + H^+$	$SO_4^{\bullet-} + H_2O_2 \rightarrow SO_4^{2-} + HO_2^\bullet + H^+$
$Cl_2^{\bullet-} + Fe^{2+} \rightarrow Cl^- + FeCl_2^+$	$SO_4^{\bullet-} + Fe^{2+} \rightarrow SO_4^{2-} + Fe^{3+}$
$Fe^{2+} + Cl^- \leftrightarrow FeCl^+$	$Fe^{2+} + SO_4^{2-} \leftrightarrow FeSO_4$
$Fe^{3+} + Cl^- \leftrightarrow FeCl^{2+}$	$Fe^{3+} + SO_4^{2-} \leftrightarrow FeSO_4^+$
$Fe^{3+} + 2Cl^- \leftrightarrow FeCl_2^+$	$Fe^{3+} + 2SO_4^{2-} \leftrightarrow Fe(SO_4)_2^-$
Second-order rate constants: $Cl_2^{\bullet-} = 10^3$-10^8 M^{-1} s^{-1}; $SO_4^{\bullet-} = 10^6$-10^9 M^{-1} s^{-1}; $HO^\bullet = 10^7$-10^{10} M^{-1} s^{-1}	

Usually, the effects of inorganic salts on the overall rates of decomposition of hydrogen peroxide and organic compounds are ignored. However, a few studies examined the effects of anions on the Fenton's reaction. In a study of the degradation of 2,4-dichorophenoxyacetic acid (2,4-D) by Fenton reagent, Pignatello (1992) found that the inhibition of 2,4-D degradation with Fe^{3+}/H_2O_2 followed the order $SO_4^{2-} << Cl^- < NO_3^- \approx ClO_4^-$. It was concluded that the sulfate ligands reduced the reactivity of Fe^{3+}, while the chlorides, even at low concentrations, were responsible for hydroxyl radical scavenging which may further generate chloride radicals $Cl^{\bullet}$, which are less reactive than the hydroxyl radicals. Kiwi et al. (2000) showed a significant decrease in the rate of decoloration of Orange II by Fe^{3+}/H_2O_2 upon addition of chloride.

Moreover, the effects of chloride and sulfate ions on the rate of oxidation of organic solutes by Fe^{3+}/H_2O_2 were examined by De Laat et al. (2004). It was found that the presence of sulfates or chlorides markedly decreased the rates of decomposition of H_2O_2 by Fe^{3+} and the rates of oxidation of atrazine (0.83 μM), 4-nitrophenol (1 mM) and acetic acid (2 mM). These inhibitory effects have been attributed to the decrease of the rate of generation of hydroxyl radicals resulting from the formation of Fe^{3+} complexes and the formation of less reactive ($SO_4^{\bullet-}$) or much less reactive ($Cl_2^{\bullet-}$) inorganic radicals.

Bacardit et al. (2007) proved that neither the presence of NaCl nor Fe^{2+} concentration produces a significant influence on TOC removal. The presence of chlorides slowed down the removal rate of 4-chlorophenol (4-CP) during the photo-Fenton process; however the final substrate removal obtained was the same with that achieved in the absence of chlorides. According to their results, the presence of chlorides do not affect the mineralization degree; therefore it seems that the presence of chlorides do not affect the amount of oxidizing agents produced but the rate in which they are

produced. Consequently, the oxidation of organic matter is slower. In another study by Klamerth et al. (2009), simulated fresh water was used in order to confirm the effect of inorganic species, especially carbonates, to the photo-Fenton degradation rate of various organic contaminants. The standard moderately hard fresh water was prepared in the same way like the SW used in our study but it also contained $NaHCO_3$ (96 mg L^{-1}). The additional carbonate species (CO_3^{2-} and HCO_3^-) compete with organic contaminants for hydroxyl radical reactions, and significantly decrease the degradation efficiency. All of the investigated compounds were degraded after 30 min of illumination ($[Fe^{2+}]$=55 mg L^{-1}; $[H_2O_2]$=50 mg L^{-1}) with the exception of atrazine (12%) and caffeine (8%).

On the other hand, the presence of organic carbon and higher salt content in SWW and RE (they contain about 25 and 10 mg L^{-1} DOC, respectively) led to lower mineralization per dose of hydrogen peroxide compared to DW and SW. Substrates photodegradation and mineralization is influenced by dissolved organic matter (DOM) that interacts readily with hydroxyl radicals (Navarro et al., 2011). It should be noted that RE was subjected to solar Fenton pretreatment (5 mg L^{-1} Fe^{2+}, 50 mg L^{-1} H_2O_2, duration: 2 hours) in order to degrade partially the organic matter contained in it and therefore minimize the matrix effects for the further determination of the oxidation by-products resulted by the photocatalytic process. The main objective was to convert aromatics, double bond-containing compounds, etc. present in RE in simple aliphatics that cannot be retained by solid phase extraction or liquid chromatography. It should be mentioned that the DOC of RE after the pretreatment step was almost 9 mg L^{-1} ($[DOC]_0$=10.72 mg L^{-1}; see Table 2.3).

All the experiments described above were performed in the presence of doses of hydrogen peroxide that were totally consumed before adding a subsequent dose.

Therefore, illumination time cannot be considered for any discussion in the present work.

5.1.3 Carboxylic acids evolution

The formation of carboxylic acids (*i.e.* acetic, oxalic, propanoic or propionic and formic acid; Schematic 5.1) was monitored during the solar Fenton experiments in DW and SW. The measurements were performed using ion chromatography; thus the non-complex matrices (DW, SW) were chosen to avoid any matrix interactions. Figure 5.3 (a, b) shows the formation profile of the four acids along with the concentration profile of organic carbon (coming from acids) and DOC in the case of DW for both compounds.

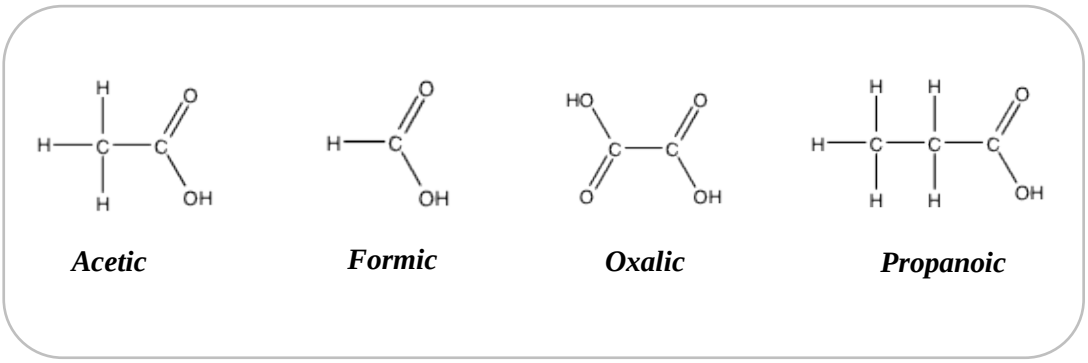

Schematic 5.1 Carboxylic acids structure (acetic; oxalic; propanoic or propionic; and formic acid).

Carboxylic and dicarboxylic acids are known to form stable iron complexes, which inhibit the reaction with hydrogen peroxide, and thus they are usually degraded slowly compared to other organics during solar Fenton process (Kavitha and Palanivelu, 2004; Radjenovic et al., 2009c; Trovo et al., 2009). Generally, organic acids are the last step before complete mineralisation.

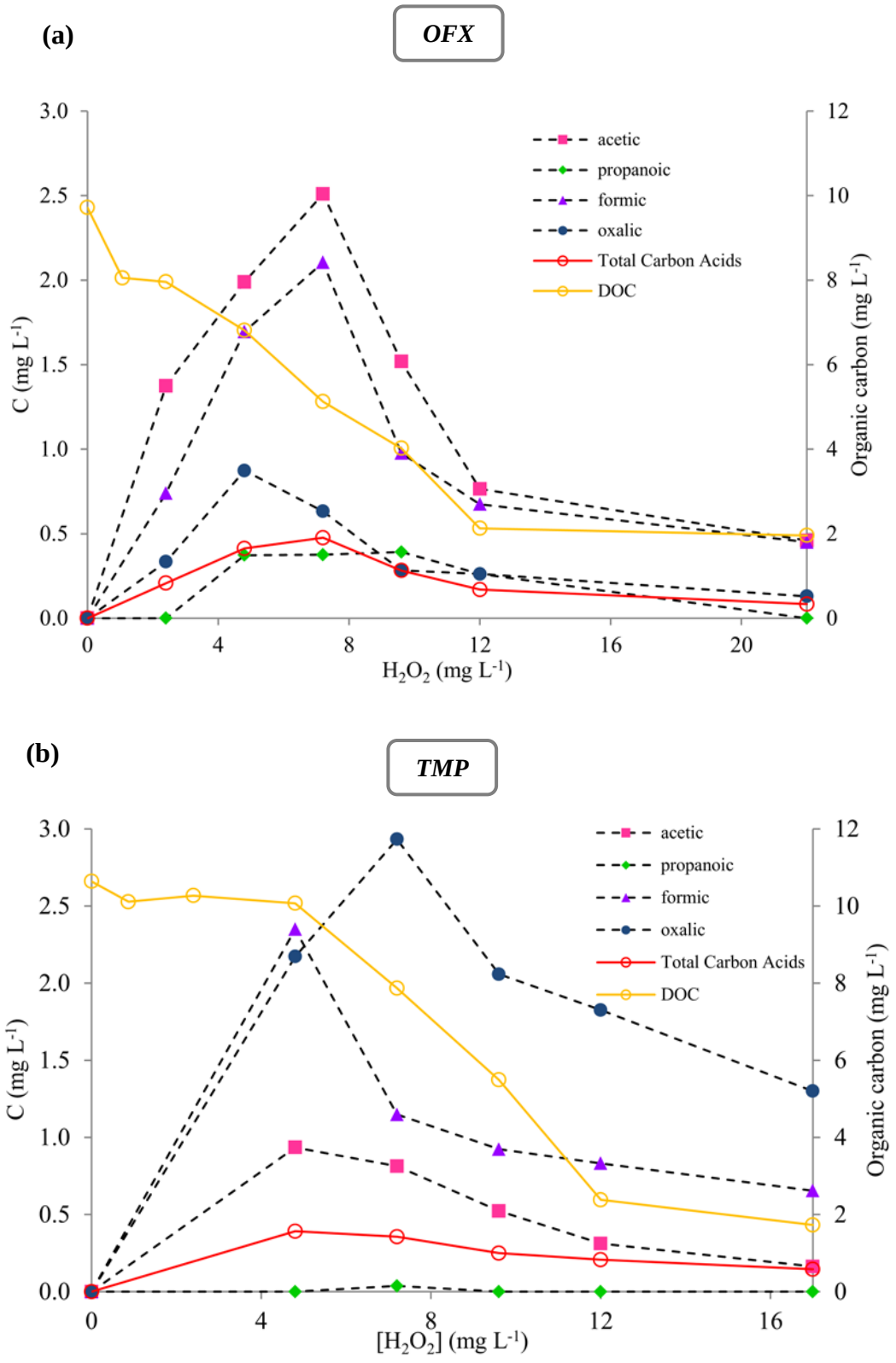

Figure 5.3 Carboxylic acids formation during degradation of: (a) OFX and (b) TMP (10 mg L^{-1}) with solar Fenton in DW. Experimental conditions: $[Substrate]_0$=10 mg L^{-1}; $[Fe^{2+}]_0$=2 mg L^{-1}; $[H_2O_2]_0$=2.5 mg L^{-1}; pH_0=2.8-2.9.

In the case of OFX, the maximum concentrations of acetic, formic, oxalic and propanoic acid detected were 2.5 (7.2 mg L^{-1} H_2O_2), 2.1 (7.2 mg L^{-1} H_2O_2), 0.87 (4.8 mg L^{-1} H_2O_2) and 0.39 mg L^{-1} (9.6 mg L^{-1} H_2O_2), respectively. At the end of the process (22 mg L^{-1} H_2O_2) 17% of the remaining DOC is attributed to these acids (Total carbon acids=0.34 mg L^{-1}, DOC=1.96 mg L^{-1}).

In the case of TMP, the maximum concentration of formic (2.35 mg L^{-1}) and acetic acid (0.93 mg L^{-1}) was reached with 4.8 mg L^{-1} H_2O_2; the maximum concentration of oxalic acid (2.93 mg L^{-1}) was observed at 7.2 mg L^{-1} peroxide consumption. However at this consumption level the concentration of the propanoic acid was much lower (0.037 mg L^{-1}). At 17 mg L^{-1} H_2O_2 consumption the acids were found at low concentrations, which is in agreement with the substantial mineralization of TMP at the end of the treatment.

Similar results were obtained during the solar Fenton process in SW and the corresponding results are depicted in Figure 5.4 (a, b). In the case of OFX, the maximum concentrations were: 2.22 mg L^{-1} for acetic (9.6 mg L^{-1} H_2O_2), 1.45 mg L^{-1} for formic (7.2 mg L^{-1} H_2O_2), 0.61 mg L^{-1} for oxalic (7.2 mg L^{-1} H_2O_2) and 0.40 mg L^{-1} for propionic (12 mg L^{-1} H_2O_2). In the case of TMP, the maximum concentration of formic acid (2.49 mg L^{-1}) was observed at 4.8 mg L^{-1} H_2O_2 while acetic (1.10 mg L^{-1}) and oxalic (2.98 mg L^{-1}) acids reached their maximum concentration using 7.2 mg L^{-1} H_2O_2. However, the elimination of these acids required higher doses of peroxide compared to that needed in DW due to the presence of anions acting as hydroxyl radical scavengers, and directly affecting the efficiency of the photocatalytic process.

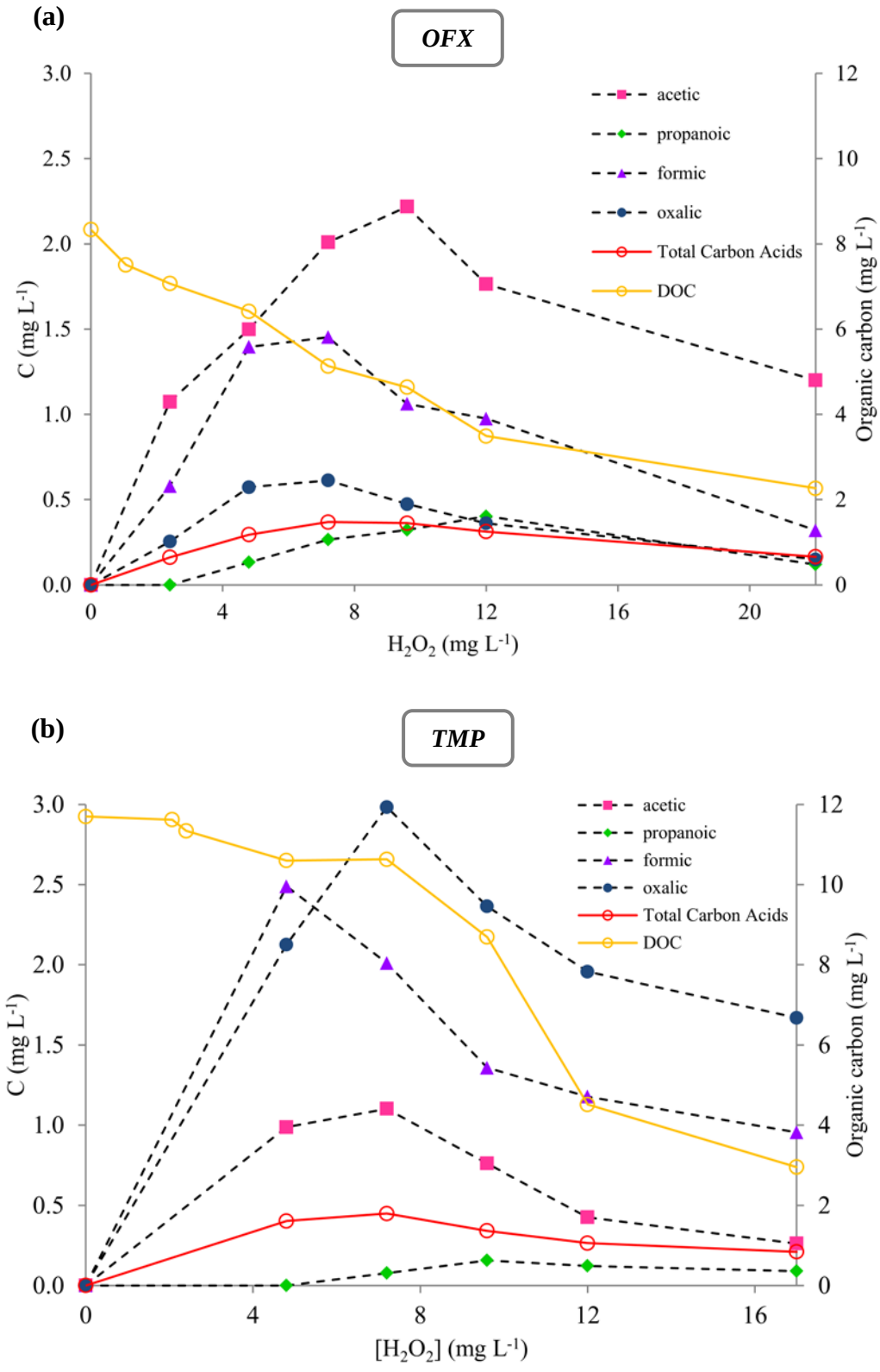

Figure 5.4 Carboxylic acids formation during degradation of: (a) OFX and (b) TMP (10 mg L^{-1}) with solar Fenton in SW. Experimental conditions: $[Substrate]_0$=10 mg L^{-1}; $[Fe^{2+}]_0$=2 mg L^{-1}; $[H_2O_2]_0$=2.5 mg L^{-1}; pH_0=2.8-2.9.

5.1.4 Evaluation of toxicity

Toxicity measurements of the treated samples were carried out to give a more complete evaluation of the efficiency of the photocatalytic process that has been used. The assays were performed in undiluted samples taken at different stages of the solar Fenton treatment using SWW and RE matrices, as it was considered more realistic than testing bioassays using DW and SW.

Figure 5.5 (a, b) shows the results as percentage of the chemiluminescence inhibition of the bacteria after 30 min of exposure for RE. In the same figure, DOC reduction in RE is also depicted. OFX untreated solution (RE spiked with 10 mg L^{-1} OFX, 0 mg L^{-1} H_2O_2 consumed) caused 33% inhibition of bacteria whereas a rapid increase was observed after solar Fenton process was applied. At 12.0 mg L^{-1} H_2O_2 consumption the inhibition was approximately 64%. As shown in Figure 5.5 (b), the inhibition of the untreated solution of TMP (RE spiked with 10 mg L^{-1} TMP, 0 mg L^{-1} H_2O_2 consumed) is 43%. The toxicity during the treatment was reduced down to 29% at 7.2 mg L^{-1} H_2O_2 consumption and there after increased to 52% at 12.0 mg L^{-1} H_2O_2 consumption.

It is important to mention that the treated samples from the SWW experiments showed no toxicity (bacteria inhibition $\leq 7\%$) after 30 min of exposure time using the same peroxide doses (Figure 5.6 (a, b)). Therefore, it was assumed that the toxicity originates from compounds present in RE and their by-products formed during solar Fenton treatment and not from the intermediates formed from the oxidation of OFX or TMP. Respirometric test was also performed in the same samples and the results showed similar behavior with those obtained by the *V. fischeri* toxicity test in each matrix.

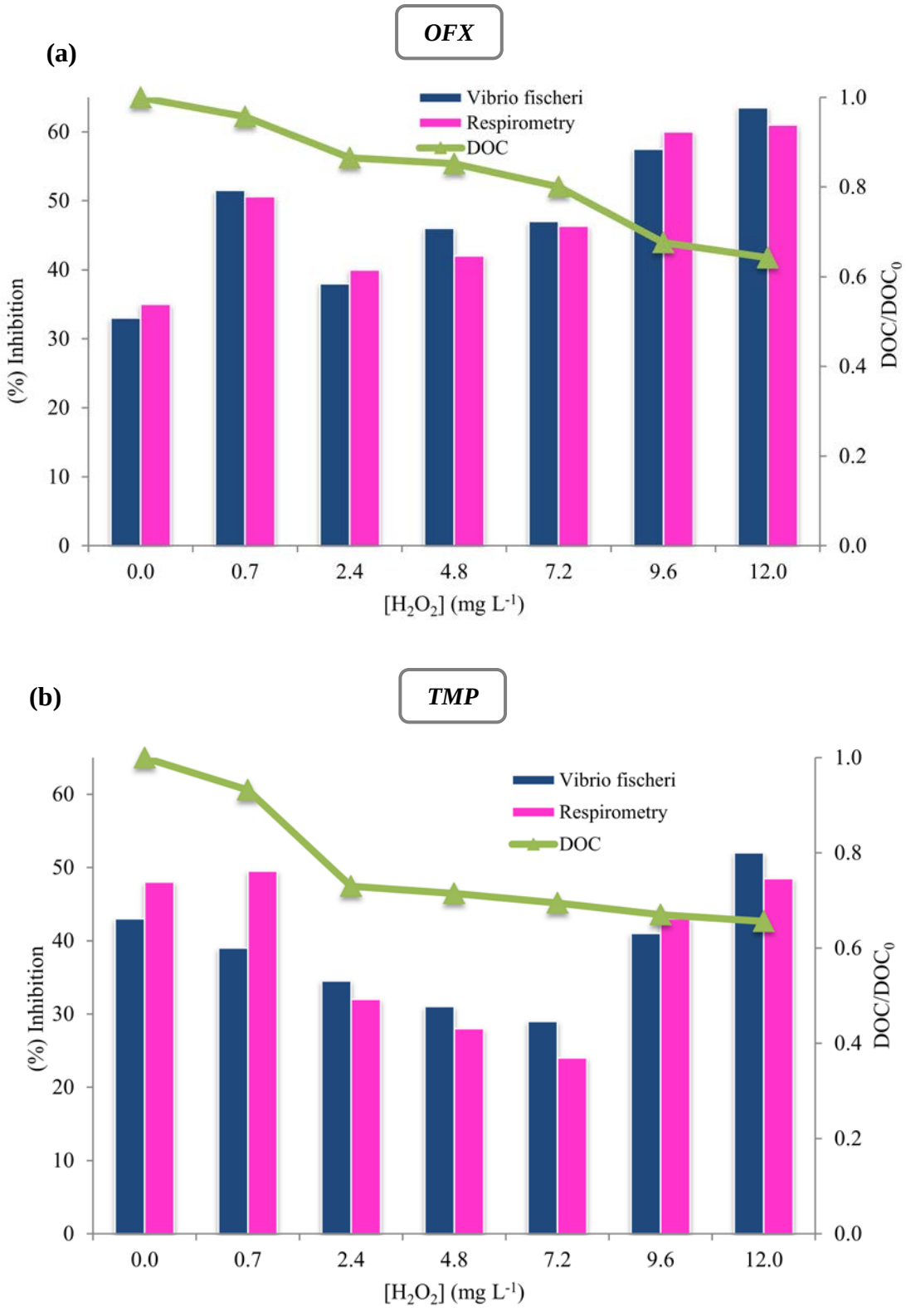

Figure 5.5 (%) Inhibition of *V. fischeri* after 30 min of exposure and inhibition of bacterial activity in activated sludge during the respirometry test for samples taken during the solar Fenton process in RE. DOC profile is also depicted in the each figure.

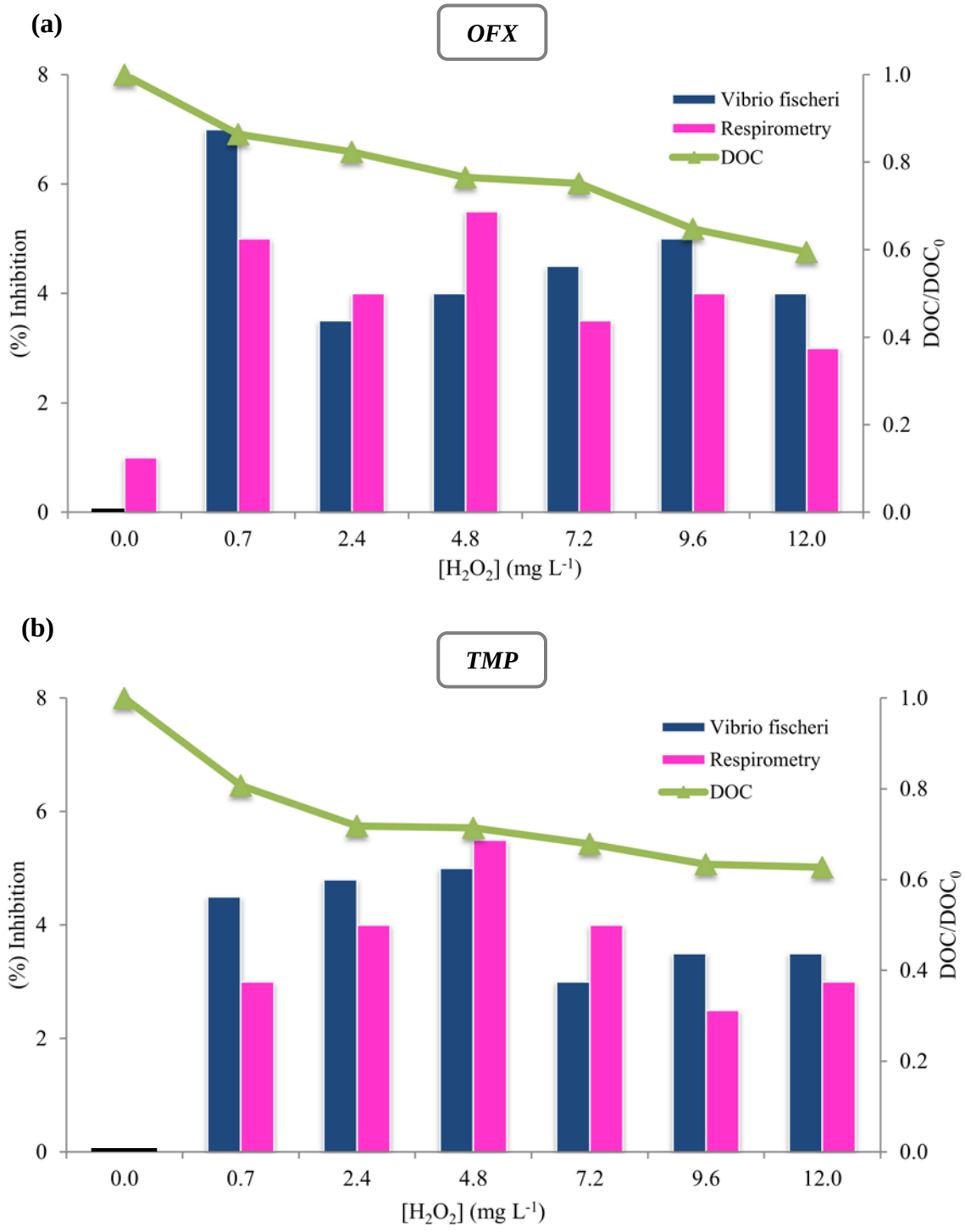

Figure 5.6 (%) Inhibition of *V. fischeri* after 30 min of exposure and inhibition of bacterial activity in activated sludge during the respirometry test for samples taken during the photo-Fenton process in SWW. DOC profile is also depicted in the same figure.

Very interesting was the fact that the final treated samples are characterized by higher toxicity compared to the initial indicating that the intermediates formed were moderately toxic for the organism tested.

Similar behavior of *V. fischeri* to photo-Fenton treated samples in RE and SWW was observed in a study of Klamerth et al. (2010). The authors suggested that the increase to the bacteria inhibition during photo-Fenton treatment in RE is attributed mainly to the generation of other intermediates formed during the oxidation of organics contained in RE matrix.

5.1.5 Characterization of major transformation products by UPLC-ToF-MS/MS

In this work, in order to determine the possible intermediate products of the investigated antibiotics in each matrix studied, samples from the solar Fenton experiments were analyzed in a full-scan mode at UPLC-QqToF-MS/MS instrument. This part includes a detailed description of the transformation products and is accompanied by an extensive presentation of chromatograms and tables; therefore this section is further discussed in the next chapter (CHAPTER 6).

5.2 Pilot scale experiments at University of Cyprus

Taking into consideration that the typical environmental concentrations of antibiotics in the wastewater effluents are in the ng-μg L^{-1} range, it was decided to work with an initial concentration of 100 μg L^{-1} of OFX and TMP, which is a compromise between (i) a sufficiently high concentration to characterize the degradation kinetics using available analytical techniques; and (ii) a low enough concentration to simulate real environmental conditions.

The comparison of the data deriving from different days at different times of the day and under different solar illumination conditions was performed after applying eqn. (5.1) to ‘‘normalized illumination time’’. This equation has been reported elsewhere (Gernjak et al., 2006; Maldonado et al., 2007; Sirtori et al., 2009; Klamerth et al., 2010). In this equation t_n is the experimental time for each sample, *UV* is the average solar ultraviolet radiation (λ < 400 nm) measured between t_{n-1} and t_n, and $t_{30W,n}$ is the ‘‘normalized illumination time’’. In this case, time refers to a constant solar *UV* power of 30 W m^{-2} (typical solar *UV* power on a perfectly sunny day around noon).

$$t_{30\,W,n} = t_{30\,W,n-1} + \Delta t_n \frac{UV}{30}\frac{V_i}{V_T}; \qquad \Delta t_n = t_n - t_{n-1} \quad (n = 1, t_n = 0\ min) \quad (5.1)$$

where V_T and V_i is the total and irradiated volume, respectively.

Furthermore, considering the fact that the reaction rate during the solar Fenton process depends strongly on temperature (Zapata et al., 2009b), eqn. (5.1) is transformed (using the Arrhenius equation) to eqs. (5.2 a, 5.2 b) using the apparent rate constants of each compound at 25 ^{o}C which have been determined from the bench scale experiments.

$$t_{30WT,n} = t_{30WT,n-1} + \Delta t_n \frac{\overline{UV}}{UV}\frac{V_i}{V_T}[1 + 0.035\,(\bar{\theta} - 25^o_C)] \quad \textbf{\textit{OFX}} \qquad (5.2\text{ a})$$

$$t_{30WT,n} = t_{30WT,n-1} + \Delta t_n \frac{\overline{UV}}{UV}\frac{V_i}{V_T}[1 + 0.054\,(\bar{\theta} - 25^o_C)] \quad \textbf{\textit{TMP}} \qquad (5.2\text{ b})$$

where $t_{30WT,n}$ is the normalized time for each sample at 25 ^oC, UV is the maximum solar ultraviolent radiation (30 W m^{-2}), $\overline{UV}$ is the average solar ultraviolet radiation measured between t_{n-1} and t_n, and $\bar{\theta}$ is the average temperature between t_{n-1} and t_n. The value of 30 W m^{-2} was used as the average maximum value for the ultraviolet solar irradiation according to the UV data provided directly by the UV radiometer which is installed on the plant. The collected UV data were also confirmed with the data provided by the Cyprus Meteorological Service. Moreover, it is important to mention that the normalized illumination time $t_{30WT,n}$ calculated using the eqs. (5.2 a, 5.2 b) is lower than the actual experimental time (t_{exp}). This is because the eqs. (5.2 a, 5.2 b) include the term $\frac{V_i}{V_T}$ and the irradiated volume is significantly lower than the total volume of the treated wastewater ($V_i \approx V_T/3$).

5.2.1 Hydrolysis and photolysis experiments

To obtain relevant information about the substrates photocatalytic degradation, it was necessary to carry out experiments from which hydrolysis and direct photolysis was considered. Hydrolysis and photolysis experiments were performed at initial concentration of 100 μg L^{-1} (for each compound) in acidic pH (2.8-2.9; same pH range used for the solar Fenton process that was later on applied) and for a period of 240 min (t_{exp}). Results obtained from photolysis (solar radiation alone) indicated that photolytic process was scarcely responsible for the observed fast degradation when the antibiotic wastewater solution was irradiated in the presence of Fenton reagent. The degradation observed was 17.7% ($t_{30WT,n}$=53.9 min) for OFX and 13.7%

($t_{30WT,n}$=37 min) for TMP (Figure 5.7). Furthermore, the photolytic degradation was accompanied by a very low reduction in DOC (5-6%). The hydrolysis experiments did not exhibit significant degradation for any of the compounds (data not shown).

Competitive sunlight absorption by dissolved organic matter (DOM) and variable sorption of the compounds on organic colloids complicate the photolytic substrates degradation in natural conditions. DOM can reduce the antibiotics photolysis (which are presented at much lower concentration level than DOM) because the sensitization effect is hidden by the strong filter effect (Konstantinou et al., 2001; Navarro et al., 2011). It should be noted that the photolytic substrates degradation in the pilot scale experiments was higher compared to that observed in the bench scale study of solar Fenton (< 6%). However, the conditions were different (*i.e.* substrates concentration, solar irradiation intensity, temperature, wastewater matrix, reactor geometry) therefore we cannot export any discussion concerning these results. The acidic conditions under which the pilot scale experiments were conducted may have enhanced the photolytic behavior of the compounds as reported by Arnold and McNeill (2007).

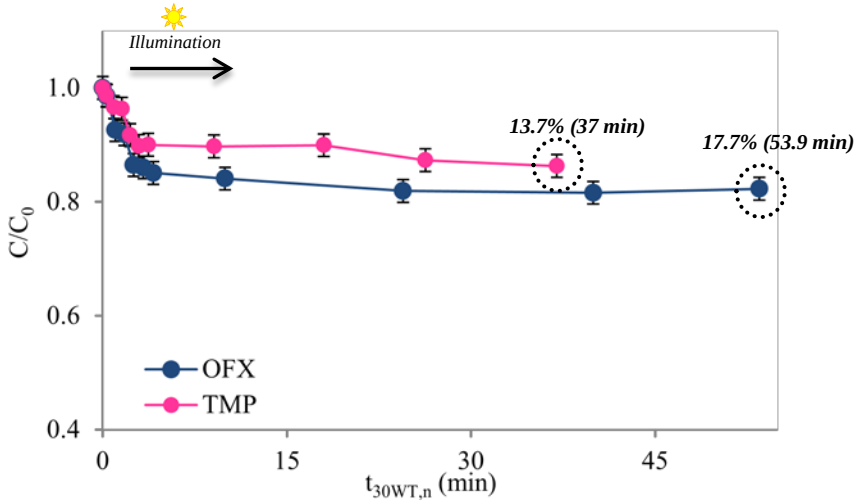

Figure 5.7 OFX and TMP degradation profile during photolysis experiments. Experimental conditions: $[Substrate]_0$=100 μg L^{-1}; pH_0=2.8-2.9.

5.2.2 Solar Fenton experiments

One important issue of the pilot scale study was to find out if the solar Fenton process is able to degrade completely the investigated compounds present at μg L^{-1} concentration level in a wastewater matrix containing dissolved organic matter (DOM) at much higher concentration level (mg L^{-1}). DOM could be considered as an important drawback for the process as it can react with the hydroxyl radicals resulting in decreased substrates degradation efficiency (Lindsey and Tarr, 2000).

For the solar Fenton experiments a concentration of iron at 5 mg L^{-1} was chosen considering the fact that this concentration is capable to achieve relatively high degradation rates (as showed in the bench scale experiments) and to avoid the requirement for iron removal at the end of the process according to the existing regulations concerning iron discharge limits. Additionally, considering the fact that hydrogen peroxide has significant economic cost, a system with low concentration of the latter was selected which would be able to give a high performance in degrading these compounds.

Preliminary solar Fenton experiments were carried out using 5 mg L^{-1} of Fe^{2+} at several H_2O_2 doses (between 25 and 100 mg L^{-1}) in order to establish the optimum peroxide dose for the antibiotics removal. It is important to point out that the concentration of soluble iron in the secondary wastewater (0.302 mg L^{-1}, see Table 2.2) is low compared with the concentration of iron added (5 mg L^{-1}) and therefore it does not change significantly the concentration of the total iron for the solar Fenton process. The complete removal of OFX and TMP substrate was accomplished with 75 mg L^{-1} of H_2O_2 within 180 min (t_{exp}) of solar irradiation; at lower H_2O_2 doses (25 and 50 mg L^{-1}) more irradiation time (t_{exp}=240 min) was needed for the complete degradation of the compounds whereas at 100 mg L^{-1} of H_2O_2 the substrates

degradation and the organic content (DOC, COD) removal profile was similar to that at 75 mg L^{-1} H_2O_2.

Figure 5.8 shows the degradation profile of both compounds at various hydrogen peroxide concentrations as a function of the $t_{30WT,n}$. The similar results obtained using 100 mg L^{-1} of H_2O_2 with that of 75 mg L^{-1} H_2O_2 are probably attributed to the enhancement of the competition reactions in the case of excess of H_2O_2, mainly the recombination of hydroxyl radicals and the reaction of hydroxyl radicals with H_2O_2, thus contributing to the hydroxyl radicals scavenging (Tamimi et al., 2008).

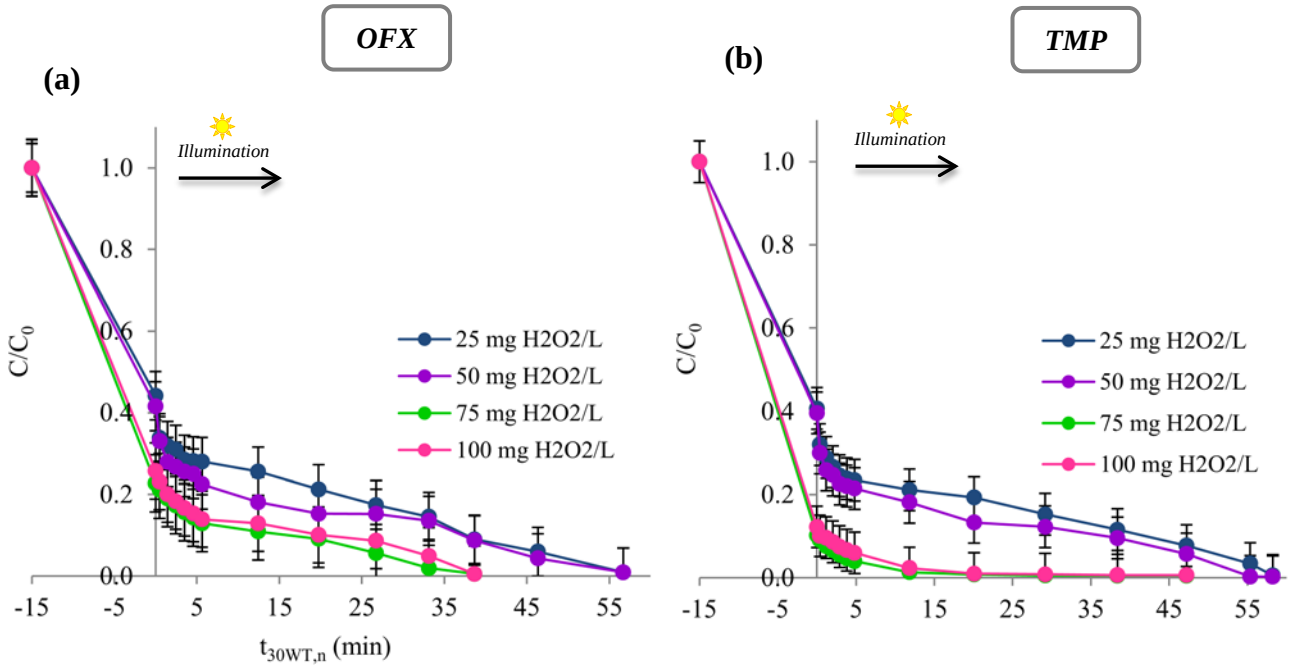

Figure 5.8 OFX and TMP substrates degradation profile at various H_2O_2 concentrations: (a) OFX and (b) TMP. Experimental conditions: $[Substrate]_0$=100 µg L^{-1}; $[Fe^{2+}]$=5 mg L^{-1}; pH_0=2.8-2.9.

Figure 5.9 (a) depicts the evolution of the photocatalytic degradation of OFX and TMP during the solar Fenton oxidation ($[Fe^{2+}]$=5 mg L^{-1}, $[H_2O_2]$=75 mg L^{-1}) vs the

normalized illumination time, $t_{30WT,n}$; in the same figure the respective curves of peroxide consumption are also presented. A similar degradation behavior was observed for both compounds. OFX was completely degraded after $t_{30WT,n}$=38.7 min of treatment (H_2O_2 consumption=33.8 mg L^{-1}) whereas TMP was completely degraded at $t_{30WT,n}$=20.1 min (H_2O_2 consumption=30.8 mg L^{-1}).

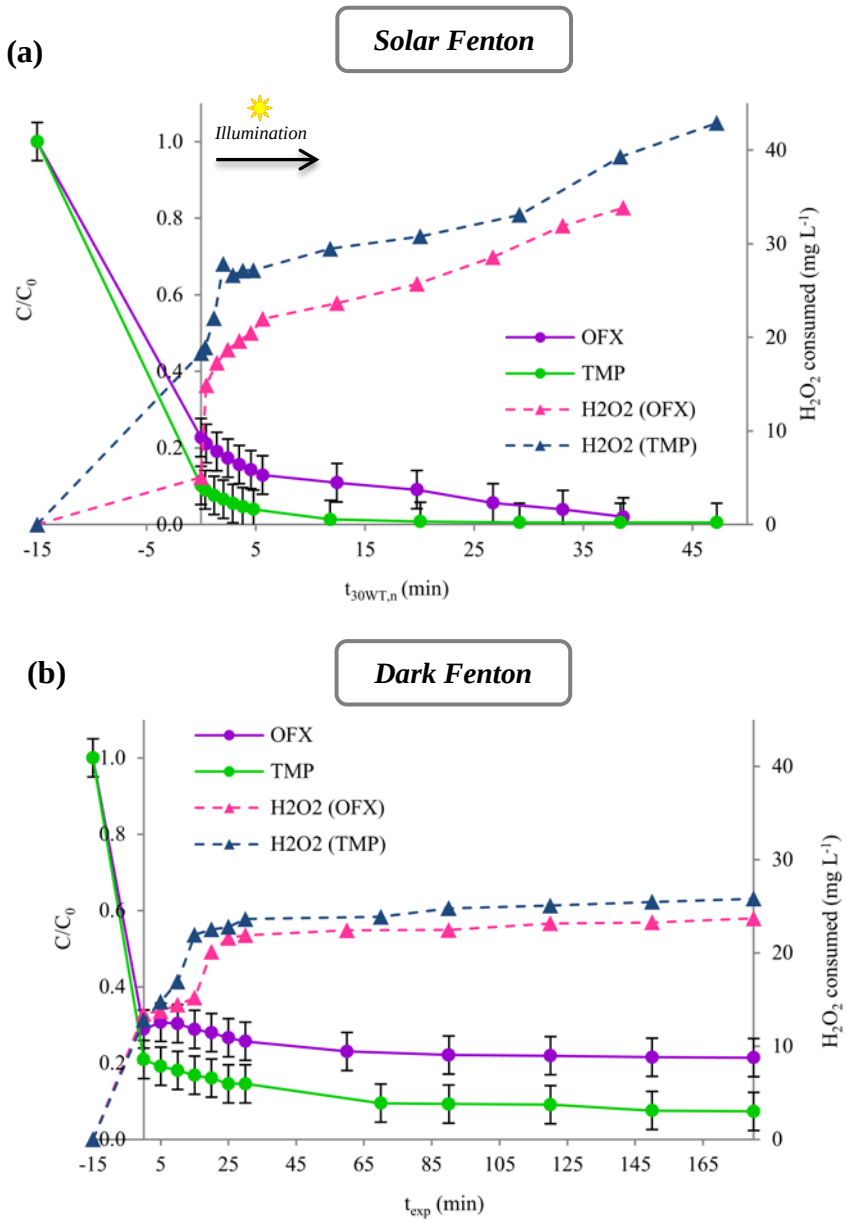

Figure 5.9 OFX and TMP degradation during: (a) solar Fenton and (b) dark Fenton experiments. Experimental conditions: $[Substrate]_0$=100 μg L^{-1}; $[Fe^{2+}]_0$=5 mg L^{-1}; $[H_2O_2]_0$=75 mg L^{-1}; pH_0=2.8-2.9.

It is important to note that degradation of the substrates started 15 min before uncovering the reactor (t_{exp}=-15 min, dark Fenton reaction) with 75.2% ($[OFX]_{residual}$=20.8 μg L^{-1}) and 82.8% ($[TMP]_{residual}$=11.4 μg L^{-1}) degradation of OFX and TMP, respectively.

The experiments were repeated under the same conditions in the absence of solar light (collectors were covered). The dark Fenton experiments were performed in order to investigate the efficiency of the process and thus the possibility of the continuous operation of the plant overnight. As shown in Figure 5.9 (b), a significant degradation of the compounds under dark conditions was achieved. The maximum degradation of the compounds during the dark Fenton was 78.6% (H_2O_2 consumption=23.7 mg L^{-1}) for OFX and 92.7% (H_2O_2 consumption=25.8 mg L^{-1}) for TMP at 180 min of treatment for both compounds.

It should be noted that, although the degradation of both compounds was complete in 180 min under solar Fenton process, DOC determinations showed no substantial mineralization. DOC was reduced to 21% after an illumination time of 180 min whereas COD abatement was found to be approximately 50% (Figure 5.10). It must be mentioned that the COD and the DOC of the treated samples is practically equivalent with the COD and DOC of the wastewater matrix considering the low concentrations of the pharmaceuticals added (each compound at concentration of 100 μg L^{-1} produce no more than 0.1 mg L^{-1} of DOC). Moreover, 80% of the initial BOD_5 was removed during the process within 180 min.

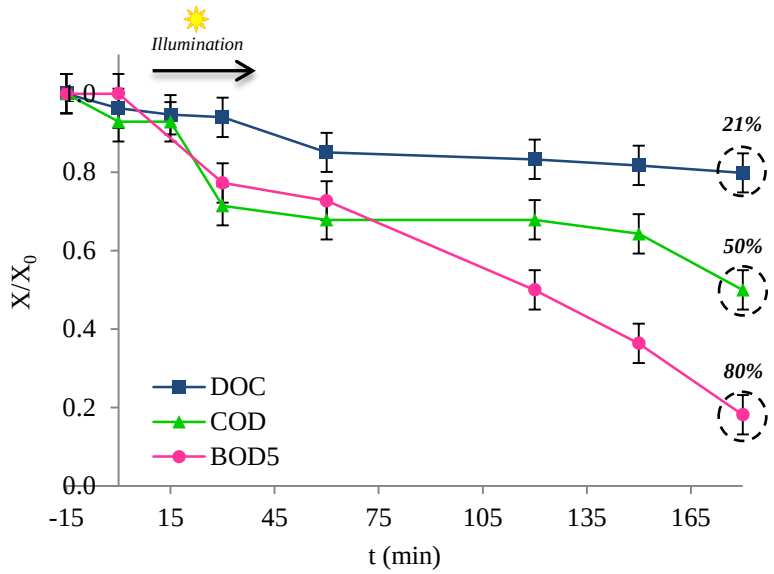

Figure 5.10 DOC, COD and BOD_5 removal during solar Fenton process. Experimental conditions: $[Substrate]_0$=100 μg L^{-1}; $[Fe^{2+}]_0$=5 mg L^{-1}; $[H_2O_2]_0$=75 mg L^{-1}; pH_0=2.8-2.9.

Additional experiments were conducted in order to determine the efficiency of the solar Fenton process without modifying the pH of the wastewater. The experiments were performed at the inherent pH value (pH ≈ 7.0) of the wastewater. This provides the advantage of avoiding the wastewater acidification which means additional cost through the consumption of reagents (H_2SO_4) and subsequent increase of the salinity of the treated water (Malato et al., 2009). Figure 5.11 shows the degradation profile of the substrates in neutral pH along with the degradation curves achieved under acidic conditions. It was demonstrated that the substrates in neutral pH were removed completely at the end of the treatment; however, the degradation proceeded with much lower rate at neutral pH compared to that observed under acidic conditions.

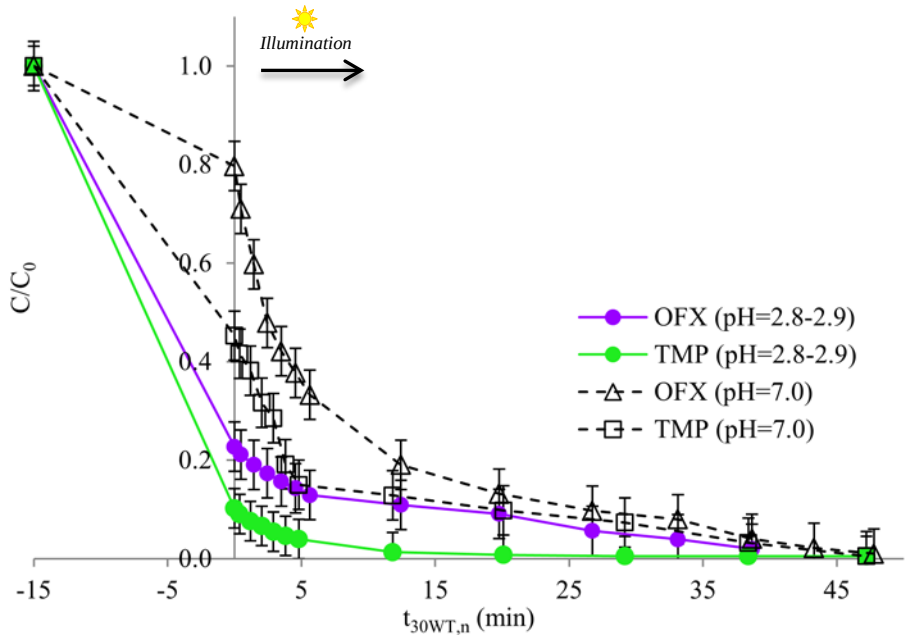

Figure 5.11 OFX and TMP degradation during solar Fenton at acidic (pH=2.8-2.9) and neutral conditions. Experimental conditions: $[Substrate]_0$=100 μg L^{-1}; $[Fe^{2+}]_0$=5 mg L^{-1}; $[H_2O_2]_0$=75 mg L^{-1}.

The complete degradation of the substrates was achieved at $t_{30WT,n}$=48.9 min for OFX and at $t_{30WT,n}$=47.2 min for TMP while DOC declined from 8.6 mg L^{-1} to 7.5 mg L^{-1} corresponding to 12% removal of the organic matter. Table 5.3 summarizes the results derived from the solar Fenton experiments under acidic and neutral conditions.

Although the pH was not adjusted, it changed to 5.7-6.1 at the end of the treatment due to the presence of organic acids in the wastewater, which are generated through the oxidation process. Moreover, at neutral pH total iron concentration decreased from 5 mg L^{-1} to approximately 3 mg L^{-1} indicating that part of the dissolved ferrous iron (which oxidized rapidly to ferric iron) was precipitated during the process while iron concentration remained constant during the experiments performed under acidic conditions. This was also confirmed by conducting the following experimental

procedure: two wastewater solutions at [Fe^{2+}]=5 mg L^{-1} were prepared at pH 3.0 and 7.0. These solutions were stirred for 2 h and then centrifuged for 20 minutes. Then, the dissolved iron in the filtered solutions was determined by atomic absorption spectroscopy. It is worth noting that during the centrifugation, a precipitate was observed in the wastewater solution at neutral pH indicating the formation of $Fe(OH)_2$. The results showed that 45% of the dissolved ferric iron formed complexes with the DOM.

Table 5.3 Comparison of the solar Fenton experiments performed under acidic and neutral pH.

Experiment	**pH 2.8-2.9**	**pH 7.0 (without adjustment)**
$t_{30WT,n}$ (min)*	OFX: 38.7 TMP: 20.1	OFX: 49.8 TMP: 47.2
DOC removal (%)	21	12
Consumed H_2O_2 (mg L^{-1})	OFX: 33.8 TMP: 30.8	OFX: 45.6 TMP: 41.2
Total iron$_{final}$ (mg L^{-1})	4.8-5.0	2.9-3.3
pH_{final}	2.61-2.65	5.7-6.1
(*) normalized illumination time for the complete degradation of the compounds		

The process pH is generally perceived as the limiting factor for the photo-Fenton system because $[Fe(OH)]^{2+}$, the most photoactive ferric iron-hydroxy complex, is predominant at acidic pH. In the presence of dissolved organic matter (DOM), strong and photoactive complexes are formed between ferric iron (Fe^{3+}) and the carboxylate or polycarboxylate groups which are the most common functional groups in DOM

(De la Cruz et al., 2012; Spuhler et al., 2010). Humic substance (HS) are the largest fraction of DOM in natural waters and are categorized as humic acid (HA) and fulvic acid (FA). They contain carboxylic acids, phenolic, alcoholic quinine, and amino and amido groups which enable them to support ion exchange and redox processes, and to form complexes (Klamerth et al., 2011). They contain also large numbers of stable free radicals which can react with various substances. The complexes of HS with Fe^{3+} have the advantage of being soluble in the wastewater matrix and so preventing the Fe^{3+} precipitation at neutral pH conditions. Another remarkable point is that they have typically higher molar absorption coefficients in the near-UV and visible regions than the aquo-Fe^{3+} complexes do (Pignatello et al., 2006). Moreover, the Fenton reaction is faster than the precipitation of Fe^{3+} therefore the process efficiency is still high at neutral conditions.

The primary step of the photoreduction of dissolved ferric iron in the solar Fenton process is a ligand-to-metal charge-transfer (LMCT) reaction. Subsequently, intermediate complexes dissociate as shown in eqn. (5.3) (Zepp et al., 1992). The ligand (*L*) can be any Lewis base able to form a complex with ferric iron (OH^-, H_2O, HO_2^-, Cl^-, $RCOO^-$, ROH, RNH_2, etc.). Depending on the reacting ligand, the product may be a hydroxyl radical such as in eqs. (5.4) and (5.5) or another radical derivated from the ligand (eqn. (5.6)).

$$[Fe^{3+}L] + h\nu \rightarrow [Fe^{3+}L]^{\bullet} \rightarrow Fe^{2+} + L^{\bullet} \quad (5.3)$$

$$[Fe(H_2O)]^{3+} + h\nu \rightarrow Fe^{2+} + HO^{\bullet} + H^{+} \quad (5.4)$$

$$[Fe(OH)]^{2+} + h\nu \rightarrow Fe^{2+} + HO^{\bullet} \quad (5.5)$$

$$[Fe(OOC\text{–}R)]^{2+} + h\nu \rightarrow Fe^{2+} + CO_2 + R^{\bullet} \quad (5.6)$$

The use of organic ligands that can complex Fe^{3+} is considered to be an important modification of the Fenton process because the continuously addition of acid in order to achieve the optimum process efficiency, makes the process unsuitable for other applications (especially in industrial scale) due to the accompanying salinity and cost increase. The formation of Fe^{3+} complexes with certain organic ligands enables the process to be carried out at higher pH (Balmer and Sulzberger, 1999). Suitable ligands should bind Fe^{3+} strongly and allow the transformation of Fe^{3+} to Fe^{2+}.

The main mechanisms (Schematic 5.2) which could possibly be involved in the solar Fenton system ($h\nu/Fe^{2+}/H_2O_2$) in the presence of DOM in neutral pH, were proposed by De la Cruz et al. (2012). The main mechanisms depicted in Schematic 5.2 through which the substrates can be degraded could be: (i) Direct photolysis of micropollutants (*P*) through an electronic excitation of the organic substrate or homolysis of the molecule to form another by-product (P_{mod}); (ii) Light (UV/visible) absorption by a photosensitizer molecule present in dissolved organic matter (DOM) which promotes it into its exited triplet state ($^3DOM^*$), and then can react with *P* or oxygen to form singlet molecular oxygen ($^1O_2$) which will react afterwards with *P* (Wenk et al., 2011; Canonica, 2007; Zepp et al., 1985); (iii) Cleavage of H_2O_2 into hydroxyl radicals by UV light (254 nm) which can then oxidize *P* (Legrini et al., 1993); (iv) Fenton reactions with oxidation of Fe^{2+} to Fe^{3+} by H_2O_2 and the formation of hydroxyl radicals which then react with *P*; (v) Formation of complexes between Fe^{3+} and DOM and absorption of light (UV/visible) undergoing via LMCT to the production of Fe^{2+} and a ligand radical (Pignatello et al., 2006); (vi) Reaction of the radical $DOM^{\bullet}_{ox}$ with O_2 leading to the formation of the radicals $O_2^{-\bullet}/HO_2^{\bullet}$; (vii) Formation of H_2O_2 in the aqueous system where the superoxide anion ($O_2^{-\bullet}$) will readily disproportionate to yield the H_2O_2 (Legrini et al., 1993); (viii) Formation of

H_2O_2 through the reaction of $O_2^{-\bullet}/HO_2^{\bullet}$, Fe^{2+} and H^+ leading to Fe^{3+} and H_2O_2, not very important at neutral pH (Feng et al., 2000) and (ix) Radical-radical ($2HO^{\bullet}$) recombination to form H_2O_2 (Legrini et al., 1993).

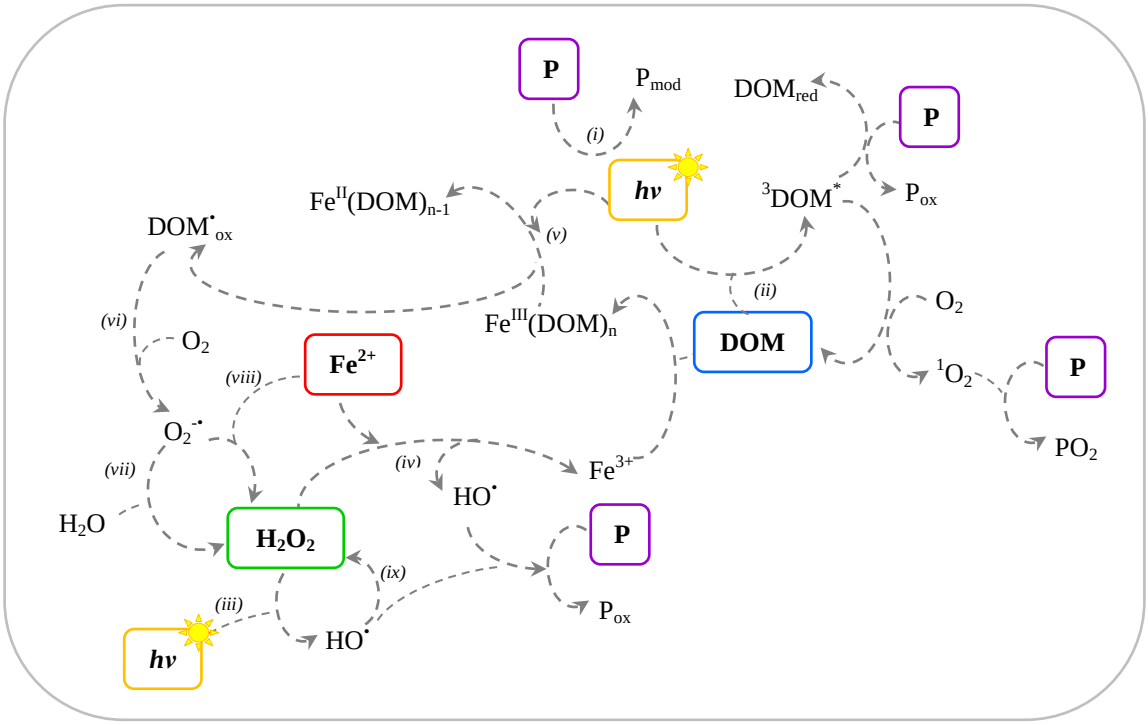

Schematic 5.2 Possible mechanisms involved in the solar Fenton system (*hv*/Fe^{2+}/H_2O_2) and DOM present in the wastewater at neutral pH (De la Cruz et al., 2012).

Few studies have focused on the photo-Fenton treatment at near neutral pH for the decontamination of municipal wastewater effluents containing micropollutants at low concentration levels (Klamerth et al., 2010; Klamerth et al., 2011; De la Cruz et al., 2012). Some chelating agents have also been proposed to be used at neutral pH. Klamerth et al. (2011) employed different iron ligands for the degradation of organic pollutants during photo-Fenton at neutral pH, such as ferrioxalate ($[Fe(C_2O_4)_3]^{3-}$) and humic acid (HA). The ferrioxalate-enhanced photo-Fenton process provided

satisfactory degradation results within a reasonable time while pollutants degradation using HA was slower and nearly complete. The addition of ferrioxalate however poses an important drawback due to the increased reagents cost and its degradation during the photochemical reactions (Malato et al., 2009).

5.2.3 Degradation kinetics

Previous studies have indicated that the kinetics of pharmaceuticals degradation by the photo-Fenton process is a pseudo-first order reaction (Lin et al., 2004; Radjenovic et al., 2009; Michael et al., 2010). Thus the concentration of the examined compounds can be given by the kinetic expression (eqn. (5.7)):

$$C = C_0 e^{-kt} \qquad \textbf{(Kinetic equation 1)} \qquad (5.7)$$

where C and C_0 are the time-dependent concentration and the initial concentration respectively, and k is the apparent pseudo-first order rate constant.

The above expression resulted considering that the reaction between $HO^{\bullet}$ and the substrate (OFX or TMP) is the rate-determining step and that $HO^{\bullet}$ rapidly achieve a constant steady-state concentration in the solution (Evgenidou et al., 2007; Radjenovic et al., 2009).

The photocatalytic disappearance of OFX and TMP (both at initial concentration of 100 μg L^{-1}) with the solar Fenton process at pilot scale experiments followed apparent first-order kinetics. This was confirmed by the linear behavior of $-ln(C/C_0)$ as a function of the normalized time $t_{30WT,n}$ in all the experiments performed (regression coefficients of the linear fitting were higher than 0.99) (Figure 5.12).

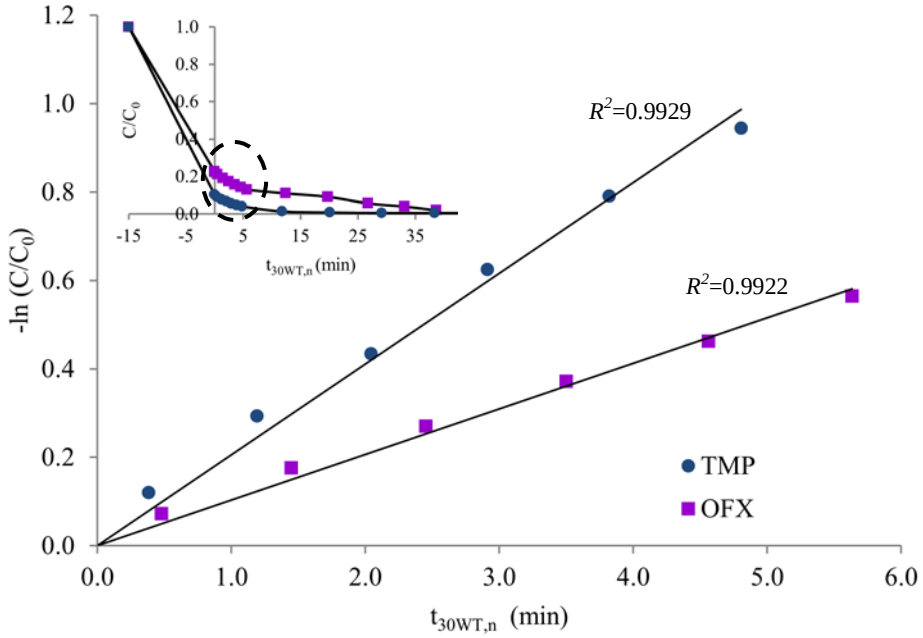

Figure 5.12 Experimental data fitting in the kinetic model which describes first order reactions. Experimental conditions: $[Substrate]_0$=100 μg L^{-1}; $[Fe^{2+}]_0$=5 mg L^{-1}; $[H_2O_2]_0$=75 mg L^{-1}; pH_0=2.8-2.9.

The kinetic expression (eqn. (5.7)) may be acceptable for a series of time-concentration data at early reaction times (usually 15-20 min). However, for wider reaction spans, this equation is unsuitable for characterizing the behaviour of the irradiated system and despite the acceptable values for the correlation coefficient (R^2) this may lead to the estimation of negative concentrations and inexistent concentration minimum values (Navvaro et al., 2011). Also, eqn. (5.7) cannot be used for the experimental data above 15-20 min due to the competitive effects of the matrix, formation of by-products, pH changes, etc. (Evgenidou et al., 2007). When the linear approach fails, other equations can be employed. A modification of the first-order kinetic expression was proposed and has been successfully used to explain

the degradation kinetics of the compounds during the photo-Fenton treatment. This empirical model is described by eqn. (5.8).

$$C = Ae^{k_1 t} + Ae^{k_2 t} \qquad \textbf{(Kinetic equation 2)} \qquad (5.8)$$

Figures 5.13 and 5.14 depict the adjustment of the experimental data for OFX and TMP to the above kinetic equations. It was observed that the experimental data fit better kinetic equation 2 for both compounds.

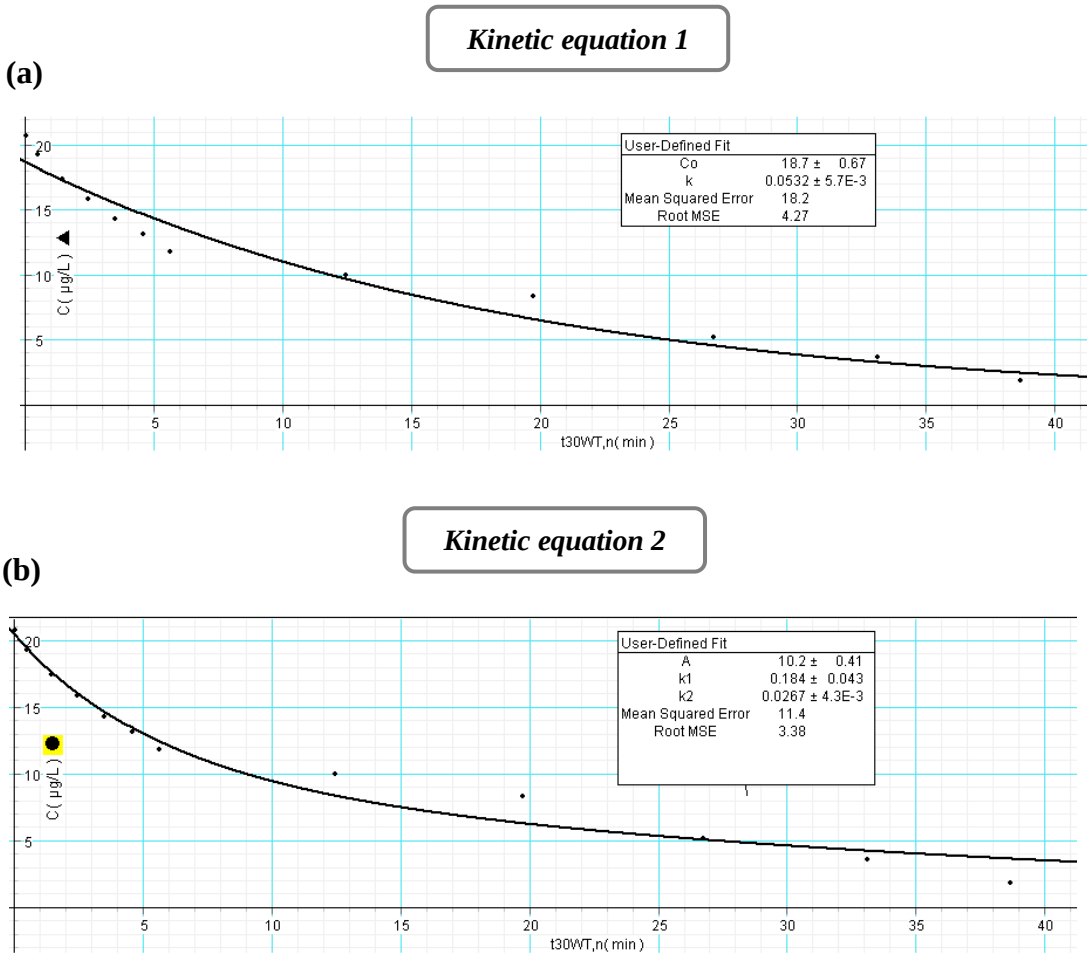

Figure 5.13 Fitting of the experimental data to the kinetic equations for solar Fenton ([substrate]$_0$=100 µg L^{-1}): (a): OFX kinetic equation 1; (b): OFX kinetic equation 2.

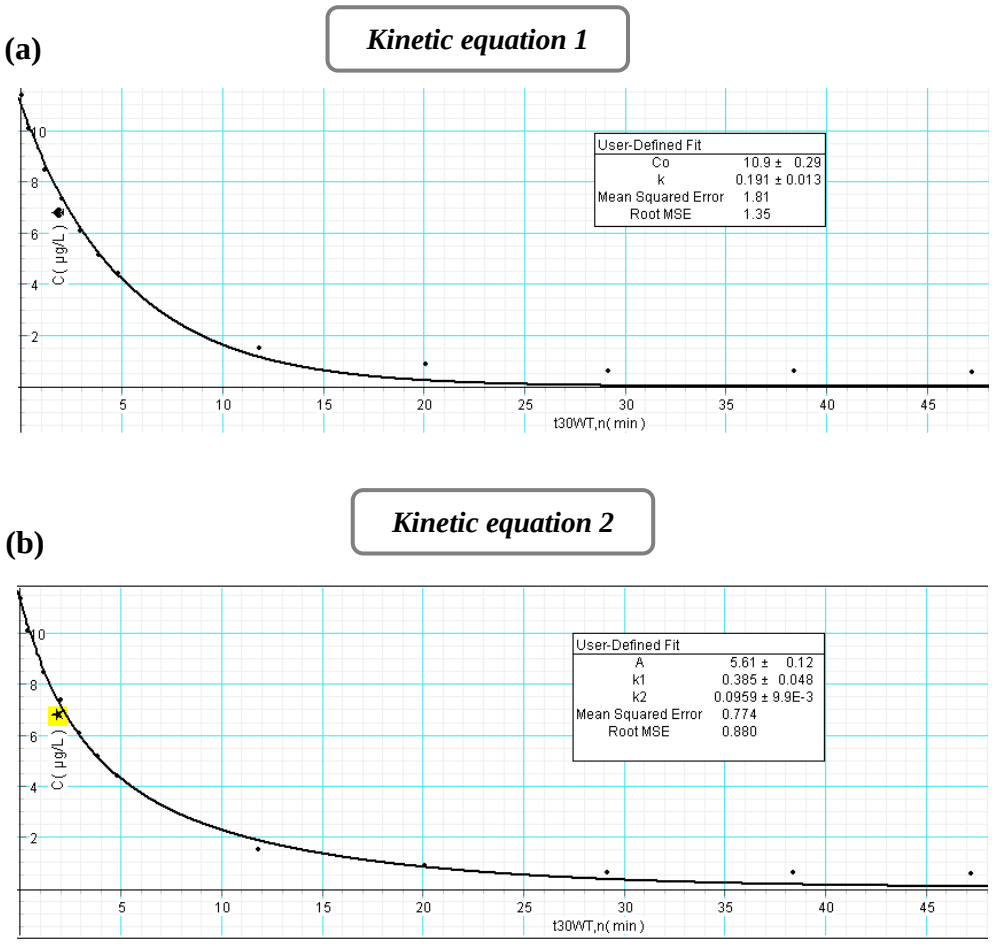

Figure 5.14 Fitting of the experimental data to the kinetic models for solar Fenton ([substrate]$_0$=100 µg L^{-1}): (a): TMP kinetic equation 1; (b): TMP kinetic equation 2.

In Table 5.4 the coefficient values are summarized with the respective mean square errors (MSE) (sum of the squares of the differences between the model predictions and the experimental data) of each equation calculated for each compound.

Table 5.4 Degradation kinetics parameters for OFX and TMP using the first-order kinetic model (kinetic equation 1) and the proposed empirical model (kinetic equation 2).

	Kinetic equation 1: $C = C_0 e^{-kt}$				***Kinetic equation 2:*** $C = Ae^{k_1 t} + Ae^{k_2 t}$				
	C_0 (μg L^{-1})	k(min^{-1})	*Adj-*R^2	*MSE*	*A*	k_1	k_2	*Adj-*R^2	*MSE*
OFX	18.7±0.67	0.0532±5.710^{-3}	0.955	18.2	10.2±0.41	0.184±0.043	0.0267±4.310^{-3}	0.998	11.4
TMP	10.9±0.29	0.191±0.013	0.939	1.81	5.61±0.12	0.385±0.048	0.0959±9.910^{-3}	0.999	0.774

The two terms of the eqn. (5.8) represent the parallel conduction of two oxidation mechanism reactions during the solar Fenton process possibly due to the presence of different hydroxyl radicals concentration areas in solution contained in a reactor volume *dV*: (i) one area (k_1) with high hydroxyl radicals concentration due to the direct photon absorption from iron; and (ii) a second area (k_2) with lower hydroxyl radicals concentration due to the filter inner effects or to the presence of natural dissolved organic matter (DOM) in the wastewater matrix (where $k_1 >> k_2$).

The inner filter effects present in the treated solution are considered as an important issue on the degradation rate during the solar Fenton process. Inner filter effects are the competitive absorption of photons by other light absorbing species, usually the various organic contaminants present in the wastewater matrix (Malato et al., 2009). Furthermore, the presence of natural organic compounds occurring in the wastewater matrix can affect the degradation rate of the target compounds since they can act as metal chelators. These compounds (such as humic acids, fulvic acids, organic colloids) exhibit significant iron complexation (or can alter the redox cycling of iron) and thereby change the formation rate of hydroxyl radicals (Lindsey and Tarr, 2000).

To assess the two models, measured and predicted values are compared in Figure 5.15 (a, b). The results demonstrate that the biphasic model (eqn. (5.8)) fits better to the experimental data (including longer timers of treatment) than the usual monophasic model (eqn. (5.7)). Also, the values of MSE obtained with eqn. (5.8) were lower for both compounds compared to that of the first-order model.

A model with more terms may appear to have a better fit simply because it has more parameters to be adjusted (or less degrees of freedom) (Perez-Moya et al., 2008). In order to compare the two models and balance their different degrees of freedom the Adjusted R^2 (*Adj-*R^2) index was used.

$$Adj - R^2 = 1 - \frac{\sum_{i=1}^{n} \frac{(y_i - \hat{y}_i)^2}{n} - p}{\sum_{i=1}^{n} \frac{(y_i - \bar{y})^2}{n} - 1} \quad (5.9)$$

where y_i is the experimental value (C_i), $\hat{y}_i$ is the model predicted values ($\hat{C}_i$), $\bar{y}$ is the average of the experimental values ($\bar{C}$), n is the number of experiments performed and p is the fit coefficient number.

This factor increases only if the addition of a new parameter improves the model more than would be expected by chance; otherwise, its value decreases (Perez-Moya et al., 2008). As shown in Table 5.4, higher values of *Adj-*R^2 were obtained using the kinetic equation 2. Although the kinetic equation 2 requires one more parameter than the simplified equation 1, the *Adj-*R^2 index shows that the extra parameter improves the data fitting; thus, it may not be neglected.

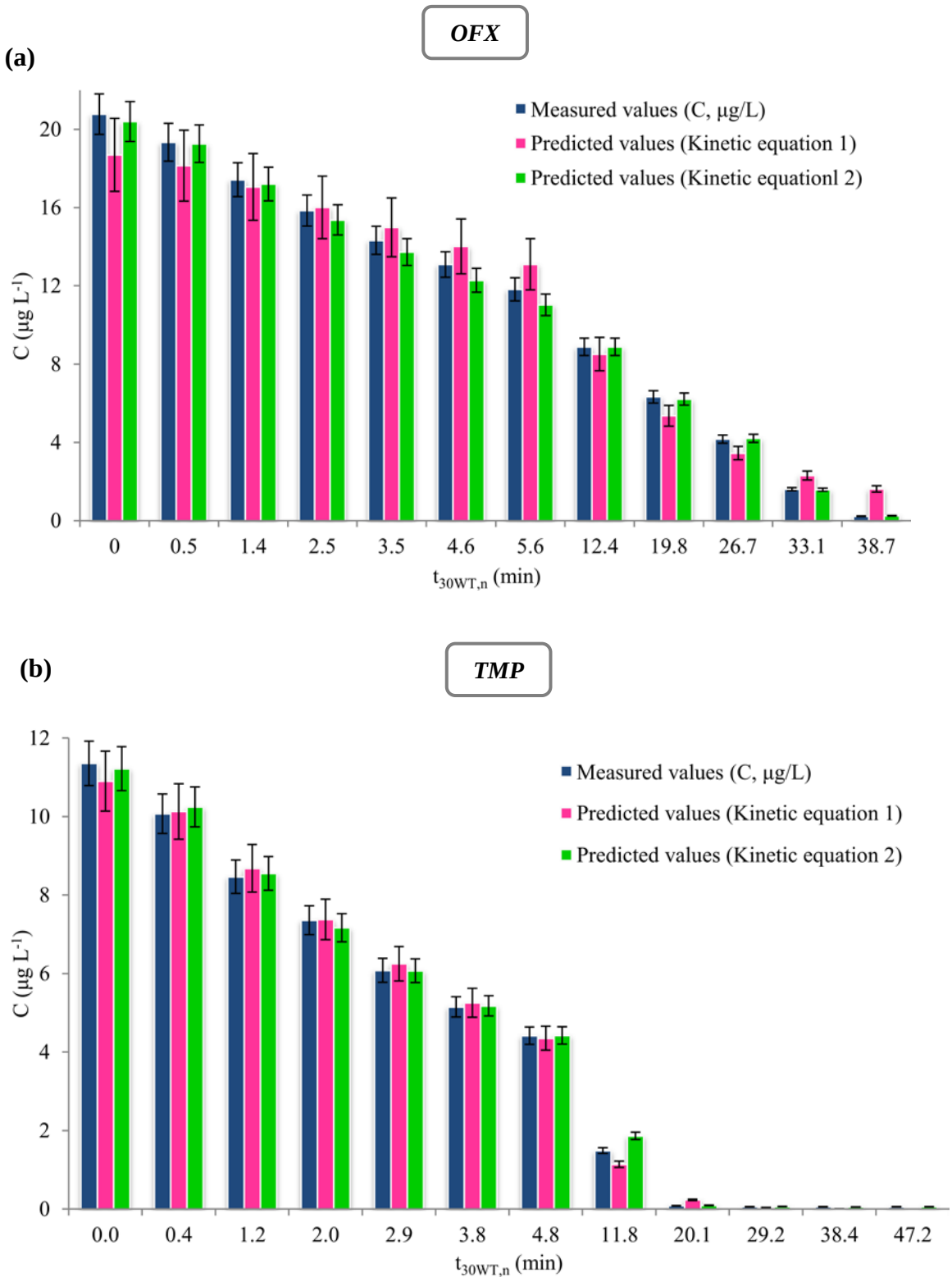

Figure 5.15 Measured and predicted values compared for each kinetic equation: (a) OFX; and (b) TMP.

5.2.4 Ecotoxicity evaluation

The oxidation by-products resulted during the application of solar Fenton process may be characterized by high toxicity (compared to the untreated sample) rendering toxicity tests as an indispensable task. These products, in our case, originated from the oxidation of OFX and TMP but also from the oxidation of the DOM present in the original secondary effluent. The possible toxicity of these products was examined by two toxicity tests considering the final use of the treated wastewater. Toxicity tests using *Daphnia magna* and three plant species (*Sorghum saccharatum*, *Lepidium sativum*, *Sinapis alba*) were considered suitable to evaluate the toxicity of the treated wastewater before its disposal to water bodies and use for agricultural irrigation, respectively.

5.2.4.1 Phytotestkit toxicity test

The test results were evaluated comparing the mean number of germinated seeds and the mean root and shoot length for the three replicates in the control and in each examined sample. The percentage effect of the chemical compounds on seed germination inhibition (GI), root growth inhibition (RI) and shoot growth inhibition (SI) was calculated applying the following formula.

$$GI\ or\ RI\ or\ SI\ (\%) = \frac{A-B}{A} \times 100 \quad (5.10)$$

where *A* is the average number of germinated seeds or average root length or average shoot length, respectively in the control and *B* is the respective value for the test solution. The experiments were performed in triplicate (RSD is depicted in Table 5.5).

Preliminary solar Fenton experiments ($[Fe^{2+}]$=5 mg L^{-1}; $[H_2O_2]$=75 mg L^{-1}; pH_0=2.8-2.9) were performed in the absence of antibiotics in order to investigate whether the toxicity effect on the plant species is mainly due to the oxidation of the DOM.

The phytotoxicity test was further conducted on samples taken from the solar Fenton process (at the same reagents concentration) at various times of treatment (0-180 min) in the presence of antibiotics. The treated samples displayed a multi-phase toxicity profile to each type of plant by means of GI, RI and SI and the results are depicted in Table 5.5. It should be noted that the results are presented as a function of the actual experimental time (t_{exp}) instead of the normalised illumination time ($t_{30WT,n}$) for comparison purposes among the three plant types and the two compounds.

5.2.4.1.1 Seed germination inhibition

In general, the solar Fenton process did not exert any significant influence on seed germination and the inhibition level was altered from 0 to 23.3%. As can be seen in Table 5.5, the raw wastewater sample (WW) before the solar Fenton process, caused low inhibition on germination for *Lepidium sativum* (3.3%) and *Sorghum saccharatum* (3.3%) and no inhibition for *Sinapis alba*. The WW toxicity remained the same when the latter was spiked with 100 μg L^{-1} of TMP (WW+TMP) and 100 μg L^{-1} of OFX (WW+OFX) indicating that the presence of the antibiotics in the WW did not have any adverse effect on the seed germination. When the solar Fenton was applied, the phytotoxic effects on seed germination varied among the plant species and the treatment time. The maximum GI was observed at 60 min of treatment for *Sinapis alba* (10%) whereas for *Lepidium sativum* and *Sorghum saccharatum* the maximum GI values were 20 and 6.7% respectively after 30 min of treatment. At the end of the treatment (180 min) the GI was eliminated for all the plant species.

Table 5.5. Seed germination inhibition (GI), root growth inhibition (RI) and shoot growth inhibition (SI) during solar Fenton process. Experimental conditions: $[Substrate]_0$=100 μg L^{-1}; $[Fe^{2+}]_0$=5 mg L^{-1}; $[H_2O_2]_0$=75 mg L^{-1}; pH_0=2.8-2.9.

Plant species	**Treatment time (min)**	**Germination inhibition (GI, %)***			**Root inhibition (RI, %)***			**Shoot inhibition (SI, %)***		
		WW	WW+TMP	WW+OFX	WW	WW+TMP	WW+OFX	WW	WW+TMP	WW+OFX
Sinapis alba	0	*ni*	*ni*	*ni*	24.0±5.2	27.2±4.7	29.1±10.8	24.5±11.7	35.2±15.1	45.4±6.2
	30	8.0±2.2	5.0±1.6	10.0±1.5	30.0±4.8	37.9±9.5	44.4±16.1	38.7±8.5	39.6±8.2	40.3±8.5
	60	10.0±5.5	13.3±2.0	10.0±2.5	35.4±11.1	52.0±13.2	42.4±8.2	47.6±13.1	48.5±5.7	47.9±8.9
	120	5.0±1.8	10.0±1.5	4.0±1.8	40.2±6.8	56.3±10.8	46.2±12.2	55.0±9.3	54.6±9.2	64.2±11.3
	150	3.3±2.1	3.3±1.9	*ni*	20.2±12.2	29.7±15.2	33.2±9.6	42.5±5.9	44.0±10.1	37.3±10.7
	180	*ni*	*ni*	*ni*	15.1±9.7	18.5±7.9	10.7±17.7	25.3±5.1	33.7±11.5	32.5±9.2
Lepidium sativum										
	0	3.3±0.0	3.3±1.5	3.3±0.0	28.3±9.9	35.7±14.3	31.0±12.1	43.1±9.2	46.6±5.9	44.6±8.7
	30	20±2.9	13.3±1.8	23.3±3.9	31.3±7.2	28.9±9.5	42.7±9.3	45.1±13.2	44.4±9.9	44.9±13.9
	60	10±1.9	6.7±2.6	10±1.5	32.5±5.5	35.7±9.0	37.8±6.9	40.2±9.4	41.3±10.4	51.9±11.4
	120	3.3±1.9	3.3±1.5	3.3±2.0	35.3±13.2	45.0±17.2	31.9±10.1	44.8±7.6	43.8±10.8	54.5±15.1
	150	3.3±0.0	3.3±0.5	3.3±0.2	21.8±18.3	29.8±11.7	28.8±15.5	37.9±5.8	39.9±7.9	36.9±5.8
	180	*ni*	*ni*	*ni*	23.7±11.2	23.3±8.6	22.1±8.9	30.0±5.0	31.6±3.2	28.0±6.4
Sorghum saccharatum										
	0	3.3±0.0	3.3±0.0	3.3±0.0	32.8±5.6	38.8±8.9	55.7±11.2	62.7±13.2	67.4±9.9	63.4±11.6
	30	6.7±1.8	3.3±0.0	3.3±1.0	33.0±8.2	28.3±10.1	50.5±8.9	67.6±10.1	65.6±13.2	75.2±9.1
	60	3.3±1.6	*ni*	3.3±1.8	38.23±7.9	47.2±12.5	52.5±10.7	73.0±9.3	71.3±15.9	76.3±14.4
	120	3.3±1.5	6.7±0.7	*ni*	42.15±11.3	47.9±5.9	41.7±10.4	75.0±9.8	79.5±10.5	84.6±12.8
	150	5.0±0.9	*ni*	6.7±2.5	45.3±9.5	32.8±5.5	38.0±11.2	64.0±8.9	61.1±9.8	57.2±9.2
	180	*ni*	*ni*	*ni*	30.2±4.8	29.2±7.1	26.8±8.3	45.7±7.7	46.3±10.2	46.9±7.6

* Values(%)±RSD(%) in relation to that in tap water
***ni*: no inhibition

In the case of the wastewater spiked with TMP, a maximum inhibition to *Lepidium sativum* (13.3%) was observed after 30 min of solar Fenton due to the subsequent formation of by-products which apparently were toxic to these seeds. The *Lepidium sativum* GI was decreased by increasing the irradiation time from 60 to 150 min, while no inhibition was detected after 180 min of treatment meaning that less toxic intermediates were formed at the end of the process. Additionally, at 60 and 120 min of treatment a maximum inhibition to *Sinapis alba* (13.3%) and *Sorghum saccharatum* (6.7%) was observed respectively whereas no negative effect on germination was achieved at the end of the treatment (180 min) for both species.

In the case of OFX wastewater spiked solution, *Lepidium sativum* displayed the same germination inhibition profile compared to that observed for TMP. The higher inhibition (23.3%) was observed after 30 min of treatment. *Sinapis alba* germination inhibition was 10% at 30 and 60 min of treatment whereas the highest inhibition of *Sorghum saccharatum* was 6.7% after 150 min of solar Fenton. Finally the inhibition on seed germination was eliminated after 180 min of irradiation for each type of plant.

In summary, the GI results obtained from the treated wastewater spiked with the antibiotics at 100 μg L^{-1} were quite similar with those observed when exposing the plant species to the wastewater treated samples alone; therefore it can be concluded that the seed germination is not affected by the presence of these antibiotics and their transformation products at the μg L^{-1} concentration level. Although data showed some variations, these can be attributed to the variations of the composition of the wastewater during the experimental period.

5.2.4.1.2 Root growth inhibition

The phytotoxicity in the treated samples expressed as root growth inhibition (RI), varied differently with relation to the inhibition of seed germination (GI). The percentage effect of the treated samples on RI was higher compared to that observed on GI. Some research studies which investigated the phytotoxicity of sewage sludges (Wong et al., 2001; Fuentes et al., 2006) pointed out the fact that the evaluation of root length is a more sensitive parameter than seed germination.

As shown in Table 5.5, a similar inhibition evolution on the root length compared to the raw wastewater (WW) was observed after spiking the wastewater with the antibiotics (WW+TMP, WW+OFX). This was confirmed by applying the student *t*-test between the measured values where no statistical differences were observed. These results indicated that the low spiked concentration level of these antibiotics (100 μg L^{-1}) did not impose any adverse effect on root growth. However, the stimulating effect to the seeds of nutrients occurring in wastewater may still prevail considering the fact that the WW contains high concentration of nitrates (36 mg L^{-1}, see Table 2.2) which are considered very important for the root development (Rizzo et al., 2009). The maximum RI observed in the case of WW alone were 40.2, 35.3 and 42.3% for *Sinapis alba*, *Lepidium sativum* and *Sorghum saccharatum*, respectively.

The RI of *Sinapis alba* in wastewater spiked with TMP was increased at 30, 60 and 120 min of the photocatalytic treatment yielding 37.9%, 52.0% and 56.3% of inhibition, respectively. Finally, samples irradiated for 150 and 180 min resulted in less toxicity displaying a decrease on RI (29.7% and 18.5% respectively) indicating the removal or transformation of the toxic by-products throughout the process. In the case of *Lepidium sativum* and *Sorghum saccharatum* the root length inhibition showed approximately the same tendency. At the end of the process the RI was

decreased yielding 23.3% and 29.2% root inhibition for *Lepidium sativum* and *Sorghum saccharatum* respectively.

In the case of OFX, the RI for *Sinapis alba* was increased after 30 min of treatment (44.4%) and remained almost constant until 120 min while it was significantly decreased (10.6%) after 180 min of irradiation. In the case of *Lepidium sativum*, RI was slightly increased during the process and dropped at the end of the treatment (24.1% at 18 min) to the same level as the WW alone. For *Sorghum saccharatum* the RI was continuously decreasing through the process to reach the level values of the WW alone.

Interestingly, however, was the fact that the RI values observed at the end of the treatment (150 and 180 min) were approximately the same in all cases (TMP, OFX, WW) indicating that the negative effect on the root growth is attributed to the DOM by-products rather than the substrates oxidation by-products.

Some other studies showed the negative effect of antibiotics at the μg L^{-1} level on the root growth (Migliore et al, 2003). Phytotoxicity of enrofloxacin on crop plants *Cucumis sativus*, *Lactuca sativa*, *Phaseolus vulgaris* and *Raphanus sativus* was determined at 50, 100 and 5000 μg L^{-1} by measuring post-germinative growth of primary root. The exposure to lower concentrations of enrofloxacin (50 and 100 μg L^{-1}) was found to cause alteration of the post-germinative development which is related to the plant drug uptake.

5.2.4.1.3 Shoot growth inhibition

The growth of the shoots was affected from the treated samples, reflecting their own specific mechanisms for growth and adaptation to the oxidation by-products. Similar

SI profile was observed in the case of WW alone and WW spiked with the antibiotics indicating that the SI was affected presumably by the DOM by-products. In the case of TMP, *Sinapis alba* SI showed similarities with the RI, however the SI at the end of the process was higher compared to that of RI. The highest SI was 54.6% after 120 min (similar to the RI, 56.3%) whereas after 180 min the SI was decreased to 43.7%. Similar behaviour was observed for the *Sorghum saccharatum* however in this case the SI values were higher than the respective values of RI. The SI was 79.5% after 120 min of treatment whereas the final SI after 180 min was 46.3%. In the case of *Lepidium sativum* no significant changes were obtained during the process; however at the end of the treatment the SI was lower (31.6%, 180 min) than the initial (46.6%) indicating the high efficiency of the process in removing the toxic compounds. Similar SI profile was observed in the case of OFX (Table 5.5).

The results described above demonstrate the capacity of the applied advanced process to reduce the phytotoxicity to the examined plant species. The three plant species displayed an interesting profile concerning the germination, root and shoot inhibition stimulated by the presence of antibiotics in wastewater but mainly the varying response to the oxidation by-products. According to our knowledge, there is limited literature dealing with this toxicity assay although this important aspect is of great importance considering the consequent use of the treated domestic wastewater for agricultural irrigation purposes.

Naddeo et al. (2009) studied the ecotoxicity to *Lepidium sativum* before and after the ultrasonic irradiation treatment in urban wastewater effluent spiked with pharmaceuticals (diclofenac, amoxicillin and carbamazepine). It was found that the inhibition of *Lepidium sativum*, in terms of germination, in the presence of the pharmaceuticals mixture was stimulated instead of inducing any toxicity effect and

this might be attributed to the fact that the samples, spiked with very low drug concentrations, were able to act as a provider of additional nutrient elements. In another study of Rizzo et al. (2009) the photocatalytic effect (TiO_2 process) on *Lepidium sativum* germination using both spiked distilled water and actual wastewater solutions with pharmaceuticals (diclofenac, amoxicillin and carbamazepine) was investigated. The photocatalytic treatment did not completely reduce the phytotoxicity under the investigated conditions (maximum catalyst loading and irradiation time 0.8 g TiO_2 L^{-1} and 120 min respectively) and a drastic decrease in germination index was observed, indicating the formation of oxidation intermediates which were toxic to *Lepidium sativum* seeds. The potential impact of six antibiotics (chlortetracycline, tetracycline, tylosin, sulfamethoxazole, sulfamethazine and trimethoprim) on plant growth and soil quality was studied by Liu et al. (2009) by using the seed germination test. The phytotoxic effects varied between the antibiotics and between plant species (sweet oat, rice and cucumber). Among the three plants, sweet oat was the most sensitive plant to the six antibiotics although with varying toxicity values. Tetracyclines and sulfonamides were more toxic to plant seed germination while tylosin and trimethoprim were less toxic to seed germination.

The above plant species was tested on the antibiotic contaminated wastewater samples before and after the solar Fenton process at a pilot scale for the first time; therefore a comparison with other studies cannot be done. However, the samples' effect potency was further investigated towards *D.magna* species.

5.2.4.2 Daphnia magna toxicity test

In all the tests performed (wastewater with and without the antibiotics), solar Fenton process was observed to induce the same variation in the toxicity profile (expressed as % immobilization) indicating that the presence of OFX and TMP (and their by-products) at the low concentration level of μg L^{-1} did not affect *D.magna* species. It should be noted that previous studies revealed toxic effects of these antibiotics to *D.magna* at higher concentration level (> 10 mg L^{-1}) though (Isidori et al., 2005; Kim et al., 2007; Hapeshi et al., 2010; Rizzo et al., 2009; Fatta-Kassinos et al., 2011b). The results are depicted in Figure 5.16.

Primarily, in order to determine the toxicity of the secondary treated wastewater (WW) used for the whole experimental procedure, a set of control toxicity tests was performed by exposing *D.magna* to the wastewater samples. The control tests showed no toxicity to *D.magna* after 24 h exposure time; however after 48 h of exposure time the immobilization of daphnids was increased to (13.3-20.0)±0.8%.

The toxicity of the treated samples taken at 30 min of the photocatalytic process was dramatically increased to 40±0.2% and 60±0.4% after 24 and 48 h of exposure respectively. This increase is attributed to the organic intermediates formed rapidly from the oxidation of the DOM, causing toxicity effects on the daphnids especially at longer exposure times. Also, the high values of toxicity during the first stages of the process, is probably because of the slower decrease of the DOC that allows greater accumulation of by-products.

After 60 min of treatment, a decrease of immobilization was observed (which means that the oxidation of the by-products formed at 30 min and consequently the formation of new intermediates was still going on) but after 120 min of irradiation the toxicity of the samples increased indicating the formation of more toxic oxidation by-products. This may attributed to the competition mechanisms related to the

degradation of organics (including the antibiotics), the complete oxidation of organics to CO_2 and the formation of the toxic compounds. From that time and onwards a continuous decrease was observed. After 150 min of irradiation a significant decrease on immobilization after 24 h of exposure (25±1%) was observed due to the potential formation of less toxic by-products. Finally, after 180 min of photo-treatment the immobilization of daphnids after 24 h of exposure was 13.3±0.6% while after 48 h of exposure the respective value was 33.3±0.7%

Since the toxicity of the treated samples after 180 min of solar Fenton process was higher than that of the untreated wastewater, additional experiments were carried out to investigate whether the residual toxicity could be reduced in longer treatment time. The results showed a decrease in daphnids immobilization (~6.7%) after 300 min indicating the removal of the toxic compounds.

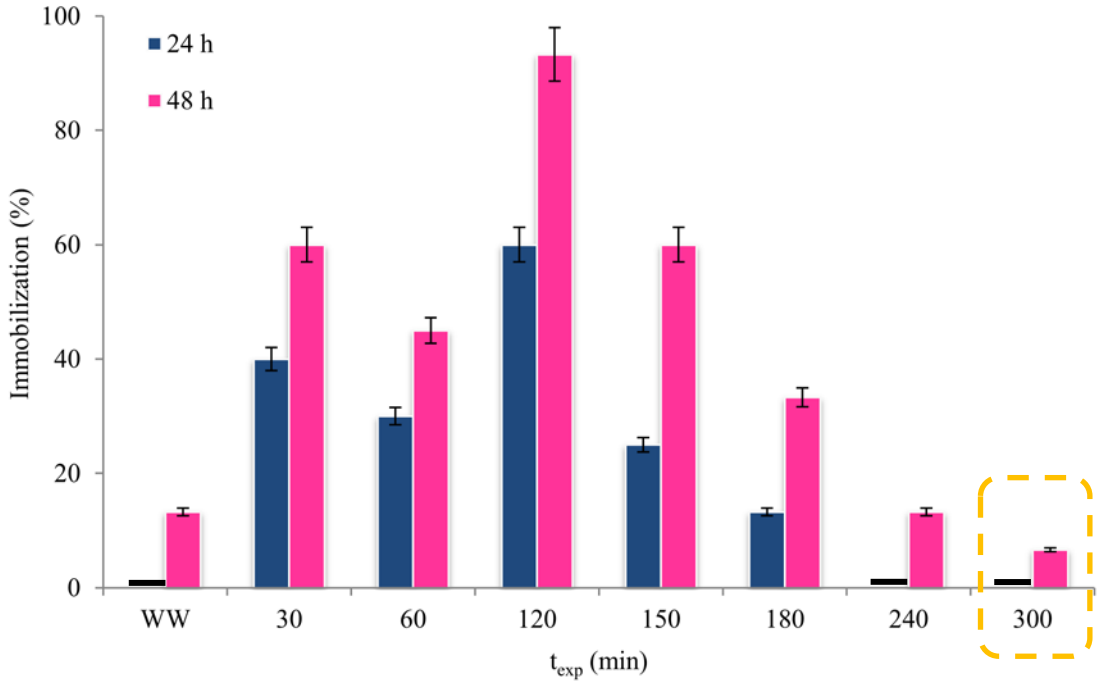

Figure 5.16 Evolution of toxicity to *D.magna* during solar Fenton process. Experimental conditions: $[Fe^{2+}]_0$=5 mg L^{-1}; $[H_2O_2]_0$=75 mg L^{-1}; pH_0=2.8-2.9.

The examined species displayed an interesting profile concerning their sensitivity by the presence of antibiotics in wastewater and also the varying response to the oxidation by-products. It can be emphasized that the by-products formed during the DOM oxidation seem to play more significant role in the toxicity changes to the plants and microorganisms than the by-products resulted from the substrates degradation. Therefore, more species from varying taxonomy and the aquatic environment must to be used in such studies for obtaining more integrated results.

5.2.5 Antibiotic resistant enterococci bacteria removal

It appears from the literature that the greatest risk related to the presence of antibiotics in the environment is their potential to select for antibiotic resistance among bacteria (Akiyama and Savin, 2010; Novo and Manaia, 2010). Although antibiotics are found in the wastewater effluents at sub-inhibitory levels, relatively low concentrations of antimicrobial agents can still promote bacterial resistance (Castiglioni et al., 2008). It has been reported that more than 70% of bacteria are insensitive against at least one antibiotic (Salvador et al., 2007). Acquisition and further spread of antibiotic resistance determinants among pathogens is becoming one of the most relevant problems for treatment of infectious diseases (Kumarasamy et al., 2010). Hence, controlling antibiotic resistant bacteria in the effluents of municipal wastewater treatment plants (WWTPs) should be a concern in order to help reduce health risks from microbial pathogens during reclaimed water reuse. Studies focusing exclusively on wastewater treatment systems regarding antibiotic resistance are, however, limited.

Enterococci are lactic acid bacteria associated with enteric systems and are relevant indicators of fecal contamination. Given their ubiquity and close contact with humans, enterococci are also considered important vectors of antibiotic resistance (European Antimicrobial Resistance Surveillance System: EARSS). Moreover, these bacteria are implicated in a wide variety of human diseases, with urinary tract infections being the most common while bacteraemia/endocarditis being the most severe (Blanch et al., 2003; Cattoir et al., 2009). These bacteria are released into the environment via wastewater effluents and are often used as indicators of microbial quality in waters. The high persistence of enterococci in the environment initially supported the view that species identification could provide a tool for the determination of faecal pollution sources (Blanch et al., 2003). This study is focused on Enterococci resistant bacteria which have a higher survival rate in the aquatic media and are more resistant in disinfectant conditions than other bacteria (*e.g. E. coli*) (Lanao et al., 2012).

Among the trimethoprim-resistant bacteria, enterococci remain the least studied, probably due to the controversial role of TMP as a therapeutic option (Hamilton-Miller, 1988; Murray, 1989; Coque et al., 1999; Cattoir et al., 2009). In addition, TMP analogs developed in recent years have demonstrated good activity against enterococci. TMP inhibits the enzyme dihydrofolate reductase (DHFR), which catalyses the reduction of dihydrofolate to tetrahydrofolate in prokaryotic and eukaryotic cells (Hitchins, 1973; Cattoir et al., 2009). Several studies have demonstrated that high-level resistance to TMP can be attributed to more than one mechanism of resistance. The most frequent mechanism of resistance to TMP is the production of an additional drug-resistant DHFR (*dfr* gene), often found on mobile genetic elements (*e.g.* plasmids, transposons) (Amyes and Towner, 1990). TMP resistance plasmids have been found in various enterobacteria.

While more than 15 DHFRs conferring high-level resistance to TMP have been identified in gram-negative bacteria, only four are known in gram-positive organisms: (i) S1DHFR encoded by *dfrA* (found in *Staphylococcus aureus*, *Staphylococcus epidermidis*, *Staphylococcus hominis*, and *Staphylococcus haemolyticus*) and (ii) S2DHFR encoded by *dfrD* (found in *Staphylococcus haemolyticus* and, recently, in *Listeria monocytogenes*), (iii) S3DHFR encoded by *dfrG*; and (iv) E1DHFR encoded by *dfrF* (Coque et al., 1999; Cattoir et al., 2009). Some reports showed a bactericidal effect of TMP in combination with sulfamethoxazole against *Enterococcus faecalis* and *Enterococcus casseliflavus* strains (Coque et al., 1999).

Among the quinolone antibiotics, ofloxacin and ciprofloxacin exhibit the greatest intrinsic activity against a variety of Gram-positive bacteria, including staphylococci, enterococci, and various streptococci (Eliopoulos et al., 1996). Ofloxacin is an equimolar ratio of two isomers (racemate mixture); however the high antimicrobial activity of the mixture is attributed to the activity of the S(-)-isomer form (Hayakawa et al., 1986). As a result, S(-)-ofloxacin demonstrates approximately twice the activity of ofloxacin. For this reason, this isomer is independently synthesised (namely levofloxacin) and evaluated for its antibacterial activity (Eliopoulos et al., 1996; Okeri and Arhewoh, 2008).

Fluoroquinolones are known to have two enzyme targets, DNA gyrase and topoisomerase IV, in the bacterial cell; both of these targets are essential for bacterial DNA replication (Hopper, 2000). These drugs appear to antagonize the A subunit of the bacterial enzyme DNA gyrase and thus inhibit DNA replication (Nakanishi et al., 1991). The resistance to the fluoroquinolones likely involves mutations altering the A subunit of DNA gyrase and other processes such as decreased drug permeation (Wolfson and Hooper, 1985; Korten et al., 1994). Additionally, expression or

overexpression of multidrug efflux pumps (which can actively remove antibacterial agents from the organisms' cells) may also contribute to fluoroquinolone resistance in a wide variety of bacterial organisms.

The main bacterial mechanisms of antibiotic resistance described above are illustrated in Schematic 5.3.

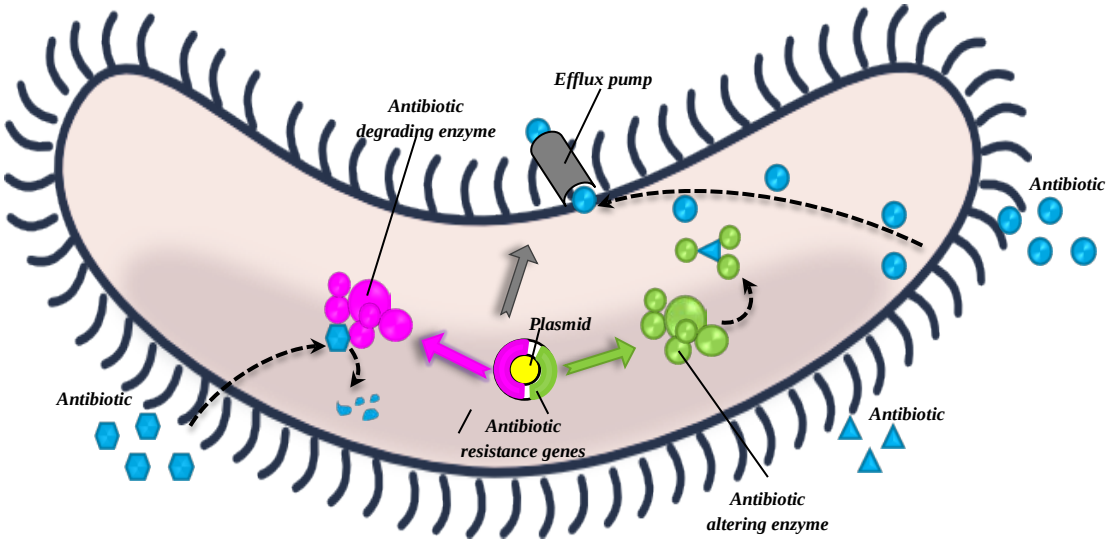

Schematic 5.3 Main bacterial mechanisms of antibiotic resistance.

For each antibiotic, the antibiotic resistance (%) was calculated by directly comparing the counts on the antibiotic plate with the corresponding counts on the plate without antibiotic (eqn. (5.11)).

$$\%\text{Resistance} = \frac{\left(\frac{\text{CFU}}{\text{mL}}\right)_{\text{medium with antibiotic}}}{\left(\frac{\text{CFU}}{\text{mL}}\right)_{\text{medium without antibiotic}}} \times 100 \qquad (5.11)$$

The bacterial removal rate for each treated sample was estimated for each antibiotic as:

$$\%\text{Removal rate} = \left[1 - \frac{\left(\frac{\text{CFU}}{\text{mL}}\right)_{\text{in treated sample}}}{\left(\frac{\text{CFU}}{\text{mL}}\right)_{\text{in raw wastewater}}}\right] \times 100 \qquad (5.12)$$

The average bacterial density of enterococci in the examined samples expressed in CFU mL^{-1} against the treatment time is shown in Figure 5.17 whereas Figure 5.18 depicts the average resistance percentage profile during the process. It was observed that enterococci presented significantly lower counts in the solar Fenton treated samples compared to the untreated wastewater effluent sample. The average of enterococci population in the initial wastewater sample was 2.53×10^{3} whereas the bacteria population was completely eliminated at the end of the treatment (t_{exp}=180 min). Comparing the resistance rates for the two antibiotics tested, it was observed that OFX resistance was almost double of that of TMP. This is in agreement with previous studies which report high quinolone resistance in the species *Enterococcus faecium* and *E. faecalis*; the most frequent species of enterococci in wastewaters (Ferreira da Silva et al., 2006). However, irrespective of the initial resistance rates, the antibiotic resistant enterococci were eliminated at the end of the process.

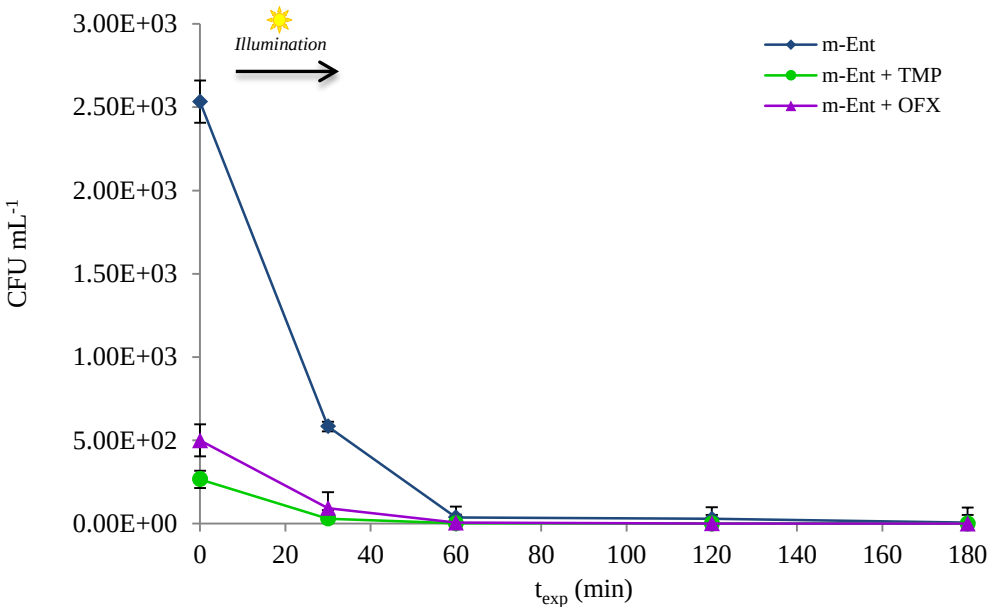

Figure 5.17 Number of enterococci (bacterial density expressed as CFU mL^{-1}) present in the solar Fenton treated samples.

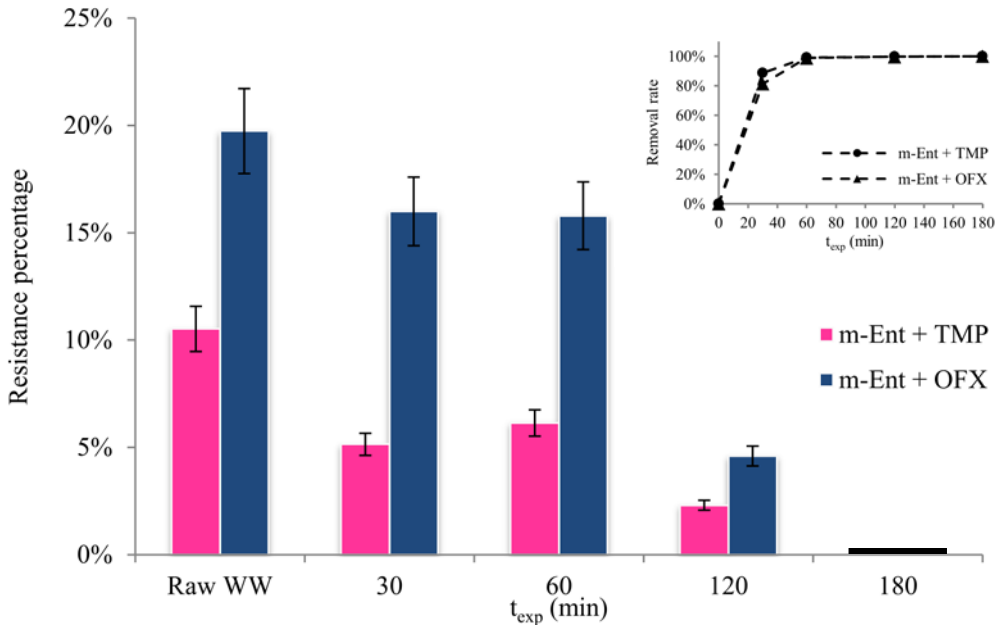

Figure 5.18 Antibiotic resistance evolution during the solar Fenton process (Inset graph: Removal rate against treatment time).

The need for acidic pH (pH ≈ 2.8-2.9) during the Fenton process, receives in general a strong criticism. At pH around 3 though, most microorganisms are inactivated (Malato et al., 2009). Moreover, hydrogen peroxide and iron can migrate inside the bacteria cells and cause damage to cell functions by catalysing the production of reactive oxygen radicals (Keyer and Imlay, 1996). Additionally, the synergistic effect of hydrogen peroxide and solar photons leads to the inactivation and death of bacteria.

Recent studies investigated the efficiency of the conventional wastewater treatment plants on removing antibiotic resistant bacteria (Akiyama and Savin, 2010; Luczkiewicz et al., 2010; Manaia et al., 2010; Novo and Manaia, 2010). Generally, it was observed that the microbiological quality of the treated effluent, in terms of predictability of the antibiotic resistance rates and homogeneity of the removal of organisms belonging to different resistance groups is strongly influenced by the treatment process (*i.e.* activated sludge) and the operating conditions. Moreover, studies on the effect of chlorination on antibiotic resistant bacteria have shown to be conflicting; few studies have inspected the regrowth or reactivation of antibiotic resistant bacteria after chlorination in wastewater (Huang et al., 2011). Studies on the effect of chlorination on antibiotic resistant bacteria can be traced back to 1970s, where chlorination was shown to influence the proportion of multiple-antibiotic resistant bacteria in drinking water and wastewater (Grabow and van Zyl, 1976; Armstrong et al., 1982).

It should be noted that the studies conducted so far in the area of advanced wastewater treatment dealt with the disinfection efficiency and not with the removal of the antibiotic resistant bacteria. Vidal et al. (1999) published the first pilot plant study about TiO_2 solar photocatalysis for water disinfection. This group evaluated the performance of a low-cost compound parabolic concentrator (CPC) prototype built along this work and explored the feasibility of this concept as the basis for the solar photocatalytic oxidation facilities of water supplies. The results obtained for *Escherichia coli* and *Enterococcus faecalis* (initial concentration ~10^2-10^4 CFU mL^{-1}), with TiO_2 photocatalysis ([TiO_2]=0.5 g L^{-1}), showed a 5-log decrease after 30 min of solar irradiation. The feasibility of using TiO_2 solar photocatalysis to disinfect water supplies was also investigated by Fernández et al. (2005). This study reviewed

the viability of solar photocatalysis for disinfection in low cost compound parabolic collectors, using sunlight and TiO_2 semiconductor, both applied as slurry and supported. It was found that the total deactivation of *Escherichia coli* is attributed to the combined effect of sunlight and the oxidant species generated in the TiO_2 in suspensions and or by supported TiO_2. However, while sunlight deactivates *Escherichia coli*, bacteria can still be detected.

Over the past several years, there has been a growing interest in the application of solar Fenton for water disinfection, with *Escherichia coli* being the most widely investigated bacterium. Pulgarin and co-workers (2005) showed that the inactivation of *Escherichia coli* under sunlight could be enhanced by adding Fe^{2+} or Fe^{3+} and H_2O_2. They also showed that some organic and inorganic molecules in the water matrix were responsible for the reduced disinfection efficiency of photo-Fenton (Rincón and Pulgarin, 2006). Spuhler et al. (2010) proved that solar photo-Fenton system at low concentrations of reagents (0.6 mg L^{-1} of Fe^{2+}, 10 mg L^{-1} H_2O_2) and at near neutral pH was efficient for *Escherichia coli* bacterial inactivation.

5.2.6 Economic estimation for the photocatalytic process

There is limited literature (Hernández-Sancho et al., 2010; Jordá et al., 2011) dealing with wastewater treatment process economics although this aspect is very important issue. Furthermore, there are hardly any exhaustive reports which address the issue of economic feasibility of the use of advanced oxidation for wastewater treatment on industrial scale (Mahamuni and Adewuyi, 2010).

Based on the experimental and operational data recorded during the operational period of the solar pilot plant unit and the basic design parameters applied, a scale up

extrapolation was carried out. The aim of this task was to establish the overall cost for a full scale installation operating for a period of 5 years. For this purpose, a simple methodology was developed based on the investment cost estimation along with the operational (including mainly electric power and consumables) and the maintenance cost.

In order to estimate the cost of the full scale treatment plant the following were considered:

- The advanced oxidation treatment aims at the degradation of OFX and TMP.
- The hydraulic capacity of the scale up unit is based on an expected effluent flow from a sewage treatment plant serving a community of 1000 PE. This is based on the water consumption of 150 L per person per day meaning a total of 150 m^3 day^{-1}.
- The operating daily time is 10 h. This was based on the findings from the operation of the existing pilot unit.
- The extrapolation to full scale plant is based on the specific flow rate of 250 L h^{-1} that was considered as the optimum flow rate for the operation of the existing pilot unit.

5.2.6.1 System sizing

In order to estimate the cost for the full scale plant, the system sizing was determined. The main parts are given below:

- Storage tank volume: The storage tank was calculated based on the total maximum daily flow (150 m^3 day^{-1}) delivered by the WWTP of 1000 PE capacity. The treatment unit will be operated for a period of 10 h per day. This implies that

over a period of 14 h the storage tank needs to have adequate storage volume. Based on the theoretical average flow of 6.25 $m^3 h^{-1}$ the storage tank volume must be 87.5 m^3. A safety factor of 1.2 was introduced to give a total net volume of 105 m^3.

- Air blower: The air requirements for mixing are calculated on the basis of 1 $m^3 h^{-1}$ of air per m^3 of effluent volume stored in the buffer tank. The maximum storage capacity of the storage tank is 105 m^3 requiring a total air flow of 105 $m^3 h^{-1}$. An air blower with nominal power of 2.2 kW and absorbed power of 1.6 kW is able to deliver the above air flow at a back pressure of 350 mbar that is adequate for a storage tank with 3.0 m max water level. This air flow rate is adequate to ensure a dissolved oxygen level above 2 mg L^{-1} that is the minimum required.

- Feed pump: The feed rate was calculated on the basis of the total maximum daily flow delivered by the WWTP, which is 150 m^3 and the operating time of the treatment unit. A feed pump with a nominal power of 1.1 kW and absorbed power of 1.0 kW is able to deliver 15 $m^3 h^{-1}$ at 1.5 bar pressure that is adequate to overcome head losses in the network piping and the CPCs assemblies.

- Chemical dosing systems: The sizing of the different dosing systems was based on the required chemicals concentrations and the feed rate to the treatment unit. Chemicals' concentrations are relatively low and standard diaphragm type dosing pumps of 0.08 kW can easily satisfy the dosing rates required. A total of three dosing pumps are required.

- CPCs: The sizing of the solar collectors is based on the empirical data collected during the operation of the pilot plant unit. The existing CPCs assembly was operated at a flow rate of 600 L h^{-1}. The same assembly can be used in multiples

to satisfy the total flow rate of a full scale plant. Based on a feed flow rate of 15 $m^3 h^{-1}$ for the full scale plant and the above specific flow rate per assembly, a total of 25 CPC assemblies connected in series are required.

5.2.6.2 Investment, operation and maintenance cost estimation

The investment cost of a full scale unit for the treatment of 150 m^3 day^{-1} secondary wastewater effluent is illustrated in Table 5.6.

Table 5.6 Investment cost estimation based on 2012 prices.

Item	Units	Unit cost (€)	Total cost (€)
Air blower balance tank	1	4.250,00	4.250,00
Air diffusion system	1	3.500,00	3.500,00
Feed pumps	2	1.450,00	2.900,00
Level sensor in balance tank	1	750,00	750,00
$FeSO_4.7H_2O$ dosing system	1	3.200,00	3.200,00
H_2O_2 dosing system	1	3.200,00	3.200,00
H_2SO_4 dosing system	1	3.500,00	3.500,00
pH sensor/controller	1	4.200,00	4.200,00
H_2O_2 sensor/controller	1	4.800,00	4.800,00
DO sensor controller	1	4.250,00	4.250,00
UV sensor	1	2.800,00	2.800,00
Electromagnetic flow meter-Feed line	1	3.500,00	3.500,00
Electromagnetic flow meter-Return line	1	3.500,00	3.500,00
CPCs assemblies	25	5.500,00	137.500,00
Interconnection piping	1	5.000,00	5.000,00
Electrical control panel	1	8.500,00	8.500,00
Mechanical installations	1	3.600,00	3.600,00
Electrical installations	1	2.000,00	2.000,00
Testing and commissioning	1	1.200,00	1.200,00
Operating and maintenance manuals	1	500,00	500,00

	Total cost	**202.650,00 €**

Energy consumption estimation (kWh) was based on the electrical power consumption (kW) (mainly pumping) multiplied by the unit operating time (in hours). Table 5.7 presents the calculations made giving a total energy consumption of 44.86 kWh.

Table 5.7 Electric power cost estimation.

Item	**Absorbed power (kW)**	**Operating time (h)**	**Power consumption (kWh)**
Air blower balance tank	1.56	16.00	24.96
Feed pumps	1.00	10.00	10.00
$FeSO_4.7H_2O$ dosing system	0.33	10.00	3.30
H_2O_2 dosing system	0.33	10.00	3.30
H_2SO_4 dosing system	0.33	10.00	3.30
	Total power consumption		**44.86**

Based on the above data, the specific power consumption per m^3 of treated wastewater is 0.23 kWh per m^3. With an average cost of 0.17 € per kWh, the cost per m^3 is 0.039 € m^{-3} or 5.86 € day^{-1} for the total flow of 150 m^3. The projected power consumption cost is 2.140,70 € $year^{-1}$ or 10.703,50 € for 5 years.

The per day cost of the chemicals (H_2O_2, $FeSO_4.7H_2O$, H_2SO_4) are depicted in Table 5.8. It is worth noting the fact that hydrogen peroxide consumption is one of the most important factors accounting for the reagents cost of the solar Fenton process.

Table 5.8 Reagents cost estimation.

Chemical	Dose	Cost per day (€ day^{-1})
$FeSO_4.7H_2O$	5 mg L^{-1}	0.338
H_2O_2 (30%, w/w)	75 mg L^{-1}	13.5
H_2SO_4	25 mL	1.5

The maintenance cost (inspection, replacement and repair) were estimated as a percentage of the total investment cost. For this type of plants 1.5% of the initial investment cost per annum can be considered representative. This approach gives an annual maintenance cost of 3.039,75 € or 15.198,75 € over the period of 5 years.

The total cost of the full scale unit for the treatment of 150 m^3 day^{-1} secondary wastewater effluent is summarized in Table 5.9 and it was found to be 0.85 € m^{-3}. This value is in agreement with a previous study of the photo-Fenton process in a pilot-scale set-up (Jordá et al., 2011).

Table 5.9 Total cost estimation for 5 years operational period.

Expense	Cost (€)
Total investment	202.650,00
Electric power	10.703,50
Chemicals	27991,85
Maintenance and repairs	15.198,75
Total ownership cost for 5 years	**231.552,25**

DOC removal was lower in the case of SW compared to DW, which can be attributed to the presence of inorganic anions which may act as scavengers of the HO•. Furthermore, the presence of higher organic and salt content in SWW and RE led to lower mineralization per dose of hydrogen peroxide compared to DW and SW. Toxicity evolution is attributed to the compounds present in RE and their by-products formed during solar Fenton treatment and not to the intermediates formed by the oxidation of the parent antibiotics. Solar Fenton process was proved to be an efficient method for the elimination of these antibiotics at concentration level of $\mu g\ L^{-1}$ with relatively high degradation rates. A modification of the first-order kinetic expression was proposed and has been successfully applied to explain the degradation kinetics of the compounds during the solar Fenton treatment. The results demonstrated the capacity of the solar Fenton process to reduce the initial toxicity against the examined plant species (Sorghum saccharatum, Lepidium sativum, Sinapis alba) and the water flea Daphnia magna. Enterococci, including those resistant to OFX and TMP, were completely eliminated at the end of the treatment. Solar Fenton was proved to be an efficient and cost effective method considering the requirement for safe wastewater reuse for agriculture irrigation purposes.

CHAPTER 6: CHARACTERIZATION OF TRANSFORMATION PRODUCTS BY UPLC-TOF-MS/MS

A variety of photodegradation by-products are formed during the solar Fenton process; however, very often not much attention is paid to the possible formation of these by-products which, would allow the degradation process to be better understood and evaluated. The identification of transformation products and the elucidation of photocatalysis-reaction pathways are important in optimizing the overall process efficiency, as they are very often related to toxicity and biodegradability evolution (Amat et al., 2009). Transformation products (TPs) generated during the pilot-scale solar Fenton treatment of TMP were elucidated and the possible influence of the water-matrix composition on the degradation pathway was determined.

Identification of all the TPs present in the treated samples is a difficult task especially because of the differences in concentration at which they are generated and extracted by the SPE method used. This task represents a particular analytical challenge because the TPs formed are new chemical entities, for which standards are not available. Thus, analytical methods that combine high separation efficiency with a maximum of structural information are required. Recent advances in mass spectrometric instrumentation have provided the environmental scientists with highly valuable tools to gain deeper insight into transformation processes of pharmaceutical compounds present in environmental matrices (Pérez et al., 2007).

Ultra performance liquid chromatography interfaced with time-of-flight tandem mass spectrometry (UPLC-ToF-MS/MS) technology was adopted to detect the possible degradation transformation products formed during the solar Fenton reactions. This method permits the acquisition of full-scan product ion spectra, with the accurate

mass of the product ions, thus yielding results of much higher degree of certainty making it useful for structure elucidation of unknown compounds, as well as for identifying target compounds (Lambropoulou et al., 2011). The approach to identify TPs using the above analytical technique was by screening the total ion chromatogram (TIC), acquired in full-scan mode and then selecting a specific protonated molecule for further product ion scans. The MS^2 experiments improved the selectivity of the analyses, providing the structural information together with accurate mass measurements of product ions, providing thus precision in the low ppm range (Reemtsma, 2003). The analyses were performed under the conditions described in the experimental section 2.3.4 (CHAPTER 2). With the objective of exploring the TPs of the examined antibiotics, a relatively low amount of H_2O_2 (2.5 mg L^{-1} in doses) was used in the photocatalytic experiments, which enabled obtaining slow kinetics and provided favourable conditions for the determination of TPs.

The degradation pathways and the production of intermediates depend on the type of advanced treatment applied, even though the processes are driven by the same reactive species, which are mainly hydroxyl radicals. The degradation pathway is of course related to the specific structure characteristics of the examined compound (Fatta-Kassinos et al., 2011b). In the case of aromatic pollutants, the degradation mainly involves the: (i) hydroxylation of the organic π-system by an electrophilic attack from hydroxyl radicals; (ii) demethylation-hydroxylation; and (iii) cleavage on α-position from the aromatic moiety and ring opening (Legrini et al., 1993).

6.1 Evolution profile of the main TPs formed during the TMP solar Fenton treatment

As many as 21 compounds were tentatively identified as TPs formed during the solar Fenton treatment of TMP (*m/z* 291; $C_{14}H_{19}N_4O_3$). The structure elucidation relied on proposing elemental compositions for the ion masses obtained by accurate mass measurements along with interpretation of the fragmentation pathways deduced from the product ion spectra. The low errors reported (below 5 ppm) guarantee the correct assignation of the ion elemental composition of the ions in all the cases.

Figure 6.1 depicts the chromatographic peak of TMP at t_R = 2.40 min that exhibited a molecular ion peak at *m/z* 291. The collision-induced-dissociation experiments with TMP (molecular ion $[M + H]^+$ 291) revealed the formation of only two fragment ions at *m/z* 261 and 230, as a consequence of the loss of two methylene groups and one $-C_2H_5O_2$ group, respectively.

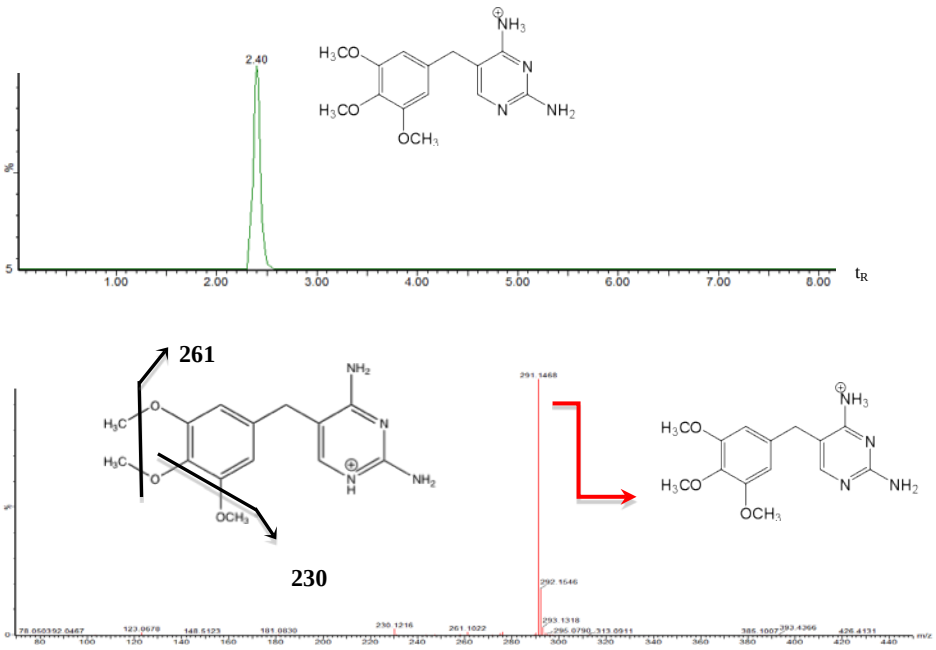

Figure 6.1 Extracted ion chromatograph (XIC) and mass spectra of a standard solution of TMP (10 mg L^{-1}).

The analyses generated a large amount of information which is recorded in Table 6.1. Table 6.1 illustrates summary data related to the experimental and calculated masses of the protonated ion, the error between them, the double-bond equivalents (DBE) and the proposed empirical formula corresponding to the compounds identified. Possible elemental compositions, based on accurate mass, were calculated using the elemental composition calculator embedded into the MassLynx^{TM} software. The aforementioned data were obtained under optimized conditions of collision energy and cone voltage of the ToF mass spectrometer.

The 21 photoproducts generated distinct sets of fragment ions which allowed pinpointing the site of modification among the two TMP substructures; 1,2,3-trimethoxybenzene and 2,4-diaminopyrimidine.

Table 6.1 Accurate mass measurement of product ions of TMP and its photo transformation products (TPs) as determined by UPLC-ToF-MS/MS.

Compound	**t_R(min)**	**Elemental Formula**	**Mass (*m/z*)**		**Error**			**Water matrix**
			Theoretical	Experimental	mDa	ppm	DBE (*)	
TMP	2.40	$C_{14}H_{19}N_4O_3$	291.1468	291.1457	1.1	3.8	7.5	DW, SW, RE, SWW
		$C_{12}H_{13}N_4O_3$	261.0878	261.0883	2.5	5.2	8.5	
		$C_{12}H_{14}N_4O$	230.1198	230.1216	1.5	4	7.5	
P1	3.17	$C_{14}H_{17}N_4O_4$	305.1260	305.1250	1.0	3.3	8.5	DW, SW, RE, SWW
		$C_{13}H_{13}N_4O_4$	289.0937	289.0933	-0.7	1.2	9.5	
P2	1.76	$C_{13}H_{15}N_4O_5$	307.1051	307.1042	0.9	2.9	8.5	DW, SW, RE, SWW
		$C_{14}H_{17}N_4O_3$	289.1102	289.1100	1.9	4	8.5	
		$C_{12}H_{11}N_4O_3$	259.0845	259.0845	2.4	4.1	9.5	
P3	2.52	$C_{13}H_{15}N_4O_4$	307.1417	307.1042	1.5	3.5	8.5	DW, SW, RE, SWW
		$C_{12}H_{13}N_4O_3$	277.0821	277.0817	0.7	2.8	8.5	
		$C_5H_7N_4$	123.0578	123.0574	-1.4	0.8	4.5	
P4	2.15	$C_{14}H_{21}N_4O_5$	325.1513	325.1512	0.1	0.3	6.5	DW, SW, RE, SWW
		$C_{10}H_{13}O_3$	181.0858	181.0865	-0.3	1.6	4.5	
P5	3.14	$C_{14}H_{19}N_4O_5$	323.1367	323.1355	1.2	3.7	7.5	DW, SW, RE, SWW
		$C_{14}H_{17}N_4O_4$	305.1138	305.1134	2.2	4.0	8.5	
		$C_{11}H_{13}N_4O_3$	249.0967	249.0965	0.9	3.3	7.5	
P6	2.01	$C_{14}H_{19}N_4O_5$	323.1367	323.1354	-1.5	0.1	7.5	DW, SW, RE, SWW
		$C_{14}H_{17}N_4O_4$	305.1138	305.1125	0.3	2.5	8.5	
		$C_{13}H_{15}N_4O_4$	291.1126	291.1118	-4	-2.5	7.5	
		$C_{11}H_{13}N_4O_3$	249.0967	249.0966	1.6	-0.5	7.5	
P7	3.04	$C_{14}H_{19}N_4O_5$	323.1367	323.1355	-1.5	-0.4	7.5	DW, SW,

								RE, SWW
P8	0.87	$C_{13}H_{15}N_4O_5$	307.1059	307.1042	1.7	5.5	8.5	DW, SW, RE, SWW
		$C_{10}H_9N_4O_3$	233.0656	233.06565	-0.2	2.4	8.5	
P9	1.57	$C_{13}H_{15}N_4O_5$	307.1060	307.1042	1.8	5.9	8.5	DW, SW, RE, SWW
P10	1.87	$C_{13}H_{17}N_4O_5$	309.1199	309.1199	0.0	0.0	7.5	DW, SW, RE, SWW
		$C_{11}H_{15}N_4O_4$	267.1086	267.1085	-0.9	1.3	6.5	
P11	2.52	$C_{13}H_{17}N_4O_5$	308.1461	308.1453	0.1	2.3	7.5	DW, SW, RE, SWW
P12	1.16	$C_{14}H_{19}N_4O_7$	355.1268	355.1254	1.4	3.9	7.5	DW, SW, RE, SWW
		$C_{14}H_{19}N_4O_6$	339.1270	339.1263	0.1	2.4	7.5	
P13	1.34	$C_{14}H_{19}N_4O_7$	355.1268	355.1265	0.1	2.7	7.5	DW, SW, RE, SWW
P14	2.01	$C_{14}H_{19}N_4O_7$	355.1268	355.1267	-0.8	1.5	7.5	DW, SW, RE, SWW
		$C_{14}H_{19}N_4O_6$	339.1270	339.1255	-2.3	0.1	7.5	
P15	1.47	$C_{13}H_{19}N_4O_5$	311.1347	311.1355	-0.8	-2.6	6.5	DW, SW, RE, SWW
		$C_{13}H_{19}N_4O_3$	279.0558	279.0773	-5.8	-2.4	6.5	
		$C_{11}H_{15}N_4O_3$	251.0618	251.0664	-4.7	-1.6	4.5	
P16	0.75	$C_{13}H_{19}N_4O_5$	311.1071	311.1355	-28.4	-91.3	6.5	DW, SW, RE, SWW
P17	1.81	$C_{13}H_{19}N_4O_4$	295.1396	295.1406	-1.0	-3.4	6.5	DW, SW, RE, SWW
		$C_5H_7N_4O_2$	155.0435	155.0433	0.4	2.3	4.5	
P18	1.03	$C_{12}H_{13}N_4O_4$	277.0835	277.0833	-1.5	0.32	8.5	DW, SW, RE, SWW
		$C_{12}H_{11}N_4O_3$	259.0789	259.0788	-3.5	-0.8	9.5	
P19	0.92	$C_{12}H_{13}N_4O_4$	277.0835	277.0829	-6.7	-3.8	8.5	DW, SW, RE, SWW
P20	0.47	$C_5H_7N_4O$	139.0621	139.0620	0.1	0.7	4.5	DW, SW, RE, SWW
		$C_2H_4N_3O$	86.0344	86.0341	2.4	3.8	2.5	
P21	0.35	$C_5H_7N_4O_2$	155.0578	155.0570	3.5	5.2	4.5	DW, SW, RE, SWW
		$C_5H_5N_4O$	137.0460	137.0464	-0.7	1.2	5.5	
(*) DBE=Double Bond Equivalent								

At this point, it is worth noting that not only the relative mass errors served as a criterion in proposing the most likely elemental composition, but calculation of the corresponding double-bond equivalents (DBE) afforded a straightforward means of confirming the empirical formula.

On the basis of the results presented herein and previous studies on the TMP photooxidation (Luo et al., 2012; Sirtori et al., 2010), biodegradation (Eichhorn et al., 2005) and metabolism of TMP (Klooster et al., 1992; Bergh and Breytenbach, 1990; Nordholm and Dalgaard, 1984), three competitive pathways are suggested (Schematic 6.1), in which hydroxylation, demethylation, cleavage of TMP molecule, and oxidation of hydroxyl groups are described as major transformation steps. It should be noted that in the four examined matrices (DW, SW, SWW and RE), TMP

undergoes the same hydroxylation, demethylation and cleavage reactions generating the same intermediates; however, some important differences in the pathway mechanism were observed and these are discussed further below.

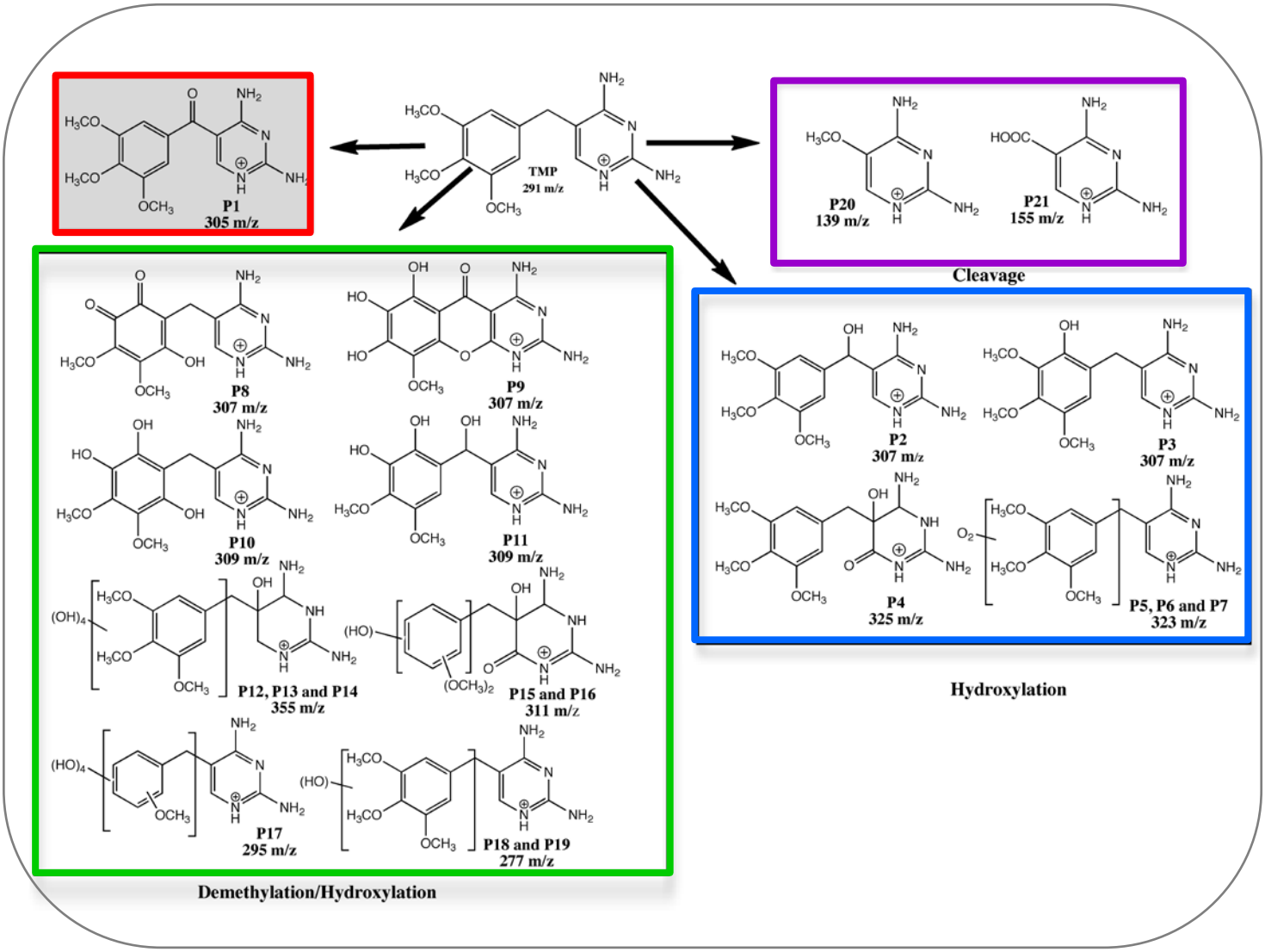

Schematic 6.1 Photodegradation products identified during solar Fenton treatment of TMP in four environmental matrices (DW, SW, SWW and RE): Structures and *m/z* of protonated ions.

The primary product (**P1**) was identified as trimethoxybenzoylpyrimidine (*m/z* 305; $C_{14}H_{17}N_4O_4$, protonated molecule), which appeared during the first stage (0-4.8 mg L^{-1} H_2O_2), and was regarded as the promoter of a series of photoreactions involving hydroxyl radicals. These reactions included hydroxylation, demethylation and finally cleavage of the TMP molecule as shown in Schematic 6.2.

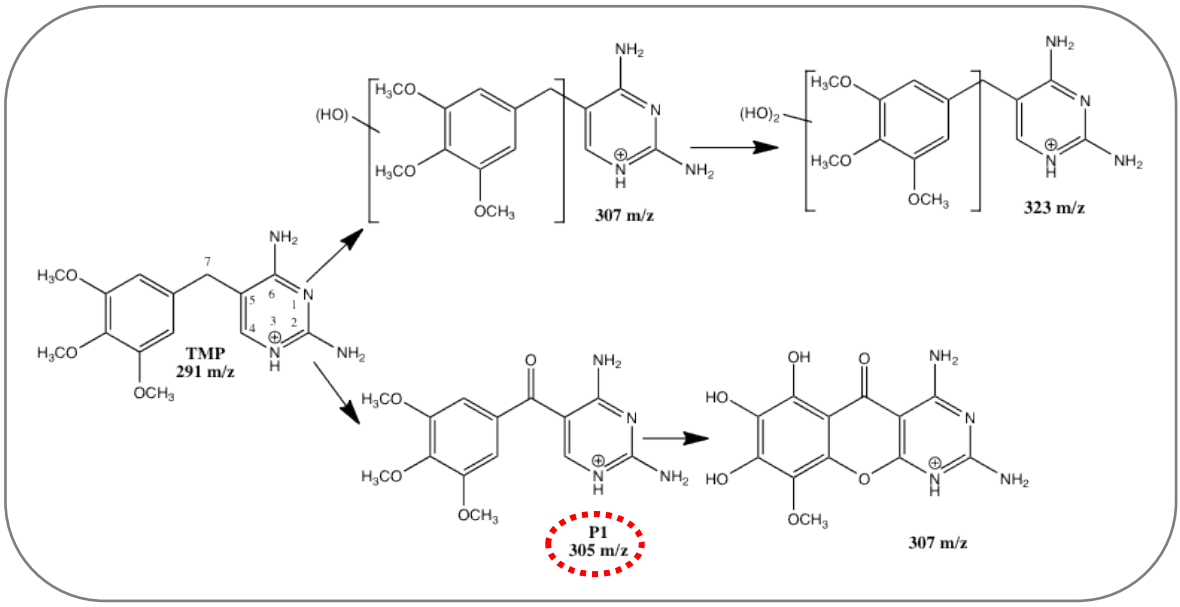

Schematic 6.2 Proposed degradation pathway for the oxidation of TMP (**P1**: promoter product).

Hydroxylation reactions resulted in polyhydroxylated compounds with the general formula $C_{14}H_{19}N_4O_{3+x}$, for the protonated ion, with x varying from 1 to 4. As hydroxyl radicals do not exhibit a high degree of selectivity towards various functional groups, several isobaric compounds, corresponding to positional isomers, were detected. Two separate monohydroxylated (x=1) products (**P2**, **P3**) were observed, corresponding to the addition of 16 mass units to the TMP molecule (*m/z* 307; $C_{14}H_{19}N_4O_4$).

The formation mechanism of **P2** has recently been proposed by Luo et al. (2012). Hydrogen abstraction is the pathway for hydroxyl radicals' reaction with -CH_2- groups resulting in a carbon-centered radical, followed by reaction with O_2 to form peroxyl radicals (eqn. (6.1)). These peroxyl radicals are relatively unreactive, and usually decay via bimolecular self-termination reactions to form tetroxide species (eqn. (6.2)) which then undergo unimolecular decomposition to form an alcohol (**P2**) and a ketone (eqn. (6.3)). The structure of **P2** has previously been proposed by Eichhorn et al. (2005).

$$R_1R_2CH^{\bullet} + O_2 \rightarrow R_1R_2CHO_2^{\bullet} \quad (6.1)$$

$$2\ R_1R_2CHO_2^{\bullet} \rightarrow R_1R_2CHO{-}O{-}O{-}OHCR_2R_1 \quad (6.2)$$

$$R_1R_2CHO{-}O{-}O{-}OHCR_2R_1 \rightarrow R_1R_2C{=}O + R_1R_2CHOH + O_2 \quad (6.3)$$

The electrophilic addition of the hydroxyl radical to the aromatic ring forms a resonance-stabilized carbon-centered radical, with subsequent addition of oxygen and elimination of a hydroperoxyl radical yielding the phenolic product **P3** (Song et al., 2008, 2008b).

Furthermore, three dihydroxylated (x=2) isomer products (**P5**, **P6**, **P7**) corresponding to the addition of 32 mass units to the TMP molecule (*m/z* 323; $C_{14}H_{19}N_4O_5$) were identified as a result of further oxidation with the above primary phenolic degradation product (**P3**).

P4 (*m/z* 325; $C_{14}H_{19}N_4O_7$) was also formed. **P4** molecular composition indicates that one oxygen atom was introduced into TMP molecule by forming a keto-derivative. **P4** has previously been reported as a degradation product of TMP in nitrifying activated sludge (Eichhorn et al., 2005).

In parallel with hydroxylation, demethylation reactions were also demonstrated by the presence of protonated ions with the general formula $C_{14-y}H_{19-2y}N_4O_{3+x}$, with y varying from 1 to 3. **P8** and **P9** degradation products (*m/z* 307; $C_{13}H_{17}N_4O_5$) are the major products during hydroxylation-demethylation mechanism. The degradation product **P8** resulted from the addition of two hydroxyl radicals on the aromatic ring and then by a further oxidation of the two alcohol groups forming a keto-derivative. The DBE value (DBE=7.5) is in line with the formation of two ketones in the **P8** product. **P9** is a result of an intramolecular bond which undergoes spontaneous cyclization to the benzooxazole derivatives from the promoter product **P1**.

Figure 6.2 shows the total ion chromatograph (TIC) for the sample taken after 2.4 mg L^{-1} H_2O_2 consumption during the solar Fenton treatment at various cone voltages (CV) and collision voltages (CE).

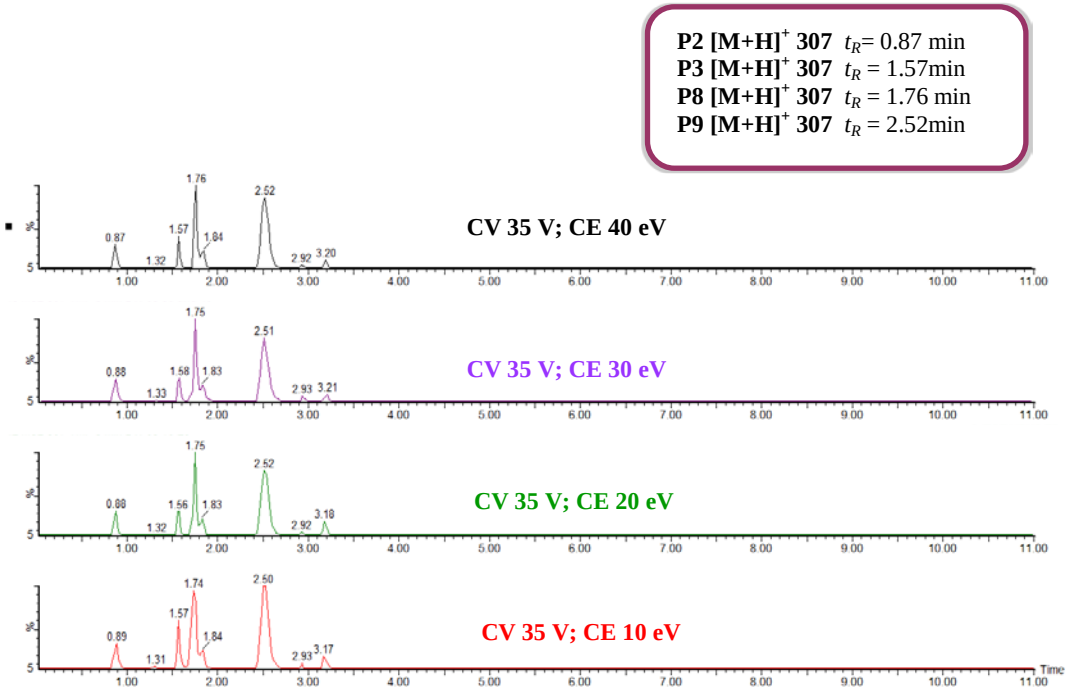

Figure 6.2 Total ion chromatograph (TIC) of **P2**, **P3**, **P8** and **P9** at 2.4 mg L^{-1} H_2O_2 consumption.

Based on the interpretation of the fragmentation patterns and the accurate mass data as listed in Table 6.1, the proposed structures of the **P3** fragmentation ions are compiled in Figure 6.3.

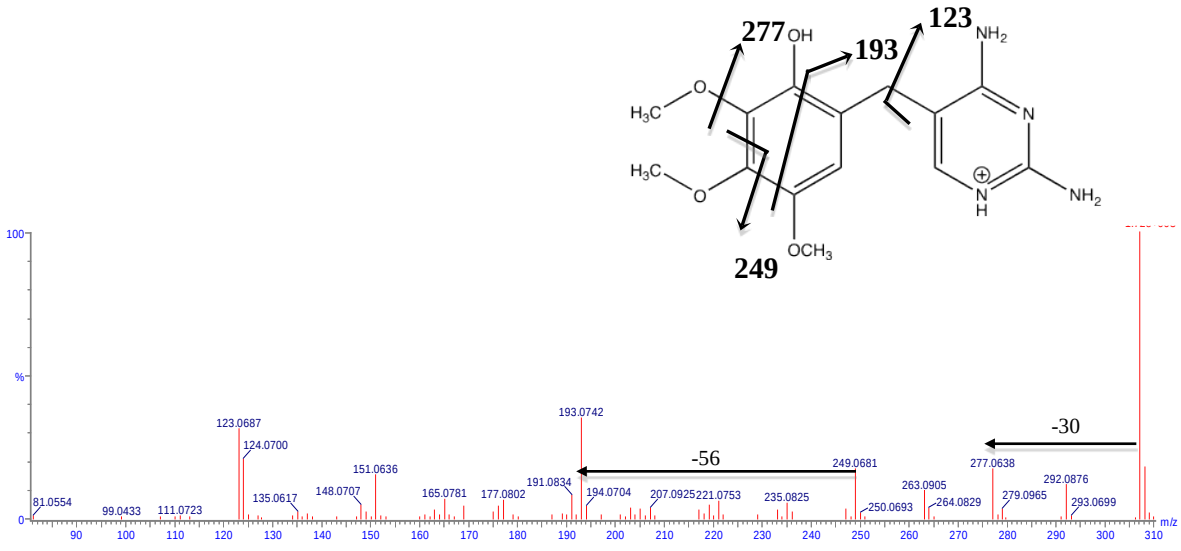

Figure 6.3 (+)ESI-QqToF-MS^2 spectra of photodegradation product **P3**.

As regards **P3**, which is 16 Da more than the parent compound (one OH according to Table 6.1), the sequence of neutral losses becomes -30 Da / -56 Da, eventually leading to the fragment ion *m/z* 277 and *m/z* 249, respectively; therewith demonstrating again that the central 2,4-diaminopyrimidine ring remained intact. The loss of 28 Da from *m/z* 277, typical for the elimination of CO, led to the appearance of the mass ion *m/z* 249, which with further loss of CO group resulted in the *m/z* 193 fragment ion. Moreover, the photoproduct *m/z* 307 at the same time generated the fragmentation products at *m/z* 123 (–$C_8H_8O_4$ loss).

Subsequent hydroxyl radical attack could lead either to the formation of mono- (**P18** and **P19**, *m/z* 277), bi- (**P15** and **P16**, *m/z* 311; Figure 6.4), tri- (**P10** and **P11**, *m/z* 309), tetra- (**P17**, *m/z* 295) and penta-hydroxylated (**P12**, **P13** and **P15**, *m/z* 355) products. As it is shown, several isobaric compounds, corresponding to positional

isomers, were detected. However, differentiation of positional isomers was not always feasible by UPLC–ToF–MS. The product with *m/z* 277 is attributed to *ipso* attack of the hydroxyl radical at a methoxy position resulting in a phenol.

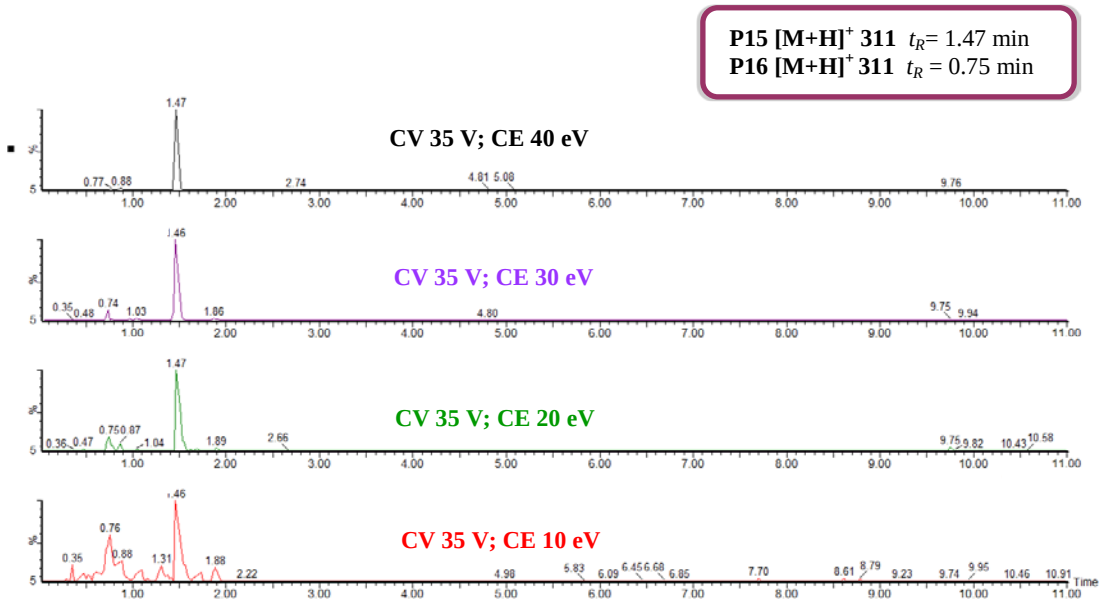

Figure 6.4 Total ion chromatograph (TIC) of **P15** at 2.4 mg L^{-1} H_2O_2 consumption.

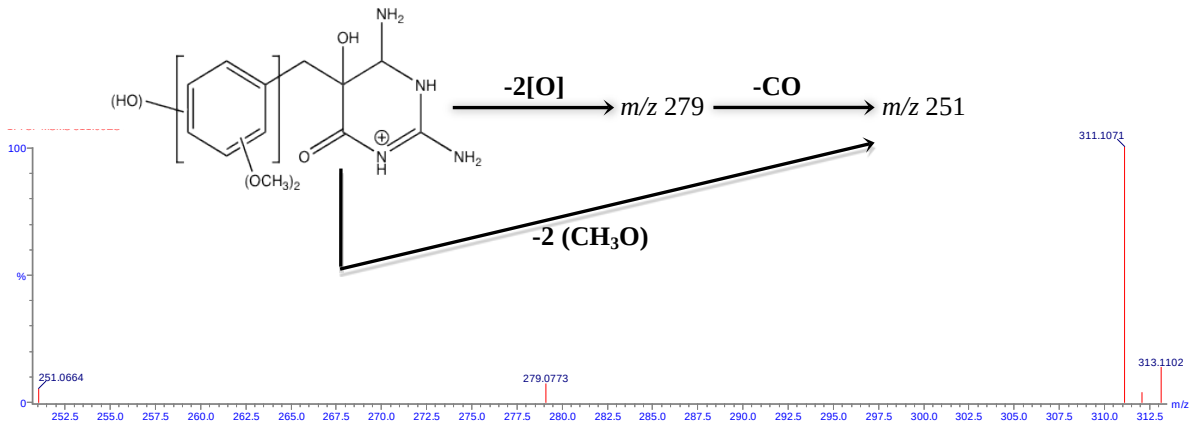

Figure 6.5 (+)ESI-QqToF-MS^2 spectra of photodegradation product **P15**.

The structure ($C_{13}H_{19}N_4O_5^+$) of **P15** was confirmed by the appearance of two characteristic fragments. The loss of 32 Da, typical for the elimination of –2[O], led to

the appearance of the mass ion at *m/z* 279, which with further loss of CO group resulted in the *m/z* 251 fragment ion. The second one possibly derived from the loss of 2[-CH_2O] group from the molecular ion at *m/z* 311.

It should be noted that most of the photoproducts generated during photocatalysis maintained the two-ring TMP structure and major changes occurred in the trimethoxybenzyl moiety. These TPs undergo the same mechanism, via hydroxylation, oxidation, demethylation and decarboxylation and finally are transformed to lower molecular weight products before mineralization. In addition to the assigned product ions encompassing both aromatic rings, two further fragment ions, $C_5H_7N_4O$ (**P20**; *m/z* 139) and $C_5H_7N_4O_2$ (**P21**; *m/z* 155) were observed arising from the cleavage of the protonated molecule at either side of the central methylene group (C7 atom; see Schematic 6.2 for atom numbering). These TPs were present at a higher concentration level at the end of the experiments. All the above described intermediates were further transformed by an oxidative opening of the aromatic ring, giving rise to the formation of smaller and more oxidized molecules, such as short carboxylic acids (*e.g.* formic, acetic, oxalic; these acids, particularly C2 and C3-acids, are very important intermediates as they provide evidence for the oxidative ring opening). The evolution of carboxylic acids was described in the previous chapter.

6.2 TPs evolution in four different water matrices

The formation of TPs expressed as the relative intensity of TPs measured by integration of LC-MS peaks of the corresponding TPs against the peroxide consumption are depicted in Figures 6.6-6.9.

P4, **P5** and **P6** may be proposed as the main TPs during the first stages of photocatalytic process in DW (Figure 6.6 (a)). All the TPs derived from the hydroxylation (**P2-P7**) and demethylation-hydroxylation (**P8-P19**) reactions as well as the promoter product **P1** disappeared at 7.2 mg L^{-1} of peroxide consumption. At this concentration level, cleavage products were detected at the maximum concentration (Figure 6.6 (c)) and disappeared when the consumption of peroxide was equal to 12 mg L^{-1}. It should be noted that the incomplete mineralization of TMP in DW experiments is attributed to the formation of carboxylic acids.

During photodegradation of TMP in SW, TMP undergoes the same degradation pathway reactions as already discussed in DW, generating the same TPs; however some important differences were observed. All the TPs derived from the hydroxylation reactions (**P2-P7**) as well as the promoter product **P1** were detected at lower intensities compared to DW and disappeared at 7.2 mg L^{-1} of peroxide consumption (Figure 6.7 (a)). On the contrary, some of the demethylation-hydroxylation products (**P15; P17-P19**) unlike in DW, they remained abundant in the solution until the end of the experiments (12 mg L^{-1} H_2O_2) (Figure 6.7 (b)). Additionally, photo-induced cleavage products (**P20** and **P21**) were detected at maximum concentration at 9.6 mg L^{-1} H_2O_2 consumption and remained until the end of the treatment (Figure 6.7 (c)). Therefore, incomplete mineralization in SW could be attributed to the presence of the aforementioned TPs and carboxylic acids as well. These results confirmed the higher DOC concentration remaining at the end of SW experiments (~4.5 mg L^{-1} at 12 mg L^{-1} H_2O_2) compared to that observed in DW experiments (~2.4 mg L^{-1} at 12 mg L^{-1} H_2O_2).

The presence of inorganic anions in the SW matrix inhibits the reaction of TMP with hydroxyl radicals which negatively affect the degradation rate and the formation of

TPs. Moreover, these results indicate that differences in the TPs formation profile exists when TMP is in SW or DW, probably as a consequence of the high concentration of SO_4^{2-} and Cl^-, which quench the ketone triplet state (Gan et al., 2008), inhibiting the $HO^\bullet$ conducted mechanism and generating a preferential route in which **P15** and **P17-P19** remain as the major transformation products.

The formation of TPs in the more complex matrices (SWW and RE) exhibited different behavior compared to DW and SW. Hydroxylation products (**P2-P7**) as well as the promoter **P1** disappeared from the treated samples at 9.6 mg L^{-1} H_2O_2 consumption in both matrices (Figure 6.8 (a) and Figure 6.9 (a)). On the other hand, demethylation-hydroxylation products (**P8-P10**; **P12-P15**; **P17-P19**) were detected at 12 mg L^{-1} H_2O_2 consumption except **P16** which was removed at 9.6 mg L^{-1} H_2O_2 consumption. Additionally the cleavage products (**P20**, **P21**) were detected at the end of the treatment at higher intensities. These results indicate the negative effect of the high organic content present in the SWW and RE matrices in the degradation pathway. This small decay in TPs formation in RE can be possibly due to the presence of dissolved organic matter (DOM) and some ions such as nitrite and nitrate.

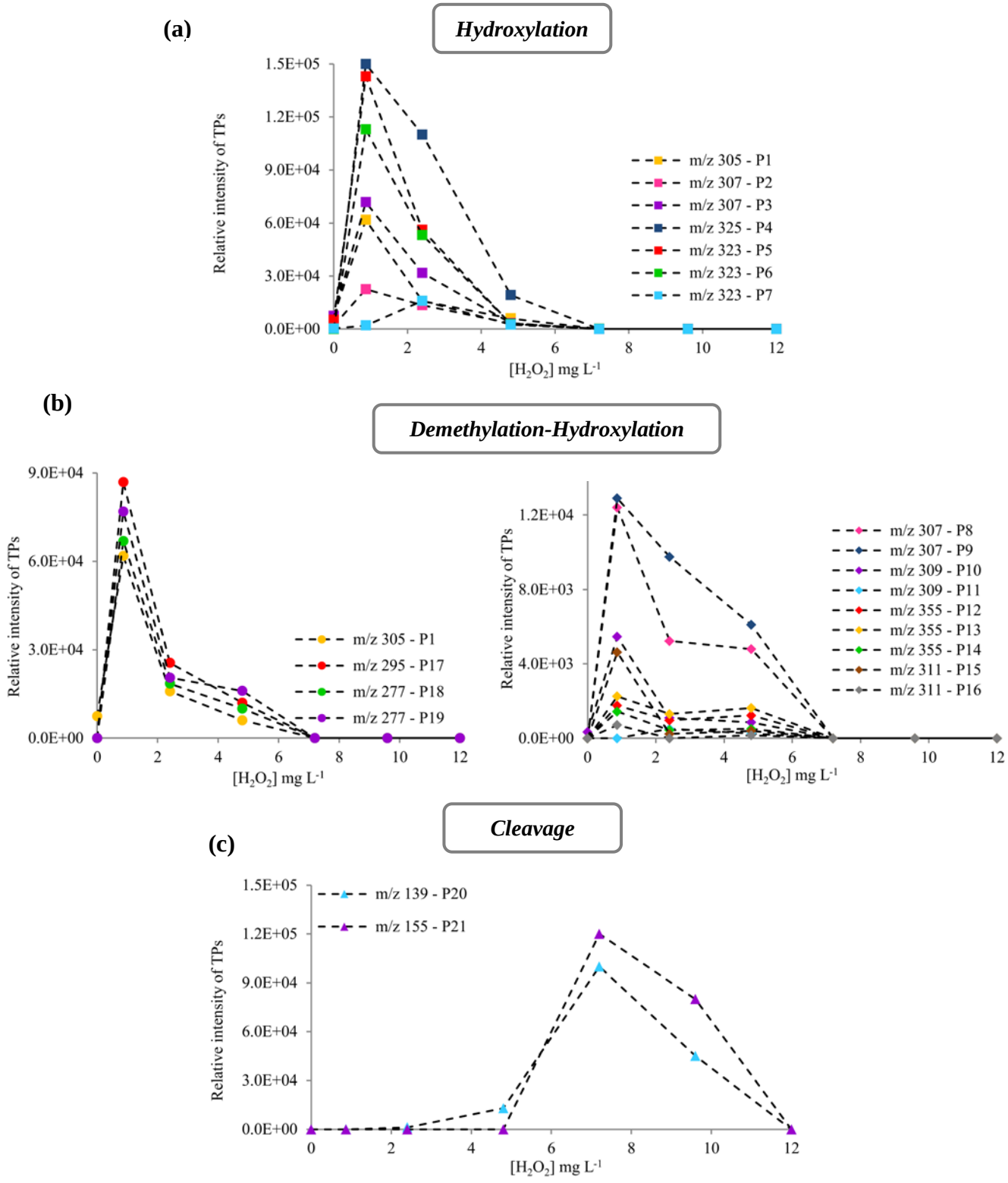

Figure 6.6 Abundance of the main photo-transformation products of TMP generated during solar Fenton experiments in demineralized water (DW): (a) Hydroxylation; (b) Demethylation/Hydroxylation; and (c) Cleavage. The promoter product **P1** is depicted in graphs (a) and (b).

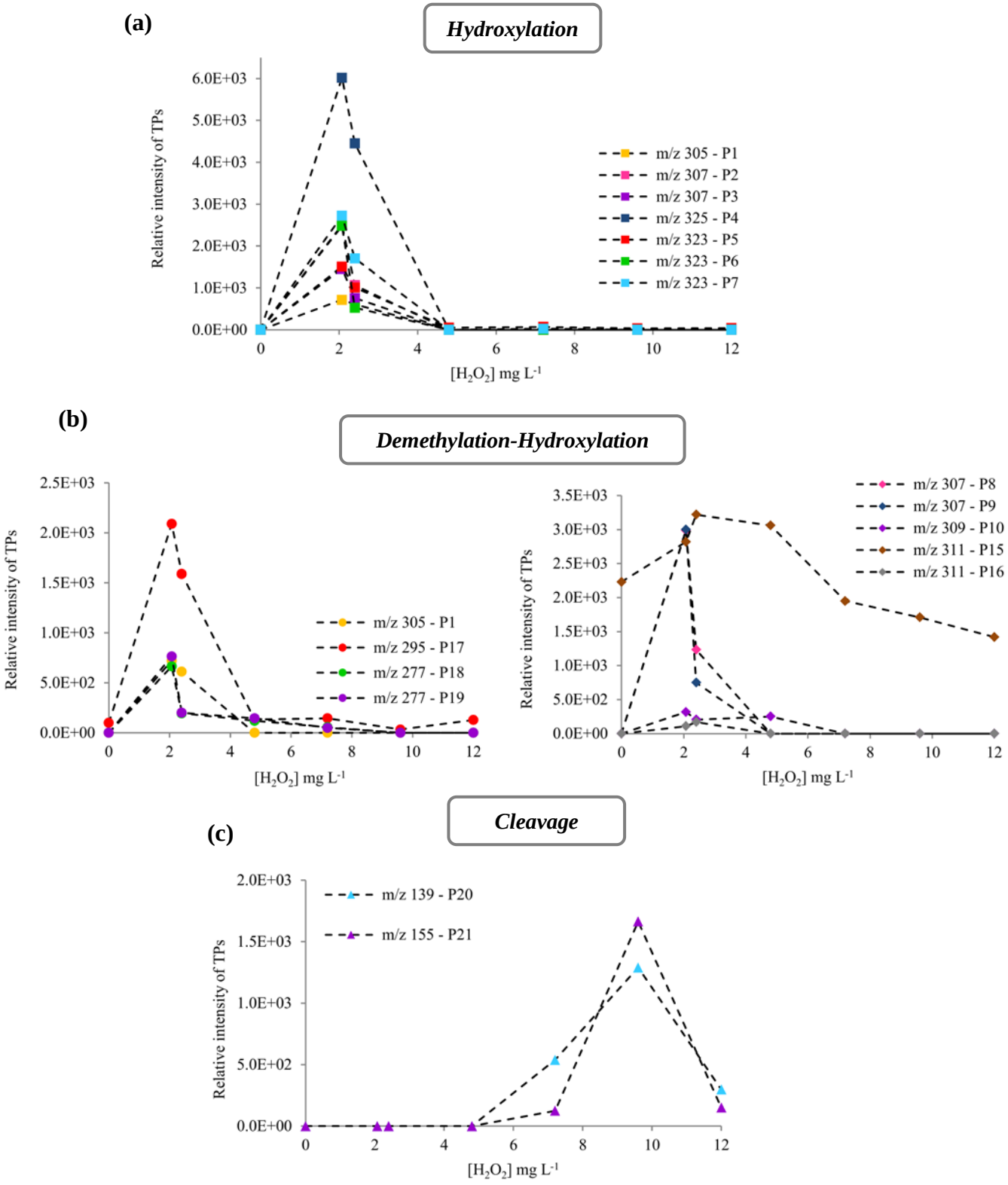

Figure 6.7 Abundance of the main photo-transformation products of TMP generated during solar Fenton experiments in simulated natural freshwater (SW): (a) Hydroxylation; (b) Demethylation/Hydroxylation; and (c) Cleavage. The promoter product **P1** is depicted in graphs (a) and (b).

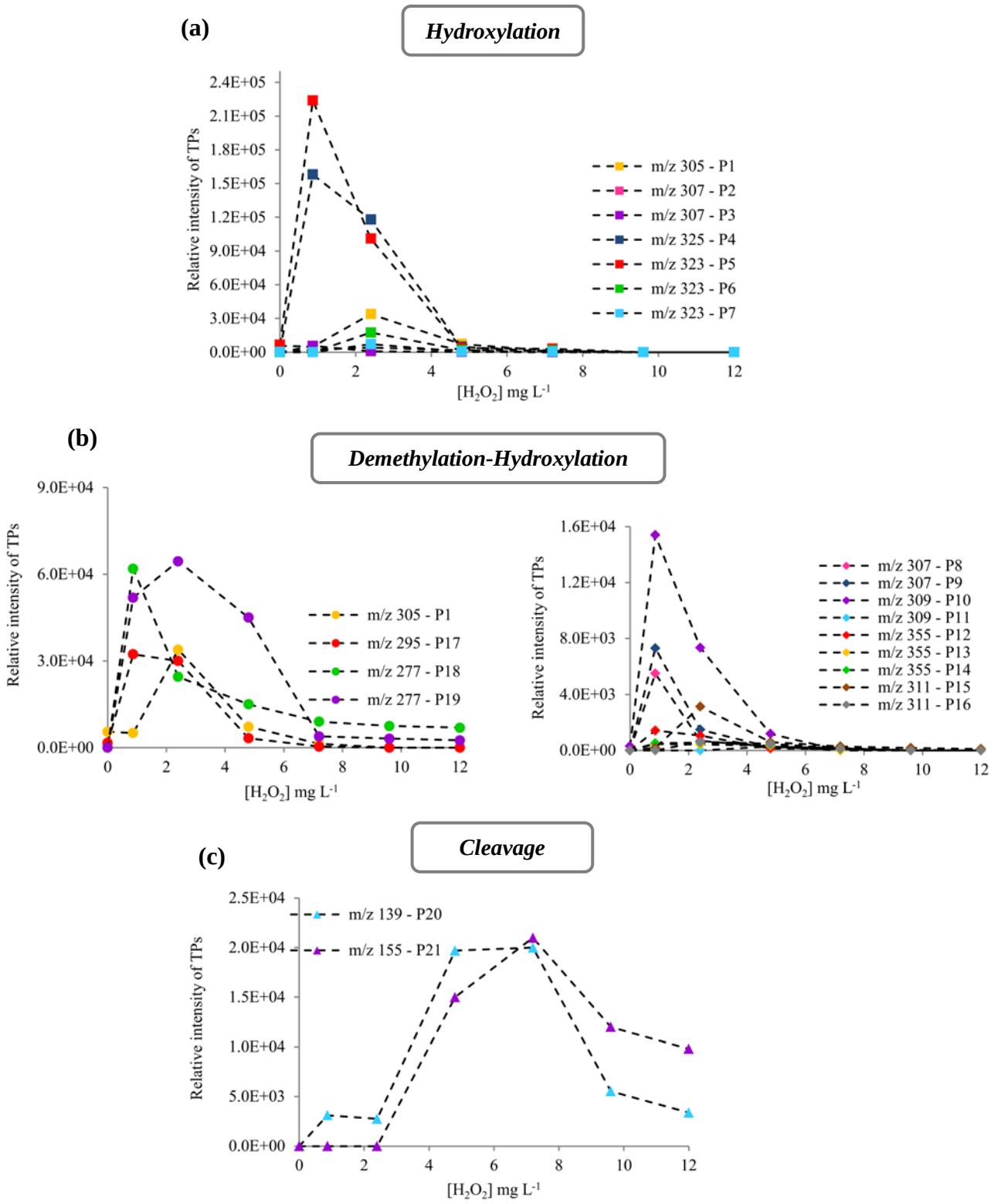

Figure 6.8 Abundance of the main photo-transformation products of TMP generated during solar Fenton experiments in simulated wastewater (SWW): (a) Hydroxylation; (b) Demethylation/Hydroxylation; and (c) Cleavage. The promoter product **P1** is depicted in graphs (a) and (b).

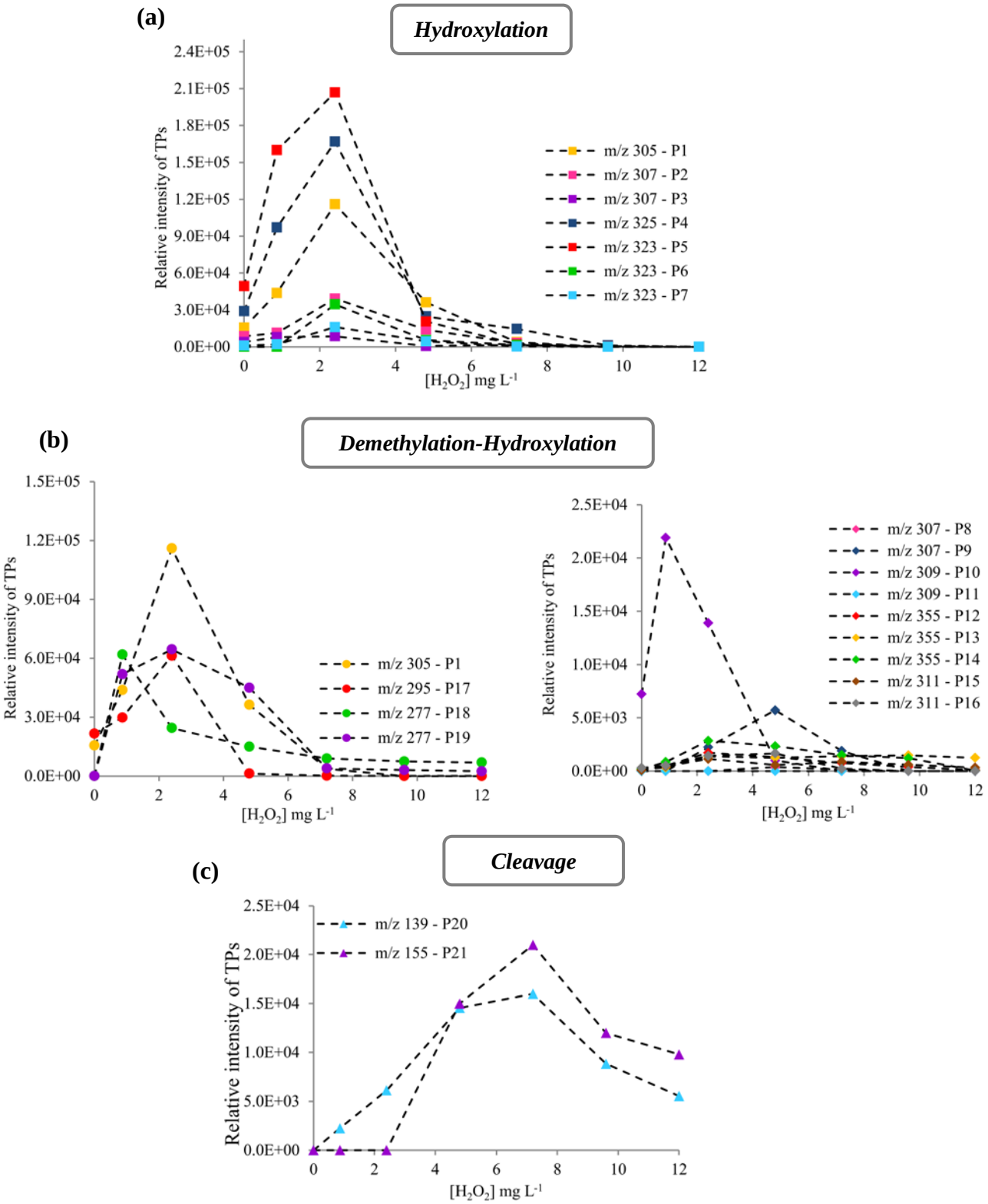

Figure 6.9 Abundance of the main photo-transformation products of TMP generated during solar Fenton experiments in real effluent (RE): (a) Hydroxylation; (b) Demethylation/Hydroxylation; and (c) Cleavage. The promoter product **P1** is depicted in graphs (a) and (b).

The reaction routes proposed, although with some similarities, differ from others previously reported in the literature. TMP follows similar, but not identical, reaction pathways in photocatalytic experiments as reported by Sirtori et al. (2010) and Luo et al. (2012). It is worth pointing out that Sirtori et al. (2010) did not detect **P21** in the cleavage mechanism during TMP heterogeneous photocatalytic treatment (TiO_2) in DW whereas two new TPs (*m/z* 339; *m/z* 341) were elucidated in demethylation-hydroxylation reactions. Sirtori et al. (2010) reported also the formation of a new TP (*m/z* 141) in the cleavage mechanism during photolysis experiments with a solar simulator. In a recent study conducted by Luo et al. (2012) some similar TPs were proposed (except *m/z* 262) during photolysis experiments; however no cleavage mechanisms were described in this study.

Some of the identified TPs are similar to those found in metabolic studies of TMP, while several new products have been found additionally. Metabolites of TMP (**P2**, **P3**) were reported by Nordholm and Dalgaard (1984) and Klooster et al. (1992). Bergh et al. (1989) reported the degradation products formed during thermally and photochemically catalysed hydrolysis or oxidation of TMP. The major changes occurred in the 2,4-diaminoprimidine moiety while **P1** and **P3** were also detected. In a later study of Bergh and Breytenbach (1990), five degradation products of TMP were detected in pharmaceutical suspensions which were similar with those observed by Bergh et al. (1989). Table 6.2 summarizes the so far conducted studies concerning the TMP TPs identification, formed under different processes (*i.e.* oxidation, hydrolysis, photolysis, and metabolism) as reported in the literature.

The number of identified TPs of TMP revealed the complexity involved with the solar Fenton process and proposed the existence of various degradation routes resulting in multi-step and interconnected pathways. The matrix composition affected

the formation of TPs suggesting that the hydroxyl radicals generated during the process were scavenged by anions and organics present in the solution.

Table 6.2 Various studies for TMP TPs identification as reported in the literature.

Process	Reference
Photolysis Demineralized water =spiked with [TMP]=20 mg L^{-1} and [Humic acid]= 20 mg L^{-1} Solar simulator	*Luo et al., (2012)*
TiO_2 photocatalysis Demineralized water and simulated seawater spiked with [TMP]=20 mg L^{-1} [TiO_2]=200 mg L^{-1} Solar pilot plant	*Sirtori et al., (2010)*
Biodegradation Nitrifying activated sludge spiked with [TMP]=20 mg L^{-1}	*Eichhorn et al., 2005*
Metabolism Rat hepatocytes	*Klooster et al. (1992)*
Metabolism Pharmaceutical tablets and suspensions	*Bergh and Breytenbach (1990)*
Hydrolysis and Oxidation Acidic and alkaline mediums Direct sunlight	*Bergh et al. (1989)*
Metabolism Pig urine	*Nordholm and Dalgaard (1984)*

A large number of compounds generated by the photocatalytic transformation of TMP were identified by UPLC-ToF/MS. The number of identified TPs revealed the complexity involved with the solar Fenton process and proposed the existence of various degradation routes resulting in multi-step and interconnected pathways. The matrix composition affected the formation of TPs suggesting that the hydroxyl radicals generated during the process were scavenged by anions and organics present in the solution; however hydroxylation, demethylation and cleavage reactions were observed in all water matrices.

CHAPTER 7: CONCLUSIONS

7.1 General conclusions

The main conclusions of this thesis are divided in three distinct sections. In the first one the conclusions concerning the development and validation of a UPLC-MS/MS method for the detection and quantification of OFX and TMP in secondary treated wastewaters are mentioned. In the second section the main conclusions concerning the bench scale degradation study of OFX and TMP wastewater spiked solutions during the homogeneous solar Fenton process ($h\nu/Fe^{2+}/H_2O_2$) and the heterogeneous photocatalysis with titanium dioxide (TiO_2) suspensions are reported. Finally, the last section includes the main conclusions derived from the pilot scale experiments.

7.1.1 UPLC-MS/MS method

In this work, a sensitive and highly selective method was developed and validated to study the degradation of OFX and TMP spiked in secondary treated domestic effluents at low concentration level.

- Column BEH Shield RP18 was found to be the most efficient for separation and determination of OFX and TMP using 0.1 mM ammonium acetate in water + 0.01% formic acid (A_1) and 0.1 mM ammonium acetate in methanol + 0.01% formic acid (A_2) as mobile phase.
- The method was optimized and showed very good performance characteristics (R^2>99% and R^2>98% in the range of 0.1-100 μg L^{-1} and 0.01-0.1 μg L^{-1} respectively, RSD in the range of 0.98-1.54% for 0.01-1.0 μg L^{-1} and 2.36-14.65% for 10-100 μg L^{-1} for OFX and in the range of 0.85-3.66% for 0.01-1.0 μg L^{-1} and

2.59-5.54% for 10-100 μg L^{-1} for TMP, LOD 4.6 and 5.5 ng L^{-1} for OFX and TMP respectively, LOQ 8.8 and 9.5 ng L^{-1} for OFX and TMP respectively, overall recovery ≥ 90%) and was successfully applied to study the degradation kinetics of the selected antibiotics during the solar Fenton process applied.

7.1.2 Bench scale experiments

Two different advanced oxidation processes (AOPs), solar Fenton homogeneous photocatalysis (*hv*/Fe^{2+}/H_2O_2) and heterogeneous photocatalysis with titanium dioxide (TiO_2) suspensions, were studied for the chemical degradation of two antibiotics (OFX and TMP) in secondary treated domestic effluents. Bench scale experiments using a solar simulator and a photochemical batch reactor were carried out to evaluate the influence of various operational parameters on the degradation rate of OFX and TMP substrates and to select the optimum oxidation conditions.

The evaluation of the processes was performed by studying the degradation/removal of the antibiotics in the wastewater solution by UV/Vis spectrophotometry and chromatographic analysis (UPLC-MS/MS) and by monitoring the reduction of dissolved organic carbon (DOC) during the process. A *Daphnia magna* bioassay was also used to evaluate the potential toxicity of the parent compounds and their photo-oxidation by-products during different stages of the oxidation process.

The main conclusions drawn from the bench scale study are summarized as follows:

- The experiments showed that OFX and TMP substrates at concentration of 10 mg L^{-1} can be successfully totally removed by solar Fenton at low iron ($[Fe^{2+}]_0$=5 mg L^{-1}) and low initial hydrogen peroxide ($[H_2O_{2(OFX)}]_0$=2.714 mmol L^{-1}; $[H_2O_{2(TMP)}]_0$=3.062 mmol L^{-1}) concentrations within 30 min of treatment.

However, the maximum degradation of OFX and TMP substrates with the heterogeneous photocatalysis was 60% and 68% respectively using [TiO_2]=3 g L^{-1}. Therefore, solar Fenton was proved to be more efficient for the degradation of these antibiotics than TiO_2 photocatalysis.

- The mineralization was lower compared to the degradation of OFX and TMP substrates indicating the formation of stable oxidation by-products during the application of both processes. Also, substrates mineralization was influenced by dissolved organic matter (DOM) which reacts with the hydroxyl radicals. The highest DOC removal achieved was approximately 41% and 44% in the case of OFX and TMP wastewater spiked solution respectively, within 120 min of solar Fenton treatment. On the contrary, TiO_2 photocatalysis was less efficient for the DOC removal compared to solar Fenton yielding 10% and 13% removal for OFX and TMP wastewater solutions, respectively.

- OFX and TMP substrates degradation followed both for solar Fenton and TiO_2 process, a first-order kinetic law in the first 20 min; however the degradation rate was higher in homogeneous photocatalysis. The degradation followed the Langmuir-Hinshelwood (L-H) kinetic model in the case of heterogeneous photocatalysis.

- The kinetic parameters (the rate constant (k), the half-life time ($t_{1/2}$) and the initial rate of degradation (r_0)) were influenced by the operating conditions employed such as the concentration of iron salt and hydrogen peroxide, the pH of solution, the solar irradiation, the temperature and the initial concentration of the substrate in the case of solar Fenton process.

- In the presence of higher iron concentration, the process was accelerated mainly by the photocatalytic regeneration of ferrous from ferric iron resulting to the rapid generation of additional hydroxyl radicals. When iron concentration is low, part of the hydrogen peroxide is decomposed into molecular oxygen and water but does not participate in the oxidation of the antibiotic substrates.

- The degradation of both compounds was increased when increasing the concentration of hydrogen peroxide. However, at higher oxidant concentrations an adverse effect on the substrates degradation was observed due to the recombination of the $HO^{\bullet}$ produced as well as the reaction of $HO^{\bullet}$ with H_2O_2, contributing to the $HO^{\bullet}$ scavenging capacity.

- The photolysis (solar radiation alone) and the combined action of solar radiation and Fe^{2+} at acidic conditions showed no significant degradation of the investigated compounds. Under the presence of hydrogen peroxide, 30% of OFX and 35% of TMP substrate was degraded within 120 min due to the photochemical cleavage of H_2O_2 to yield $HO^{\bullet}$ by solar light absorption. In the dark Fenton, OFX and TMP degradation was completed at 90 and 120 min respectively whereas the substrates' oxidation was strongly accelerated by solar irradiation (solar Fenton) and was completed at 30 min for both compounds.

- As already proved by various other studies, our investigation confirmed the fact that during the solar Fenton process, the pH range should be kept between the optimum range of 2.8-3.0. At pH 2.8-3.0 the predominant species is the $[FeOH(H_2O)_5]^{2+}$ complex (the most photoactive ferric iron-water complex) which is able to undergo excitation.

- The highest treatment efficiency (*i.e.* faster substrate degradation, shorter illumination time required for complete removal and less hydrogen peroxide consumption) was obtained at 45 ^{o}C. An increase of the temperature from 15 ^{o}C to 45 ^{o}C led to an increased degradation rate constant for both compounds. The rate constant (k) vs $1/T$ was found to be linear, obeying Arrhenius equation indicating the dependence of OFX and TMP degradation on T.

- The degradation rate was found to increase by decreasing the substrate concentration from 2 to 20 mg L^{-1}. However, OFX and TMP degradation proceeded more slowly at 100 μg L^{-1} compared to that at mg L^{-1} level (except 20 mg L^{-1}) probably due to the presence of various complex organics in the wastewater matrix which prevent the generated $HO^{\bullet}$ to attack the substrate molecules.

- The oxidation of OFX and TMP substrates by TiO_2 process was affected by the various operating conditions employed such as the concentration of catalyst, the initial substrate concentration and the solution pH.

  - The results demonstrated that the degradation of the antibiotics and the initial degradation rate (r_0) increased by increasing the catalyst concentration up to a level after which a sharp drop of the r_0 was observed. The total active surface area was increased by increasing catalyst amount up to a level which corresponds to the optimum of light absorption. Above the optimum amount of TiO_2 the increased turbidity of the solution reduced the light transmission through the solution.

- The adsorption on the catalyst surface and the degradation rate of the substrates was strongly depended on the solution pH. The effect of the pH of the solution on the photocatalytic degradation of OFX and TMP cannot be explained in terms of the ionization state of the catalyst and the substrate alone, since both have either negative or positive charges at alkaline or acidic conditions, respectively. Consequently, this behavior may be due to the relative contribution of various complex reactions.
- With the addition of an oxidant into illuminated semiconducting suspensions a synergistic effect that led to an enhancement of the substrates degradation was observed. The replacement of peroxide with peroxydisulfate, led to even higher degradation rates due to the prevention of the recombination of the e_{CB}^{-} – h_{VB}^{+} pair but also due to the photolytic activity of the oxidant.

▪ Substrates decomposition was accompanied by the formation of intermediates that should always been taken into consideration because they can increase the effluent final toxicity. A different behaviour of daphnids immobilization was observed for each antibiotic during the two oxidation processes applied. The AOP systems that have been used were able to achieve a reduction of the toxicity of the treated solution.

7.1.3 Pilot scale experiments

This study investigated the application of the solar Fenton process for the degradation of OFX and TMP at a pilot-scale. A compound parabolic collector (CPC) pilot plant was used for the photocatalytic experiments. The main objectives of the pilot scale study were: (i) to elucidate the possible oxidation intermediates formed during the TMP solar Fenton treatment and determine the effect that the water matrix might have when applying this process; and (ii) to investigate the efficiency of the solar Fenton in degrading the two antibiotics at low concentration level (μg L^{-1}).

The main conclusions drawn from the pilot scale study of the solar Fenton process are listed below:

- DOC removal was found to be dependent on the chemical composition of the water matrix. The DOC removal needed a little bit more of hydrogen peroxide in the case of SW compared to DW, which can be attributed to the presence of various anions which act as scavengers of the hydroxyl radicals. On the other hand, the presence of organic carbon and higher salt content in SWW and RE led to lower mineralization per dose of hydrogen peroxide compared to DW and SW.
- The elimination of carboxylic acids required higher doses of peroxide in SW compared to that needed in DW due to the presence of anions acting as hydroxyl radical scavengers, and directly affecting the efficiency of the photocatalytic process.
- The toxicity assays (*V. fischeri*, respirometry) which were performed in samples taken at different stages of the solar Fenton treatment using SWW and RE matrices indicated that the toxicity originates from compounds present in RE and their by-products formed during solar Fenton treatment and not from the intermediates

formed from the oxidation of OFX or TMP. The final treated samples are characterized by higher toxicity compared to the initial indicating that the intermediates formed were moderately toxic for the organism tested.

- Results obtained from photolysis (solar radiation alone) at initial concentration of 100 μg L^{-1} indicated that the photolytic process was scarcely responsible for the observed fast degradation when the antibiotics wastewater solution was irradiated in the presence of Fenton reagent.
- The initial concentration of each contaminant (100 μg L^{-1}) was low enough to optimize the solar Fenton process under realistic environmental conditions and high enough to study the degradation behaviour of the selected contaminants by a fast and reliable UPLC-MS/MS method. OFX and TMP at the μg L^{-1} level can be successfully degraded with solar Fenton at low iron (5 mg L^{-1}) and low initial hydrogen peroxide (75 mg L^{-1}) concentration.
- OFX and TMP substrates were removed completely at the end of the solar Fenton treatment without modifying the pH of the wastewater; however the degradation proceeded with much lower rate at neutral pH compared to that observed at acidic conditions. In the presence of dissolved organic matter (DOM), photoactive complexes with ferric iron were formed which have the advantage of being soluble in the wastewater matrix and so preventing the Fe^{3+} precipitation in neutral pH conditions.
- The photocatalytic removal of OFX and TMP (at 100 μg L^{-1}) with the solar Fenton process followed apparent first-order kinetics. A modification of the first-order kinetic expression was proposed and was successfully used to explain the

degradation kinetics of the compounds during the solar Fenton treatment yielding lower mean square error (*MSE*) values.

- Solar Fenton was proved to be an efficient method considering the wastewater reuse for agriculture irrigation purposes and recharging groundwater aquifers. The results demonstrated the capacity of the solar Fenton process to reduce the toxicity to the examined plant species (*Sorghum saccharatum*, *Lepidium sativum*, *Sinapis alba* and microorganisms *D.magna*. In general, the solar Fenton process did not exert any significant influence on seed germination which was found to be affected by the DOM by-products and not by the presence of the antibiotics and their by-products at the μg L^{-1} concentration level. Root and shoot growth on the other hand, were more sensitive and were affected by the organic by-products formed during the oxidation of DOM. In the case of *D.magna* it was found that the presence of OFX and TMP (and their by-products) at the low concentration level of μg L^{-1} did not affect these species and the toxicity changes were attributed to the DOM by-products.

- Solar Fenton process contributed significantly reductions on the prevalence of enterococci, including those resistant to TMP or OFX, in the treated samples. Comparing the resistance for both antibiotics tested, it was observed that OFX resistance was almost double of that of TMP.

- A process cost estimation based on the experimental and operational data recorded during the operational period of the solar pilot plant unit was carried out. For this purpose, the investment cost along with the operational cost (including mainly electric power and consumables) and the maintenance cost were estimated. The total cost of a full scale unit for the solar Fenton treatment of 150 m^3 day^{-1} secondary wastewater effluent was found to be 0.85 € m^{-3}.

- 21 compounds were identified as possible TPs formed during the solar Fenton treatment of TMP. Three competitive pathways were suggested in which hydroxylation, demethylation, cleavage of TMP molecule, and oxidation of hydroxyl groups are described as major transformation steps. The incomplete mineralization of TMP in DW was attributed to the formation of carboxylic acids while in SW could be attributed to the presence of the photo-induced cleavage TPs and carboxylic acids as well. The differences in the TPs formation profile in SW and DW were observed probably as a consequence of the high concentration of SO_4^{2-} and Cl^-. The formation of TPs in the more complex matrices (SWW and RE) exhibited different behavior compared to DW and SW indicating the adverse effect of the high organic content present in the SWW and RE matrices in the degradation pathway.

An advanced oxidation treatment using the Fenton process tends to be a feasible and efficient method for the removal of antibiotics at low concentration levels in secondary domestic wastewater effluents. The Fenton process requires relatively inexpensive and easily transported chemicals and, in the case of the photo-Fenton process, solar irradiation can be applied making the process a cost-effective one. Its application was proved to be capable for removing the initial toxic effects on various microorganisms and plant species and also the antibiotic resistant enterococci.

7.2 Future work

Some further studies which are proposed to be carried out are as follows:

- Elucidate the oxidation intermediates produced during the pilot-scale solar Fenton treatment of OFX.
- Study the application of the solar Fenton process for the degradation of complex mixtures of micropollutants. The mixtures may consist of compounds that are characterized by the same mechanism of action or other contaminants which belong to different chemical groups.
- Determine other adverse effects of antibiotics and their transformation products such as genotoxitocity (DNA-damaging) and mutagenicity (DNA-mutation).
- Develop accurate and reliable analytical methodologies for the determination of antibiotic metabolites in various environmental compartments (*e.g.* wastewater effluents).
- Study the coupling of a solar Fenton process with other wastewater treatment process (or integration of the process into an existing WWTP), and treatment of two or more wastewater streams (*i.e.* hospital effluents combined with urban wastewater).
- Evaluate the use of the solar Fenton treated effluents for crops (*e.g* vegetables) irrigation.
- Evaluate in more depth the efficiency of the solar Fenton process to the antibiotic resistance evolution in various bacteria species.

REFERENCES

Abellán, M.N., Giménez, J., Esplugas, S., 2009. Photocatalytic degradation of antibiotics: The case of sulfamethoxazole and trimethoprim. *Catalysis Today* **144**, 131-136.

Abo-Farha, S.A., 2010. Comparative study of oxidation of some azo dyes by different advanced oxidation processes: Fenton, Fenton-Like, Photo-Fenton and Photo-Fenton-Like. *Journal of American Science* **6** (10), 128-142.

Adams, C., Asce, M., Wang, Y., Loftin, K., Meyer, M., 2002. Removal of antibiotics from surface and distilled water in conventional water treatment processes. *Journal of Environmental Engineering* **128** (3), 253-260.

Akiyama, T., Savin, M.C., 2010. Populations of antibiotic-resistant coliform bacteria change rapidly in a wastewater effluent dominated stream. *Science of the Total Environment* **408**, 6192-6201.

Aksu, Z., Tunç, O., 2005. Application of biosorption for penicillin G removal: comparison with activated carbon. *Process Biochemistry* **40**, 831-847.

Amat, A.M., Arques, A., García-Ripoll, A., Santos-Juanes, L., Vicente, R., Oller, I., Maldonado, M.I., Malato, S., 2009. A reliable monitoring of the biocompatibility of an effluent along an oxidative pre-treatment by sequential bioassays and chemical analyses. *Water Research* **43**, 784-792.

Amyes, S.G.B., Towner, K.J., 1990. Trimethoprim resistance; epidemiology and molecular aspects. *Journal of Medical Microbiology* **31**, 1-19.

Andreozzi, R., Caprio, V., Insola, A., Marotta, R., 1999. Advanced oxidation processes (AOP) for water purification and recovery. *Catalysis Today* **53**, 51-59.

Andreozzi, R., Raffaele, M., Nicklas, P., 2003. Pharmaceuticals in STP effluents and their solar photodegradation in aquatic environment. *Chemosphere* **50**, 1319-1330.

Andreozzi, R., Canterino, M., Marotta, R., Paxeus, N., 2005. Antibiotic removal from wastewaters: the ozonation of amoxicillin. *Journal of Hazardous Materials* **122**, 243-250.

Andrews, J.M., 2009. BSAC standardized disc susceptibility testing method (version 8). *Journal of Antimicrobial Chemotherapy* **64**, 454-489.

Armstrong, J.L., Calomaris, J.J., Seidler, R.J., 1982. Selection of antibiotic-resistant standard plate count bacteria during water treatment. *Applied and Environmental Microbiology* **44**, 308-316.

Arnold, W.A, McNeill, K., 2007. Transformation of pharmaceuticals in the environment: Photolysis and other abiotic processes. *Comprehensive Analytical Chemistry* **50**, Petrović, M., Barceló, D. (Eds), Chapter 3.2, 361-385.

Arslan Alaton, I., Dogruel, S., 2004. Pre-treatment of penicillin formulation effluent by advanced oxidation processes. *Journal of Hazardous Materials* **B112**, 105-113.

Arslan Alaton, I., Dogruel, S., Baykal, E., Gerone, G., 2004. Combined chemical and biological oxidation of penicillin formulation effluent. *Journal of Environmental Management* **73**, 155-163.

Arslan-Alaton, I., Balcioğlu, I.A., 2002. Biodegradability assessment of ozonated raw and biotreated pharmaceutical wastewater. *Archives of Environmental Contamination and Toxicology* **43**, 425-431.

Ash, R., Mauck, B., Morgan, M., 2002. Antibiotic resistance of Gram-negative bacteria in rivers, United States. *Emerging Infectious Diseases* **8**, 713-716.

Auerbach, E.A., Seyfried, E.E., McMahon, K.D., 2007. Tetracycline resistance genes in activated sludge wastewater treatment plants. *Water Research* **41**, 1143-1151.

Babíc, S., Aŝperger, D., Mutavdži´, D., Horvat, A.J.M., Kaŝtelan-Macan, M., 2006. Solid phase extraction and HPLC determination of veterinary pharmaceuticals in wastewater. *Talanta* **70**, 732-738.

Babuponnusami, A., Muthukumar, K., 2011. Advanced oxidation of phenol: A comparison between Fenton, electro-Fenton, sono-electro-Fenton and photo-electro-Fenton processes. *Chemical Engineering Journal* **183**, 1-9.

Bacardit, J., Sto1tzner, J, Chamarro, E., Esplugas, S., 2007. Effect of Salinity on the Photo-Fenton Process. *Industrial and Engineering Chemistry Research* **46**, 7615-7619.

Backhaus, T., Grimme, L.H., 1999. The toxicity of antibiotic agents to the luminescent bacterium *Vibrio fischeri*. *Chemosphere* **38**, 3291-3301.

Baeza, C., Knappe, D.R.U., 2011. Transformation kinetics of biochemically active compounds in low-pressure UV photolysis and UV/H_2O_2 advanced oxidation processes. *Water Research* **45**, 4531-4543.

Baker, D.R., Kasprzyk-Hordern, B., 2011. Multi-residue analysis of drugs of abuse in wastewater and surface water by solid-phase extraction and liquid chromatography-positive electrospray ionisation tandem mass spectrometry. *Journal of Chromatography A* **1218**, 1620-1631.

Balcıoğlu, I. A., Ötker, M., 2003. Treatment of pharmaceutical wastewater containing antibiotics by O_3 and O_3/H_2O_2 processes. *Chemosphere* **50**, 85-95.

Balmer, M.E., Sulzberger, B., 1999. Atrazine degradation in irradiated iron/oxalate systems: Effects of pH and oxalate. *Environmental Science and Technology* **33**, 2418-2424.

Baquero, F., Martínez, J.L., Cantó, R., 2008. Antibiotics and antibiotic resistance in water environments, Current Opinion in Biotechnology 19, 260-265.

Barb, W.G., Baxendale, J.H., George, P., Hargrave, K.R., 1951. Reactions of ferrous and ferric ions with hydrogen peroxide. Part I-The ferrous ion reaction. Transactions of Faraday Society 47, 462-500.

Barbarin, N, Henion, J.D., Wu, Y., 2002. Comparison between liquid chromatography-UV detection and liquid chromatography-mass spectrometry for the characterization of impurities and/or degradants present in trimethoprim tablets. *Journal of Chromatography A* **970**, 141-154.

Batt, A.L., Snow, D.D., Aga, D.S., 2006. Occurrence of sulphonamide antimicrobials in private water wells in Washington County, Idaho, USA. *Chemosphere* **64**, 1963-1971.

Batt, A.L., Kim, S., Aga, D.S., 2007. Comparison of the occurrence of antibiotics in four full-scale wastewater treatment plants with varying designs and operations. *Chemosphere* **68**, 428-435.

Batt, A. L., Kostich, M. S., Lazorchak, J.M., 2008. Analysis of Ecologically Relevant Pharmaceuticals in Wastewater and Surface Water Using Selective Solid-Phase Extraction and UPLC-MS/MS. *Analytical Chemistry* **80**, 5021-5030.

Bautitz, I.R, Nogueira, R.F.P, 2007. Degradation of tetracycline by photo-Fenton process-Solar irradiation and matrix effects. *Journal of Photochemistry and Photobiology A: Chemistry* **187**, 33-39.

Baxendale, J.H., Evans, M.G., Park, G.S., 1946. The mechanism and kinetics of the initiation of polymerisation by systems containing hydrogen peroxide. *Transactions of the Faraday Society* **42**, 155-169.

Becker, M., Zittlau, E., Petz, M., 2004. Residue analysis of 15 penicillins and cephalosporins in bovine muscle, kidney and milk by liquid chromatography-tandem mass spectrometry. *Analytica Chimica Acta* **520**, 19-32.

Bendz, D., Paxéus, N.A., Ginn, T.R., Loge, F.J., 2005. Occurrence and fate of pharmaceutically active compounds in the environment, a case study: Hoje River in Sweden. *Journal of Hazardous Materials* **122**, 195-204.

Bergh, J.J., Breytenbach, J.C., Wessels, P.L., 1989. Degradation of TMP. *Journal of Pharmaceutical Sciences* **78**, 348-350.

Bergh, J.J., Breytenbach, J.C., 1990. High-performance liquid chromatographic analysis of trimethoprim in the presence of its degradation products. *Journal of Chromatography A* **513**, 392-396.

Bixio, D., Thoeye, C., De Koning, J., Joksimovic, D., Savic, D., Wintgens, T., Melind, T., 2006. Wastewater reuse in Europe. *Desalination* **187**, 89-101.

Biyela, P.T., Lin, J., Bezuidenhou, C.C., 2004. The role of aquatic ecosystems as reservoirs of antibiotic resistant bacteria and antibiotic resistance genes. *Water Science and Technology* **50**, 45-50.

Blanch, A.R, Caplin, J.L., Iversen, A., Kuhn, I., Manero, A., Taylor, H.D., Vilanova, X., 2003. Comparison of enterococcal populations related to urban and hospital wastewater in various climatic and geographic European regions. *Journal of Applied Microbiology* **94**, 994-1002.

Blom, J.D., 2009. A Dictionary of Hallucinations, Springer.

Boreen, A.L., Arnold, W.A., McNeill, K., 2003. Photodegradation of pharmaceuticals in the aquatic environment: A review. *Aquatic Sciences* **65**, 320-341.

Bouzaida, I., Ferronato, C., Chovelon, J.M., Rammah, M.E., Herrmann, J.M., 2004. Heterogeneous photocatalytic degradation of the anthraquinonic dye, Acid Blue 25 (AB25): a kinetic approach. *Journal of Photochemistry and Photobiology A: Chemistry* **168**, 23-30.

Boxall, A.B.A., Sinclair, C.J., Fenner, K., Kolpin, D., Maund, S.J., 2004. When synthetic chemicals degrade on the environment. *Environmental Science and Technology* **38**, 368-375.

Bray, W.C., Gorin, M.H., 1932. Ferryl ion, A compound of tetravalent iron. *Journal of the American Chemistry Society* **54**, 2124.

Brown, K.D., Kulis, J., Thomson, B., Chapman, T. H., Mawhinney, D.B., 2006. Occurrence of antibiotics in hospital, residential, and dairy effluent, municipal wastewater, and the Rio Grande in New Mexico. *Science of the Total Environment* **366**, 772-783.

Buda, F., Ensing, B., Gribnau, M.C.M, Baerends, E.J, 2001. DFT study of the active intermediate in the Fenton reaction. *Chemistry-A European Journal* **7** (13), 2775-2783.

Byrns, G., 2001. The fate of xenobiotic organic compounds in wastewater treatment plants. *Water Research* **35** (10), 2523-2533.

Cahill, J.D., Furlong, E.T., Burkhardt, M.R., Kolpin, D., Anderson, L.G., 2004. Determination of pharmaceutical compounds in surface- and ground-water samples by solid-phase extraction and high-performance liquid chromatography-

electrospray ionization mass spectrometry. *Journal of Chromatography A* **1041**, 171-180.

Cai, Z., Zhang, Y., Pan, H., Tie, X., Ren, Y., 2008. Simultaneous determination of 24 sulfonamide residues in meat by ultra-performance liquid chromatography tandem mass spectrometry. *Journal of Chromatography A* **1200**, 144-155.

Candela, L., Fabregat, S., Josa, A., Suriol, J., Vigués, N., Mas, J., 2007. Assessment of soil and groundwater impacts by treated urban wastewater reuse. A case study: Application in a golf course (Girona, Spain). *Science of the Total Environment* **374**, 26-35.

Canonica, S., 2007. Oxidation of aquatic organic contaminants induced by excited triplet states. *Chimia* **61** (10), 641-644.

Carballa, M., Omil, F., Lema, J.M., Llompart, M., Garcia-Jares, C., Rodriguez, I., Gomez, M., Ternes, T., 2004. Behavior of pharmaceuticals, cosmetics and hormones in a sewage treatment plant. *Water Research* **38**, 2918-2926.

Castiglioni, S., Pomati, F., Miller, K., Burns, B.P., Zuccato, E., Calamari, D., Neilan, B.A., 2008. Novel homologs of the multiple resistance regulator *marA* in antibiotic-contaminated environments. *Water Research* **42**, 4271-4280.

Cattoir, V., Huynh, T.M., Bourdon, N., Auzou, M., Leclercq, R., 2009. Trimethoprim resistance genes in vancomycin-resistant *Enterococcus faecium* clinical isolates from France. *International Journal of Antimicrobial Agents* **34** (4), 390-392.

Cervera, M.I., Medina, C., Portolés, T., Pitarch, E., Beltrán, J., Serrahima, E., Pineda, L., Muñoz, G., Centrich, F., Hernández, F., 2010. Multi-residue determination of 130 multiclass pesticides in fruits and vegetables by gas chromatography coupled

to triple quadrupole tandem mass spectrometry. *Analytical and Bioanalytical Chemistry* **397**, 2873-2891.

Cha, J.M., Yang, S., Carlson, K.H., 2006. Trace determination of β-lactam antibiotics in surface water and urban wastewater using liquid chromatography combined with electrospray tandem mass spectrometry. *Journal of Chromatography A* **1115**, 46-57.

Chander, Y., Kumar, K., Goyal, S.M., Gupta, S.C., 2005. Antibacterial activity of soil-bound antibiotics. *Journal of Environmental Quality* **34**, 1952-1957.

Chang, H., Hua, J., Asamib, M., Kunikane, S., 2008. Simultaneous analysis of 16 sulfonamide and trimethoprim antibiotics in environmental waters by liquid chromatography-electrospray tandem mass spectrometry. *Journal of Chromatography A* **1190**, 390-393.

Chen, Q., Wu, P, Dang, Z., Zhu, N., Li, P., Wu, J., Wang, X., 2010. Iron pillared vermiculite as a heterogeneous photo-Fenton catalyst for photocatalytic degradation of azo dye reactive brilliant orange X-GN. *Separation and Purification Technology* **71**, 315-323.

Choi, K.J., Kim, S.G., Kim, C.W., Kim, S.H., 2007. Determination of antibiotic compounds in water by on-line SPE-LC/MSD. *Chemosphere* **66**, 977-984.

Ciesla, P., Kocot, P., Mytych, P., Stasicka, Z., 2004. Review: homogenous photocatalysis by transition metal complexes in the environment. *Journal of Molecular Catalysis A: Chemical* **224**, 17-33.

Clara, M., Strenn, B., Gans ,O., Martinez, E., Kreuzinger, N., Kroiss, H., 2005. Removal of selected pharmaceuticals, fragrances and endocrine disrupting

compounds in a membrane bioreactor and conventional wastewater treatment plants. *Water Research* **39**, 4797-4807.

Clesceri, L.S., Greenberg, A.E., Eaton, A.D., Eds. Standard Methods for the Examination of Water and Wastewater, 20th ed.; American Public Health Association, American Water Works Association, Water Environment Federation, Baltimore, Maryland, 1998.

Coque, T.M., Singh, K.V., Weinstock, G.M., Murray, B.E., 1999. Characterization of dihydrofolate reductase genes from trimethoprim-susceptible and trimethoprim-resistant strains of *Enterococcus faecalis*. *Antimicrobial Agents Chemotherapy* **43** (1), 141-147.

Costanzo, S. D., Murby, J., Bates, J., 2005. Ecosystem response to antibiotics entering the aquatic environment. *Marine Pollution Bulletin* **51**, 218-223.

Cotter, R.J. (ed). Time-of-flight mass spectrometry. American Chemical Society, Washington DC, 1992.

Cyprus Law on the pollution of water bodies: 106(I)/2002

D'Costa, V.M., McGrann, K.M., Hughes, D.W., Wright, G.D., 2006. Sampling the antibiotic resistome. *Science* **311**, 374-377.

Daneshvar, N., Salari, D., Khataee, A.R., 2004. Photocatalytic degradation of azo dye acid red 14 in water on ZnO as an alternative catalyst to TiO_2. *Journal of Photochemistry and Photobiology A: Chemistry* **162**, 317-322.

Davis, A.P., Huang, C.P., 1989. Removal of phenols from water by a photocatalytic oxidation process. *Water Science Technology* **21** (6-7): 455-464.

De la Cruz, N., Giménez, J., Esplugas, S., Grandjean, D., de Alencastro, L.F., Pulgarín, C., 2012. Degradation of 32 emergent contaminants by UV and neutral photo-fenton in domestic wastewater effluent previously treated by activated sludge. *Water Research* **46**, 1947-1957.

De la Torre, A., Iglesias, I., Carballo, M., Ramírez, P., Muñoz, M.J., 2012. An approach for mapping the vulnerability of European Union soils to antibiotic contamination. *Science of the Total Environment* **414**, 672-679.

De Laat, J., Le, G.T., Legube, B., 2004. A comparative study of the effects of chloride, sulfate and nitrate ions on the rates of decomposition of H_2O_2 and organic compounds by Fe(II)/H_2O_2 and Fe(III)/H_2O_2. *Chemosphere* **55**, 715-723.

Dedola, G., Fasani, E., Albini, A., 1999. The photoreactions of trimethoprim in solution. *Journal of Photochemistry and Photobiology A: Chemistry* **123**, 47-51.

Diaz-Cruz, M.S., Lopez de Alda, M.J., Barcelo, D., 2003. Environmental behavior and analysis of veterinary and human drugs in soils, sediments and sludge. *Trends in Analytical Chemistry* **22** (6), 340-351.

Ding, C., He, J., 2010. Effect of antibiotics in the environment on microbial populations. *Applied Microbiology and Biotechnology* **87**, 925-941.

Dodd, M.C., Buffle, M., von Gunten, U, 2006. Oxidation of Antibacterial Molecules by Aqueous Ozone: Moiety-Specific Reaction Kinetics and Application to Ozone-Based Wastewater Treatment. *Environmental Science and Technology* **40**, 1969-1977.

Dodd, M.C., Huang, C.H., 2007. Aqueous chlorination of the antibacterial agent trimethoprim: Reaction kinetics and pathways. *Water Research* **41**, 647- 655.

Dong, M.M., Mezyk, S.P., Rosario-Ortiz, F.L., 2010. Reactivity of effluent organic matter (EfOM) with hydroxyl radical as a function of molecular weight. *Environmental Science and Technology* **44** (15), 5714-5720.

Dongre, V.G., Karmuse, P.P., Rao, P.P., Kumar, A., 2008. Development and validation of UPLC method for determination of primaquine phosphate and its impurities. *Journal of Pharmaceutical and Biomedical Analysis* **46**, 236-242.

Drewes, J.E., Bellona, C., Oedekoven, M., Xu, P., Kim, T.U., Amy, G., 2006. Rejection of wastewater-derived micropollutants in high-pressure membrane applications leading to indirect potable reuse. *Environmental Progress* **24** (4), 400-409.

Drewes, J.E., 2007. Removal of pharmaceutical residues during wastewater treatment. *Comprehensive Analytical Chemistry* **50**, Petrović, M., Barceló, D., Eds., Chapter 4.1, 427-449.

Dunford, H.B., 2002. Oxidations of iron(II)/(III) by hydrogen peroxide: from aquo to Enzyme. *Coordination Chemistry Reviews* **233-234**, 311-318.

Duong, H.A., Pham, N.H., Nguyen, H.T., Hoang, T.T., Pham, H.V., Pham, V.C, Berg, M., Giger, W., Alder, A.C., 2008. Occurrence, fate and antibiotic resistance of fluoroquinolone antibacterials in hospital wastewaters in Hanoi, Vietnam. *Chemosphere* **72**, 968-973.

Eichhorn, P., Ferguson, P.L., Pérez, S., Aga, D.S., 2005. Application of ion trap-MS with H/D exchange and QqTOF-MS in the identification of microbial degradates of trimethoprim in nitrifying activated sludge. *Analytical Chemistry* **77**, 4176-4184.

Eliopoulos, G.M., Wennersten, C.B., Moellering, R.C., 1996. Comparative in vitro activity of levofloxacin and ofloxacin against Gram-positive bacteria. *Diagnostic Microbiology and Infectious Disease* **25**, 35-41.

Elmolla, E.S., Chaudhuri, M., 2011. The feasibility of using combined TiO_2 photocatalysis-SBR process for antibiotic wastewater treatment. *Desalination* **272**, 218-224.

El-Morsi, T.M., Emara, M.M., Abd El Bary, H.M.H., Abd-El-Aziz, A.S., Friesen, K.J., 2002. Homogeneous degradation of 1,2,9,10-tetrachlorodecane in aqueous solutions using hydrogen peroxide, iron and UV light. *Chemosphere* **47**, 343-348.

Ensing, B., Buda, F., Blochl, P.E, Baerends, E.J., 2002. A Car-Parrinello study of the formation of oxidizing intermediates from Fenton's reagent in aqueous solution. *Physical Chemistry Chemical Physics* **4**, 3619-3627.

Eriksson, E., Auffarth, K., Eilersen, A.M., Henze, M., Ledin, A., 2003. Household chemicals and personal care products as sources for xenobiotic organic compounds in grey wastewater. *Water SA* **29**, 135-146.

Esplugas, S., Bila, D.M., Krause, L.G.T., Dezotti, M., 2007. Ozonation and advanced oxidation technologies to remove endocrine disrupting chemicals (EDCs) and pharmaceuticals and personal care products (PPCPs) in water effluents. *Journal of Hazardous Materials* **149**, 631-642.

Evgenidou, E., Fytianos, K., Poulios, I., 2005. Photocatalytic oxidation of dimethoate in aqueous solutions. *Journal of Photochemistry and Photobiology A: Chemistry* **175**, 29-38.

Evgenidou, E., Konstantinou, I., Fytianos, K., Poulios, I., 2007. Oxidation of two organophosphorous insecticides by the photo-assisted Fenton reaction. *Water Research* **41**, 2015-2027.

Evgenidou, E., Bizani, E., Christophoridis, C., Fytianos, K., 2007b. Heterogeneous photocatalytic degradation of prometryn in aqueous solutions under UV–Vis irradiation. *Chemosphere* **68**, 1877-1882.

Evgenidou, E., Konstantinou, I., Fytianos, K., Poulios, I., Albanis, T., 2007c. Photocatalytic oxidation of methyl parathion over TiO_2 and ZnO suspensions. *Catalysis Today* **124**, 156-162.

Fatta, D., Nikolaou, A., Achilleos, A., Meric, S., 2007. Analytical methods for tracing pharmaceutical residues in water and wastewater. *Trends in Analytical Chemistry* **26** (6), 515-533.

Fatta-Kassinos, D., Hapeshi, E., Achilleos, A. Meric, S. Gros, M. Petrovic, M. Barcelo, D., 2010. Existence of pharmaceutical compounds in tertiary treated urban wastewater that is utilized for reuse applications. *Water Resources Manegement* **25**, 1183-1193.

Fatta-Kassinos, D., Meric, S., Nikolaou, A. 2011. Pharmaceutical residues in environmental waters and wastewater: current state of knowledge and future research. *Analytical and Bioanalytical Chemistry* **399**, 251-275.

Fatta-Kassinos, D., Vasquez, M.I., Kümmerer, K., 2011b.Transformation products of pharmaceuticals in surface waters and wastewater formed during photolysis and advanced oxidation processes-Degradation, elucidation of byproducts and assessment of their biological potency. *Chemosphere* **85**, 693-709.

Fatta-Kassinos, D., Kalavrouziotis, I.K., Koukoulakis, P.H., Vasquez, M.I., 2011c. The risks associated with wastewater reuse and xenobiotics in the agroecological environment. *Science of the Total Environment* **409**, 3555-3563.

Faust, B.C., Hoigne, J., 1990. Photolysis of Fe(III)-hydroxyl complexes as sources of OH radicals in clouds, fog and rain. *Atmospheric Environment* **24**, 79-89.

Feng, Q.Z., Zhao, L.X., Yan, W., Lin, J.M., Zheng, Z.X., 2009. Molecularly imprinted solid-phase extraction combined with high performance liquid chromatography for analysis of phenolic compounds from environmental water samples. *Journal of Hazardous Materials* **167**, 282-288.

Feng, W., Nansheng, D., 2000. Photochemistry of hydrolytic iron (III) species and photoinduced degradation of organic compounds. A mini-review. *Chemosphere* **41**, 1137-1147.

Fenton, H.J.H., 1894. The oxidation of tartaric acid in presence of iron. *Proceedings of the Chemical Society* **10**, 157-158.

Fenton, H. J. H., 1899. Oxidation of certain organic acids in the presence of ferrous salts. *Proceedings of the Chemical Society* **15**, 224-228.

Fentona, R., Chemizmu, K.D., 2009. Fenton reaction-Controversy concerning the chemistry. *Ecological Chemistry and Engineering S* **16** (3), 347-358.

Fernández, P., Blanco, J., Sichel, C., Malato, S., 2005. Water disinfection by solar photocatalysis using compound parabolic collectors. *Catalysis Today* **101**, 345-352.

Ferreira da Silva, M., Tiago, I., Verissimo, A., Boaventura, R.A.R., Nunes, O.C., Manaia, C.M., 2006. Antibiotic resistance of *enterococci* and related bacteria in an urban wastewater treatment plant. *FEMS Microbial Ecology* **55**, 322-329.

Figueroa, R.A., MacKay, A.A., 2005. Sorption of Oxytetracycline to Iron Oxides and Iron Oxide-Rich Soils. *Environmental Science and Technology* **39**, 6664-6671

Flynn, C.M., 1984. Hydrolysis of inorganic iron(III) salts. *Chemical Reviews* **84** (1), 31-41.

Fresta, M., Furneri, P.M., Mezzasalma, E., Nicolosi V.M., Puglisi, G., 1996. Correlation of trimethoprim and brodimoprim physicochemical and lipid membrane interaction properties with their accumulation in human neutrophils. *Antimicrobial agents and chemotherapy* **40**, 2865-2873.

Froehner, K., Backhaus, T., Grimme, L.H., 2000. Bioassays with *Vibrio fischeri* for the assessment of delayed toxicity. *Chemosphere* **40**, 821-828.

Fuentes, A., Lorens, M., Saez, J., Aguilar, M.I., Pérez-Marin, A.B., Ortuno, J.F., Meseguer, V.F., 2006. Ecotoxicity, phytotoxicity and extractability of heavy metals from different stabilized sewage sludges. *Environmental Pollution* **143**, 355-360.

Gan, D., Jia, M., Vaughan, P.P., Falvey, D.E., Blough, N.V., 2008. Aqueous photochemistry of methyl-benzoquinone. *Journal of Physical Chemistry A* **112**, 2803-2812.

Garcia-Montano, J., Torrades, F., Garcıa-Hortal, J.A., Domenech, X., Peral, J., 2006. Degradation of Procion Red H-E7B reactive dye by coupling a photo-Fenton system with a sequencing batch reactor. *Journal of Hazardous Materials* **B134**, 220-229.

Gernjak, W., Fuerhacker, M., Fernández-Ibanez P., Blanco, J., Malato, S., 2006. Solar photo-Fenton treatment-Process parameters and process control. *Applied Catalysis B: Environmental* **64**, 121-130.

Ghosh, B.C., Deb, N., Mukherjee, A.K., 2010. Determination of individual proton affinities of ofloxacin from its UV-Vis absorption, fluorescence and charge-transfer spectra: Effect of inclusion in cyclodextrin on the proton affinities. *Journal of Physical Chemistry* **B114**, 9862-9871.

Giraldo, A.L., Penuela, G.A., Torres-Palma, R.A., Pino, N.J., Palominos, R.A., Mansilla, H.D., 2010. Degradation of the antibiotic oxolinic acid by photocatalysis with TiO_2 in suspension. *Water Research* **44**, 5158-5167.

Gob, S., Oliveros, E., Bossmann, S.H., Braun, A.M., Nascimento, C.A.O., Guardani, R., 2001. Optimal experimental design and artificial neural networks applied to the photochemically enhanced Fenton reaction. *Water Science and Technology* **44** (5), 339-345.

Göbel, A., Thomsen, A., McArdell, C.S., Joss, A., Giger, W., 2005. Occurrence and sorption behavior of sulfonamides, macrolides, and trimethoprim in activated sludge treatment. *Environmental Science and Technology* **39**, 3981-3989.

Göbel, A., McArdell, C.S., Joss, A., Siegrist, H, Giger, W., 2007. Fate of sulfonamides, macrolides, and trimethoprim in different wastewater treatment technologies. *Science of the Total Environment* **372**, 361-371.

Goldstein, S., Meyerstein, D., Czapski, G., 1993. The Fenton reagents. *Free Radical Biology & Medicine* **15**, 435-445.

Golet, E.M., Alder, A.C., Giger, W., 2002. Environmental exposure and risk assessment of fluoroquinolone antibacterial agents in wastewater and river water

of the Glatt Vally watershed, Switzerland. *Environmental Science and Technology* **36**, 3645-3651.

Golet, E.M., Xifra, I., Siegrift, H., Alder, A.C., Giger, W., 2003. Environmental exposure assessment of fluoroquinolone antibacterial agents from sewage to soil. *Environmental Science and Technology* **37**, 3243-3249.

Goslich, R., Dillert, R., Bahnemann, D., 1997. Solar water treatment: Principles and reactors. *Water Science and Technology* **35** (4), 137-148.

Goswami, D.Y., 1997. A review of engineering developments of aquoues phase solar photocatalytic detoxification and disinfection processes. *Journal of Solar Energy Engineering* **119** (2), 101-107.

Grabow, W.O.K., van Zyl, M., 1976. Behavior in conventional sewage purification processes of coliform bacteria with transferable or non-transferable drug-resistance, *Water Research* **10**, 717-723.

Gracia-Lor, E., Sancho, J.V., Hernández, F., 2010. Simultaneous determination of acidic, neutral and basic pharmaceuticals in urban wastewater by ultra high-pressure liquid chromatography-tandem mass spectrometry. *Journal of Chromatography A*, **1217**, 622-632.

Gros, M., Petrovíc, M., Barceló, D., 2006. Development of a multi-residue analytical methodology based on liquid chromatography-tandem mass spectrometry (LC-MS/MS) for screening and trace level determination of pharmaceuticals in surface and wastewaters. *Talanta* **70**, 678-690.

Guardabassi, L., Wong, D.M.A., Dalsgaard, A., 2002. The effects of tertiary wastewater treatment on the prevalence of antimicrobialresistant bacteria. *Water Research* **36**, 1955-1964

Gulkowska, A., Leung, H.W., So, M.K., Taniyasu, S., Yamashita, N., Yeung, L.W.Y., Richardson, B.J., Lei, A.P., Giesy, J.P., Lam, P.K.S., 2008. Removal of antibiotics from wastewater by sewage treatment facilities in Hongkong and Shenzhen, China. *Water Research* **42**, 395-403.

Haber, F., Willstatter, R., 1931. Unpaarigkeit und Radikalketten im Reaktionsmchanismus organischer und enzymatischer. *Ber Deutsch Chem Ges* **64**, 2844-2856.

Haber, F., Weiss, J.J., 1934. The catalytic decomposition of H_2O_2 by iron salts. *Proceedings of the Royal Society A* **147**,332-351.

Hamilton-Miller, J.M.T., 1988. Reversal of activity of trimethoprim against Gram-positive cocci by thymidine, thymine and "folates". *Journal of Antimicrobial Chemotherapy* **22**, 35-39.

Hapeshi, E., Achilleos, A., Vasquez, M.I., Michael, C., Xekoukoulotakis, N.P., Mantzavinos, D., Kassinos, D., 2010. Drugs degrading photocatalytically: Kinetics and mechanisms of ofloxacin and atenolol removal on titania suspensions. *Water Research* **44** (6), 1737-1746.

Hayakawa, I., Atarashi, S., Yokohama, S., Imamura, M., Sakano, K.I., Furukawa, M., 1986. Synthesis and antibacterial activities of optically active ofloxacin. *Antimicrobial Agents and Chemotherapy* **29**, 163-164.

Hennion, M.C., 1999. Solid-phase extraction: method development, sorbents, and coupling with liquid chromatography. *Journal of Chromatography A* **856**, 3-54.

Hernandez, F., Portoles, T., Pitarch, E., Lopez, F.J., Beltran, J., Vazquez, C., 2005. Potential of gas chromatography coupled to triple quadrupole mass spectrometry

for quantification and confirmation of organohalogen xenoestrogen compounds in human breast tissues. *Analytical Chemistry* **77**, 7662-7672.

Hernández-Sancho, F., Molinos-Senante, M., Sala-Garrido, R., 2010. Economic valuation of environmental benefits from wastewater treatment processes: An empirical approach for Spain. *Science of the Total Environment* **408**, 953-957.

Hernando, M.D., Fernández-Alba, A.R., Tauler, R., D. Barceló, D., 2005. Toxicity assays applied to wastewater treatment. *Talanta* **65**, 358-366.

Hernando, M.D., Mezcua, M., Fernandez-Alba, A.R., Barcelo, D., 2006. Environmental risk assessment of pharmaceutical residues in wastewater effluents, surfacewaters and sediments. Talanta 1st Swift-WFD workshop on validation of Robustness of sensors and bioassays for Screening Pollutants-1st SWIFT-WFD 2004 **69**, 334-342.

Hernando, M.D., Gómez, M.J., Agüera, A., Fernández-Alba, A.R., 2007. LC-MS analysis of basic pharmaceuticals (beta-blockers and anti-ulcer agents) in wastewater and surface water. *Trend of Analytical Chemistry* **26**, 581-594.

Herrmann, J.M, Guillard, C., Pichat, P., 1993. Heterogeneous photocatalysis: an emerging technology for water treatment. *Catalysis Today* **7**, 7-20.

Herrmann, J.M., 2010. Fundamentals and misconceptions in photocatalysis. *Journal of Photochemistry and Photobiology A: Chemistry* **216**, 85-93.

Himmelfarb, M.Z., Zikk, D., Rapoport, Y., Redianu, C., Shalit, I., 1993. Granulation tissue concentrations of ofloxacin after oral administration in invasive external otitis. *European Archives of Otorhinolaryngology* **250**, 15-17.

Himmelsbach, M., Buchberger, W., Klampfl, C.W., 2006. Determination of antidepressants in surface and waste water samples by capillary electrophoresis

with electrospray ionization mass spectrometric detection after preconcentration using off-line solid-phase extraction. *Electrophoresis* **27,** 1220-1226.

Hirsch, R., Ternes, T., Haberer, K., Kratz, K.L., 1999. Occurrence of antibiotics in the aquatic environment. *Science of the Total Environmental* **225**, 109-118.

Hitchins, G.H., 1973. Mechanism of action of trimethoprim-sulfamethoxazole. *Journal of Infectious Diseases* **128**, 433-436.

Hochstrat , R., Wintgens, T., 2003. AQUAREC, Report on Milestone M3.I, Draft of wastewater reuse potential estimation, Interim report.

Hoffmann, E., Stroobant, V. Mass spectrometry. Principles and Applications. 3rd edition. Wiley, 2007.

Hoffmann, M.R., Martin, S.T., Choi, W., Bahnemann, D.W., 1995. Environmental applications of semiconductor photocatalysis. *Chemical Reviews* **95**, 69-96.

Homem, V., Santos, L., 2011. Degradation and removal methods of antibiotics from aqueous matrices-A review. *Journal of Environmental Management* **92** (10), 1-44.

Hooper, D.C., 2000. Mechanisms of Action and Resistance of Older and Newer Fluoroquinolones. *Clinical Infectious Diseases* **31**, 24-28.

Hu, L., Martin, H.M., Strathmann, T.J., 2010. Oxidation kinetics of antibiotics during water treatment with potassium permanganate. *Environmental Science and Technology* **44**, 6416-6422.

Huang, J.J., Hu, H.Y., Tang, F., Li, Y., Lu, S.Q., Lu, Y., 2011. Inactivation and reactivation of antibiotic-resistant bacteria by chlorination in secondary effluents of a municipal wastewater treatment plant. *Water Research* **45**, 2775-2781.

Huber, M.M., Gobel, A., Joss, A., Hermann, N., Loffler, D., McArdell, C.S., Ried, A., Siegrist, H., Ternes, T.A., von Gunten, U., 2005. Oxidation of pharmaceuticals during ozonation of municipal wastewater effluents: A pilot study. *Environmental Science and Technology* **39**, 4290-4299.

Huston, P.L., Pignatello, J.J., 1999. Degradation of selected pesticide active ingredients and commercial formulations in water by the photo-assisted Fenton reaction. *Water Research* **33** (5), 1238-1246.

Ibanez, M., Guerrero, C., Sancho, J.V., Hernandez, F., 2009. Screening of antibiotics in surface and wastewater samples by ultra-high-pressure liquid chromatography coupled to hybrid quadrupole time-of-flight mass spectrometry. *Journal of Chromatography A* **1216**, 2529-2539.

Ikehata, K., Naghashkar, N.J., Ei-Din, M.G., 2010. Degradation of aqueous pharmaceuticals by ozonation and advanced oxidation processes: a review. *Ozone: Science & Engineering* **28** (6), 353-414.

Isidori, M., Lavorgna, M., Nardelli, A., Pascarella, L., Parrella, A., 2005. Toxic and genotoxic evaluation of six antibiotics on non-target organisms. *Science of the Total Environment* **346**, 87-98.

ISO 11348-3:2007. Water quality-Determination of the inhibitory effect of water samples on the light emission of *Vibrio fischeri* (Luminescent bacteria test)-Part 3: Method using freeze-dried bacteria.

ISO 6332:1988. Water quality-Determination of iron-Spectrometric method using 1,10-phenanthroline.

ISO 6341:1996. Water quality-Determination of the inhibition of the mobility of *Daphnia magna Straus* (Cladocera, Crustacea)-Acute toxicity test.

ISO 8245:2000. Water quality-Guidelines for the determination of total organic carbon (TOC) and dissolved organic carbon (DOC).

Jennings, V.L.K., Rayner-Brandes, M.H., Bird, D.J., 2001. Assessing chemical toxicity with the bioluminescent photobacterium (*Vibrio fischeri*): A comparison of three commercial systems. *Water Research* **35**, 3448-3456.

Jeong, J., Song, W., Cooper, W.J., Jung, J., Greaves, J., 2010. Degradation of tetracycline antibiotics: Mechanisms and kinetic studies for advanced oxidation/reduction processes. *Chemosphere* **78**, 533-540.

Ji, L.G., Chen, W., Duan, L., Zhu, D., 2009. Mechanisms for strong adsorption of tetracycline to carbon nanotubes: A comparative study using activated carbon and graphite as adsorbents. *Environmental Science and Technology* **43**, 2322-2327.

Jiao, S., Zheng, S., Yin, D.,Wang, L., Chen, L., 2008. Aqueous photolysis of tetracycline and toxicity of photocatalytic products to luminescent bacteria. *Chemosphere* **73**, 377-382.

Jin, H., Kumar, A.P., Paik, D., Ha, K., Yoo, Y., Lee, Y., 2010. Trace analysis of tetracycline antibiotics in human urine using UPLC-QToF mass spectrometry. *Microchemical Journal* **94**, 139-147.

Jones, O.A.H., Voulvoulis, N., Lester, J.N., 2007. The occurrence and removal of selected pharmaceutical compounds in a sewage treatment works utilising activated sludge treatment. *Environmental Pollution* **145** (3), 738-744.

Jordá, L.S.J., Martín, M.M.B., Gómez, E.O., Reina, A.C., Sánchez, I.M.R., López, J.L.C., Pérez, J.A.S., 2011. Economic evaluation of the photo-Fenton process. Mineralization level and reaction time: The keys for increasing plant efficiency. *Journal of Hazardous Materials* **186**, 1924-1929.

Joss, A., Kellera, E., Aldera, A.C., Gobel, A., McArdell, C.S., Ternes, T., Siegrista, H., 2005. Removal of pharmaceuticals and fragrances in biological wastewater treatment. *Water Research* **39**, 3139-3152.

Kanay, H., 1983. Drug-resistance and distribution of conjugative R-plasmids in E. coli strains isolated from healthy adult animals and humans. *Japanese Journal of Veterinary Science* **45**, 171-178.

Karthikeyan, K.G., Meyer, M.T., 2006. Occurrence of antibiotics in wastewater treatment facilities in Wisconsin, USA. *Science of the Total Environment* **361**, 196-207.

Kasprzyk-Hordern, B., Dinsdale, R.M., Guwy, A.J., 2007. Multi-residue method for the determination of basic/neutral pharmaceuticals and illicit drugs in surface water by solid-phase extraction and ultra performance liquid chromatography-positive electrospray ionisation tandem mass spectrometry. *Journal of Chromatography A* **1161**, 132-145.

Kasprzyk-Hordern, B., Dinsdale, R.M., Guwy, A.J., 2008. The effect of signal suppression and mobile phase composition on the simultaneous analysis of multiple classes of acidic/neutral pharmaceuticals and personal care products in surface water by solid-phase extraction and ultra performance liquid chromatography-negative electrospray tandem mass spectrometry. *Talanta* **74**, 1299-1312.

Kavitha, V., Palanivelu, K., 2004. The role of ferrous ion in Fenton and photo-Fenton processes for the degradation of phenol. *Chemosphere* **55**, 1235-1243.

Keyer, K., James, A.I., 1996. Superoxide accelerates DNA damage by elevating free-iron levels. *Proceedings of the National Academy of Sciences of the United States of America* **93**, 13635-13640.

Khan, S.J., Ongerth, J.E., 2005. Occurrence and removal of pharmaceuticals at an Australian sewage treatment plant. *Water* **32** (4), 80-85.

Kim, Y., Choi, K., Jung, J., Park, S., Kim, P.G., Park, J., 2007. Aquatic toxicity of acetaminophen, carbamazepine, cimetidine, diltiazem and six major sulfonamides, and their potential ecological risks in Korea. *Environment International* **33**, 370-375.

Kim, I., Yamashita, N., Tanaka, H., 2009. Performance of UV and UV/H_2O_2 processes for the removal of pharmaceuticals detected in secondary effluent of a sewage treatment plant in Japan. Journal of Hazardous Materials 166, 1134-1140.

Kimura, K., Toshima, S., Amy, G., Watanabe, Y., 2004. Rejection of neutral endocrine disrupting compounds (EDCs) and pharmaceutical active compounds (PhACs) by RO membranes. *Journal of Membrane Science* **245**, 71-78.

Kitteringham, N.R., Jenkins, R.E., Lane, C.S., Elliott, V.L., Parka, B.K. 2009. Multiple reaction monitoring for quantitative biomarker analysis in proteomics and metabolomics. *Journal of Chromatography B*, **877**, 1229-1239.

Kiwi, J., Lopez, A., Nadtochenko, V., 2000. Mechanism and kinetics of the OH-radical intervention during Fenton oxidation in the presence of a significant amount of radical scavenger (Cl^-). *Environmental Science and Technology* **34**, 2162-2168.

Klamerth, N., Miranda, N., Malato, S., Agüera, A., Fernández-Alba, A. R., Maldonado, M. I., Coronado, J .M., 2009. Degradation of emerging contaminants

at low concentrations in MWTPs effluents with mild solar photo-Fenton and TiO_2. *Catalysis Today* **144**, 124-130.

Klamerth, N., Rizzo, L., Malato, S., Maldonado, M. I., Aguera, A., Fernández-Alba, A.R., 2010. Degradation of fifteen emerging contaminants at μg L^{-1} initial concentrations by mild solar photo-Fenton in MWTP effluents. *Water Research* **44**, 545-554.

Klamerth, N., Malato, S., Maldonado, M.I., Agüera, A., Fernández-Alba, A., 2011. Modified photo-Fenton for degradation of emerging contaminants in municipal wastewater effluents. *Catalysis Today* **161**, 241-246.

Klavarioti, M., Mantzavinos, D., Kassinos, D., 2009. Removal of residual pharmaceuticals from aqueous systems by advanced oxidation processes. *Environment International* **35**, 402-417.

Klooster, G.A.E., Kolker, H.J., Woutersen-van Nijnanten, F.M.A., 1992. Determination of trimethoprim and its oxidative metabolites in cell culture media and microsomal incubation mixtures by high-performance liquid chromatography. *Journal of Chromatography B* **579** (2), 355-360.

Knackmuss, H.J., 1996. Basic knowledge and perspectives of bioelimination of xenobiotic compounds. Journal of Biotechnology 51 (1996) 287-295.

Kong, W.D., Zhu, Y.G., Liang, Y.C., Zhang, J., Smith, F.A., Yang, M., 2007. Uptake of oxytetracycline and its phytotoxicity to alfalfa (*Medicago sativa* L.). *Environmental Pollution* **147** (1), 87-193.

Konstantinou, I.K., Albanis, T.A., 2004. TiO_2-assisted photocatalytic degradation of azo dyes in aqueous solution: kinetic and mechanistic investigations A review. *Applied Catalysis B: Environmental* **49**, 1-14.

Konstantinou, I.K., Zarkadis, A.K., Albanis, T.A., 2001. Organic compounds in the environment photodegradation of selected herbicides in various natural waters and soils under environmental conditions. *Journal of Environmental Quality* **30**, 121-130.

Koo, G.N., Lee, B.H., Han, S.W., Kim, S.K., Lee, H.M., 2008. Molecular dynamics study on the binding of S- and R-Ofloxacin to $[d(ATAGCGCTAT)]_2$ oligonucleotide: Effects of protonation states. *Bullettin of the Korean Chemical Society* **29** (11), 2103-2108.

Kormann, C., Bahnemann, D.W., Hoffmann, M.R., 1991. Photolysis of chloroform and other organic molecules in aqueous TiO_2 suspensions. *Environmental Science and Technology* **25**, 494-500.

Korten, V., Huang, W.M., Murray, B.E., 1994. Analysis by PCR and direct DNA sequencing of gyrA mutations associated with fluoroquinolone resistance in *Enterococcus faecalis*. *Antimicrobial Agents and Chemotherapy* **38** (9), 2091-2094.

Kosutíc, K., Dolar, D., Asperger, D., Kunst, B., 2007. Removal of antibiotics from a model wastewater by RO/NF membranes. *Separation and Purification Technology* **53**, 244-249.

Kremer, M.L., 1999. Mechanism of the Fenton reaction. Evidence for a new intermediate. *Physical Chemistry Chemical Physics* **1**, 3595-3605.

Kritikos, D.E., Xekoukoulotakis, N.P., Psillakis, E., Mantzavinos, D., 2007. Photocatalytic degradation of reactive black 5 in aqueous solutions: Effect of operating conditions and coupling with ultrasound irradiation. *Water Research* **41**, 2236-2246.

Krýsová, H., Jirkovský, J., Krýsa, J., Mailhot, G., Bolte, M., 2003. Comparative kinetic study of atrazine photodegradation in aqueous $Fe(ClO_4)_3$ solutions and TiO_2 suspensions. Applied Catalysis B: Environmental 40, 1-12.

Kulshrestha, P.J., Giese, R.F., Aga, D.S., 2004. Investigating the Molecular Interactions of Oxytetracycline in Clay and Organic Matter: Insights on Factors affecting its mobility in soil. *Environmental Science and Technology* **38**, 4097-4105.

Kumar, K.V., Porkodi, K., Rocha, F., 2008. Langmuir-Hinshelwood kinetics-A theoretical study. *Catalysis Communications* **9**, 82-84.

Kumarasamy, K.K., Toleman, M.A., Walsh, T.R., Bagaria, J., Butt, F., Balakrishnan, R., Chaudhary, U., Doumith, M., Giske, C.G., Irfan, S., Krishnan, P., Kumar, A.V., Maharjan, S., Mushtaq, S., Noorie, T., Paterson, D.L., Pearson, A., Perry, C., Pike, R., Rao, B., Ray, U., Sarma, J.B., Sharma, M., Sheridan, E., Thirunarayan, M.A., Turton, J., Upadhyay, S., Warner, M., Welfare, W., Livermore, D.M., Woodford, N., 2010. Emergence of a new antibiotic resistance mechanism in India, Pakistan, and the UK: a molecular, biological, and epidemiological study. *The Lancet Infectious Diseases* **10**, 597-602.

Kümmerer, K., 2004. Resistance in the environment. *Journal of Antimicrobial Chemotherapy* **54**, 311-320.

Kümmerer, K., 2009. Antibiotics in the aquatic environment-A review-Part I. *Chemosphere* **75**, 417-434.

Kuo, W.S., Wu, L.N., 2010. Fenton degradation of 4-chlorophenol contaminated water promoted by solar irradiation. *Solar Energy* **84**, 59-65.

Kusari, S., Prabhakaran, D., Lamshöft, M., Spiteller, M., 2009. In vitro residual antibacterial activity of difloxacin, sarafloxacin and their photoproducts after photolysis in water. *Environmental Pollution* **157**, 2722-2730.

Lambropoulou, D.A., Konstantinou, I.K., Albanis, T.A., Fernandez-Alba, A.R., 2011. Photocatalytic degradation of the fungicide Fenhexamid in aqueous TiO_2suspensions: Identification of intermediates products and reaction pathways. *Chemosphere* **83**, 367-378.

Lanao, M., Ormad, M.P., Mosteo, R., Ovelleiro, J.L., 2012. Inactivation of *Enterococcus* sp. by photolysis and TiO_2 photocatalysis with H_2O_2 in natural water. *Solar Energy* **86**, 619-625.

Lapertot, M., Pulgarín, C., Fernández-Ibáñez, P., Maldonado, M.I., Pérez-Estrada, L., Oller, I., Gernjak, W., Malato, S., 2006. Enhancing biodegradability of priority substances (pesticides) by solar photo-Fenton. *Water Research* **40**, 1086-1094.

Larson, R.A., Schlauch, M.B., Marley, K.A., 1991. Ferric ion promoted photodecomposition of triazines. *Journal of Agriculture and Food Chemistry* **39** (11), 2057-2061.

Lee, C., Yoon, J., 2004. Temperature dependence of hydroxyl radical formation in the hv/Fe^{3+}/H_2O_2 and Fe^{3+}/H_2O_2 systems. *Chemosphere* **56**, 923-934.

Lee, H., Peart, T.E., Svoboda, M.L., 2007. Determination of ofloxacin, norfloxacin, and ciprofloxacin in sewage by selective solid-phase extraction, liquid chromatography with fluorescence detection, and liquid chromatography-tandem mass spectrometry. *Journal of Chromatography A* **1139**, 45-52.

Legrini, O., Oliveros, E., Braun, A.M., 1993. Photochemical processes for water treatment. *Chemical Reviews* **93** (2), 671-698.

Le-Minh, N., Khan, S.J., Drewes, J.E., Stuetz, R.M., 2010. Fate of antibiotics during municipal water recycling treatment processes. *Water Research* **44**, 4295-4323.

Lhiaubet-Vallet, V., Bosca, F., Miranda, M.A., 2009. Photosensitized DNA damage: the case of fluoroquinolones. *Photochemistry and Photobiology* **85**, 861-868.

Li, B., Zhang, T., 2011. Mass flows and removal of antibiotics in two municipal wastewater treatment plants. *Chemosphere* **83** (9), 1284-1289.

Li, B., Zhang, T., Xua, Z., Fang, H.H.P., 2009. Rapid analysis of 21 antibiotics of multiple classes in municipal wastewater using ultra performance liquid chromatography-tandem mass spectrometry. *Analytica Chimica Acta* **645**, 64-72.

Li, S., Li, X., Wang, D., 2004. Membrane (RO-UF) filtration for antibiotic wastewater treatment and recovery of antibiotics. *Separation and Purification Technology* **34**, 109-114.

Li, N., Zhang, Y.H., Xiong, X.L., Li, Z.G., Jin, X.H., Wu, Y.N., 2005. Study of the physicochemical properties of trimethoprim with β-cyclodextrin in solution. *Journal of Pharmaceutical and Biomedical Analysis* **38**, 370-374.

Li, W., Nanaboina, V., Zhou, Q., Korshin, G.V., 2012. Effects of Fenton treatment on the properties of effluent organic matter and their relationships with the degradation of pharmaceuticals and personal care products. *Water Research* **46**, 403-412.

Liang, J., Komarov, S., Hayashi, N., Kasai, E., 2007. Improvement in sonochemical degradation of 4-chlorophenol by combined use of Fenton-like reagents. *Ultrasonics Sonochemistry* **14**, 201-207.

Lin, A.Y.C., Yu, T.H., Lateef, S.K., 2009. Removal of pharmaceuticals in secondary wastewater treatment processes in Taiwan. *Journal of Hazardous Materials* **167**, 1163-1169.

Lin, A.Y.C., Lin, C., Chiou ,J., Hong, P.K.A., 2009b. O_3 and O_3/H_2O_2 treatment of sulfonamide and macrolide antibiotics in wastewater. *Journal of Hazardous Materials* **171**, 452-458.

Lin, K., Yuan, D., Chen, M., Deng, Y., 2004. Kinetics and products of photo-Fenton degradation of triazophos. *Journal of Agriculture and Food Chemistry* **52**, 7614-7620.

Lindberg, R.H., Björklundb, K., Rendahl, P., Johansson, M.I., Tysklind, M., Andersson, B.A.V., 2007. Environmental risk assessment of antibiotics in the Swedish environment with emphasis on sewage treatment plants. *Water Research* 41, 613-619.

Lindberg, R.H., Wennberg, P., Johansson, M.I., Tysklind, M., Andersson, B.A.V., 2005. Screening of human antibiotic substances and determination of weekly mass flows in five sewage treatment plants in Sweden. *Environmental Science and Technology* **39**, 3421-3429.

Lindsey, M.E., Tarr, M.A., 2000. Inhibition of Hydroxyl Radical Reaction with Aromatics by Dissolved Natural Organic Matter. *Environmental Science and Technology* **34**, 444-449.

Lindsey, M.E., Tarr, M.A., 2000. Quantitation of hydroxyl radical during Fenton oxidation following a single addition of iron and peroxide. *Chemosphere* **41**, 409-417.

Linsebigler, A.L., Lu, G., Yates, J.T., 1995. Photocatalysis on TiO_2 surfaces: Principles, mechanisms and selected results. *Chemical Reviews* **95**, 735-758.

Litter, M.I., 2005. Introduction to photochemical advanced oxidation processes for water treatment. *Environmental Chemistry* **2**, Part M, 325-366.

Liu, F., Ying, G., Tao, R., Zhao, J.L., Yang, J.F., Zhao, L.F., 2009. Effects of six selected antibiotics on plant growth and soil microbial and enzymatic activities. *Environmental Pollution* **157**, 1636-1642.

Liu, Y., Zhang, X., Xue, X., Liang, X., 2008. Improved concentration technique for purified preparative fractions via solid phase extraction using oasis HLB as sorbent. *Journal of Biotechnology* **136**, S83.

Loftin, K.A., Adams, C.D., Meyer, M.T., Surampalli, R., 2008. Effects of ionic strength, temperature, and pH on degradation of selected antibiotics. *Journal of Environmental Quality* **37**, 378-386.

Lucas, M.S., Peres, J.A., 2006. Decolorization of the azo dye Reactive Black 5 by Fenton and photo-Fenton oxidation. *Dyes and Pigments* **71**, 236-244.

Luczkiewicz, A., Jankowska, K., Fudala-Ksiazek, Olanczuk-Neyman, K., 2010. Antimicrobial resistance of fecal indicators in municipal wastewater treatment plant. *Water Research* **44**, 5089-5097.

Luo, X., Zheng, Z., Greaves, J., Cooper, W.J., Song, W., 2012. Trimethoprim: Kinetic and mechanistic considerations in photochemical environmental fate and AOP treatment. *Water Research* **46**, 1327-1336.

Lykkeberg, A.K., Sorensen, B.H., Cornett, C., Tjornelund, J., Hansen, S.H., 2004. Quantitative analysis of oxytetracycline and its impurities by LC-MS-MS, Journal of *Pharmaceutical and Biomedical Analysis* **34**, 325-332.

Macrì, A., Stazi, A.V., Dojmi di Delupis, G., 1988. Acute toxicity of furazolidone on *Artemia salina*, *Daphnia magna*, and *Culex pipiens molestus* larvae. *Ecotoxicology and Environmental Safety* **16**, 90-94.

Mahamuni, N.N., Adewuyi, Y.G., 2010. Advanced oxidation processes (AOPs) involving ultrasound for waste water treatment: A review with emphasis on cost estimation. *Ultrasonics Sonochemistry* **17**, 990-1003.

Malato, S., Blanco, J., Maldonado, M.I., Fernández-Ibáñez, P., Campos, A., 2000. Optimising solar photocatalytic mineralisation of pesticides by adding inorganic oxidising species; application to the recycling of pesticide containers. *Applied Catalysis B: Environmental* **28**, 163-174.

Malato, S., Blanco, J., Maldonado, M.I., Oller, I., Gernjak, W., Pérez-Estrada, L., 2007. Coupling solar photo-Fenton and biotreatment at industrial scale: Main results of a demonstration plant. *Journal of Hazardous Materials* **146**, 440-446.

Malato, S., Fernández-Ibáñez, P., Maldonado, M.I., Blanco, J., Gernjak, W., 2009. Decontamination and disinfection of water by solar photocatalysis: Recent overview and trends. *Catalysis Today* **147**, 1-59.

Maldonado, M. I., Passarinho, P. C., Oller, I., Gernjak, W., Fernández, P., Blanco, J., Malato, S., 2007. Photocatalytic degradation of EU priority substances: A comparison between TiO_2 and Fenton plus photo-Fenton in a solar pilot plant. *Journal of Photochemistry and Photobiology A* **185**, 354-363.

Manaia, C.M., Novo, A., Coelho, B., Nunes, O.C., 2010. Ciprofloxacin resistance in domestic wastewater treatment plants. *Water Air Soil Pollution* **208**, 335-343.

Mantzavinos, D., Sahibzada, M., Livingston, A.G., Metcalfe, I.S., Hellgardt, K., 1999. Wastewater treatment: wet air oxidation as a precursor to biological treatment. *Catalysis Today* **53**, 93-106.

Martinez, J.L., 2009. Environmental pollution by antibiotics and by antibiotic resistance determinants. *Environmental Pollution* **157**, 2893-2902.

Massey, L.B., Haggard, B.E., Galloway, J.M., Loftin, K.A., Meyer, M.T., Green, W.R., 2010. Antibiotic fate and transport in three effluent-dominated Ozark streams. *Ecological Engineering* **36**, 930-938.

McArdell, C.S., Molnar, E., Suter, M.J.F., Giger, W., 2003. Occurrence and fate of macrolide antibiotics in wastewater treatment plants and in the Glatt Valley Watershed, Switzerland. *Environmental Science Technology* **37**, 5479-5486.

Melero, J.A., Calleja, G., Martinez, F., Molina, R., Pariente, M.I., 2007. Nanocomposite Fe_2O_3/SBA-15: An efficient and stable catalyst for the catalytic wet peroxidation of phenolic aqueous solutions. *Chemical Engineering Journal* **131**, 245-256.

Mendez-Arriaga, F., Esplugas, S., Gime, J., 2010. Degradation of the emerging contaminant ibuprofen in water by photo-Fenton. *Water Research* **44**, 589-595.

Mengelers, M.J.B., Oorsprong, M.B.M, Kuiper, H.A, Aerts, M.M.L, Van Gogh, E.R, Van Miert, A.S.J.P.A.M, 1989. Determination of sulfadimethoxine, sulfamethoxazole, trimethoprim and their main metabolites in porcine plasma by column switching HPLC. *Journal of Pharmaceutical & Biomedical Analysis* **7** (12), 1765-1776.

Merz, J.H., Waters, W.A., 1947. The mechanism of oxidation of alcohols with Fenton's reagent. *Discussion of the Faraday Society* **2**, 179-188.

Miao, X.S., Bishay, F., Chen, M., Metcalfe, C.D., 2004. Occurrence of antimicrobials in the final effluents of wastewater treatment plants in Canada. *Environmental Science and Technology* **38** (13), 3533-3541.

Michael, I., Hapeshi, E., Michael, C., Fatta-Kassinos, D., 2010. Solar Fenton and solar TiO_2 catalytic treatment of ofloxacin in secondary treated effluents: Evaluation of operational and kinetic parameters. *Water Research* **44**, 5450-5462.

Migliore, L., Cozzolino, S., Fiori, M., 2003. Phytotoxicity to and uptake of enrofloxacin in crop plants. *Chemosphere* **52**, 1233-1244.

Miller, C.M., Valentine, R.L., Roehl, M.E., Alvarez, P.J.J., 1996. Chemical and microbiological assessment of pendimethalin-contaminated soil after treatment with Fenton's reagent. *Water Research* **30**, 2579-2586.

Moncayo-Lasso, A., Pulgarin, C., Benítеza, N., 2008. Degradation of DBPs' precursors in river water before and after slow sand filtration by photo-Fenton process at pH 5 in a solar CPC reactor. *Water Research* **42**, 4125-4132.

Monk, J.P, Campoli-Richards, D.M., 1987. Ofloxacin. A review of its antibacterial activity, pharmacokinetic properties and therapeutic use. *Drugs* **33** (4), 346-391.

Morse, A., Jackson, A., 2004. Fate of amoxicillin in two water reclamation systems. *Water Air and Soil Pollution* **157** (1-4), 117-132.

Munter, R., 2001. Advanced oxidation processes-current status and prospects. *Proceedings of Estonian Academy of Sciences Chemistry* **50**, 59-80.

Murray, B.E., 1989. Antibiotic treatment of enterococcal infection. *Antimicrobial Agents and Chemotherapy* **33**, 1411.

Muruganandham, M., Swaminathan, M., 2004. Decolourisation of Reactive Orange 4 by Fenton and photo-Fenton oxidation technology. *Dyes and Pigments* **63**, 315-321.

Naddeo, V., Meric, S., Kassinos, D., Belgiorno, V., Guida, M., 2009. Fate of pharmaceuticals in contaminated urban wastewater effluent under ultrasonic irradiation. *Water Research* **43**, 4019-4027.

Nakada, N., Shinohara, H., Murata, A., Kiri, K., Managaki, S., Sato, N., Takada, H., 2007. Removal of selected pharmaceuticals and personal care products (PPCPs) and endocrine-disrupting chemicals (EDCs) during sand filtration and ozonation at a municipal sewage treatment plant. *Water Research* **41**, 4373-4382.

Nakanishi, N., Yoshida, S., Wakebe, H., Inoue, M., Mitsuhashi, S., 1991. Mechanisms of Clinical Resistance to Fluoroquinolones in *Enterococcus faecalis*. *Antimicrobial Agents and Chemotherapy* **35** (6), 1053-1059.

National prescriptions, National Organization for Medicines, Athens, Greece, 2000.

Nau, R., Kinzig, M., Dreyhaupt, T., Kolenda, H., Sorgel, F., Prange, H.W., 1994. Kinetics of ofloxacin and its metabolites in cerebrospinal fluid after a single intravenous infusion of 400 milligrams of ofloxacin. *Antimicrobial Agents and Chemotherapy* **38** (8), 1849-1853.

Navarro, S., Fenoll, J., Vela, N., Ruiz, E., Navarro, G., 2011. Removal of ten pesticides from leaching water at pilot plant scale by photo-Fenton treatment. *Chemical Engineering Journal* **167**, 42-49.

Neyens, E., Baeyens, J., 2003. A review of classic Fenton's peroxidation as an advanced oxidation technique. Journal of Hazardous Materials B98, 33-50.

Ni, Y., Qi, Z, Kokot, S., 2006. Simultaneous ultraviolet-spectrophotometric determination of sulfonamides by multivariate calibration approaches. *Chemometrics and Intelligent Laboratory Systems* **82**, 241-247.

Nikolaou, A., Meric, S., Fatta D., 2007. Occurrence patterns of pharmaceuticals in water and wastewater environments. *Analytical and Bioanalytical Chemistry* **387**, 1225-1234.

Nogueira, R.F.P., Oliveira, M.C., Paterlini, W.C., 2005. Simple and fast spectrophotometric determination of H_2O_2 in photo-Fenton reactions using metavanadate. *Talanta* **66**, 86-91.

Nordholm, L., Dalgaard, L., 1984. Determination of trimethoprim metabolites including conjugates in urine using high-performance liquid chromatography with combined ultraviolet and electrochemical detection. *Journal of Chromatography B* ***305***, 391-399.

Novo, A., Manaia, C.M., 2010. Factors influencing antibiotic resistance burden in municipal wastewater treatment plants. *Applied Microbiology and Biotechnology* **87**, 1157-1166.

Núñez, L., García-Hortal, J.A., Torrades, F., 2007. Study of kinetic parameters related to the decolourization and mineralization of reactive dyes from textile dyeing using Fenton and photo-Fenton processes. *Dyes and Pigments* **75**, 647-652.

Ochsenkuehn-Petropoulou, M. Analytical methods. Spectrometric methods. Simmetria, 2006.

OECD Guidelines for testing of Chemicals, simulation test-aerobic sewage treatment 303A, 1999.

Ohno, T., Sarukawa, K., Tokieda, K., Matsumura, M., 2001. Morphology of a TiO_2 photocatalyst (Degussa, P-25) consisting of anatase and rutile crystalline phases. *Journal of Catalysis* **203,** 82-86.

Okeri, H.A., Arhewoh, I.M., 2008. Analytical profile of the fluoroquinolone antibacterials. I. Ofloxacin. *African Journal of Biotechnology* **7** (6), 670-680.

Oller, I., Gernjak, W., Maldonado, M.I., Pérez-Estrada L.A., Sánchez-Pérez, J.A., Malato, S., 2006. Solar photocatalytic degradation of some hazardous water-soluble pesticides at pilot-plant scale. *Journal of Hazardous Materials* **B138**, 507-517.

Pailler, J.Y., Krein, A., Pfister, L., Hoffmann, L., Guignard, C., 2009. Solid phase extraction coupled to liquid chromatography-tandem mass spectrometry analysis of sulfonamides, tetracyclines, analgesics and hormones in surface water and wastewater in Luxembourg. *Science of the Total Environment* **407**, 4736-4743.

Park, H.R., Oh, C.H., Lee, H.C., Choi, J.G., Jung, B.I., Bark, K.M., 2006. Quenching of ofloxacin and flumequine fluorescence by divalent transition metal cations. *Bulletin of the Korean Chemical Society* **27** (12), 2002-2010.

Parsons, S. (ed). Advanced oxidation processes for water and wastewater treatment. *International Water Association (*IWA), London, 2004.

Parvez, S., Venkataraman, C., Mukherji, S., 2006. A review on advantages of implementing luminescence inhibition test (*Vibrio fischeri*) for acute toxicity prediction of chemicals. *Environmental International* **32**, 265-268.

Peng, X., Wang, Z., Kuang, W., Tan, J., Li, K., 2006. A preliminary study on the occurrence and behavior of sulfonamides, ofloxacin and chloramphenicol antimicrobials in wastewaters of two sewage treatment plants in Guangzhou, China. *Science of the Total Environment* **371**, 314-322.

Pérez, M., Torrades, F., Domènech, X., Peral, J., 2002. Fenton and photo-Fenton oxidation of textile effluents. *Water Research* 36, 2703-2710.

Pérez, S., Eichhorn, P., Aga, D.S., 2005. Evaluating the biodegradability of sulfamethazine, sulfamethoxazole, sulfathiazole and trimethoprim at different stages of sewage treatment. *Environmental Toxicology and Chemistry* **24** (6), 1361-1367.

Pérez, S., Eichhorn, P., Barcelo, D., 2007. Structural characterization of photodegradation products of enalapril and its metabolite enalaprilat obtained under simulated environmental conditions by hybrid quadrupole-linear ion trap-MS and quadrupole-time-of-flight-MS. *Analytical Chemistry* **79**, 8293-8300.

Perez-Estrada, L.A., Malato, S., Gernjak, W., Agüera, A., Thurman, E.M., Ferrer, I., Fernádez-Alba, A.R., 2005. Photo-Fenton Degradation of Diclofenac: Identification of main intermediates and degradation pathway. *Environmental Science and Technology* **39**, 8300-8306.

Perez-Moya, M., Graells, M., Buenestado, P., Mansilla, H.D., 2008. A comparative study on the empirical modeling of photo-Fenton process performance. *Applied Catalysis B: Environmental* **84**, 313-323.

Petrović, M., Hernando, M.D, Dıaz-Cruz, M.S, Barceló, D., 2005. Liquid chromatography-tandem mass spectrometry for the analysis of pharmaceutical

residues in environmental samples: a review. *Journal of Chromatography A* **1067**, 1-14.

Petrović, M., Gros, M, Barceló, D., 2006. Multi-residue analysis of pharmaceuticals in wastewater by ultra-performance liquid chromatography-quadrupole-time-of-flight mass spectrometry. *Journal of Chromatography A* **1124**, 68-81.

Petrović, M., Gros, M., Barceló, D., 2007. Multi-residue analysis of pharmaceuticals using LC-tandem MS and LC-hybrid MS. *Comprehensive Analytical Chemistry* **50**, 157-183.

Pignatello, J.J., 1992. Dark and photoassisted Fe^{3+}-catalyzed degradation of chlorophenoxy herbicides by hydrogen peroxide. *Environmental Science and Technology* **26**, 944-951.

Pignatello, J.J., Oliveros, E., MacKay, A., 2006. Advanced oxidation processes for organic contaminant destruction based on the Fenton reaction and related chemistry. *Critical Reviews in Environmental Science and Technology* **36**, 1-84.

Poole, C.F., Gunatilleka, A.D., Sethuraman, R., 2000. Contributions of theory to method development in solid-phase extraction. *Journal of Chromatography A* **885**, 17-39.

Poulios, I., Avranas, A., Rekliti, E., Zouboulis, A., 2000. Photocatalytic oxidation of Auramine O in the presence of semiconducting oxides. *Journal of Chemical Technology and Biotechnology* **75**, 205-212.

Poulios, I., Kositzi, M., Kouras, A., 1998. Photocatalytic decomposition of triclopyr over aqueous semiconductor suspensions. *Journal of Photochemistry and Photobiology A: Chemistry* **115**, 175-183.

Poulopoulos, S.G., Nikolaki, M., Karampetsos, D., Philippopoulos, C.J., 2008. Photochemical treatment of 2-chlorophenol aqueous solutions using ultraviolet radiation, hydrogen peroxide and photo-Fenton reaction. *Journal of Hazardous Materials* **153**, 582-587.

Putra, E.K., Pranowo, R., Sunarso, J., Indraswati, N., Ismadji, S., 2009. Performance of activated carbon and bentonite for adsorption of amoxicillin from wastewater: Mechanisms, isotherms and kinetics. *Water Research* **43**, 2419-2430.

Radjenovic, J., Godehardt, M., Petrovic, M., Hein, A., Farre, M., Jekel, M., Barcelo, D., 2009. Evidencing generation of persistent ozonation products of antibiotics roxithromycin and trimethoprim. *Environmental Science and Technology* **43**, 6808-6815.

Radjenovic, J., Petrovic, M., Barcelo, D., 2009b. Fate and distribution of pharmaceuticals in wastewater and sewage sludge of the conventional activated sludge (CAS) and advanced membrane bioreactor (MBR) treatment. *Water Research* **43**, 831-841.

Radjenovic, J., Sirtori, C., Petrovic, M., Barcelo, D., Malato, S., 2009c. Solar photocatalytic degradation of persistent pharmaceuticals at pilot-scale: Kinetics and characterization of major intermediate products. *Applied Catalysis B: Environmental* **89**, 255-264.

Reemtsma, T., 2003. Liquid chromatography–mass spectrometry and strategies for trace-level analysis of polar organic pollutants. *Journal of Chromatography A* **1000**, 477-501.

Renew, J.E., C.H, Huang, 2004. Simultaneous determination of fluoroquinolone, sulfonamide, and trimethoprim antibiotics in wastewater using tandem solid phase

extraction and liquid chromatography–electrospray mass spectrometry. *Journal of Chromatography A* **1042**, 113-121.

Rincón, A.G., Pulgarin, C., 2006. Comparative evaluation of Fe^{3+} and TiO_2 photoassisted processes in solar photocatalytic disinfection of water. *Applied Catalysis B: Environmental* **63**, 222-231.

Rivera-Utrilla, J., Prados-Joya, G., Sánchez-Polo, M., Ferro-García, M.A., Bautista-Toledo, I., 2009. Removal of nitroimidazole antibiotics from aqueous solution by adsorption/bioadsorption on activated carbon. *Journal of Hazardous Materials* **170**, 298-305.

Rizzo, L., Meric, S., Guida, M., Kassinos, D., Belgiorno, V., 2009. Heterogenous photocatalytic degradation kinetics and detoxification of an urban wastewater treatment plant effluent contaminated with pharmaceuticals. *Water Research* **43**, 4070-4078.

Rizzo, L., 2011. Bioassays as a tool for evaluating advanced oxidation processes in water and wastewater treatment. *Water Research* **45**, 4311-4340.

Roberts, P.H., Thomas, K.V., 2006. The occurrence of selected pharmaceuticals in wastewater effluent and surface waters of the lower Tyne catchment. *Science of the Total Environment* **356**, 143-153.

Robertson, P.K.J., 1996. Semiconductor photocatalysis: an environmentally acceptable alternative production technique and effluent treatment process. *Journal of Cleaner Production* **4** (34), 203-212.

Rosal, R., Rodríguez, A., Perdigón-Melón, J.A. , Petre, A., García-Calvo, E., Gómez , M. J., Aguera, A., Fernández-Alba, A. R., 2010. Occurrence of emerging

pollutants in urban wastewater and their removal through biological treatment followed by ozonation. *Water Research* **44**, 578-588.

Ryan, C.C., Tan, D.T, Arnold, W.A, 2011. Direct and indirect photolysis of sulfamethoxazole and trimethoprim in wastewater treatment plant effluent. *Water Research* **45**, 1280-1286.

Safarzadeh-Amiri, A., Bolton, J.R., Carter, S.R., 1996. The use of iron in advanced oxidation processes. *Journal of Advanced Oxidation Technology* **1**, 18-26.

Sahar, E., David, I., Gelman, Y., Chikurel, H., Aharoni, A., Messalem, R., Brenner, A., 2010. The use of RO to remove emerging micropollutants following CAS/UF or MBR treatment of municipal wastewater. *Desalination* **273** (1), 142-147.

Sakthivel, S., Neppolian, B., Shankar, M.V., Arabindoo, B., Palanichamy, M., Murugesan, V., 2003. Solar photocatalytic degradation of azo dye: comparison of photocatalytic efficiency of ZnO and TiO_2. *Solar Energy Materials & Solar Cells* **77**, 65-82.

Salvador, J.P., Adrian, J., Galve, R., Pinacho, D.G., Kreuzer, M., Sánchez-Baeza, F., Marco, M.P., 2007. Application of bioassays/biosensors for the analysis of pharmaceuticals in environmental samples. *Comprehensive Analytical Chemistry* **50**, Petrović, M., Barceló, D. (Eds), Chapter 2.8, 279-334.

Santos, M.S., Peres, J.A., 2006. Decolorization of the azo dye reactive black 5 by Fenton and photo-Fenton oxidation. *Dyes Pigments* **71**, 236-244.

Santos, A., Yustos, P., Rodriguez, S., Simon, E., Garcia-Ochoa, F., 2007. Abatement of phenolic mixtures by catalytic wet oxidation enhanced by Fenton's pretreatment: Effect of H_2O_2 dosage and temperature. *Journal of Hazardous Materials* **146**, 595-601.

Saritha, P., Aparna, C., Himabindu, V., Anjaneyulu, Y., 2007. Comparison of various advanced oxidation processes for the degradation of 4-chloro-2nitrophenol. *Journal of Hazardous Materials* **149**, 609-14.

Schafer, A.I., Kalinowski, J., Puhler, A., 1994. Increased fertility of corynebacterium glutamicum recipients in intergeneric matings with *Escherichia coli* after stress exposure. *Applied and Environmental Microbiology* **60** (2), 756-759.

Schiavello, 1993. Some working principles of heterogeneous photocatalysis by semiconductors. *Electrochimicha Acta* **38** (1), 11-14.

Schwartz, T., Kohnen, W., Jansen, B., Obst, U., 2003. Detection of antibiotic-resistance genes in wastewater, surface water and drinking water biofilms. *FEMS Microbiology Ecology* **43**, 325-335.

Seifrtová, M., Nováková, L., Lino, C., Pena, A., Solich, P., 2009. An overview of analytical methodologies for the determination of antibiotics in environmental waters. *Analytica Chimica Acta* **649**, 158-179.

Senta, I., Terzić, S., Ahel, M., 2008. Simultaneous determination of sulfonamides, fluoroquinolones, macrolides and trimethoprim in wastewater and river water by LC-Tandem-MS. *Chromatographia* 68, 747-758.

Serpone, N., Sauvé, G., Koch, R., Tahiri, H., Pichat, P., Piccinini, P., Pelizzetti, E., Hidaka, H., 1996. Standardization protocol of process effiniencies and activation parameters in heterogeneous photocatalysis: relative photonic efficiencies ζ_r. *Journal of Photochemistry and Photobiology A: Chemistry* **94**, 191-203.

Serrano, P.H., 2005. Responsible use of antibiotics in aquaculture. Fisheries Technical Paper 469, Food and Agriculture Organization of the United Nations (FAO), Rome.

Sirtori, C., Zapata, A., Oller, I., Gernjak, W., Aguera, A., Malato, S., 2009. Decontamination industrial pharmaceutical wastewater by combining solar photo-Fenton and biological treatment. *Water Research* **43**, 661-668.

Sirtori, C., Aguera, A., Gernjak. W., Malato, S., 2010. Effect of water-matrix composition on trimethoprim solar photodegradation kinetics and pathways. *Water Research* **44** (9), 2735-2744.

Song, W., Chen, W., Cooper, W.J., Greaves, J., Miller, G.E., 2008. Free-radical destruction of β-lactam antibiotics in aqueous solution. *Journal of Physical Chemistry A* **112**, 7411-7417.

Song, W., Cooper, W.J., Mezyk, S.P., Greaves, J., Peake, B.M., 2008b. Free radical destruction of β-blockers in aqueous solution. *Environmental Science and Technology* **42**, 1256-1261.

Spongberg, A.L., Witter, J.D., 2008. Pharmaceutical compounds in the wastewater process stream in Northwest Ohio. *Science of the Total Environment* **397**, 148-157.

Spuhler, D., Rengifo-Herrera, J.A., Pulgarin, C., 2010. The effect of Fe^{2+}, Fe^{3+}, H_2O_2 and the photo-Fenton reagent at near neutral pH on the solar disinfection (SODIS) at low temperatures of water containing *Escherichia coli* K12. *Applied Catalysis B: Environmental* **96**, 126-141.

Sui, Q., Huang, J., Deng, S., Yu, G., Fan, Q., 2010. Occurrence and removal of pharmaceuticals, caffeine and DEET in wastewater treatment plants of Beijing, China. *Water Research* **44**, 417-426.

Sun, Y., Pignatello, J.J., 1992. Chemical treatment of pesticides wastes. Evaluation of Fe(III) chelates for catalytic hydrogen peroxide oxidation of 2,4-D at circumneutral pH. *Journal of Agriculture and Food Chemistry* **40**, 322-327.

Sychev, A.Y., Isak, V.G., 1995. Iron compounds and the mechanisms of the homogeneous catalysis of the activation of O_2 and H_2O_2 and of the oxidation of organic substrates. *Russian Chemical Reviews* **64** (12), 1105-1129.

Tamimi, M., Qourzal, S., Barka, N., Assabbane, A., Ait-Ichou, Y., 2008. Methomyl degradation in aqueous solutions by Fenton's reagent and the photo-Fenton system. *Separation and Purification Technology* **61**, 103-108.

Tekin, H., Bilkay, O., Ataberk, S.S., Balta, T.H., Ceribasi, I.H., Sanin, F.D., 2006. Use of Fenton oxidation to improve the biodegradability of a pharmaceutical wastewater. *Journal of Hazardous Materials* **136**, 258-265.

Ternes, T., Bonerz, M., Schmidt, T., 2001. Determination of neutral pharmaceuticals in wastewater and rivers by liquid chromatography-electrospray tandem mass spectrometry. *Journal of Chromatography A* **938**, 175-185.

Ternes, T.A., Stuber, J., Herrmann, N., McDowell, D., Ried, A., Kampmann, M., Teiser, B., 2003. Ozonation: a tool for removal of pharmaceuticals, contrast media and musk fragrances from wastewater? *Water Research* **37**, 1976-1982.

Ternes, T.A., Bonerz, M., Herrmann, N., Teiser, B., Andersen, H.R., 2007. Irrigation of treated wastewater in Braunschweig, Germany: An option to remove pharmaceuticals and musk fragrances. *Chemosphere* **66**, 894-904.

Thomulka, K.W., McGee, D.J., 1993. Detection of biohazardous materials in water by measuring bioluminescence reduction with the marine organism *Vibrio harveyi*. *Journal of Environmental Science and Health A* 28, 2153-2166.

Torrades, F., Perez, M., Mansilla, H.D., Peral, J., 2003. Experimental design of Fenton and photo-Fenton reactions for the treatment of cellulose bleaching effluents. *Chemosphere* **53**, 1211-1220.

Trovo, A.G., Melo, S.A.S, Nogueira, R.F.P, 2008. Photodegradation of the pharmaceuticals amoxicillin, bezafibrate and paracetamol by the photo-Fenton process-Application to sewage treatment plant effluent. *Journal of Photochemistry and Photobiology A: Chemistry* **198**, 215-220.

Trovo, A.G., Nogueira, R.F.P., Aguera, A., Fernandez-Alba, A.R., Sirtori, C., Malato, S., 2009. Degradation of sulfamethoxazole in water by solar photo-Fenton. Chemical and toxicological evaluation. *Water Research* **43**, 3922-3931.

Tühkanen, T.A. 2004. UV/H_2O_2 processes. *International Water Association* (IWA), Parsons, S. (Ed.), Chapter 4, 234-333.

Vidal, A., Díaz, A.I., El Hraiki, A., Romero, M., Muguruza, I., Senhaji, F., González, J., 1999. Solar photocatalysis for detoxification and disinfection of contaminated water: pilot plant studies. *Catalysis Today* **54**, 283-290.

Walling, C., 1975. Fenton's reagent revisited *Account of Chemical Research* **8**, 125-131.

Walter, M.V., Vennes, J.W., 1985. Occurrence of multiple-antibiotic-resistant enteric bacteria in domestic sewage and oxidation lagoons. *Applied and Environmental Microbiology* **50** (4), 930-933.

Watkinson, A.J., Murbyc, E.J., Costanzo, S.D., 2007. Removal of antibiotics in conventional and advanced wastewater treatment: Implications for environmental discharge and wastewater recycling. *Water Research* **41**, 4164-4176.

Watkinson, A.J., Murbyd, E.J., Kolpine, D.W., Costanzof, S.D., 2009. The occurrence of antibiotics in an urban watershed: From wastewater to drinking water. *Science of the Total Environment* **407**, 2711-2723.

Wenk, J., Von Gunten, U., Canonica, S., 2011. Effect of dissolved organic matter on the transformation of contaminants induced by excited triplet states and the hydroxyl radical. *Environmental Science and Technology* **45** (4), 1334-1340.

Westerhoff, P., Yoon, Y., Snyder., S., Wert, E., 2005. Fate of endocrine-disruptor, pharmaceutical, and personal care product chemicals during simulated drinking water treatment processes. *Environmental Science and Technology* **39**, 6649-6663.

Wolfson, J.S., Hooper, D.C., 1985. The fluoroquinolones: structures, mechanisms of action and resistance, and spectra of activity in vitro. *Antimicrobial Agents and Chemotherapy* **28** (4), 581-586.

Wollenberger, L., Halling-Sorensen, B., Kusk, K.O., 2000. Acute and chronic toxicity of veterinary antibiotics to *Daphnia magna*. *Chemosphere* **40**, 723-730.

Wong, J.W.C., Lia, K., Fanga, M., Sub, D.C., 2001. Toxicity evaluation of sewage sludges in Hong Kong. *Environment International* **27**, 373-380.

Xekoukoulotakis, N.P., Xinidis, N., Chroni, M., Mantzavinos, D., Venieri, D., Hapeshi, E., Fatta-Kassinos, D., 2010. UV-A/TiO_2 photocatalytic decomposition of erythromycin in water: Factors affecting mineralization and antibiotic activity. *Catalysis Today* **151**, 29-33.

Xekoukoulotakis, N.P., Drosou, C, Brebou., C., Chatzisymeon, E., Hapeshi, E., Fatta-Kassinos, D., Mantzavinos, D., 2011. Kinetics of UV-A/TiO_2 photocatalytic degradation and mineralization of the antibiotic sulfamethoxazole in aqueous matrices. *Catalysis Today* **16**, 163-168.

Xiao, Y., Chang, H., Jia, A., Hu, J., 2008. Trace analysis of quinolone and fluoroquinolone antibiotics from wastewaters by liquid chromatography-electrospray tandem mass spectrometry. *Journal of Chromatography A* **1214**, 100-108.

Xu, P., Drewes, J.E., Kim, T.U., Bellona, C., Amy, G., 2006. Effect of membrane fouling on transport of organic contaminants in NF/RO membrane applications. *Journal of Membrane Science* **279** (1-2), 165-175.

Xu, W., Zhang, G., Li, X., Zou, S., Li, P., Hu, Z., Li, J., 2007. Occurrence and elimination of antibiotics at four sewage treatment plants in the Pearl River Delta (PRD), South China. *Water Research* **41**, 4526-4534.

Xu, X.R., Li, X.Y., Li, X.Z., Li, H.B., 2009. Degradation of melatonin by UV, UV/H_2O_2, Fe^{2+}/H_2O_2 and UV/Fe^{2+}/H_2O_2 processes. *Separation and Purification Technology* **68**, 261-266.

Yang, S., Carlson, K.H., 2004. Solid-phase extraction-high-performance liquid chromatography-ion trap mass spectrometry for analysis of trace concentrations of macrolides antibiotics in natural and waste water matrices. *Journal of Chromatography A* **1038**, 141-155.

Yang, S., Cha, J., Carlson, K., 2005. Simultaneous extraction and analysis of 11 tetracycline and sulfonamide antibiotics in influent and effluent domestic wastewater by solid-phase extraction and liquid chromatography-electrospray ionization tandem mass spectrometry. *Journal of Chromatography A* **1097**, 40-53.

Yang, Y., Wang, P., Shi, S., Liu, Y., 2009. Microwave enhanced Fenton-like process for the treatment of high concentration pharmaceutical wastewater. *Journal of Hazardous Materials* **168**, 238-245.

Yasojima, M., Nakada, N., Komori, K., Suzuki, Y., Tanaka, H., 2006. Occurrence of levofloxacin, clarithromycin and azithromycin in wastewater treatment plant in Japan. *Water Science and Technology* **53** (11), 227-233.

Yu, T., Lin, A.Y., Lateef, S.K., Lin, C., Yang, P., 2009. Removal of antibiotics and non-steroidal anti-inflammatory drugs by extended sludge age biological process. *Chemosphere* **77**, 175-181.

Yuan, F., Hu, C., Hu, X., Wie, D., Chen, Y., Qu, J., 2011. Photodegradation and toxicity changes of antibiotics in UV and UV/H_2O_2 process. *Journal of Hazardous Materials* **185**, 1256-1263.

Zapata, A., Velegraki, T., Sanchez-Pérez, J.A., Mantzavinos, D., Maldonado, M.I., Malato, S., 2009. Solar photo-Fenton treatment of pesticides in water: Effect of iron concentration on degradation and assessment of ecotoxicity and biodegradability. *Applied Catalysis B: Environmental* **88**, 448-454.

Zapata, A., Oller, I., Bizani, E., Sánchez-Peérez, J.A., Maldonado, M.I., Malato, S., 2009b. Evaluation of operational parameters involved in solar photo-Fenton degradation of a commercial pesticide mixture. *Catalysis Today* **144**, 94-99.

Zazo, J.A., Casas, J.A., Mohedano, A.F., Rodriguez, J.J., 2009. Semicontinuous Fenton oxidation of phenol in aqueous solution. A kinetic study. *Water Research* **43**, 4063-4069.

Zepp, R.G., Schlotzhauer, P.F., Sink, R.M., 1985. Photosensitized transformations involving electronic energy transfer in natural waters: role of humic substances. *Environmental Science and Technology* **19** (1), 74-81.

Zepp, R.G., Faust, B.C., Hoigné, J., 1992. Hydroxyl radical formation in aqueous reactions (pH 3-8) of iron(II) with hydrogen peroxide: The photo-Fenton reaction. *Environmental Science and Technology* **26**, 313-319.

Zhang, G., Ji, S., Xi, B., 2006. Feasibility study of treatment of amoxillin wastewater with a combination of extraction, Fenton oxidation and reverse osmosis. *Desalination* **196**, 32-42.

Zhang, Y., Marrs, C.F., Simon, C., Xi, C., 2009. Wastewater treatment contributes to selective increase of antibiotic resistance among *Acinetobacter* spp. *Science of the Total Environment* **407**, 3702-3706.

Zhu, J., Snow, D.D., Cassada, D.A., Monson, S.J., Spalding, R.F., 2001. Analysis of oxytetracycline, tetracycline, and chlortetracycline in water using solid-phase extraction and liquid chromatography-tandem mass spectrometry. *Journal of Chromatography A* **928**, 177-186.

Zorita, S., Mårtensson, L., Mathiasson, L., 2009. Occurrence and removal of pharmaceuticals in a municipal sewage treatment system in the south of Sweden. *Science of the Total Environment* **407**, 2760-2770.

Zuccato, E., Castiglioni, S., Fanelli, R., 2005. Identification of the pharmaceuticals for human use contaminating the Italian aquatic environment. *Journal of Hazardous Materials* 122, 205-209.

Zuccato, E., Castiglioni, S., Bagnati, R., Melis, M., Fanelli, R., 2010. Source, occurrence and fate of antibiotics in the Italian aquatic environment. *Journal of Hazardous Materials* **179**, 1042-1048.

ANNEX: SUPPORTING INFORMATION

Table A1. Removal of antibiotics from wastewater effluents through conventional treatment processes.

Table A2. Removal of antibiotics from wastewater effluents through advanced treatment processes.

Table A1. Removal of antibiotics from wastewater effluents through conventional treatment processes.

Antibiotic group Antibiotic	Location	Initial concentration (ng L^{-1})	Treatment process	Effluent concentration (ng L^{-1}) Removal efficiency (%)	Reference
β-Lactams					
Amoxicillin	Brisbane (Australia)	280	Screened influent; Primary Settling Tank (PST): HRT_{PST}=5.5 h; Bioreactor (BRT): SRT=12.5 days; Final Settling Tank (FST): HRT_{FST}=9 h	PST / 270 (3.6%*) BRT / *nd* (100%*) FST / 30 (89%*)	*Watkinson et al., 2007*
	Italy and Switzerland (Milan, Varese, Como, Lugano)	Milan / *nd* Varese / 6.05±10.5 Como / 21±15 Lugano / 382±453	Pre-treatment; Primary treatment (primary settling); Secondary treatment (CAS); UV-light tertiary treatment (Varese).	Milan / *nd* Varese / *nd* (100%*) Como / *nd* (100%*) Lugano / 37±24 (90%*)	*Zuccato et al., 2010*
	South-East Queensland (Australia)	6940	*na*	50 (99%*)	*Watkinson et al., 2009*
Ampicillin	Fort Collins (Colorado)	17	Pretreatment; Primary clarification; Intermediate clarification; Secondary clarification; Chlorine disinfection	13 (23.5%*)	*Cha et al., 2006*
	Hong Kong (Stanley and Shatin)	Shatin / 389.5±11.2 Stanley / *nd*	*na*	Shatin / 126.4±6.6 (67.5%**) Stanley / *nd*	*Li et al., 2009*
	Hong Kong (Stanley and Shatin)	Shatin / (<34.4) Stanley / 77.2-383	Shatin (Anoxic-Aerobic CAS); Stanley (Anoxic-Aerobic CAS and Chlorination)	Shatin (*ne*) Stanley (82%**) Disinfection (91%**) Final (97%**)	*Li and Zhang, 2011*
Cephalexin	Brisbane (Australia)	2000	*na*	78.2 (96%*)	*Costanzo et al., 2005*
	Brisbane (Australia)	5600	Screened influent; Primary Settling Tank (PST): HRT_{PST}=5.5 h; Bioreactor (BRT): SRT=12.5 days; Final Settling Tank (FST): HRT_{FST}=9 h	PST / 3900 (30%*) BRT / *nd* (100%*) FST / *nd* (100%*)	*Watkinson et al., 2007*
	Hong Kong and Shenzhen (China) (Wan Chai [1], Shatin [2], Tai Po [3], Stonecutters Island [4], Nan Shan [5])	670-2900	[1] (Primary treatment); [2] (Screening; Settlement of grit particles; Primary sedimentation; Biological treatment); [3] (Removal of solids and grit; Primary sedimentation; Biological treatment; Anaerobic digestion); [4] (Chemically enhanced primary treatment); [5] (Primary treatment)	240-1800 (~9-89%**)	*Gulkowska et al., 2008*
	Taipei (Taiwan)	1563-4367	$WWTP_1$ (Screening and sedimentation; CAS and sedimentation; UV); $WWTP_2$ (Grit removal and screening and sedimentation, deep shaft and step aeration and sedimentation; Chlorination); $WWTP_3$ (Screening; Trickling filter and sedimentation; Chlorination); $WWTP_4$ (Screening and grit removal and sedimentation; CAS and sedimentation; Chlorination)	10-994 (36-99.8%**)	*Lin et al., 2009*
	South-East Queensland (Australia)	64000	*na*	250 (99.6%*)	*Watkinson et al., 2009*
	Hong Kong (Stanley and Shatin)	Shatin / 534.9±20.2 Stanley / 175.4±8.3	*na*	Shatin / 375.6±19.7 (30.4%**) Stanley/ *nd* (100%**)	*Li et al., 2009*
	Hong Kong (Stanley and Shatin)	Shatin / 658-1718 Stanley / 65.7-525	Shatin (Anoxic-Aerobic CAS); Stanley (Anoxic-Aerobic CAS and Chlorination)	Shatin (53%**) Stanley (91%**) Disinfection (99%**) Final (100%**)	*Li and Zhang, 2011*
Penicillin G	Hong Kong and Shenzhen (China) (Wan Chai [1], Shatin [2], Tai Po [3], Stonecutters Island [4], Nan Shan [5])	29	[1] (Primary treatment); [2] (Screening; Settlement of grit particles; Primary sedimentation; Biological treatment); [3] (Removal of solids and grit; Primary sedimentation; Biological treatment; Anaerobic digestion); [4] (Chemically enhanced primary treatment); [5] (Primary treatment)	*na* (< LOD**)	*Gulkowska et al., 2008*
	South-East Queensland (Australia)	10	*na*	300 (29%*)	*Watkinson et al., 2009*
Penicillin V	Brisbane (Australia)	160	Screened influent; Primary Settling Tank (PST): HRT_{PST}=5.5 h;	PST / 10 (94%*)	*Watkinson et al., 2007*

			Bioreactor (BRT): SRT=12.5 days; Final Settling Tank (FST): HRT_{FST}=9 h	BRT / 20 (87.5%*) FST / 80 (50%*)	
	South-East Queensland (Australia)	13800	*na*	2000 (86%*)	*Watkinson et al., 2009*
Cloxacillin	Brisbane (Australia)	320	Screened influent; Primary Settling Tank (PST): HRT_{PST}=5.5 h; Bioreactor (BRT): SRT=12.5 days; Final Settling Tank (FST): HRT_{FST}=9 h	PST / *nd* (100%*) BRT / *nd* (100%*) FST / *nd* (100%*)	*Watkinson et al., 2007*
	Fort Collins (Colorado)	13	Pretreatment; Primary clarification; Intermediate clarification; Secondary clarification; Chlorine disinfection	9 (31%*)	*Cha et al., 2006*
	South-East Queensland (Australia)	4600	*na*	700 (85%*)	*Watkinson et al., 2009*
Cefaclor	Brisbane (Australia)	980	Screened influent; Primary Settling Tank (PST): HRT_{PST}=5.5 h; Bioreactor (BRT): SRT=12.5 days; Final Settling Tank (FST): HRT_{FST}=9 h	PST / 800 (18%*) BRT / *nd* (100%*) FST / 60 (94%*)	*Watkinson et al., 2007*
	South-East Queensland (Australia)	6150	*na*	1800 (71%*)	*Watkinson et al., 2009*
Cefotaxim	Hong Kong and Shenzhen (China) (Wan Chai [1], Shatin [2], Tai Po [3], Stonecutters Island [4], Nan Shan [5])	24-1100	[1] (Primary treatment); [2] (Screening; Settlement of grit particles; Primary sedimentation; Biological treatment); [3] (Removal of solids and grit; Primary sedimentation; Biological treatment; Anaerobic digestion); [4] (Chemically enhanced primary treatment); [5] (Primary treatment)	34 (< LOD**)	*Gulkowska et al., 2008*
	Hong Kong (Stanley and Shatin)	Shatin / 38.4-93.0 Stanley / *nd*	Shatin (Anoxic-Aerobic CAS); Stanley (Anoxic-Aerobic CAS and Chlorination)	Shatin (~43%**) Stanley (*ne)* Disinfection (*ne*) Final (*ne*)	*Li and Zhang, 2011*
Cephapirin	Fort Collins (Colorado)	18	Pretreatment; Primary clarification; Intermediate clarification; Secondary clarification; Chlorine disinfection	15 (17%*)	*Cha et al., 2006*
Oxacillin	Fort Collins (Colorado)	14	Pretreatment; Primary clarification; Intermediate clarification; Secondary clarification; Chlorine disinfection	8 (43%*)	*Cha et al., 2006*
Macrolides					
Roxithromycin	Brisbane (Australia)	18	Screened influent; Primary Settling Tank (PST): HRT_{PST}=5.5 h; Bioreactor (BRT): SRT=12.5 days; Final Settling Tank (FST): HRT_{FST}=9 h	PST / 9 (50%*) BRT / 60 (< 0*) FST / 100 (< 0*)	*Watkinson et al., 2007*
	Switzerland (Kloten-Opfikon (WWTP-K); Altenrhein (WWTP-A))	10-40	Primary treatment (screen, aerated grit-removal tank, primary clarifier); Secondary treatment (WWTP-K: CAS; WWTP-A: CAS and FBR); Tertiary treatment (sand filtration).	Primary / 10-50 Secondary / 10-30 Tertiary / 10-30	*Göbel et al., 2005*
	South-East of Austria	25-117	Screen; Grit chamber; Two aeration tanks; Two secondary clarifiers for final sedimentation.	36-69 (<0*)	*Clara et al., 2005*
	Switzerland (Kloten-Opfikon (WWTP-K); Altenrhein (WWTP-A))	10-40	Primary treatment (screen, aerated grit-removal tank, primary clarifier); Secondary treatment (WWTP-K: CAS; WWTP-A: CAS and FBR); Tertiary treatment (sand filtration).	Primary (3-9%**) Secondary (-18-38%**)	*Göbel et al., 2007*
	South-East Queensland (Australia)	500	*na*	500 (0%*)	*Watkinson et al., 2009*
	Hong Kong (Stanley and Shatin)	Shatin / 25.3±0.7 Stanley / 3.5±0.2	*na*	Shatin / 14.2±1.1 (43.9%**) Stanley / 2.9±0.0 (17.1%**)	*Li et al., 2009*
	Braunschweig (Germany)	810±420	Screen; Aerated grid-removal tank; Primary clarifier; CAS; Phosphate removal; Nitrification-denitrification.	540±70 (33%**)	*Ternes et al., 2007*
	Guangzhou and Hong Kong (South China) Kaifaqu (A), Liede (B), New Territory (C), Kowloon (D)	A / 102±32 B / 164±31 C / 75±14 D / 156±29	A (Primary treatment; CAS; Chlorine); B (Primary treatment; Oxidation ditch; UV); C (Primary treatment; CAS); D (Primary treatment; Chemically enhanced; Chlorine).	A / 36±21 (65%*) B / 278±46 (<0*) C / 35±8 (53%*) D / 37±11 (76%*)	*Xu et al., 2007*
	Switzerland (Kloten-Opfikon (WWTP-K); Altenrhein (WWTP-A))	50	Primary treatment (screen, aerated grit-removal tank, primary clarifier); Secondary treatment (WWTP-K: CAS; WWTP-A: CAS	40 (20%*)	*Joss et al., 2005*

			and a FBR); Tertiary treatment (sand filtration).		
	Hong Kong (Stanley and Shatin)	Shatin / 35.6-135 Stanley / 4.2-141	Shatin (Anoxic-Aerobic CAS); Stanley (Anoxic-Aerobic CAS and Chlorination)	Shatin (46%**) Stanley (40%**) Disinfection (18%**) Final (53%**)	*Li and Zhang, 2011*
Azithromycin	Croatia	152	CAS	96 (37%*)	*Gros et al., 2006*
	Switzerland (Kloten-Opfikon (WWTP-K); Altenrhein (WWTP-A))	90-380	Primary treatment (screen, aerated grit-removal tank, primary clarifier); Secondary treatment (WWTP-K: CAS; WWTP-A: CAS and FBR); Tertiary treatment (sand filtration).	Primary / 80-320 Secondary / 40-380 Tertiary / 80-400	*Göbel et al., 2005*
	Switzerland (Kloten-Opfikon (WWTP-K); Altenrhein (WWTP-A))	90-380	Primary treatment (screen, aerated grit-removal tank, primary clarifier); Secondary treatment (WWTP-K: CAS; WWTP-A: CAS and FBR); Tertiary treatment (sand filtration).	Primary (10-33%**) Secondary (-26-55%**)	*Göbel et al., 2007*
	South-western Kentucky	4.5-53	Large grit removal; Returned Activated Sludge; Post-Clarifier/Pre-Chlorination; Oxidation ditch; Post-Chlorination	4-23 (11-57%*)	*Loganathan et al., 2009*
	Cyprus	WWTP I / 1150 WWTP II / 660 WWTP III / 1680	WWTP I: Primary treatment; Secondary treatment (oxidation ditches, secondary settlement); Tertiary treatment (sand filtration, chlorination). WWTP II: Primary treatment; Secondary treatment (CAS); Tertiary treatment (sand filtration, chlorination). WWTP III: Primary treatment; Secondary treatment (phosphorus biological removal, nitrification and denitrification, secondary clarifiers); Tertiary treatment (sand filtration, chlorination)	Secondary WWTP I / 1600 (<0*) WWTP II / 300 (55%*) WWTP III / 530 (68%*) Outlet WWTP I / 180 (84%*) WWTP II / 200 (70%*) WWTP III / 30 (98%*)	*Fatta et al., 2010*
Tylosin	Brisbane (Australia)	55	Screened influent; Primary Settling Tank (PST): HRT_{PST}=5.5 h; Bioreactor (BRT): SRT=12.5 days; Final Settling Tank (FST): HRT_{FST}=9 h	PST / *nd* (100%*) BRT / 20 (64%*) FST / 65 (< 0*)	*Watkinson et al., 2007*
	Italy and Switzerland (Milan, Varese, Como, Lugano)	Milan / 4.0±3.0 Varese / *nd* Como / *nd* Lugano / *nd*	Pre-treatment; Primary treatment (primary settling); Secondary treatment (CAS); UV-light tertiary treatment (Varese).	Milan / 1.6±1.7 (60%*) Varese / *nd* Como / *nd* Lugano / *nd*	*Zuccato et al., 2010*
	South-East Queensland (Australia)	60	*na*	3400 (< 0*)	*Watkinson et al., 2009*
	Northern Colorado (USA)	1150±70	*na*	60±4 (95%*)	*Yang et al., 2004*
Clarithromycin	Taipei (Taiwan)	59-1433	$WWTP_1$ (Screening and sedimentation; CAS and sedimentation; UV); $WWTP_2$ (Grit removal and screening and sedimentation, deep shaft and step aeration and sedimentation; Chlorination); $WWTP_3$ (Screening; Trickling filter and sedimentation; Chlorination); $WWTP_4$ (Screening and grit removal and sedimentation; CAS and sedimentation; Chlorination)	12-32 (99%**)	*Lin et al., 2009*
	Switzerland (Kloten-Opfikon (WWTP-K); Altenrhein (WWTP-A))	330-600	Primary treatment (screen, aerated grit-removal tank, primary clarifier); Secondary treatment (WWTP-K: CAS; WWTP-A: CAS and FBR); Tertiary treatment (sand filtration).	Primary / 160-440 Secondary / 150-460 Tertiary / 110-350	*Göbel et al., 2005*
	Switzerland (Kloten-Opfikon (WWTP-K); Altenrhein (WWTP-A))	330-660	Primary treatment (screen, aerated grit-removal tank, primary clarifier); Secondary treatment (WWTP-K: CAS; WWTP-A: CAS and FBR); Tertiary treatment (sand filtration).	Primary (11-14%**) Secondary (-45-20%**)	*Göbel et al., 2007*
	Italy and Switzerland (Milan, Varese, Como, Lugano)	Milan / 322±74 Varese / 121±60 Como / 939±407 Lugano / 318±45	Pre-treatment; Primary treatment (primary settling); Secondary treatment (CAS); UV-light tertiary treatment (Varese).	Milan / 104±28 (68%*) Varese / 52±41 (57%*) Como / 500±80 ng L^{-1} (47%*) Lugano / 437±70 ng L^{-1} (<0*)	*Zuccato et al., 2010*
	Northwest Ohio (USA)	105.7-724.2	*na*	(<LOQ)-610.6 (16%*)	*Spongberg et al., 2008*
	Braunschweig (Germany)	460±100	Screen; Aerated grid-removal tank; Primary clarifier; CAS;	210±40 (54%**)	*Ternes et al., 2007*

			Phosphate removal; Nitrification-denitrification.		
Erythromycin	Howdon (UK)	71-141	Coarse screening; Preliminary clarification; Activated sludge treatment and trickling filter system; Settlement tanks; High-pressure 254 nm UV disinfection.	145-290 (79%**)	*Roberts and Thomas, 2006*
	Italy and Switzerland (Milan, Varese, Como, Lugano)	Milan / 0.39±0.3 Varese / 4.6±2.8 Como / *nd* Lugano / 0.56±1.1	Pre-treatment; Primary treatment (primary settling); Secondary treatment (CAS); UV-light tertiary treatment (Varese).	Milan / 34±5.3 (< 0*) Varese / 27±15 (< 0*) Como / 6.5±1.2 Lugano / 59±12 (< 0*)	*Zuccato et al., 2010*
	Cyprus	WWTP I / 380 WWTP II / 280 WWTP III / 700	WWTP I: Primary treatment; Secondary treatment (oxidation ditches, secondary settlement); Tertiary treatment (sand filtration, chlorination). WWTP II: Primary treatment; Secondary treatment (activated sludge treatment); Tertiary treatment (sand filtration, chlorination). WWTP III: Primary treatment; Secondary treatment (phosphorus biological removal, nitrification and denitrification, secondary clarifiers); Tertiary treatment (sand filtration, chlorination)	Secondary WWTP I / 200 (47%*) WWTP II / 250 (11%*) WWTP III / 420 (40%*) Outlet WWTP I / 30 (92%*) WWTP II / 400 (<0*) WWTP III / <LOD (100%*)	*Fatta et al., 2010*
	Braunschweig (Germany)	830±270	Screen; Aerated grid-removal tank; Primary clarifier; CAS; Phosphate removal; Nitrification-denitrification.	620±440 (25%**)	*Ternes et al., 2007*
	Guangzhou and Hong Kong (South China) Kaifaqu (A), Liede (B), New Territory (C), Kowloon (D)	A / 751±109 B / 1978±233 C / 253±22 D / 469±38	A (Primary treatment; CAS; Chlorine); B (Primary treatment; Oxidation ditch; UV); C (Primary treatment; CAS); D (Primary treatment; Chemically enhanced; Chlorine).	A / 430±73 (43%*) B / 2054±386 (<0*) C / 216±34 (15%*) D / 259±20 (45%*)	*Xu et al., 2007*
Erythromycin-H_2O	Hong Kong and Shenzhen (China) (Wan Chai [1], Shatin [2], Tai Po [3], Stonecutters Island [4], Nan Shan [5])	470-810	[1] (Primary treatment); [2] (Screening; Settlement of grit particles; Primary sedimentation; Biological treatment); [3] (Removal of solids and grit; Primary sedimentation; Biological treatment; Anaerobic digestion); [4] (Chemically enhanced primary treatment); [5] (Primary treatment)	510-850 (-12-19%**)	*Gulkowska et al., 2008*
	Taipei (Taiwan)	226-1537	$WWTP_1$ (Screening and sedimentation; CAS and sedimentation; UV); $WWTP_2$ (Grit removal and screening and sedimentation, deep shaft and step aeration and sedimentation; Chlorination); $WWTP_3$ (Screening; Trickling filter and sedimentation; Chlorination); $WWTP_4$ (Screening and grit removal and sedimentation; CAS and sedimentation; Chlorination)	361-811 (56%**)	*Lin et al., 2009*
	Switzerland (Kloten-Opfikon (WWTP-K); Altenrhein (WWTP-A))	60-190	Primary treatment (screen, aerated grit-removal tank, primary clarifier); Secondary treatment (WWTP-K: CAS; WWTP-A: CAS and FBR); Tertiary treatment (sand filtration).	Primary / 40-190 Secondary / 50-140 Tertiary / 60-110	*Göbel et al., 2005*
	Wisconsin (USA)	(<50)-1300	CAS	(<50)-300 (43.8-100%**)	*Karthikeyan and Meyer, 2006*
	Switzerland (Kloten-Opfikon (WWTP-K); Altenrhein (WWTP-A))	60-190	Primary treatment (screen, aerated grit-removal tank, primary clarifier); Secondary treatment (WWTP-K: CAS; WWTP-A: CAS and FBR); Tertiary treatment (sand filtration).	Primary (-8-4%**) Secondary (-22-7%**)	*Göbel et al., 2007*
	Italy and Switzerland (Milan, Varese, Como, Lugano)	Milan / *nd* Varese / *nd* Como / 25±5.7 Lugano / *nd*	Pre-treatment; Primary treatment (primary settling); Secondary treatment (CAS); UV-light tertiary treatment (Varese).	Milan / *nd* Varese / *nd* Como/ 17±4.5 (32%*) Lugano / *nd*	*Zuccato et al., 2010*
	Hong Kong (Stanley and Shatin)	Shatin / 16.7±0.8 Stanley / 51.3±1.9	*na*	Shatin / 96.3±6.0 (55.6%**) Stanley / 37.9±0.6 (26.1%**)	*Li et al., 2009*
	Northern Colorado (USA)	200±10	*na*	80±5 (60%*)	*Yang et al., 2004*
	Hong Kong (Stanley and Shatin)	Shatin / 258-409 Stanley / 169-374	Shatin (Anoxic-Aerobic CAS); Stanley (Anoxic-Aerobic CAS and Chlorination)	Shatin (15%**) Stanley (26%**)	*Li and Zhang, 2011*

				Disinfection (24%**) Final (43%**)	
Spiramycin	Italy and Switzerland (Milan, Varese, Como, Lugano)	Milan / 24±11 Varese / 234±155 Como / 97±23 Lugano / 1.7±1.5	Pre-treatment; Primary treatment (primary settling); Secondary treatment (activated sludge process); UV-light tertiary treatment (Varese).	Milan / 121±30 (<0*) Varese /146±63 ng L^{-1} (38%*) Como / 75±24 ng L^{-1} (23%*) Lugano / 393±179 (< 0*)	*Zuccato et al., 2010*
Sulfonamides					
Sulfamethoxazole	Brisbane (Australia)	500	Screened influent; Primary Settling Tank (PST): HRT_{PST}=5.5 h; Bioreactor (BRT): SRT=12.5 days; Final Settling Tank (FST): HRT_{FST}=9 h	PST / 570 (< 0*) BRT / 200 (60%*) FST / 320 (36%*)	*Watkinson et al., 2007*
	Taipei (Taiwan)	179-1760	$WWTP_1$ (Screening and sedimentation; CAS and sedimentation; UV); $WWTP_2$ (Grit removal and screening and sedimentation, deep shaft and step aeration and sedimentation; Chlorination); $WWTP_3$ (Screening; Trickling filter and sedimentation; Chlorination); $WWTP_4$ (Screening and grit removal and sedimentation; CAS and sedimentation; Chlorination)	47-964 (26-88%**)	*Lin et al., 2009*
	Fort Collins (Colorado)	1090	Pretreatment; Primary clarification; Intermediate clarification; Secondary clarification; Chlorine disinfection	210 (~81%**)	*Yang et al., 2005*
	Korea	450	CAS	(<30) (>93%*)	*Choi et al., 2007*
	Croatia	590	CAS	390 (34%*)	*Gros et al., 2006*
	Switzerland (Kloten-Opfikon (WWTP-K); Altenrhein (WWTP-A))	230-570	Primary treatment (screen, aerated grit-removal tank, primary clarifier); Secondary treatment (WWTP-K: CAS; WWTP-A: CAS and FBR); Tertiary treatment (sand filtration).	Primary / 90-640 Secondary / 130-840 Tertiary / 211-860	*Göbel et al., 2005*
	Rio Grande (Colorado) (Magdalena; Hagerman; Socorro; Portales; Santa Fe; Albuquerque)	390	CAS	310 (20%**)	*Brown et al., 2006*
	South-East of Austria	24-145	Screen; Grit chamber; Two aeration tanks; Two secondary clarifiers for final sedimentation.	18-91 (25-37%*)	*Clara et al., 2005*
	Guangzhou (China)	$GZ\text{-}WWTP_2$ / 5450 $GZ\text{-}WWTP_1$ / 7910	$GZ\text{-}WWTP_1$ (Sedimentation; CAS; Filtration); $GZ\text{-}WWTP_2$ (CAS; Filtration; Chlorination).	$GZ\text{-}WWTP_1$ Primary / 9460 (<0*) Secondary / *nq* Tertiary / *nd* $GZ\text{-}WWTP_2$ Primary / *nq* Secondary / *nq* Tertiary/ *nd*	*Peng et al., 2006*
	Sweden (Stockholm; Gothenburg; Umeå; Kalmar; and Floda)	(<80)-674	Chemical removal of phosphorus; Primary clarification; CAS with nitrogen removal (except Umeå and Floda); Secondary clarification.	(<80)-304 (42%**)	*Lindberg et al., 2005*
	Kallby (Sweden)	20	Bar screening; Grit removal; Primary clarification; Activated sludge; Secondary sedimentation; Chemical phosphorous removal; Final sedimentation.	70 (<0**)	*Bendz et al., 2005*
	Wisconsin (USA)	(<50)-1250	CAS	(<50)-370 (17.8-100%**)	*Karthikeyan and Meyer, 2006*
	Galicia (Spain)	So / 580 (inlet to the grit removal unit) Sps / 470 (inlet to the primary sedimentation tank) Sb / 640 (inlet to the biological reactor)	Pre-treatment (coarse screening, bar racks, fine screening and aerated chambers for grit and fat removal); Primary treatment (circular sedimentation tanks); Secondary treatment (conventional activated sludge process); Sedimentation tank (final effluent of the plant).	250 (67%**)	*Carballa et al., 2004*

		Sss / 250 (inlet to the secondary sedimentation tank)			
	Switzerland (Kloten-Opfikon (WWTP-K); Altenrhein (WWTP-A))	230-570	Primary treatment (screen, aerated grit-removal tank, primary clarifier); Secondary treatment (WWTP-K: CAS; WWTP-A: CAS and FBR); Tertiary treatment (sand filtration).	Primary (-21-(-5)%**) Secondary (-138-60%**)	*Göbel et al., 2007*
	Italy and Switzerland (Milan, Varese, Como, Lugano)	Milan / 40±21 Varese / 97±38 Como / 33±44 Lugano / 33±15	Pre-treatment; Primary treatment (primary settling); Secondary treatment (CAS); UV-light tertiary treatment (Varese).	Milan / 16±2.8 (60%*) Varese / 11±19 (89%*) Como / 30±5.6 (9%*) Lugano / 15±11 (55%*)	*Zuccato et al., 2010*
	South-East Queensland (Australia)	3000	*na*	200 (93%*)	*Watkinson et al., 2009*
	Hong Kong (Stanley and Shatin)	Shatin / 146.5±10.6 Stanley / 355.5±17.2	*na*	Shatin / 46.6±2.6 (68.2%**) Stanley/ 15.3±0.3 (95.7%**)	*Li et al., 2009*
	Taiwan	500-10000	Extended sludge age biological technology (HRT=12 h; SRT> 200 days; MLSS=16000 mg L^{-1})	(65-96%**)	*Yu et al., 2009*
	California (WWTP I) and Arizona (WWTP II) (Georgia)	*na*	Primary (screening and sedimentation); Secondary (activated sludge and trickling filter); Tertiary (biological nutrient removal and disinfection). WWTP I: chlorination ,WWTP II: UV	WWTP I Secondary / (<60)-640 Chlorination / (<50)-70 WWTP II Secondary / 100-1600 UV / 330-2140	*Renew and Huang, 2004*
	Beggen (Luxemburg)	13-155	*na*	4-39 (69-75%*)	*Pailler et al., 2009*
	Erie County (New York) (Amherst, East Aurora, Holland, Lackawanaa).	*na*	Amherst: Primary treatment; Secondary treatment (Stage1: conventional activated sludge; Stage 2: nitrification); Tertiary treatment (Sand filtration and chlorination). East Aurora: No Primary treatment; Secondary treatment (Extended aeration; Ferrous chloride addition); Tertiary treatment (Sand filtration and UV radiation). Holland: Primary treatment; Secondary treatment (Rotating biological contactors); Tertiary treatment (Sand filtration and UV radiation). Lackawana: Primary treatment; Secondary treatment (Pure oxygen activated sludge); Chlorination.	Amherst (Primary / 2800±300; Stage1 / 1200±3; Stage2 / 700±40; Tertiary / 630±60; Final / 680±30) East Aurora (Primary / 880±80 ; Secondary / 200±3; Tertiary / 190±5 ; Final / 220±20) Holland (Primary / 750±40; Secondary / 480±30; Tertiary / 450±20; Final / 500±60) Lackawana (Primary / 720±60; Secondary / 460±40; Final / 380±30)	*Batt et al., 2007*
	Braunschweig (Germany)	820±230	Screen; Aerated grid-removal tank; Primary clarifier; CAS; Phosphate removal; Nitrification-denitrification.	620±90 (24%**)	*Ternes et al., 2007*
	Guangzhou and Hong Kong (South China) Kaifaqu (A), Liede (B), New Territory (C), Kowloon (D)	A / 16±5 B / 118±17 C / 10±3 D / 25±7	A (Primary treatment; CAS; Chlorine); B (Primary treatment; Oxidation ditch; UV); C (Primary treatment; CAS); D (Primary treatment; Chemically enhanced; Chlorine).	A / 16±7 (0%) B / 78±13 (34%*) C / 12±3 (<0*) D / 9±4 (64%*)	*Xu et al., 2007*
	Hong Kong (Stanley and Shatin)	Shatin / 52.0-127 Stanley / 163-230	Shatin (Anoxic-Aerobic CAS); Stanley (Anoxic-Aerobic CAS and Chlorination)	Shatin (90%**) Stanley (62%**) Disinfection (27%**) Final (73%**)	*Li and Zhang, 2011*
N^4-Sulfamethoxazole	Switzerland (Kloten-Opfikon (WWTP-K); Altenrhein (WWTP-A))	850-1600	Primary treatment (screen, aerated grit-removal tank, primary clarifier); Secondary treatment (WWTP-K: CAS; WWTP-A: CAS and FBR); Tertiary treatment (sand filtration).	Primary / 570-1200 Secondary / (<20)-150 Tertiary / (<20)-180	*Göbel et al., 2005*

	Switzerland (Kloten-Opfikon (WWTP-K); Altenrhein (WWTP-A))	850-1600	Primary treatment (screen, aerated grit-removal tank, primary clarifier); Secondary treatment (WWTP-K: CAS; WWTP-A: CAS and FBR); Tertiary treatment (sand filtration).	Primary (9-21%**) Secondary (81-96%**)	*Göbel et al., 2007*
	Switzerland (Kloten-Opfikon (WWTP-K); Altenrhein (WWTP-A))	1000	Primary treatment (screen, aerated grit-removal tank, primary clarifier); Secondary treatment (WWTP-K: CAS; WWTP-A: CAS and a FBR); Tertiary treatment (sand filtration).	60 (94%*)	*Joss et al., 2005*
Sulfamethazine	Fort Collins (Colorado)	150	Pretreatment; Primary clarification; Intermediate clarification; Secondary clarification; Chlorine disinfection	(<30) (>80%*)	*Yang et al., 2005*
	Korea	4010	CAS	(<30) (>99%*)	*Choi et al., 2007*
	Wisconsin (USA)	110-210	CAS	(<50) (100%**)	*Karthikeyan and Meyer, 2006*
	Taiwan	2000-10000	Extended sludge age biological technology (HRT=12 h; SRT> 200 days; MLSS=16000 mg L^{-1})	(32-85%**)	*Yu et al., 2009*
	Northwest Ohio (USA)	(<LOQ)-26.9	*na*	<LOQ (100%*)	*Spongberg et al., 2008*
	Hong Kong (Stanley and Shatin)	Shatin / 3.2-54.7 Stanley / 17.8	Shatin (Anoxic-Aerobic CAS); Stanley (Anoxic-Aerobic CAS and Chlorination)	Shatin (100%**) Stanley (100%**) Disinfection (*ne*) Final (100%**)	*Li and Zhang., 2011*
Sulfadiazine	Guangzhou (China)	GZ-$WWTP_2$ / 5100 GZ-$WWTP_1$ / 5150	GZ-$WWTP_1$ (Sedimentation; CAS; Filtration); GZ-$WWTP_2$ (CAS; Filtration; Chlorination).	GZ-$WWTP_1$ Primary / 4180 (19%*) Secondary / *nd* Tertiary / *nd* GZ-$WWTP_2$ Primary / *nd* Secondary / *nd* Tertiary / *nd*	*Peng et al., 2006*
	Hong Kong (Stanley and Shatin)	Shatin / 73.0±2.3 Stanley / *nd*	*na*	Shatin / 16.2±0.0 (72.8%**) Stanley / *nd*	*Li et al., 2009*
	Guangzhou and Hong Kong (South China) Kaifaqu (A), Liede (B), New Territory (C), Kowloon (D)	A / *nd* B / 72±22 C / *nd* D / *nd*	A (Primary treatment; CAS; Chlorine); B (Primary treatment; Oxidation ditch; UV); C (Primary treatment; CAS); D (Primary treatment; Chemically enhanced; Chlorine).	A / 36±13 (50%*)	*Xu et al., 2007*
	Hong Kong (Stanley and Shatin)	Shatin / 36.0-55.4 Stanley / 4.4-530	Shatin (Anoxic-Aerobic CAS); Stanley (Anoxic-Aerobic CAS and Chlorination)	Shatin (100%**) Stanley (87%**) Disinfection (4%**) Final (88%**)	*Li and Zhang, 2011*
Sulfathiazole	Brisbane (Australia)	40	Screened influent; Primary Settling Tank (PST): HRT_{PST}=5.5 h; Bioreactor (BRT): SRT=12.5 days; Final Settling Tank (FST): HRT_{FST}=9 h	PST / *nd* (100%*) BRT / *nd* (100%*) FST / 5 (88%*)	*Watkinson et al., 2007*
	Korea	10570	CAS	180 (98%*)	*Choi et al., 2007*
	South-East Queensland (Australia)	300	*na*	600 (< 0*)	*Watkinson et al., 2009*
	Beggen (Luxemburg)	(1.0)-2.0	*na*	(<1.0) (100%*)	*Pailler et al., 2009*
Sulfamerazine	Korea	1530	CAS	(<30) (>98%*)	*Choi et al., 2007*
Sulfachloropyridazine	Korea	1560	CAS	60 (>93%*)	*Choi et al., 2007*

Sulfadimethoxine	Fort Collins (Colorado)	70	Pretreatment; Primary clarification; Intermediate clarification; Secondary clarification; Chlorine disinfection	(<30) (>57%*)	*Yang et al., 2005*
	Korea	460	CAS	(<30) (>93%*)	*Choi et al., 2007*
	Taiwan	2000-10000	Extended sludge age biological technology (HRT=12 h; SRT> 200 days; MLSS=16000 mg L^{-1})	(61-96%**)	*Yu et al., 2009*
	Northwest Ohio (USA)	(<(LOQ)-2.6)	*na*	(<LOQ)-1.9 (27%*)	*Spongberg et al., 2008*
	Beggen (Luxemburg)	(1.0)-26	*na*	(1.0)-9.0 (65%*)	*Pailler et al., 2009*
Sulfapyridine	Switzerland (Kloten-Opfikon (WWTP-K); Altenrhein (WWTP-A))	60-150	Primary treatment (screen, aerated grit-removal tank, primary clarifier); Secondary treatment (WWTP-K: CAS; WWTP-A: CAS and FBR); Tertiary treatment (sand filtration).	Primary (-29-20%**) Secondary (-107-72%**)	*Göbel et al., 2007*
Sulfasalazine	Brisbane (Australia)	60	Screened influent; Primary Settling Tank (PST): HRT_{PST}=5.5 h; Bioreactor (BRT): SRT=12.5 days; Final Settling Tank (FST): HRT_{FST}=9 h	PST / 15 (75%*) BRT / *nd* (100%*) FST / 10 (83%*)	*Watkinson et al., 2007*
	South-East Queensland (Australia)	100	*na*	150 (< 0*)	*Watkinson et al., 2009*
Sulfamonomethoxine	Korea	3110	CAS	(<30) (>99%*)	*Choi et al., 2007*
Sulfisoxazole	Northwest Ohio (USA)	(<LOQ)-22.1)	*na*	(<LOQ)-11.9 (46%*)	*Spongberg et al., 2008*
Sulfadimidine	Guangzhou and Hong Kong (South China) Kaifaqu (A), Liede (B), New Territory (C), Kowloon (D)	A / 25±12 B / 696±212 C / *nd* D / *nd*	A (Primary treatment; CAS; Chlorine); B (Primary treatment; Oxidation ditch; UV); C (Primary treatment; CAS); D (Primary treatment; Chemically enhanced; Chlorine).	A / 12±6 (52%*) B / 346±54 (50%*)	*Xu et al., 2007*
Quinolones					
Norfloxacin	Brisbane (Australia)	*na*	*na*	210	*Costanzo et al., 2005*
	Brisbane (Australia)	210	Screened influent; Primary Settling Tank (PST): HRT_{PST}=5.5 h; Bioreactor (BRT): SRT=12.5 days; Final Settling Tank (FST): HRT_{FST}=9 h	PST / 145 (31%*) BRT / 15 (93%*) FST / 40 (81%*)	*Watkinson et al., 2007*
	Hong Kong and Shenzhen (China) (Wan Chai [1], Shatin [2], Tai Po [3], Stonecutters Island [4], Nan Shan [5])	110-460	[1] (Primary treatment); [2] (Screening; Settlement of grit particles; Primary sedimentation; Biological treatment); [3] (Removal of solids and grit; Primary sedimentation; Biological treatment; Anaerobic digestion); [4] (Chemically enhanced primary treatment); [5] (Primary treatment)	85-320 (-20-78%**)	*Gulkowska et al., 2008*
	Zurich-Werdholzli (Switzerland)	431±45	Screens; Combined grid; Fat removal tank; Primary clarification; Activated sludge; Secondary clarifiers (SRT=11days); Denitrification; Flocculation-filtration.	Primary / 383±61 (11%*) Secondary / 69±15 (84%*) Tertiary / 51±7 (88%*)	*Golet et al., 2003*
	Kristianstad (Sweden) ($WWTP_1$-$WWTP_5$)	$WWTP_1$ / 18±2.5 $WWTP_2$ / 27±3.0 $WWTP_3$ / 19.0±1.5 $WWTP_4$ / (<5.5) $WWTP_5$ / (<5.5)	Screens; Grit-aerated chamber; CAS; Chemical removal; Sand filtration.	(>70%**)	*Zorita et al., 2009*
	Sweden (Stockholm; Gothenburg; Umeå; Kalmar; and Floda)	66-174	Chemical removal of phosphorus; Primary clarification; CAS with nitrogen removal (except Umeå and Floda); Secondary clarification.	(<7)-37 (87%**)	*Lindberg et al., 2005*
	Gao Beidian (Beijing, China)	339	Primary treatment; Secondary treatment processes	85 (75%*)	*Xiao et al., 2008*
	Glatt Valley Watershed (Switzerland)	388± 112	Secondary treatment	57±12 (82±3%**)	*Golet et al., 2002*

	South-East Queensland (Australia)	220	*na*	250 (< 0*)	*Watkinson et al., 2009*
	Hong Kong (Stanley and Shatin)	Shatin / 59.5±3.7 Stanley / *nd*	*na*	Shatin / 13.9±0.5 (76.6%**) Stanley/ *nd*	*Li et al., 2009*
	Guangzhou and Hong Kong (South China) Kaifaqu (A), Liede (B), New Territory (C), Kowloon (D)	A / 229±42 B / 179±41 C / 54±10 D / 263±36	A (Primary treatment; CAS; Chlorine); B (Primary treatment; Oxidation ditch; UV); C (Primary treatment; CAS); D (Primary treatment; Chemically enhanced; Chlorine).	A / 44±19 (81%*) B / 62±13 (65%*) C / 27±6 (50%*) D / 85±12 (68%*)	*Xu et al., 2007*
Ciprofloxacin	Brisbane (Australia)	90	*na*	138.2 (<0*)	*Costanzo et al., 2005*
	Brisbane (Australia)	4600	Screened influent; Primary Settling Tank (PST): HRT_{PST}=5.5 h; Bioreactor (BRT): SRT=12.5 days; Final Settling Tank (FST): HRT_{FST}=9 h	PST / 6900 (< 0*) BRT / 742 (84%*) FST / 720 (84%*)	*Watkinson et al., 2007*
	Zurich-Werdholzli (Switzerland)	427±69	Screens; Combined grid; Fat removal tank; Primary clarification; Activated sludge; Secondary clarifiers (SRT=11days); Denitrification; Flocculation-filtration.	Primary / 331±53 (22%*) Secondary / 95±15 (78%*) Tertiary / 71±11 (83%*)	*Golet et al., 2003*
	Kristianstad (Sweden) ($WWTP_1$-$WWTP_5$).	$WWTP_1$ / 320±10 $WWTP_2$ / 310±20 $WWTP_3$ / 94.0±12.0 $WWTP_4$ / 28.0±5.5 $WWTP_5$ / 31.5±4.0	Screens; Grit-aerated chamber; CAS; Chemical removal; Sand filtration.	(>90%**)	*Zorita et al., 2009*
	Sweden (Stockholm; Gothenburg; Umeå; Kalmar; and Floda)	90-300	Chemical removal of phosphorus; Primary clarification; CAS with nitrogen removal (except Umeå and Floda); Secondary clarification.	7-60 (87%**)	*Lindberg et al., 2005*
	Wisconsin (USA)	(<50)-310	CAS	(<50)-60 (22.2-100%**)	*Karthikeyan and Meyer, 2006*
	Gao Beidian (Beijing, China)	80	Primary treatment; Secondary treatment processes	27 (66%*)	*Xiao et al., 2008*
	Glatt Valley Watershed (Switzerland)	434±93	Secondary treatment	72±14 (82±3%**)	*Golet et al., 2002*
	Italy and Switzerland (Milan, Varese, Como, Lugano)	Milan / 32±12 Varese / 203±121 Como / 108±15 Lugano / 4.9±6.0	Pre-treatment; Primary treatment (primary settling); Secondary treatment (CAS); UV-light tertiary treatment (Varese).	Milan / 24±4.5 (25%*) Varese / 60±46 (70%*) Como / *nd* (100%*) Lugano / *nd* (100%*)	*Zuccato et al., 2010*
	South-East Queensland (Australia)	1100	*na*	*nd* (100%*)	*Watkinson et al., 2009*
	Hong Kong (Stanley and Shatin)	Shatin / 720.0±30.4 Stanley / 99.2±5.1	*na*	Shatin / 73.3±3.0 (89.8%**) Stanley / 7.6±0.7 (92.3%**)	*Li et al., 2009*
	Northwest Ohio (USA)	11.4-377.2	*na*	88-109.9 (71%*)	*Spongberg et al., 2008*
	California (WWTP I) and Arizona (WWTP II) (Georgia)	*na*	Primary (screening and sedimentation); Secondary (activated sludge and trickling filter); Tertiary (biological nutrient removal and disinfection). WWTP I: chlorination ,WWTP II: UV	WWTP I Secondary / (<30)-100 Chlorination / (<20) WWTP II Secondary / 80-370 UV / (<20)	*Renew and Huang, 2004*
	Erie County (New York) (Amherst, East Aurora, Holland, Lackawanaa).	*na*	Amherst: Primary treatment; Secondary treatment (Stage1: conventional activated sludge; Stage 2: nitrification); Tertiary treatment (Sand filtration and chlorination). East Aurora: No Primary treatment; Secondary treatment (Extended aeration; Ferrous chloride addition); Tertiary treatment (Sand	Amherst (Primary / 1100±100; Stage 1 / 450±1; Stage 2 / 450±4; Tertiary / 450±3; Final / 540±5) East Aurora (Primary / 610±30;	*Batt et al., 2007*

			filtration and UV radiation). Holland: Primary treatment; Secondary treatment (Rotating biological contactors); Tertiary treatment (Sand filtration and UV radiation). Lackawana: Primary treatment; Secondary treatment (Pure oxygen activated sludge); Chlorination.	Secondary / 290±30; Tertiary / 220±9; Final / 220±7) Holland (Primary / 1400±300; Secondary / 590±10; Tertiary / 450±60; Final / 340±60) Lackawana (Primary / 920±50; Secondary / 460±10; Final / 270±20)	
	Varese Olona (Italy)	1674.20	*na*	626.50 (63%*)	*Castiglioni et al., 2008*
	Hong Kong (Stanley and Shatin)	Shatin / 555-1033 Stanley / 98.6-235	Shatin (Anoxic-Aerobic CAS); Stanley (Anoxic-Aerobic CAS and Chlorination)	Shatin (18%**) Stanley (55%**) Disinfection (18%**) Final (66%**)	*Li and Zhang., 2011*
Enrofloxacin	Brisbane (Australia)	100	Screened influent; Primary Settling Tank (PST): HRT_{PST}=5.5 h; Bioreactor (BRT): SRT=12.5 days; Final Settling Tank (FST): HRT_{FST}=9 h	PST / 20 (80%*) BRT / 5 (95%*) FST / 10 (90%*)	*Watkinson et al., 2007*
	South-East Queensland (Australia)	40	*na*	50 (< 0*)	*Watkinson et al., 2009*
Ofloxacin	Taipei (Taiwan)	115-1274	$WWTP_1$ (Screening and sedimentation; CAS and sedimentation; UV); $WWTP_2$ (Grit removal and screening and sedimentation, deep shaft and step aeration and sedimentation; Chlorination); $WWTP_3$ (Screening; Trickling filter and sedimentation; Chlorination); $WWTP_4$ (Screening and grit removal and sedimentation; CAS and sedimentation; Chlorination)	53-991 (2-88%**)	*Lin et al., 2009*
	Rio Grande (Colorado) (Magdalena; Hagerman; Socorro; Portales; Santa Fe; Albuquerque)	470	CAS	110 (77%**)	*Brown et al., 2006*
	Kristianstad (Sweden) ($WWTP_1$-$WWTP_5$).	$WWTP_1$ / 22.5±2.5 $WWTP_2$ / 30.0±3.0 $WWTP_3$ / 19.5±3.0 $WWTP_4$ / 9.0±1.5 $WWTP_5$ / 10.0±1.0	Screens; Grit-aerated chamber; CAS; Chemical removal; Sand filtration.	(56%**)	*Zorita et al., 2009*
	Guangzhou (China)	GZ-$WWTP_1$ / 5560 GZ-$WWTP_2$ / 3520	GZ-$WWTP_1$ (Sedimentation; CAS; Filtration); GZ-$WWTP_2$ (CAS; Filtration; Chlorination).	GZ-$WWTP_1$ Primary / 5700 (<0*) Secondary / 860 (85%*) Tertiary / 740 (87%*) GZ-$WWTP_2$ Primary / *nq* Secondary / *nd* Tertiary / *nd*	*Peng et al., 2006*
	Sweden (Stockholm; Gothenburg; Umeå; Kalmar; and Floda)	7-287	Chemical removal of phosphorus; Primary clarification; CAS with nitrogen removal (except Umeå and Floda); Secondary clarification.	7-52 (86%**)	*Lindberg et al., 2005*
	Gao Beidian (Beijing, China)	1208	Primary treatment; Secondary treatment processes	503 (58%*)	*Xiao et al., 2008*
	Italy and Switzerland (Milan, Varese, Como, Lugano)	Milan / 7.7±6.9 Varese / 184±134 Como / 20±25 Lugano / 0.31±0.60	Pre-treatment; Primary treatment (primary settling); Secondary treatment (CAS); UV-light tertiary treatment (Varese).	Milan / 5.3±1.6 (31%*) Varese / 77±56 (58%*) Como / 4.9±8.4 (75%*) Lugano / *nd* (100%*)	*Zuccato et al., 2010*

	Hong Kong (Stanley and Shatin)	Shatin / 335.9±16.7 Stanley / 104.4±4.4	*na*	Shatin / 556.4±28.7 (-65.6%**) Stanley/ 2.1±0.3 (98.0%**)	*Li et al., 2009*
	California (WWTP I) and Arizona (WWTP II) (Georgia)	*na*	Primary (screening and sedimentation); Secondary (activated sludge and trickling filter); Tertiary (biological nutrient removal and disinfection). WWTP I: chlorination ,WWTP II: UV	WWTP I Secondary / (<30)-350 Chlorination / (<20)-50 WWTP II Secondary / 140-260 UV / 100-210	*Renew and Huang, 2004*
	Cyprus	WWTP I / 22620 WWTP II / 34740 WWTP III / 59380	WWTP I: Primary treatment; Secondary treatment (oxidation ditches, secondary settlement); Tertiary treatment (sand filtration, chlorination). WWTP II: Primary treatment; Secondary treatment (activated sludge treatment); Tertiary treatment (sand filtration, chlorination). WWTP III: Primary treatment; Secondary treatment (phosphorus biological removal, nitrification and denitrification, secondary clarifiers); Tertiary treatment (sand filtration, chlorination)	Secondary WWTP I / 3020 (87%*) WWTP II / 5930 (83%*) WWTP III / 3330 (94%*) Outlet WWTP I / 1290 (94%*) WWTP II / 4820 (86%*) WWTP III / 1900 (97%*)	*Fatta et al., 2010*
	Varese Olona (Italy)	539.80	*na*	183.10 (66%*)	*Castiglioni et al., 2008*
	Guangzhou and Hong Kong (South China) Kaifaqu (A), Liede (B), New Territory (C), Kowloon (D)	A / 137±58 B / 359±52 C / 80±12 D / 368±23	A (Primary treatment; CAS; Chlorine); B (Primary treatment; Oxidation ditch; UV); C (Primary treatment; CAS); D (Primary treatment; Chemically enhanced; Chlorine).	A / 41±8 (70%*) B / 137±28 (62%*) C / 48±7 (40%*) D / 165±15 (55%*)	*Xu et al., 2007*
	Hong Kong (Stanley and Shatin)	Shatin / 478-1042 Stanley / 188-327	Shatin (Anoxic-Aerobic CAS); Stanley (Anoxic-Aerobic CAS and Chlorination)	Shatin (26%**) Stanley (59%**) Disinfection (39%**) Final (74%**)	*Li and Zhang, 2011*
Nalidixic acid	Brisbane (Australia)	200	Screened influent; Primary Settling Tank (PST): HRT_{PST}=5.5 h; Bioreactor (BRT): SRT=12.5 days; Final Settling Tank (FST): HRT_{FST}=9 h	PST / *nd* (100%*) BRT / 1 (100%*) FST / *nd* (100%*)	*Watkinson et al., 2007*
	Taipei (Taiwan)	26-372	$WWTP_1$ (Screening and sedimentation; CAS and sedimentation; UV); $WWTP_2$ (Grit removal and screening and sedimentation, deep shaft and step aeration and sedimentation; Chlorination); $WWTP_3$ (Screening; Trickling filter and sedimentation; Chlorination); $WWTP_4$ (Screening and grit removal and sedimentation; CAS and sedimentation; Chlorination)	40-200 (37-46%**)	*Lin et al., 2009*
	South-East Queensland (Australia)	200	*na*	450 (< 0*)	*Watkinson et al., 2009*
Pipemidic acid	Gao Beidian (Beijing, China)	54	Primary treatment; Secondary treatment processes	12 (78%*)	*Xiao et al., 2008*
Flerofloxacin	Gao Beidian (Beijing, China)	28	Primary treatment; Secondary treatment processes	5.8 (79%*)	*Xiao et al., 2008*
Lomefloxacin	Gao Beidian (Beijing, China)	98	Primary treatment; Secondary treatment processes	17 (83%*)	*Xiao et al., 2008*
Gatifloxacin	Gao Beidian (Beijing, China)	111	Primary treatment; Secondary treatment processes	56 (50%*)	*Xiao et al., 2008*
Moxifloxacin	Gao Beidian (Beijing, China)	44	Primary treatment; Secondary treatment processes	17 (61%*)	*Xiao et al., 2008*
Trimethoprim					

	Brisbane (Australia)	930	Screened influent; Primary Settling Tank (PST): HRT_{PST}=5.5 h; Bioreactor (BRT): SRT=12.5 days; Final Settling Tank (FST): HRT_{FST}=9 h	PST / 480 (48%*) BRT / 30 (97%*) FST / 70 (93%*)	*Watkinson et al., 2007*
	Hong Kong and Shenzhen (China) (Wan Chai [1], Shatin [2], Tai Po [3], Stonecutters Island [4], Nan Shan [5])	120-320	[1] (Primary treatment); [2] (Screening; Settlement of grit particles; Primary sedimentation; Biological treatment); [3] (Removal of solids and grit; Primary sedimentation; Biological treatment; Anaerobic digestion); [4] (Chemically enhanced primary treatment); [5] (Primary treatment)	120-230 (~ -17-62%**)	*Gulkowska et al., 2008*
	Taipei (Taiwan)	259-949	$WWTP_1$ (Screening and sedimentation; CAS and sedimentation; UV); $WWTP_2$ (Grit removal and screening and sedimentation, deep shaft and step aeration and sedimentation; Chlorination); $WWTP_3$ (Screening; Trickling filter and sedimentation; Chlorination); $WWTP_4$ (Screening and grit removal and sedimentation; CAS and sedimentation; Chlorination)	203-415 (~22-56%**)	*Lin et al., 2009*
	Croatia	1172	CAS	290 (75%*)	*Gros et al., 2006*
	Switzerland (Kloten-Opfikon (WWTP-K); Altenrhein (WWTP-A))	210-440	Primary treatment (screen, aerated grit-removal tank, primary clarifier); Secondary treatment (WWTP-K: CAS; WWTP-A: CAS and FBR); Tertiary treatment (sand filtration).	Primary / 80-340 Secondary / 80-400 Tertiary / 20-310	*Göbel et al., 2005*
	Rio Grande (Colorado) (Magdalena; Hagerman; Socorro; Portales; Santa Fe; Albuquerque)	590	CAS	180 (69%**)	*Brown et al., 2006*
	Sweden (Stockholm; Gothenburg; Umeå; Kalmar; and Floda)	99-1300	Chemical removal of phosphorus; Primary clarification; CAS with nitrogen removal (except Umeå and Floda); Secondary clarification.	66-1340 (3%**)	*Lindberg et al., 2005*
	Wisconsin (USA)	140-1100	CAS	(<50)-550 (50-100%**)	*Karthikeyan and Meyer, 2006*
	Kallby (Sweden)	80	Bar screening; Grit removal; Primary clarification; Activated sludge; Secondary sedimentation; Chemical phosphorous removal; Final sedimentation.	40 (49%**)	*Bendz et al., 2005*
	Howdon (UK)	213-300	Coarse screening; Preliminary clarification; Activated sludge treatment and trickling filter system; Settlement tanks; High-pressure 254 nm UV disinfection.	218-322 (3%**)	*Roberts and Thomas., 2006*
	Switzerland (Kloten-Opfikon (WWTP-K); Altenrhein (WWTP-A))	210-440	Primary treatment (screen, aerated grit-removal tank, primary clarifier); Secondary treatment (WWTP-K: CAS; WWTP-A: CAS and FBR); Tertiary treatment (sand filtration).	Trimethoprim Primary (-13-31%**) Secondary (-40-20%**)	*Göbel et al., 2007*
	Beijing (China)	400	Primary treatment; Secondary biological treatment (A and D: anaerobic/anoxic/oxic [A^2/O]) CAS; B: anoxic/oxic [A/O]) CAS; C: Oxidation ditch [OD].	Primary (~20%**) Secondary (76±24%**)	*Sui et al., 2010*
	South-East Queensland (Australia)	4300	*na*	250 (94*)	*Watkinson et al., 2009*
	Hong Kong (Stanley and Shatin)	Shatin / 128.7±5.5 Stanley / 161.2±10.7	*na*	Shatin / 66.2±0.7 (48.6%**) Stanley / 10.8±1.1 (93.3%**)	*Li et al., 2009*
	Taiwan	1000	Extended sludge age biological technology (HRT=12 h; SRT> 200 days; MLSS=16000 mg L^{-1})	(74%**)	*Yu et al., 2009*
	California (WWTP I) and Arizona (WWTP II) (Georgia)	*na*	Primary (screening and sedimentation); Secondary (activated sludge and trickling filter); Tertiary (biological nutrient removal and disinfection). WWTP I: chlorination ,WWTP II: UV	WWTP I Secondary / 30-1210 Chlorination / (<40) WWTP II Secondary / 270-1220 UV / (<40)-1760	*Renew and Huang, 2004*

	Erie County (New York) (Amherst, East Aurora, Holland, Lackawanaa).	*na*	Amherst: Primary treatment; Secondary treatment (Stage1: conventional activated sludge; Stage 2: nitrification); Tertiary treatment (Sand filtration and chlorination). East Aurora: No Primary treatment; Secondary treatment (Extended aeration; Ferrous chloride addition); Tertiary treatment (Sand filtration and UV radiation). Holland: Primary treatment; Secondary treatment (Rotating biological contactors); Tertiary treatment (Sand filtration and UV radiation). Lackawana: Primary treatment; Secondary treatment (Pure oxygen activated sludge); Chlorination.	Amherst (Primary / 7900±400; Stage 1 / 7600±500; Stage 2 / 2500±300; Tertiary / 2600±200; Final / 2400±200) East Aurora (Primary / 7000±1000; Secondary / 300±30; Tertiary / 270±20; Final / 210±9) Holland (Primary / 2300±500; Secondary / 580±20; Tertiary / 570±10; Final / 540±50) Lackawana (Primary / 2100±400; Secondary / 590±3; Final / 360±40)	*Batt et al., 2007*
	Cyprus	WWTP I / 50 WWTP II / 140 WWTP III / 350	WWTP I: Primary treatment; Secondary treatment (oxidation ditches, secondary settlement); Tertiary treatment (sand filtration, chlorination). WWTP II: Primary treatment; Secondary treatment (activated sludge treatment); Tertiary treatment (sand filtration, chlorination). WWTP III: Primary treatment; Secondary treatment (phosphorus biological removal, nitrification and denitrification, secondary clarifiers); Tertiary treatment (sand filtration, chlorination)	Secondary WWTP I / <LOD (100%*) WWTP II / 90 (36%*) WWTP III / 60 (83%*) Outlet WWTP I / <LOD (100%*) WWTP II / <LOD (100%*) WWTP III / <LOD (100%*)	*Fatta et al., 2010*
	Braunschweig (Germany)	1100±260	Screen; Aerated grid-removal tank; Primary clarifier; CAS; Phosphate removal; Nitrification-denitrification.	340±80 (69%**)	*Ternes et al., 2007*
	Hong Kong (Stanley and Shatin)	Shatin / 100-154 Stanley / 136-172	Shatin (Anoxic-Aerobic CAS); Stanley (Anoxic-Aerobic CAS and Chlorination)	Shatin (13%**) Stanley (42%**) Disinfection (40%**) Final (65%**)	*Li and Zhang., 2011*
Tetracyclines					
Tetracycline	Brisbane (Australia)	35	Screened influent; Primary Settling Tank (PST): HRT_{PST}=5.5 h; Bioreactor (BRT): SRT=12.5 days; Final Settling Tank (FST): HRT_{FST}=9 h	PST / *nd* (100%*) BRT / 20 (43%*) FST / 30 (14%*)	*Watkinson et al., 2007*
	Hong Kong and Shenzhen (China) (Wan Chai [1], Shatin [2], Tai Po [3], Stonecutters Island [4], Nan Shan [5])	96-1300	[1] (Primary treatment); [2] (Screening; Settlement of grit particles; Primary sedimentation; Biological treatment); [3] (Removal of solids and grit; Primary sedimentation; Biological treatment; Anaerobic digestion); [4] (Chemically enhanced primary treatment); [5] (Primary treatment)	180-620 (-88-73%**)	*Gulkowska et al., 2008*
	Taipei (Taiwan)	46-234	$WWTP_1$ (Screening and sedimentation; CAS and sedimentation; UV); $WWTP_2$ (Grit removal and screening and sedimentation, deep shaft and step aeration and sedimentation; Chlorination); $WWTP_3$ (Screening; Trickling filter and sedimentation; Chlorination); $WWTP_4$ (Screening and grit removal and sedimentation; CAS and sedimentation; Chlorination)	16-38 (66-90%**)	*Lin et al., 2009*
	Fort Collins (Colorado)	200	Pretreatment; Primary clarification; Intermediate clarification; Secondary clarification; Chlorine disinfection	(<30) (>~85%*)	*Yang et al., 2005*
	Korea	110	CAS	(<30) (>73%*)	*Choi et al., 2007*
	Wisconsin (USA)	240-790	CAS	(<50)-160 (67.9-100%**)	*Karthikeyan and Meyer, 2006*
	South-East Queensland (Australia)	100	*na*	20 (80*)	*Watkinson et al., 2009*

	Hong Kong (Stanley and Shatin)	Shatin / 270.8±16.1 Stanley / 134.5±10.8	*na*	Shatin / 89.4±4.2 (67.0%**) Stanley / *nd (*100%**)	*Li et al., 2009*
	Northwest Ohio (USA)	29.3-38.9	*na*	(<LOQ)-34.4 (12%*)	*Spongberg et al., 2008*
	Beggen (Luxemburg)	(1.0)-85	*na*	(1.0)-24 (72%*) Removal: ~72%*	*Pailler et al., 2009*
	Erie County (New York) (Amherst, East Aurora, Holland, Lackawanaa).	*na*	Amherst: Primary treatment; Secondary treatment (Stage1: conventional activated sludge; Stage 2: nitrification); Tertiary treatment (Sand filtration and chlorination). East Aurora: No Primary treatment; Secondary treatment (Extended aeration; Ferrous chloride addition); Tertiary treatment (Sand filtration and UV radiation). Holland: Primary treatment; Secondary treatment (Rotating biological contactors); Tertiary treatment (Sand filtration and UV radiation). Lackawana: Primary treatment; Secondary treatment (Pure oxygen activated sludge); Chlorination.	Amherst (Primary / 1100±100; Stage 1 / 410±20; Stage 2 / 170±10; Tertiary / 170±2; Final / 160±1) East Aurora (Primary / 320±30; Secondary / 75±3; Tertiary / 61±9; Final / 61±3) Holland (Primary / 580±20; Secondary / 240±20; Tertiary / 220±40; Final / 210±2) Lackawana (Primary / 430±200; Secondary / 240±20; Final / 290±30)	*Batt et al., 2007*
	Hong Kong (Stanley and Shatin)	Shatin / 221-353 Stanley / 59.8-110	Shatin (Anoxic-Aerobic CAS); Stanley (Anoxic-Aerobic CAS and Chlorination)	Shatin (24%**) Stanley (36%**) Disinfection (13%**) Final (39%**)	*Li and Zhang, 2011*
Chlortetracycline	Fort Collins (Colorado)	270	Pretreatment; Primary clarification; Intermediate clarification; Secondary clarification; Chlorine disinfection	60 (~78%**)	*Yang et al., 2005*
	Korea	970	CAS	40 (>96%*)	*Choi et al., 2007*
	South-East Queensland (Australia)	200	*na*	250 (< 0*)	*Watkinson et al., 2009*
	Hong Kong (Stanley and Shatin)	Shatin / 155 Stanley / 178	Shatin (Anoxic-Aerobic CAS); Stanley (Anoxic-Aerobic CAS and Chlorination)	Shatin (85%**) Stanley (82%**) Disinfection (6%**) Final (83%**)	*Li and Zhang., 2011*
Doxycycline	Brisbane (Australia)	65	Screened influent; Primary Settling Tank (PST): HRT_{PST}=5.5 h; Bioreactor (BRT): SRT=12.5 days; Final Settling Tank (FST): HRT_{FST}=9 h	PST / 40 (78%*) BRT / 20 (69%*) FST / 40 (78%*)	*Watkinson et al., 2007*
	Fort Collins (Colorado)	210	Pretreatment; Primary clarification; Intermediate clarification; Secondary clarification; Chlorine disinfection	70 (~67%**)	*Yang et al., 2005*
	Korea	220	CAS	30 (86%*)	*Choi et al., 2007*
	Sweden (Stockholm; Gothenburg; Umeå; Kalmar; and Floda)	(<64)-2480	Chemical removal of phosphorus; Primary clarification; CAS with nitrogen removal (except Umeå and Floda); Secondary clarification.	(<64)-915 (~70%**)	*Lindberg et al., 2005*
	South-East Queensland (Australia)	650	*na*	150 (77%*)	*Watkinson et al., 2009*
Oxytetracycline	Korea	240	CAS	(<30) (>88%*)	*Choi et al., 2007*
	South-East Queensland (Australia)	350	*na*	70 (80%*)	*Watkinson et al., 2009*
	Beggen (Luxemburg)	(1.0)-7.0	*na*	(1.0)-5.0 (29%*)	*Pailler et al., 2009*
	Hong Kong (Stanley and Shatin)	Shatin / 53.5-107 Stanley / *nd*	Shatin (Anoxic-Aerobic CAS); Stanley (Anoxic-Aerobic CAS and Chlorination)	Shatin (44%**)	*Li and Zhang, 2011*
Minocycline	Korea	380	CAS	(<30) (>92%*)	*Choi et al., 2007*
Democlocycline	Korea	270	CAS	30 (89%*)	*Choi et al., 2007*

Meclocycline-Sulfosalicylate	Korea	500	CAS	180 (64%*)	*Choi et al., 2007*
Lincosamides					
Lincomycin	Brisbane (Australia)	80	Screened influent; Primary Settling Tank (PST): HRT_{PST}=5.5 h; Bioreactor (BRT): SRT=12.5 days; Final Settling Tank (FST): HRT_{FST}=9 h	PST / 70 (12.5%*) BRT / 50 (37.5%*) FST / 60 (25%*)	*Watkinson et al., 2007*
	Italy and Switzerland (Milan, Varese, Como, Lugano)	Milan / 15±3.7 Varese / 3.9±3.0 Como / 10±6.6 Lugano / 0.54±0.2	Pre-treatment; Primary treatment (primary settling); Secondary treatment (CAS); UV-light tertiary treatment (Varese).	Milan / 4.9±1.5 (67%*) Varese / 2.8±1.5 (28%* Como / 5.8±2.7 (42%*) Lugano/ 1.1±1.2 9 (<0*)	*Zuccato et al., 2010*
	Five WWTPs in South-East Queensland (Australia)	500	*na*	300 (40%*)	*Watkinson et al., 2009*
	Varese Olona (Italy)	3.9	*na*	3.70 (5%*)	*Castiglioni et al., 2008*
Clindomycin	Brisbane (Australia)	5	Screened influent; Primary Settling Tank (PST): HRT_{PST}=5.5 h; Bioreactor (BRT): SRT=12.5 days; Final Settling Tank (FST): HRT_{FST}=9 h	PST / 5 (0%*) BRT / 5 (0%*) FST / 5 (0%*)	*Watkinson et al., 2007*
	South-East Queensland (Australia)	60	*na*	70 (< 0*)	*Watkinson et al., 2009*
	Northwest Ohio (USA)	6.8-13.3	*na*	14.9-32.5 (<0*)	*Spongberg et al., 2008*
Polyether ionophores					
Monensin	Brisbane (Australia)	190	Screened influent; Primary Settling Tank (PST): HRT_{PST}=5.5 h; Bioreactor (BRT): SRT=12.5 days; Final Settling Tank (FST): HRT_{FST}=9 h	PST / 10 (95%*) BRT / 1 (99.5%*) FST / *nd* (100%*)	*Watkinson et al., 2007*
Salisomycin	South-East Queensland (Australia)	300	*na*	*nd* (100%*)	*Watkinson et al., 2009*
Glycopeptides					
Vancomycin	Italy and Switzerland (Milan, Varese, Como, Lugano)	Milan / 9.6±1.8 Varese / 14±20 Como / *nd* Lugano / *nd*	Pre-treatment; Primary treatment (primary settling); Secondary treatment (activated sludge process); UV-light tertiary treatment (Varese).	Milan / 5.2±0.5 (46%*) Varese / 10±13 (29%*) Como / 9.4±6.7 Lugano / 24±13	*Zuccato et al., 2010*
	Hong Kong (Stanley and Shatin)	Shatin / (<36.5)-60.6 Stanley / *nd*	Shatin (Anoxic-Aerobic CAS); Stanley (Anoxic-Aerobic CAS and Chlorination)	Vamcomycin Shatin (52%**)	*Li and Zhang, 2011*

NOTES

- CAS: Conventional activated sludge treatment
- **(*)** Removal efficiencies, not reported by authors in the cited study, are calculated from the average influent and effluent concentrations which were stated in the study.
- **(**)** Removal efficiencies reported by authors in the cited study
- Value in the parenthesis is the limit of detection (LOD)
- Negative removal values result from an observed increase of loads from inflow to outflow of wastewater treatment.
- *nd*: not detected; *na*: not available; *ne:* not evaluated; *nq:* not quantified

Table A2. Removal of antibiotics from wastewater effluents through advanced treatment processes.

Advanced treatment process Antibiotic Group	OZONATION				
	Type of wastewater (location)	**Initial concentration**	**Treatment process**	**Results/findings (Removal efficiency)**	**Reference**
β-Lactams					
Cephalexin	Secondary effluent (Kloten-Opfikon, Switzerland)	1 μM	Batch experiments, O_3 dose=0.5-5.0 mg L^{-1}	O_3 dose=3 mg L^{-1} (100%)	*Dodd et al., 2006*
Penicillin	Antibiotic formulation effluent (Turkey)	*na*	O_3 dose =2500 mg (L h)$^{-1}$; pH=2.5–12.0 O_3+H_2O_2 [H_2O_2]=2-40 mM); pH=10.5	COD removal O_3: (10-56%) O_3+H_2O_2 (20 mM): (83%)	*Arslan Alaton et al., 2004*
	Antibiotic formulation effluent (Turkey)	*na*	O_3 dose =2760 mg (L h)$^{-1}$; pH=3-11.5	COD removal O_3/pH 3: (15%) O_3/pH 7: (28%) O_3/pH 11: (49%) TOC removal O_3/pH 3: (2%) O_3/pH 7: (23%) O_3/pH 11: (52%)	*Arslan Alaton and Dogruel, 2004*
Penicillin	Secondary effluent (Kloten-Opfikon, Switzerland)	1 μM	Batch experiments, O_3 dose=0.5-5.0 mg L^{-1}	O_3 dose=5 mg L^{-1} (100%)	*Dodd et al., 2006*
Penicillin V	Synthetic wastewater (Turkey)	*na*	(a) O_3 (flow=100 L h^{-1}, O_3 dose=2.96 g L^{-1} h^{-1}); (b) O_3/H_2O_2 ([H_2O_2]=20 mM)	(a) (80% in 60 min) (b) (100% in 60 min)	*Balcioglu and Otker, 2003*
Ceftriaxone	Synthetic wastewater (Turkey)	*na*	(a) O_3 (flow=100 L h^{-1}, O_3 dose=2.96 g L^{-1} h^{-1}); (b) O_3/H_2O_2 ([H_2O_2]=20 mM)	(a) (>99% in 60 min) (b) (100% in 60 min)	*Balcioglu and Otker, 2003*
Macrolides					
Roxithromycin	Secondary effluent (Kloten-Opfikon, Switzerland)	1 μM	Batch experiments, O_3 dose=0.5-5.0 mg L^{-1}	O_3 dose=1 mg L^{-1} (55%)	*Dodd et al., 2006*
	CAS and MBR effluent (Kloten-Opfikon, Switzerland)	2 μg L^{-1}	O_3 dose=0-5 mg L^{-1}; flow=200 ±10 L h^{-1} (only column 1).	O_3 dose ≥ 2 mg L^{-1} (≥90%)	*Huber et al., 2005*
	Secondary effluent (German)	0.54±0.04 μg L^{-1}	Ozonation-UV treatment plant O_3=100 g h^{-1}, O_3 dose= 5-15 mg L^{-1}, 2 diffuser/PVC bubble columns	O_3 dose= 5-15 mg L^{-1} (≥ 91%)	*Ternes et al., 2003*
	Secondary wastewater effluent (Spain)	*na*	Batch experiments, O_3 flow=35 L h^{-1}, O_3 dose=20 mg L^{-1}.	(100%)	*Radjenovic et al., 2009*
	CAS and sand filtration (Tokyo)	27.2 ng L^{-1}	O_3 dose=3 mg L^{-1}, Retention time=27 min	(90.9%)	*Nakada et al., 2007*
Azithromycin	Secondary effluent (Kloten-Opfikon, Switzerland)	1 μM	Batch experiments, O_3 dose=0.5-5.0 mg L^{-1}	O_3 dose: 1 mg L^{-1} (62%)	*Dodd et al., 2006*
	CAS and sand filtration (Tokyo)	*nd*	O_3 dose=3 mg L^{-1}, Retention time=27 min	(92.6%)	*Nakada et al., 2007*
	CAS effluent (Alcala de Henares, Madrid)	235 ng L^{-1}	AirSep AS-12 PSA oxygen generation unit	O_3 dose<50 μM (100%)	*Rosal et al., 2010*
Tylosin	Secondary effluent (Kloten-Opfikon, Switzerland)	1 μM	Batch experiments, O_3 dose=0.5-5.0 mg L^{-1}	O_3 dose=3 mg L^{-1} (100%)	*Dodd et al., 2006*
	Pharmaceutical effluent (Taiwan)	40 mg L^{-1}	O_3/O_2 mixture, O_3 dose(v/v)=5.3%, flow=1.6 L min^{-1}.	(>99%)	*Lin et al., 2009b*
Clarythromycin	Secondary effluent (German)	0.21±0.02 μg L^{-1}	Ozonation-UV treatment plant O_3=100 g h^{-1}, O_3 dose= 5-15 mg L^{-1}, 2 diffuser/PVC bubble columns	O_3 dose=5-15 mg L^{-1} (≥ 76%)	*Ternes et al., 2003*
	CAS and sand filtration (Tokyo)	228 ng L^{-1}	O_3 dose=3 mg L^{-1}, Retention time=27 min	(84.69%)	*Nakada et al., 2007*
	CAS effluent (Alcala de Henares, Madrid)	39 ng L^{-1}	AirSep AS-12 PSA oxygen generation unit	O_3 dose<50 μM (100%)	*Rosal et al., 2010*

Erythromycin	Secondary effluent (German)	0.62±0.24 μg L^{-1}	Ozonation-UV treatment plant O_3=100 g h^{-1}, O_3 dose= 5-15 mg L^{-1}, 2 diffuser/PVC bubble columns	O_3 dose =5-15 mg L^{-1} (≥ 92%)	*Ternes et al., 2003*
	CAS effluent (Alcala de Henares, Madrid)	72 ng L^{-1}	AirSep AS-12 PSA oxygen generation unit	O_3 dose<90 μM (100%)	*Rosal et al., 2010*
	Pharmaceutical effluent (Taiwan)	40 mg L^{-1}	O_3/O_2 mixture, O_3 dose(v/v)=5.3%, flow=1.6 L min^{-1}.	(>99%)	*Lin et al., 2009b*
Erythromycin-H_2O	CAS and sand filtration (Tokyo)	150 ng L^{-1}	O_3 dose=3 mg L^{-1}, Retention time=27 min	(88.7%)	*Nakada et al., 2007*
Sulfonamides					
Sulfamethoxazole	Secondary effluent (Kloten-Opfikon, Switzerland)	1 μM	Batch experiments, O_3 dose=0.5-5.0 mg L^{-1}	O_3 dose=3 mg L^{-1} (100%)	*Dodd et al., 2006*
	CAS and MBR effluent (Kloten-Opfikon, Switzerland)	2 μg L^{-1}	O_3 dose=0-5 mg L^{-1}; flow=200 ±10 L h^{-1} (only column 1).	O_3 dose ≥ 2 mg L^{-1} (≥ 90%)	*Huber et al., 2005*
	CAS and sand filtration (Tokyo)	104 ng L^{-1}	O_3 dose=3 mg L^{-1}, Retention time=27 min	(87.4%)	*Nakada et al., 2007*
	CAS effluent (Alcala de Henares, Madrid)	95 ng L^{-1}	AirSep AS-12 PSA oxygen generation unit	O_3 dose<220 μM (100%)	*Rosal et al., 2010*
	Pharmaceutical effluent (Taiwan)	40 mg L^{-1}	O_3/O_2 mixture, O_3 dose(v/v)=5.3%, flow=1.6 L min^{-1}.	(93%)	*Lin et al., 2009b*
Sulfamethazine	Secondary effluent (German)	0.62±0.05 μg L^{-1}	Ozonation-UV treatment plant O_3=100 g h^{-1}, O_3 dose= 5-15 mg L^{-1}, 2 diffuser/PVC bubble columns.	O_3 dose =5-15 mg L^{-1} (≥ 92%)	*Ternes et al., 2003*
	Missouri River water (Jefferson City)	50 μg L^{-1}	O_3 dose=7.1 mg L^{-1}	0.3 mg L^{-1} O_3 at 1.3 min) **(**> 95%)	*Adams et al., 2002*
	Pharmaceutical effluent (Taiwan)	40 mg L^{-1}	O_3/O_2 mixture, O_3 dose(v/v)=5.3%, flow=1.6 L min^{-1}.	(95%)	*Lin et al., 2009b*
Sulfathiazole	Missouri River water (Jefferson City)	50 μg L^{-1}	O_3 dose=7.1 mg L^{-1}	0.3 mg L^{-1} O_3 at 1.3 min) **(**> 95%)	*Adams et al., 2002*
Sulfamerazine	Missouri River water (Jefferson City)	50 μg L^{-1}	O_3 dose=7.1 mg L^{-1}	0.3 mg L^{-1} O_3 at 1.3 min) **(**> 95%)	*Adams et al., 2002*
Sulfachloropyridazine	Missouri River water (Jefferson City)	50 μg L^{-1}	O_3 dose=7.1 mg L^{-1}	0.3 mg L^{-1} O_3 at 1.3 min) **(**> 95%)	*Adams et al., 2002*
Sulfadimethoxine	Missouri River water (Jefferson City)	50 μg L^{-1}	O_3 dose=7.1 mg L^{-1}	0.3 mg L^{-1} O_3 at 1.3 min) **(**> 95%)	*Adams et al., 2002*
	Pharmaceutical effluent (Taiwan)	40 mg L^{-1}	O_3/O_2 mixture, O_3 dose(v/v)=5.3%, flow=1.6 L min^{-1}.	(96%)	*Lin et al., 2009b*
Sulfapyridine	CAS and sand filtration (Tokyo)	492 ng L^{-1}	O_3 dose=3 mg L^{-1}, Retention time=27 min	(93.9%)	*Nakada et al., 2007*
	CAS effluent (Alcala de Henares, Madrid)	50 ng L^{-1}	AirSep AS-12 PSA oxygen generation unit	O_3 dose<50 μM (100%)	*Rosal et al., 2010*
Quinolones					
Norfloxacin	CAS effluent (Alcala de Henares, Madrid)	38 ng L^{-1}	AirSep AS-12 PSA oxygen generation unit	O_3 dose<90 μM (100%)	*Rosal et al., 2010*
Ciprofloxacin	Secondary effluent (Kloten-Opfikon, Switzerland)	1 μM	Batch experiments, O_3 dose=0.5-5.0 mg L^{-1}	O_3 dose=3 mg L^{-1} (100%)	*Dodd et al., 2006*
	CAS effluent (Alcala de Henares, Madrid)	522 ng L^{-1}	AirSep AS-12 PSA oxygen generation unit	O_3 dose<130 μM (100%)	*Rosal et al., 2010*
Enrofloxacin	Secondary effluent (Kloten-Opfikon, Switzerland)	1 μM	Batch experiments, O_3 dose=0.5-5.0 mg L^{-1}	O_3 dose=3 mg L^{-1} (100%)	*Dodd et al., 2006*
Trimethoprim					
	Secondary effluent (Kloten-Opfikon, Switzerland)	1 μM	Batch experiments, O_3 dose=0.5-5.0 mg L^{-1}	O_3 dose=3 mg L^{-1} (100%)	*Dodd et al., 2006*
	Secondary effluent (German)	0.34±0.04 μg L^{-1}	Ozonation-UV treatment plant O_3=100 g h^{-1}, O_3 dose= 5-15 mg L^{-1}, 2 diffuser/PVC bubble columns	O_3 dose : 5- 15 mg L^{-1} (≥ 85%)	*Ternes et al., 2003*
	Secondary wastewater effluent (Spain)	*na*	Batch experiments, O_3 flow=35 L h^{-1}, O_3 dose=20 mg L^{-1}.	100%	*Radjenovic et al., 2009*
	Missouri River water (Jefferson City)	50 μg L^{-1}	O_3 dose=7.1 mg L^{-1}	0.3 mg L^{-1} O_3 at 1.3 min) **(**> 95%)	*Adams et al., 2002*
	CAS and sand filtration (Tokyo)	53.5 ng L^{-1}	O_3 dose=3 mg L^{-1}, Retention time=27 min	(96%)	*Nakada et al., 2007*
	CAS effluent (Alcala de Henares, Madrid)	73 ng L^{-1}	AirSep AS-12 PSA oxygen generation unit	O_3 dose<90 μM (100%)	*Rosal et al., 2010*
	WWTPs in Beijing (China)	400 ng L^{-1}	O_3 dose=5 mg L^{-1}; Contact time=15 min MF/RO: Spiral-wound crossflow module	(>90%)	*Sui et al., 2010*

Tetracyclines					
Tetracycline	Secondary effluent (Kloten-Opfikon, Switzerland)	1 μM	Batch experiments, O_3 dose=0.5-5.0 mg L^{-1}	O_3 dose=1.5 mg L^{-1} (100%)	*Dodd et al., 2006*
Lincosamides					
Lincomycin	Secondary effluent (Kloten-Opfikon, Switzerland)	1 μM	Batch experiments, O_3 dose=0.5-5.0 mg L^{-1}	O_3 dose:=1 mg L^{-1} (70%)	*Dodd et al., 2006*
	CAS effluent (Alcala de Henares, Madrid)	12 ng L^{-1}	AirSep AS-12 PSA oxygen generation unit	O_3 dose<50 μM (100%)	*Rosal et al., 2010*
Aminoglycosides					
Amikacin	Secondary effluent (Kloten-Opfikon, Switzerland)	1 μM	Batch experiments, O_3 dose=0.5-5.0 mg L^{-1}	O_3 dose: 1 mg L^{-1} (25%)	*Dodd et al., 2006*
Advanced treatment process	**MEMBRANE FILTRATION (RO/MF/UF/MF) AND MEMBRANE BIOREACTOR (MBR) PROCESS**				
Antibiotic Group	**Type of wastewater (location)**	**Initial concentration**	**Treatment process**	**Results/findings (Removal efficiency)**	**Reference**
β-Lactams					
Amoxicillin	Simulated wastewater (USA)	10 mg L^{-1}	RO: plate and frame configuration, ACM-LP fully aromatic polyamide low pressure advanced composite membrane	(100%)	*Morse and Jackson, 2004*
	CAS effluent (Australia)	280 ng L^{-1}	MF/RO plant: receives ~10% of CAS effluent	MF: *nd*; RO: *nd*	*Watkinson et al., 2007*
	Wastewater from plant manufacturing AMX (China)	*na*	Laboratory-scale cross flow RO unit. Two high-pressure cross flow membrane cells (SS316, 155 cm^2) mounted with a flat-sheet polyamide RO membrane. TOC=18925 mg L^{-1} COD=80000 mg L^{-1}	RO_1 TOC=283.9 mg L^{-1} (98.5%) COD=800 mg L^{-1} (99.0%) RO_2 TOC=56.8 mg L^{-1} (99.7%) COD=240mg L^{-1} (99.7%)	*Zhang et al., 2006*
Cefaclor	CAS effluent (Australia)	980 ng L^{-1}	MF/RO plant: receives ~10% of CAS effluent	MF: *nd*; RO: *nd*	*Watkinson et al., 2007*
Cephalexin	CAS effluent (Australia)	5600 ng L^{-1}	MF/RO plant: receives ~10% of CAS effluent	MF: 100 ng L^{-1}; RO: 40 ng L^{-1}	*Watkinson et al., 2007*
Penicillin V	CAS effluent (Australia)	160 ng L^{-1}	MF/RO plant: receives ~10% of CAS effluent	MF: *nd*; RO: *nd*	*Watkinson et al., 2007*
Cloxacillin	CAS effluent (Australia)	320 ng L^{-1}	MF/RO plant: receives ~10% of CAS effluent	MF: *nd*; RO: *nd*	*Watkinson et al., 2007*
Macrolides					
Roxithromycin	Kloten-Opfikon (WWTP-K) Altenrhein in St. Gall, Austria (WWTP-A)	*na*	MBR (in WWTP-K): operated in parallel to CAS (HRT~13 h). Three different membrane filtration units: MF plate membrane module (0.4 μm); UF hollow-fibre modules (0.1 μm); UF hollow-fibre modules (0.04 μm). FBR (in WWTP-A): 8 Biostyr up-flow cells, 3.6 mm Styrofoam beads as biofilm support	MBR: 28-61% FBR: ~24%	*Göbel et al., 2007*
	CAS effluent (South-East of Austria)	26-117 ng L^{-1}	MBR (UF membrane, cross flow) pilot plant	31-42 ng L^{-1} (50-60%)	*Clara et al., 2005*
	CAS effluent (Australia)	100 ng L^{-1}	MF/RO plant: receives ~10% of CAS effluent	MF: 125 ng L^{-1}; RO: 15 ng L^{-1}	*Watkinson et al., 2007*
	CAS effluent (Tel-Aviv, Israel)	600 ng L^{-1}	MBR/RO plant: Two Zenon ZeeWeed 500 UF immersed hollow fiber membranes (total area =2 m^2). RO membrane Filmtec TW30 25-40 (surface area=2.7 m^2). CAS-UF/RO plant: UF pilot device (24 modules, 1024 m^2, ZeeWeed-1000 immersed hollow fibers). RO membrane Filmtec BW30-400 (total area= 1295 m^2).	MBR/RO MBR: (89.5±7.7%) RO: (99.6±0.4%) CAS-UF/RO UF: (81.4±10.1%) RO: (99.9±0.1%)	*Sahar et al., 2010*
Azithromycin	Kloten-Opfikon (WWTP-K)	*na*	MBR (WWTP-K): operated in parallel to CAS. Three	MBR: 4%	*Göbel et al., 2007*

	Altenrhein in St. Gall, Austria (WWTP-A)		different membrane filtration units: MF plate membrane module (0.4 μm); UF hollow-fibre modules (0.1 μm); UF hollow-fibre modules (0.04 μm). FBR (WWTP-A): 8 Biostyr up-flow cells, 3.6 mm Styrofoam beads as biofilm support.	FBR: ~12.5%	
Clarithromycin	Kloten-Opfikon (WWTP-K) Altenrhein in St. Gall, Austria (WWTP-A)	*na*	MBR (WWTP-K): operated in parallel to CAS. Three different membrane filtration units: MF plate membrane module (0.4 μm); UF hollow-fibre modules (0.1 μm); UF hollow-fibre modules (0.04 μm). FBR (WWTP-A): 8 Biostyr up-flow cells, 3.6 mm Styrofoam beads as biofilm support.	MBR: 28-61% FBR: ~10%	*Göbel et al., 2007*
	CAS effluent (Tel-Aviv, Israel)	1500 ng L^{-1}	MBR/RO plant: Two Zenon ZeeWeed 500 UF immersed hollow fiber membranes (total area =2 m^2). RO membrane Filmtec TW30 25-40 (surface area=2.7 m^2). CAS-UF/RO plant: UF pilot device (24 modules, 1024 m^2, ZeeWeed-1000 immersed hollow fibers). RO membrane Filmtec BW30-400 (total area= 1295 m^2).	MBR-/RO MBR: (91.4±5.4%) RO: (99.2±0.8%) CAS-UF/RO UF: (93.2±5.0%) RO: (99.2±0.8%)	*Sahar et al., 2010*
Erythromycin	CAS effluent (Tel-Aviv, Israel)	1000 ng L^{-1}	MBR/RO plant: Two Zenon ZeeWeed 500 UF immersed hollow fiber membranes (total area =2 m^2). RO membrane Filmtec TW30 25-40 (surface area=2.7 m^2). CAS-UF/RO plant: UF pilot device (24 modules, 1024 m^2, ZeeWeed-1000 immersed hollow fibers). RO membrane Filmtec BW30-400 (total area= 1295 m^2).	MBR/RO MBR: (90.4±8.2%) RO: (99.3±0.7%) CAS-UF/RO UF: (72.2±6.8%) RO: (99.3±0.7%)	*Sahar et al., 2010*
Erythromycin-H_2O	Kloten-Opfikon (WWTP-K) Altenrhein in St. Gall, Austria (WWTP-A)	*na*	MBR (in WWTP-K): operated in parallel to CAS (HRT~13 h). Three different membrane filtration units: MF plate membrane module (0.4 μm); UF hollow-fibre modules (0.1 μm); UF hollow-fibre modules (0.04 μm). FBR (in WWTP-A): 8 Biostyr up-flow cells, 3.6 mm Styrofoam beads as biofilm support	MBR: 28-61% FBR: ~25%	*Göbel et al., 2007*
	CAS effluent (Terrassa, Spain)	820 ng L^{-1}	Two pilot-scale MBRs were operating in parallel with activated sludge (AS) treatment: Hollow-fibre ultra-filtration membranes (HF-UF) (HRT=7.2 h); flat-sheet micro-filtration membranes (FS-MF) (HRT=15 h).	HF-UF (25.2±108.9%) FS-MF (43.0±51.5%)	*Radjenovic et al., 2009b*
Tylosin	CAS effluent (Australia)	55 ng L^{-1}	MF/RO plant: receives ~10% of CAS effluent	MF: 10 ng L^{-1}; RO: 5 ng L^{-1}	*Watkinson et al., 2007*
Sulfonamides					
Sulfamethoxazole	*na*	1 mg L^{-1}	RO membranes: Polyamide (XLE); Cellulose acetate (SC-3100). Cross flow membrane unit with a flat-sheet membrane cell Effective membrane area in the cell= 32 cm^2	XLE (70%) SC-3100 (82%)	*Kimura et al., 2004*
	Kloten-Opfikon (WWTP-K) Altenrhein in St. Gall, Austria (WWTP-A)	*na*	MBR (in WWTP-K): operated in parallel to CAS (HRT~13 h). Three different membrane filtration units: MF plate membrane module (0.4 μm); UF hollow-fibre modules (0.1 μm); UF hollow-fibre modules (0.04 μm). FBR (in WWTP-A): 8 Biostyr up-flow cells, 3.6 mm Styrofoam beads as biofilm support	MBR: >95% FBR: ~62.5%	*Göbel et al, 2007*
	CAS effluent (South-East of Austria)	145 ng L^{-1}	MBR (UF membrane, cross flow) pilot plant	56 ng L^{-1} (~61%)	*Clara et al., 2005*

	CAS effluent (Terrassa, Spain)	93 ng L^{-1}	Two pilot-scale MBRs were operating in parallel with activated sludge (AS) treatment: Hollow-fibre ultra-filtration membranes (HF-UF) (HRT=7.2 h); flat-sheet micro-filtration membranes (FS-MF) (HRT=15 h).	HF-UF (78.3±13.9%) FS-MF (80.8±12.2%)	*Radjenovic et al., 2009b*
	CAS effluent (Australia)	500 ng L^{-1}	MF/RO plant: receives ~10% of CAS effluent	MF: 445 ng L^{-1}; RO: *nd*	*Watkinson et al., 2007*
	CAS effluent (Tel-Aviv, Israel)	500 ng L^{-1}	MBR/RO plant: Two Zenon ZeeWeed 500 UF immersed hollow fiber membranes (total area =2 m^2). RO membrane Filmtec TW30 25-40 (surface area=2.7 m^2). CAS-UF/RO plant: UF pilot device (24 modules, 1024 m^2, ZeeWeed-1000 immersed hollow fibers). RO membrane Filmtec BW30-400 (total area= 1295 m^2).	MBR/RO MBR: (69.6±7.3%) RO: (97.6±2.4%) CAS-UF/RO UF: (60.3±21.7%) RO: (97.6±2.4%)	*Sahar et al., 2010*
Sulfadiazine	Model wastewater for veterinary use (Croatia)	10 mg L^{-1}	RO membranes: XLE; HR95PP; TFC-S. NF membranes: NF90; HL Desal, Osmonics Surface area of membranes: 10.8 cm^2	XLE (99.4%) HR95PP (99.4%) TFC-S (100 %) NF90 (99.4 %) HL (88.5 %)	*Kosutic et al., 2007*
Sulfaguanidine	Model wastewater for veterinary use (Croatia)	10 mg L^{-1}	RO membranes: XLE; HR95PP; TFC-S. NF membranes: NF90; HL Desal, Osmonics Surface area of membranes: 10.8 cm^2	XLE (99.3%) HR95PP (98.9%) TFC-S (100 %) NF90 (99.1 %) HL (67.3 %)	*Kosutic et al., 2007*
Sulfamethazine	Model wastewater for veterinary use (Croatia)	10 mg L^{-1}	RO membranes: XLE; HR95PP; TFC-S. NF membranes: NF90; HL Desal, Osmonics Surface area of membranes: 10.8 cm^2	XLE (99.1%) HR95PP (99.3%) TFC-S (100 %) NF90 (99.4 %) HL (96.3 %)	*Kosutic et al., 2007*
	Missouri River water (Jefferson City)	50 µg L^{-1}	Barnstead RO system: Model D2716, Cellulose acetate membrane D2731, Flow: 1.9 L min^{-1}.	(90.3%)	*Adams et al., 2002*
	CAS effluent (Tel-Aviv, Israel)	3 ng L^{-1}	MBR/RO plant: Two Zenon ZeeWeed 500 UF immersed hollow fiber membranes (total area =2 m^2). RO membrane Filmtec TW30 25-40 (surface area=2.7 m^2). CAS-UF/RO plant: UF pilot device (24 modules, 1024 m^2, ZeeWeed-1000 immersed hollow fibers). RO membrane Filmtec BW30-400 (total area= 1295 m^2).	MBR/RO MBR (90.2±9.8%) RO (93.5±6.5%) CAS-UF/RO UF (73.5±16.2%) RO (93.5±6.5%)	*Sahar et al., 2010*
Sulfathiazole	Missouri River water (Jefferson City)	50 µg L^{-1}	Barnstead RO system: Model D2716, Cellulose acetate membrane D2731, Flow: 1.9 L min^{-1}.	(90.3%)	*Adams et al., 2002*
	CAS effluent (Australia)	40 ng L^{-1}	MF/RO plant: receives ~10% of CAS effluent	MF: *nd*; RO: *nd*	*Watkinson et al., 2007*
Sulfamerazine	Missouri River water (Jefferson City)	50 µg L^{-1}	Barnstead RO system: Model D2716, Cellulose acetate membrane D2731, Flow: 1.9 L min^{-1}.	(90.3%)	*Adams et al., 2002*
Sulfachloropyridazine	Missouri River water (Jefferson City)	50 µg L^{-1}	Barnstead RO system: Model D2716, Cellulose acetate membrane D2731, Flow: 1.9 L min^{-1}.	(90.3%)	*Adams et al., 2002*
Sulfadimethoxine	Missouri River water (Jefferson City)	50 µg L^{-1}	Barnstead RO system: Model D2716, Cellulose acetate membrane D2731, Flow: 1.9 L min^{-1}.	(90.3%)	*Adams et al., 2002*
Sulfapyridine	Kloten-Opfikon (WWTP-K) Altenrhein in St. Gall, Austria (WWTP-A)	*na*	MBR (in WWTP-K): operated in parallel to CAS (HRT~13 h). Three different membrane filtration units: MF plate	MBR: >95% FBR: ~72%	*Göbel et al., 2007*

			membrane module (0.4 μm); UF hollow-fibre modules (0.1 μm); UF hollow-fibre modules (0.04 μm). FBR (in WWTP-A): 8 Biostyr up-flow cells, 3.6 mm Styrofoam beads as biofilm support		
Sulfasalazine	CAS effluent (Australia)	60 ng L^{-1}	MF/RO plant: receives ~10% of CAS effluent	MF: 55 ng L^{-1}; RO: *nd*	*Watkinson et al., 2007*
Quinolones					
Enrofloxacin	Model wastewater for veterinary use (Croatia)	10 mg L^{-1}	RO membranes: XLE (Dow/FilmTec, Midland MI); HR95PP (Dow/FilmTec, Midland MI); TFC-S (Koch Membrane Systems, Wilmington, MA). NF membranes: NF90 (Dow/FilmTec); HL Desal, Osmonics (GE Infrastructure Water Process Techn.,Vista, CA). Surface area of membranes: 10.8 cm^2	XLE (97.2%) HR95PP (98.8%) TFC-S (100%) NF90 (99.1 %) HL (99.4 %)	*Kosutic et al., 2007*
	CAS effluent (Australia)	100 ng L^{-1}	MF/RO plant: receives ~10% of CAS effluent	MF: 240 ng L^{-1}; RO: 10 ng L^{-1}	*Watkinson et al., 2007*
Norfloxacin	CAS effluent (Australia)	240 ng L^{-1}	MF/RO plant: receives ~10% of CAS effluent	MF: 190 ng L^{-1}; RO: 15 ng L^{-1}	*Watkinson et al., 2007*
Ofloxacin	CAS effluent (Terrassa, Spain)	10500 ng L^{-1}	Two pilot-scale MBRs were operating in parallel with activated sludge (AS) treatment: Hollow-fibre ultra-filtration membranes (HF-UF) (HRT=7.2 h); flat-sheet micro-filtration membranes (FS-MF) (HRT=15 h).	HF-UF (91.3±10.8%) FS-MF (95.2±2.8%)	*Radjenovic et al., 2009b*
Ciprofloxacin	CAS effluent (Australia)	4600 ng L^{-1}	MF/RO plant: receives ~10% of CAS effluent	MF: 170 ng L^{-1}; RO: *nd*	*Watkinson et al., 2007*
Nalidixic acid	CAS effluent (Australia)	200 ng L^{-1}	MF/RO plant: receives ~10% of CAS effluent	MF: 260 ng L^{-1}; RO: 75 ng L^{-1}	*Watkinson et al., 2007*
Trimethoprim					
	Model wastewater for veterinary use (Croatia)	10 mg L^{-1}	RO membranes: XLE (Dow/FilmTec, Midland MI); HR95PP (Dow/FilmTec, Midland MI); TFC-S (Koch Membrane Systems, Wilmington, MA). NF membranes: NF90 (Dow/FilmTec); HL Desal, Osmonics (GE Infrastructure Water Process Techn.,Vista, CA). Surface area of membranes: 10.8 cm^2	XLE (98.6%) HR95PP (98.2%) TFC-S (100%) NF90 (99.2 %) HL (88.8 %)	*Kosutic et al., 2007*
	Missouri River water (Jefferson City)	50 μg L^{-1}	Barnstead RO system: Model D2716, Cellulose acetate membrane D2731, Flow: 1.9 L min^{-1}.	(90.3%)	*Adams et al., 2002*
	Kloten-Opfikon (WWTP-K) Altenrhein in St. Gall, Austria (WWTP-A)	*na*	MBR (in WWTP-K): operated in parallel to CAS (HRT~13 h). Three different membrane filtration units: MF plate membrane module (0.4 μm); UF hollow-fibre modules (0.1 μm); UF hollow-fibre modules (0.04 μm). FBR (in WWTP-A): 8 Biostyr up-flow cells, 3.6 mm Styrofoam beads as biofilm support	MBR: 28-61% FBR: ~20%	*Göbel et al., 2007*
	CAS effluent (Terrassa, Spain)	204 ng L^{-1}	Two pilot-scale MBRs were operating in parallel with activated sludge (AS) treatment: Hollow-fibre ultra-filtration membranes (HF-UF) (HRT=7.2 h); flat-sheet micro-filtration membranes (FS-MF) (HRT=15 h).	HF-UF (47.5±22.5%) FS-MF (66.7±20.6%)	*Radjenovic et al., 2009b*
	CAS effluent (Australia)	930 ng L^{-1}	MF/RO plant: receives ~10% of CAS effluent	MF: 85 ng L^{-1}; RO: 10 ng L^{-1}	*Watkinson et al., 2007*
	Secondary effluent (Beijing, China)	400 ng L^{-}	UF: Dead-end ultrafiltration system (Zenon GE), 6 trains of Zee-Weed 1000 membrane, pore size of 0.02 μm (PVDF), flow=23 L $(m^2\ h)^{-1}$ MF/RO: Spiral-wound cross flow module (Filmtec, DOW).	UF (0-50%) MF/RO (>90%)	*Sui et al., 2010*

	CAS effluent (Tel-Aviv, Israel)	30 ng L^{-1}	MBR/RO plant: Two Zenon ZeeWeed 500 UF immersed hollow fiber membranes (total area =2 m^2). RO membrane Filmtec TW30 25-40 (surface area=2.7 m^2). CAS-UF/RO plant: UF pilot device (24 modules, 1024 m^2, ZeeWeed-1000 immersed hollow fibers). RO membrane Filmtec BW30-400 (total area= 1295 m^2).	MBR/RO MBR: (96±4%) RO: (97.2±2.8%) CAS-UF/RO UF: (66.4±20.5%) RO: (93.2±6.8%)	*Sahar et al., 2010*
Tetracyclines					
Oxytetracycline	Model wastewater for veterinary use (Croatia)	10 mg L^{-1}	RO membranes: XLE (Dow/FilmTec, Midland MI); HR95PP (Dow/FilmTec, Midland MI); TFC-S (Koch Membrane Systems, Wilmington, MA). NF membranes: NF90 (Dow/FilmTec); HL Desal, Osmonics (GE Infrastructure Water Process Techn,Vista, CA). Surface area of membranes: 10.8 cm^2	XLE (99.2%) HR95PP (99.3%) TFC-S (100%) NF90 (99.0 %) HL (99.2 %)	*Kosutic et al., 2007*
	Waste liquor from the crystallization unit in a pharmaceutical company (Chi Feng, Inner Mongolia, China).	1000 mg L^{-1}	RO: SEPA CELL flat sheet membrane apparatus; membrane area of 155 cm^2. UF: 0.3 MPa; UF membranes of different molecular weight cut-off (3,10, 30, 50 K Da)	< 80 mg L^{-1} (>92%)	*Li et al., 2004*
Lincosamides					
Clindamycin	CAS effluent (Australia)	5 ng L^{-1}	MF/RO plant: receives ~10% of CAS effluent	MF: 10 ng L^{-1} RO: 5 ng L^{-1}	*Watkinson et al., 2007*
Lincomycin	CAS effluent (Australia)	80 ng L^{-1}	MF/RO plant: receives ~10% of CAS effluent	MF: 35 ng L^{-1} RO: 1 ng L^{-1}	*Watkinson et al., 2007*
Advanced treatment process	**ACTIVATED CARBON ADSORPTION**				
Antibiotic Group	**Type of wastewater (location)**	**Initial concentration**	**Treatment process**	**Results/findings (Removal efficiency)**	**Reference**
β-Lactams					
Amoxicillin	Real wastewater (P.T. Coronet Crown)	317 mg L^{-1}	Activated Carbon: BET surface area=1092.951 m^2 $g^{-}1$, pore size < 20A°, dose: 1.5 g/ 50 mL solvent	16.9 mg L^{-1} (94.67%)	*Putra et al., 2009*
Penicillin G	*na*	50-1000 mg L^{-1}	HCI washed powdered activated carbon: particle size <0.15 mm, BET surface area=1000 m^2 g^{-1}, bulk density=0.46. Activated carbon 0.1 g was treated with 100 ml of PG at a defined pH, temperature and initial PG concentration	$Adsorption_{MAX}$: 375.0 mg g^{-1} (pH: 6.0, 35 ◦C) adsorption (%): 44.0-290.0 (25 ◦C) 39.6-64.4 (35 ◦C) 24.6-51.6 (45 ◦C)	*Aksu and Tunc, 2005*
Macrolides					
Erythromycin–H_2O	Four matrices: Colorado River from Lake Mead; Ohio River near Louisville; Passaic River near Totowa; Model water.	*na*	Two activated carbons: AC800 (Acticarb, Dunnellon, FL) and WPM (Calgon Carbon Corp., Pittsburgh, PA). Contact time=4 h; AC dose=1-20 mg L^{-1}	AC800 dose=5 mg L^{-1} (20%)	*Westerhoff et al., 2005*

Sulfonamides					
Sulfomethoxazole	Four matrices: Colorado River from Lake Mead; Ohio River near Louisville; Passaic River near Totowa; Model water.	*na*	Two activated carbons: AC800 (Acticarb, Dunnellon, FL) and WPM (Calgon Carbon Corp., Pittsburgh, PA). Contact time=4 h; AC dose=1-20 mg L^{-1}	AC800 dose=5 mg L^{-1} (20%)	*Westerhoff et al., 2005*
Sulfamethazine	Missouri River water (Jefferson City).	50 µg L^{-1}	Activated carbon dose=0-50 mg L^{-1}; Contact time=4 h	AC dose=10 mg L^{-1} (49%) AC dose=20 mg L^{-1} (85%) AC dose=50 mg L^{-1} (>90%)	*Adams et al., 2002*
Sulfathiazole	Missouri River water (Jefferson City).	50 µg L^{-1}	Activated carbon dose=0-50 mg L^{-1}; Contact time=4 h	AC dose=10 mg L^{-1} (70%) AC dose=20 mg L^{-1} (85%) AC dose: 50 mg L^{-1} (>90%)	*Adams et al., 2002*
Sulfamerazine	Missouri River water (Jefferson City).	50 µg L^{-1}	Activated carbon dose=0-50 mg L^{-1}; Contact time=4 h	AC dose=10 mg L^{-1} (60%) AC dose=20 mg L^{-1} (80%) AC dose=50 mg L^{-1} (>90%)	*Adams et al., 2002*
Sulfachloropyridazine	Missouri River water (Jefferson City).	50 µg L^{-1}	Activated carbon dose=0-50 mg L^{-1}; Contact time=4 h	AC dose=10 mg L^{-1} (58%) AC dose=20 mg L^{-1} (75%) AC dose=50 mg L^{-1} (>90%)	*Adams et al., 2002*
Sulfadimethoxine	Missouri River water (Jefferson City).	50 µg L^{-1}	Activated carbon dose=0-50 mg L^{-1}; Contact time=4 h	AC dose=10 mg L^{-1} (50%) AC dose=20 mg L^{-1} (80%) AC dose=50 mg L^{-1} (>90%)	*Adams et al., 2002*
Trimethoprim					
	Four matrices: Colorado River from Lake Mead; Ohio River near Louisville; Passaic River near Totowa; Model water.	*na*	Two activated carbons: AC800 (Acticarb, Dunnellon, FL) and WPM (Calgon Carbon Corp., Pittsburgh, PA). Contact time=4 h; AC dose=1-20 mg L^{-1}	AC800 dose= 5 mg L^{-1} (93%)	*Westerhoff et al., 2005*
	Missouri River water (Jefferson City).	50 µg L^{-1}	Activated carbon dose=0-50 mg L^{-1}; Contact time=4 h	AC dose=10 mg L^{-1} (55%) AC dose=20 mg L^{-1} (65%) AC dose=50 mg L^{-1} (>90%)	*Adams et al., 2002)*
Tetracyclines					
Tetracycline	*na*	*na*	Four carbonaceous adsorbents: Single walled carbon nanotubes (SWNT); Multi-walled carbon nanotubes (MWNT); Pulverized activated carbon (AC) and nonporous Graphite (G).	Adsorption efficiency: G/SWNT > MWNT >> AC	*Ji et al., 2009*
Nitroimidazoles					
Metronidazole	Motril (Granada)	100-600 mg L^{-1}	Three activated carbons (0.1 g): Sorbo (S); Merck (M) and carbon prepared by chemical activation of petroleum coke with KOH (C). S (BET=1225 m^2 g^{-1}); M (BET=1301 m^2 g^{-1}); C (BET=848 m^2 g^{-1})	Adsorption capacity S: 1.92 mmol g^{-1} M: 1.25 mmol g^{-1} C: 1.68 mmol g^{-1}	*Rivera-Utrilla et al., 2009*
Dimetridazole	Motril (Granada)	100-600 mg L^{-1}	Three activated carbons (0.1 g): Sorbo (S); Merck (M) and carbon prepared by chemical activation of petroleum coke with KOH (C). S (BET=1225 m^2 g^{-1}); M (BET=1301 m^2 g^{-1}); C (BET=848 m^2 g^{-1})	Adsorption capacity S: 1.99 mmol g^{-1} M: 1.32 mmol g^{-1} C: 2.04 mmol g^{-1}	*Rivera-Utrilla et al., 2009*
Tinidazole	Motril (Granada)	100-600 mg L^{-1}	Three activated carbons (0.1 g): Sorbo (S); Merck (M) and carbon prepared by chemical activation of petroleum coke with KOH (C). S (BET=1225 m^2 g^{-1}); M (BET=1301 m^2 g^{-1}); C (BET=848	Adsorption capacity S: 1.37 mmol g^{-1} M: 1.56 mmol g^{-1} C: 1.04 mmol g^{-1}	*Rivera-Utrilla et al., 2009*

			$m^2\ g^{-1}$)		
Ronidazole	Motril (Granada)	100-600 mg L^{-1}	Three activated carbons (0.1 g): Sorbo (S); Merck (M) and carbon prepared by chemical activation of petroleum coke with KOH (C). S (BET=1225 $m^2\ g^{-1}$); M (BET=1301 $m^2\ g^{-1}$); C (BET=848 $m^2\ g^{-1}$)	Adsorption capacity S: 1.97 mmol g^{-1} M: 1.82 mmol g^{-1} C: 1.89 mmol g^{-1}	*Rivera-Utrilla et al., 2009*
Advanced treatment process **Antibiotic Group**	**UV IRRADIATION** **Type of wastewater (location)**	**Initial concentration**	**Treatment process**	**Results/findings (Removal efficiency)**	**Reference**
β-Lactams					
Penicillin	Antibiotic formulation effluent (Turkey)	*na*	UV light (λ=253.7 nm, 1.73×10^{-4} Einstein $(Ls)^{-1}$); 60 min; pH=7; [H_2O_2]=0-40 mM	COD removal UV / pH 7: (0%) UV+H_2O_2 (40 mM) / pH 7: (11%) UV+H_2O_2 (30 mM) / pH 7: (22%) TOC removal UV / pH 7: (0%) UV+H_2O_2 (40 mM) / pH 7: (10%) UV+H_2O_2 (30 mM) / pH 7: (6%)	*Arslan Alaton and Dogruel, 2004*
Macrolides					
Clarithromycin	Effluent from secondary sedimentation and sand filter (Japan)	110-656 ng L^{-1}	3 UV lamps (λ=254 nm; intensity=1.025 mW cm^{-2}); 3 reactors in series (R_1-R_3); Air flow rate=0.5 L min^{-1}; [H_2O_2]=7.8 mg L^{-1}	UV: (24-34%) UV+ H_2O_2: (>90%)	*Kim et al., 2009*
Erythromycin	Effluent from secondary sedimentation and sand filter (Japan)	110-656 ng L^{-1}	3 UV lamps (λ=254 nm; intensity=1.025 mW cm^{-2}); 3 reactors in series (R_1-R_3); Air flow rate=0.5 L min^{-1}; [H_2O_2]=7.8 mg L^{-1}	UV: (24-34%) UV+ H_2O_2: (>90%)	*Kim et al., 2009*
Azithromycin	Effluent from secondary sedimentation and sand filter (Japan)	110-656 ng L^{-1}	3 UV lamps (λ=254 nm; intensity=1.025 mW cm^{-2}); 3 reactors in series (R_1-R_3); Air flow rate=0.5 L min^{-1}; [H_2O_2]=7.8 mg L^{-1}	UV: (24-34%) UV+ H_2O_2: (>90%)	*Kim et al., 2009*
Sulfonamides					
Sulfomethoxazole	Effluent from Blue Lake WWTP; Metro WWTP and Lake Josephine (USA)	1 μM	Photolysis experiments (Suntest CPS + solar simulator with a UV-Suprax optical filter, 765 W m^{-2})	(48%)	*Ryan et al., 2011*
	Effluent from secondary sedimentation and sand filter (Japan)	42-187 ng L^{-1}	3 UV lamps (λ=254 nm; intensity=1.025 mW cm^{-2}); 3 reactors in series (R_1-R_3); Air flow rate=0.5 L min^{-1}; [H_2O_2]=7.8 mg L^{-1}	UV: (89-100%) UV+ H_2O_2: (>90%)	*Kim et al., 2009*
Sulfamethazine	Missouri River water (Jefferson City).	50 μg L^{-1}	Mercury vapor lamp (254 nm), UV dose=0-10000 mJ cm^{-2}	UV dose=10000 mJ cm^{-2} (85%)	*Adams et al., 2002*
Sulfathiazole	Missouri River water (Jefferson City).	50 μg L^{-1}	Mercury vapor lamp (254 nm), UV dose=0-10000 mJ cm^{-2}	UV dose= 10000 mJ cm^{-2} (100%)	*Adams et al., 2002*
Sulfamerazine	Missouri River water (Jefferson City).	50 μg L^{-1}	Mercury vapor lamp (254 nm), UV dose=0-10000 mJ cm^{-2}	UV dose=10000 mJ cm^{-2} (83%)	*Adams et al., 2002*
Sulfachlorpyridazine	Missouri River water (Jefferson City).	50 μg L^{-1}	Mercury vapor lamp (254 nm), UV dose=0-10000 mJ cm^{-2}	UV dose: 10000 mJ cm^{-2} (83%)	*Adams et al., 2002*
Sulfadimethoxine	Missouri River water (Jefferson City).	50 μg L^{-1}	Mercury vapor lamp (254 nm), UV dose=0-10000 mJ cm^{-2}	UV dose: 10000 mJ cm^{-2} (85%)	*Adams et al., 2002*
	Effluent from secondary sedimentation and sand filter (Japan)	42-187 ng L^{-1}	3 UV lamps (λ=254 nm; intensity=1.025 mW cm^{-2}); 3 reactors in series (R_1-R_3); Air flow rate=0.5 L min^{-1}; [H_2O_2]=7.8 mg L^{-1}	UV: (89-100%) UV+ H_2O_2: (>90%)	*Kim et al., 2009*
Trimethoprim					

	Missouri River water (Jefferson City).	50 μg L^{-1}	Mercury vapor lamp (254 nm), UV dose=0-10000 mJ cm^{-2}	UV dose: 10000 mJ cm^{-2} (85%)	*Adams et al., 2002*
	Effluent from Blue Lake WWTP; Metro WWTP and Lake Josephine (USA)	1 μM	Photolysis experiments (Suntest CPS + solar simulator with a UV-Suprax optical filter, 765 W m^{-2})	(18%)	*Ryan et al., 2011*
Tetracyclines					
Tetracycline	Effluent from secondary sedimentation and sand filter (Japan)	4-17 ng L^{-1}	3 UV lamps (λ=254 nm; intensity=1.025 mW cm^{-2}); 3 reactors in series (R_1-R_3); Air flow rate=0.5 L min^{-1}; $[H_2O_2]$=7.8 mg L^{-1}	UV: (15%) UV+ H_2O_2: (>90%)	*Kim et al., 2009*
Oxytetracycline	Secondary wastewater (Beijing, China)	50 μM	11 W low-pressure Hg vapor lamp (λ=254 nm), photon flow= 4.5×10^{-5} E m^{-2} $s^{-}1$; UV dose=(0-320)×10^2 mJ $cm^{-}2$; 500 mL WW, $[H_2O_2]$=1 mM,	UV UV dose=30528 mJ cm^{-2} (100%) UV/H_2O_2 UV dose=7632 mJ cm^{-2} (100%)	*Yuan et al., 2011*
Doxycycline	Secondary wastewater (Beijing, China)	50 μM	11 W low-pressure Hg vapor lamp (λ=254 nm), photon flow= 4.5×10^{-5} E m^{-2} $s^{-}1$; UV dose=(0-320)×10^2 mJ $cm^{-}2$; 500 mL WW, $[H_2O_2]$=1 mM,	UV UV dose=22896 mJ cm^{-2} (100%) UV/H_2O_2 UV dose=7632 mJ cm^{-2} (100%)	*Yuan et al., 2011*
Chlorotetracycline	Effluent from secondary sedimentation and sand filter (Japan)	4-17 ng L^{-1}	3 UV lamps (λ=254 nm; intensity=1.025 mW cm^{-2}); 3 reactors in series (R_1-R_3); Air flow rate=0.5 L min^{-1}; $[H_2O_2]$=7.8 mg L^{-1}	UV: (<6.18 μg L^{-1}) (100%) UV+ H_2O_2: (>90%)	*Kim et al., 2009*
Quinolones					
	Effluent from secondary sedimentation and sand filter (Japan)	4-148 ng L^{-1}	3 UV lamps (λ=254 nm; intensity=1.025 mW cm^{-2}); 3 reactors in series (R_1-R_3); Air flow rate=0.5 L min^{-1}; $[H_2O_2]$=7.8 mg L^{-1}	UV: (86-100%) UV+ H_2O_2: (69%)	*Kim et al., 2009*
Ciprofloxacin	Secondary wastewater (Beijing, China)	50 μM	11 W low-pressure Hg vapor lamp (λ=254 nm), photon flow= 4.5×10^{-5} E m^{-2} $s^{-}1$; UV dose=(0-320)×10^2 mJ $cm^{-}2$; 500 mL WW, $[H_2O_2]$=1 mM,	UV UV dose=11448 mJ cm^{-2} (100%) UV/H_2O_2 UV dose=7632 mJ cm^{-2} (100%)	*Yuan et al., 2011*
Nalidixic acid	Effluent from secondary sedimentation and sand filter (Japan)	4-148 ng L^{-1}	3 UV lamps (λ=254 nm; intensity=1.025 mW cm^{-2}); 3 reactors in series (R_1-R_3); Air flow rate=0.5 L min^{-1}; $[H_2O_2]$=7.8 mg L^{-1}	UV: (86-100%) UV+ H_2O_2: (>90%)	*Kim et al., 2009*
Advanced treatment process **Antibiotic Group**	**FENTON (Fe^{2+}/H_2O_2)** **Type of wastewater (location)**	**Initial concentration**	**Treatment process**	**Results/findings (Removal efficiency)**	**Reference**
β-Lactams					
Amoxicillin	Wastewater from plant manufacturing AMX (China)	*na*	Fenton oxidation after extraction (dichloromethane) $[FeSO_4.7H_2O]$=10 g L^{-1}; $[H_2O_2]$=2 g L^{-1} TOC=18925 mg L^{-1} COD=80000 mg L^{-1}	TOC=2195.3 mg L^{-1} (88.4%) COD=832 mg L^{-1} (89.6%)	*Zhang et al., 2006*
	CAS effluent (Araraquara, Brazil)	42 mg L^{-1}	Black light at 365 nm and solar irradiation $[H_2O_2]$=2.0 mM [Ferrioxalate or $Fe(NO_3)_3$]=0.20 mM pH=2.5	Black light: (89% in 1 min) Solar light: (85% in 1 min) AMX degradation was not influenced by the source of the irradiation.	*Trovo et al., 2008*
Penicillin	Antibiotic formulation effluent (Turkey)	*na*	UV light (λ=253.7 nm, 1.73×10^{-4} Einstein $(Ls)^{-1}$); 60 min; pH=3; $[H_2O_2]$=20 mM; [Fe(II)]=1 mM; [Fe(III)]=1 mM.	COD removal Photo-Fenton: (56%) Photo-Fenton-like: (66%)	*Arslan Alaton and Dogruel, 2004*

				Dark Fenton: (61%) Dark Fenton-like: (46%) TOC removal Photo-Fenton: (51%) Photo-Fenton-like: (42%) Dark Fenton: (33%) Dark Fenton-like: (18%)	
	Pharmaceutical wastewater (China) COD=49912.5 mg L^{-1}; TOC=11540 mg L^{-1}	*na*	Microwave power=100-500 W; radiation time=2-10 min; pH=1-11; $[H_2O_2]$=3200-19000 mg L^{-1}; $[Fe_2(SO_4)_3]$=2000-8000 mg L^{-1}	Optimum conditions: Microwave power=300 W; radiation time=6 min; pH=4.42; $[H_2O_2]$=1300 mg L^{-1}; $[Fe_2(SO_4)_3]$=4900 mg L^{-1} COD removal: (57.53%) TOC removal: (>40%) Degradation: (55.06%)	*Yang et al., 2009*
Quinolones					
Ofloxacin	Secondary effluent (Almería, Spain)	100 μg L^{-1}	Pilot compound parabolic collector plant (CPC), $[Fe^{2+}]$= 5 mg L^{-1}, $[H_2O_2]$= 50 mg L^{-1}, t_{30W}=102 min	(100%)	*Klamerth et al., 2010*
	(Lemessos, Cyprus)	10 mg L^{-1} (0.0277 mmol L^{-1})	Batch experiments (300 mL), solar simulator (1 kW Xenon lamp) $[Fe^{2+}]$= 1-5 mg L^{-1}, $[H_2O_2]$= 1.357-8.142 mmol L^{-1}	$[Fe^{2+}]$= 5 mg L^{-1}, $[H_2O_2]$= 2.714 mmol L^{-1} (100% at 30 min)	*Michael et al., 2010*
Tetracyclines					
Tetracycline	CAS effluent (Araraquara, Brazil)	24 mg L^{-1}	Black light (15 W) and solar irradiation $[H_2O_2]$= 1-10 mM [Ferrioxalate or $Fe(NO_3)_3$]=0.20 mM pH=2.5	Black light: (80% in 3 min) Solar light: (80% in 3 min)	*Bautitz and Nogueira, 2007*
Advanced treatment process	**TiO_2 photocatalysis**				
Antibiotic Group	**Type of wastewater (location)**	**Initial concentration**	**Treatment process**	**Results/findings (Removal efficiency)**	**Reference**
β-Lactams					
Amoxicillin	Antibiotic wastewater (AW)	138±5 mg L^{-1}	$UV/H_2O_2/TiO_2$ 2000 mL of AW; $[TiO_2]$=0-1000 mg L^{-1}; $[H_2O_2]$=50-350 mg L^{-1}; T=22±2 °C UV lamp (6 W, λ≈365 nm) $UV/H_2O_2/TiO_2$/SBR 1.5 L of AW; 65 days at HRT 24 hr	$UV/H_2O_2/TiO_2$ $[TiO_2]$=1000 mg L^{-1} $[H_2O_2]$=250 mg L^{-1} 30 min, pH=5 (100%) $UV/H_2O_2/TiO_2$/SBR $[TiO_2]$=1000 mg L^{-1} $[H_2O_2]$=250 mg L^{-1} (57 % of COD); (53% of DOC)	*Elmolla and Chaudhuri, 2011*
	CAS effluent (Salerno, Italy)	10 mg L^{-1}	Batch experiments (300 mL), 125W black light fluorescent lamp (300-420 nm; photon flux= 4.7×10^{-7}einstein s^{-1}) TiO_2 Degussa P25, $[TiO_2]$=0.2-0.8 g L^{-1}	120 min, $[TiO_2]$=0.8 g L^{-1} (100%)	*Rizzo et al., 2009*
Cloxacillin	Antibiotic wastewater (AW)	138±5 mg L^{-1}	$UV/H_2O_2/TiO_2$	$UV/H_2O_2/TiO_2$	*Elmolla and Chaudhuri,*

			2000 mL of AW; $[TiO_2]$=0-1000 mg L^{-1}; $[H_2O_2]$=50-350 mg L^{-1}; T=22±2 ºC UV lamp (6 W, λ≈365 nm) $UV/H_2O_2/TiO_2$/SBR 1.5 L of AW; 65 days at HRT 24 hr	$[TiO_2]$=1000 mg L^{-1} $[H_2O_2]$=250 mg L^{-1} 30 min, pH=5 (100%) $UV/H_2O_2/TiO_2$/SBR $[TiO_2]$=1000 mg L^{-1} $[H_2O_2]$=250 mg L^{-1} (57 % of COD); (53% of DOC)	*2011*
Sulfomanides					
Sulfamethoxazole	Final effluent (Lemessos, Cyprus)	10 mg L^{-1}	Batch experiments (350 mL), 9W UVA lamp (Radium Ralutec, 9W/78, 350-400 nm), photon flux= 2.81×10^{-4} einstein min^{-1}. TiO_2 Degussa P25, $[TiO_2]$=500 mg L^{-1}	~20 min, pH=4.8<pH<5.6 (100%) 60 min, pH=7.5<pH<8.2 (>99%)	*Xekoukoulotakis et al., 2010*
Quinolones					
Ofloxacin	Final effluent (Lemessos, Cyprus)	10 mg L^{-1}	Batch experiments (350 mL), 9W UVA lamp (Radium Ralutec, 9W/78, 350-400 nm), photon flux= 3.37×10^{-6} einstein s^{-1}. TiO_2 Degussa P25, $[TiO_2]$=250 mg L^{-1}, $[H_2O_2]$= 0.14 mmol L^{-1}	~85% (Degussa P25; 250 mg L^{-1}; 30 min) ≈Hombicat UV 100 (83%) > Aldrich (73%) > Tronox A-K-1 (67%)> Tronox TR-HP-2 (39%)> Tronox TR(33%) $[H_2O_2]$=0.07 mmol L^{-1} $[TiO_2]$=250 mg L^{-1} (79% of DOC)	*Hapeshi et al., 2010*
	Secondary effluent (Lemessos, Cyprus)	10 mg L^{-1} (0.0277 mmol L^{-1}),	Batch experiments (300 mL), solar simulator (1 kW Xenon lamp) TiO_2 Degussa P25, $[TiO_2]$= 0.25-4.0 g L^{-1}, $[H_2O_2]$= 1.357-8.142 mmol L^{-1}	$[TiO_2]$= 3 g L^{-1}, 120 min (60%) $[TiO_2]$= 3 g L^{-1}, $[H_2O_2]$= 5.428 mmol L^{-1}, 120 min (67%)	*Michael et al., 2010*
Advanced treatment process **Antibiotic Group**	**ULTRASONIC IRRADIATION**				
	Type of wastewater (location)	**Initial concentration**	**Treatment process**	**Results/findings (Removal efficiency)**	**Reference**
β-Lactams					
Amoxicillin	Final effluent before disinfection (Salerno, Italy)	2.5-10.0 mg L^{-1}	Ultrasound generator: 20 kHz, titanium horn (d=1.3 cm), 25-100 W L^{-1}	100 W L^{-1} (~40%)	*Naddeo et al., 2009*

NOTES

nd: not detected; *na*: not available